CENTRO DE INVESTIGACIÓN Y DE ESTUDIOS AVANZADOS DEL INSTITUTO POLITÉCNICO NACIONAL

UNIDAD ZACATENCO

DEPARTAMENTO DE GENÉTICA Y BIOLOGÍA MOLECULAR

Células gliales de Bergmann y el reciclamiento del Glutamato

T E S I S

Que presenta

M. en C. Alain Marc Guillem Del Angel

Para obtener el grado de

DOCTOR EN CIENCIAS

EN LA ESPECIALIDAD DE

Genética y Biología Molecular

Directores de Tesis

Dr. Arturo Ortega Soto

Dra. Angelina Rodríguez Torres

México, D.F. Septiembre 2015

El presente trabajo fue realizado en el laboratorio 23 del Departamento de Genética y Biología Molecular y en el laboratorio 31 del Departamento de Toxicología del Centro de Investigaciones y Estudios Avanzados del I.P.N bajo la dirección de los Doctores Arturo Ortega Soto y Angelina Rodríguez Torres con la asesoría de los Doctores Samuel Zinker Ruzal, Bulmaro Cisneros Vega, José Antonio Arias Montaño y Francisco Castelán.

Durante la realización del presente trabajo el autor contó con el apoyo de la beca 322610 del Consejo Nacional de Ciencia y Tecnología (Conacyt).

Agradecimientos

Al Doctor Arturo Ortega (El Jefe) por sus enseñanzas y apoyo brindado durante estos 6 años de trabajo, aunque largas las horas y mas los días aprendí a pensar diferente, a tener mas confianza no solo en mi trabajo sino en mi mismo. El Jefe me hiso crecer como investigador y como persona no solo con buenos consejos sino con castigos y regaños mas que un tutor fue un mentor y ejemplo a seguir. Gracias Doctor Arturo Ortega

Agradezco la asesoría técnica de Luisa Clara Regina Hernández Kelly, Blanca Roció Ibarra López y Luis Ángel Cid Cid, del Departamento de Toxicología, Cinvestav-IPN por el entrenamiento en las metodologías realizadas en este trabajo.

Agradezco a mis compañeros de generación a Pau, Kike, Alberto, Genaro, Yuri, Martha, Aurora, Flor, Miriam, Eri, Misa, Aida, etc. Por los buenos momento que pasamos durante los cursos y las fiestas.

A mis compañeros del lab, Orqui, Miguel, Edna, Daniel, El Beto, la ardilla malvada, Marco, Gabriel e Ira por compartir los dolores y penas del lab.

A Miguel y Carlita por ser unos buenos amigos y estar ahí en las buenas y las malas

A Orqui y Dr. Edna por ser unas excelentes compañeras de lab

Al pueblo

A la doctora Ira por enseñarme a sobrevivir en el lab y la técnica de EMSA

A mis padres y abuelos porque ellos me hicieron y forjaron que sin ellos nada de esto seria posible. Porque sin su esfuerzo diario, sus enseñanzas y la disciplina que me inculcaron no habría llegado tan lejos. Les agradezco mas de lo que las palabras pueden expresar.

A Zila por lo bueno lo malo y lo peor. Mi esposa que me apoyo desde que éramos novios a seguir adelante hasta el final y presionarme sin limites

Dedico esta tesis a mi Familia.

Índice

Capítulo 1: Introducción general y liberación de Glutamina de células gliales de Bergmann 10

Glutamato 10

Receptores de Glutamato Metabotrópicos 11

Receptores Ionotrópicos de glutamato 12

Receptores AMPA 14

Receptores KA 14

Receptores NMDA 15

Transportadores de Glu 16

Transportadores de Glutamina 18

Sistema ASC 19

Sistema L 20

Sistema A 21

Sistema N 21

Células Gliales 23

Células gliales de Bergmann 24

El glutamato y su efecto sobre las células gliales de Bergmann 25

Ciclo Glutamato/Glutamina 25

Justificación 27

Objetivo General 28

Objetivos Específicos 28

Materiales y Métodos 29

Material Biológico 29

Reactivos 29

Cultivos primarios de células de Bergmann 29

Extractos de proteínas de células gliales de Bergmann 30

Inmunodetección en fase sólida 31

Ensayos de liberación de [^{3}H]-L-Gln 32

Ensayos de captura de [^{3}H]-L-Gln 32

Ensayos de captura de [^{3}H]-D-Asp 33

Ensayos de influjo de $^{45}Ca^{2+}$ en células gliales de Bergmann 33
Inmunoprecipitación de Proteínas 34
Inmunofluorescencias 34
Inmunohistoquimicas 35
Análisis estadístico 36
Resultados 37
Expresión de los transportadores de Glutamina en células de glía de Bergmann 37
Caracterización de la captura de Gln en cultivo celular de glía de Bergmann 39
Acople funcional entre GLAST y SNAT3 41
Interacción física entre GLAST y SNAT3 43
Discusión 45
Capítulo 2: Regulación de GLAST en células gliales de Bergmann por la vía del óxido nítrico/GMPc 48
Introducción 48
Justificación 51
Objetivo General 52
Objetivos Específicos 52
Resultados 53
La activación de ON/GMPc incrementa la captura de Asp en BGC 53
La via ON/GMPc regula la actividad de GLAST 55
El óxido nítrico induce influjos de Ca2+ via PKG en CGB 57
Discusión 61
Capítulo 3: Metilfenidato regula la actividad de GLAST en células gliales de Begmann 63
Introducción 63
Metilfenidato 63
Justificación 66
Objetivo General 67
Objetivos Específicos 67
Resultados 68
El metilfenidato induce un aumento en la captura de Glu en CGB. 68
MPH induce un incremento del transportador GLAST en la membrana. 69
Vías de señalización implicadas en el aumento de la captura de Glu inducidas por MPH 71
Discusión 74

Conclusiones 77
Bibliografía 78
Anexos 85

RESUMEN

El glutamato es el principal neurotransmisor excitador del sistema nervioso central, está implicado en procesos cognitivos como el aprendizaje y la memoria. El glutamato puede inducir muerte neuronal si sus concentraciones no son correctamente reguladas, los encargados de regular las concentraciones extracelulares de este aminoácido son los transportadores de aminoácidos excitadores, de los cuales se conocen 5 subtipos: GLAST, GLT-1, EAAC-1, EAAT-4, EAAT-5. De estos transportadores solo GLAST y GLT-1 tienen una expresión preferencial y son los responsables de remover el 80% del glutamato liberado en la hendidura sináptica. Estos transportadores de glutamato también tiene una función primordial en el ciclo glutamato/glutamina y debido a su alta importancia muchos estudios se ha enfocado en ellos, pero hasta la fecha no se conoce cuáles son las proteínas encargadas de devolver al glutamato en forma de glutamina a la neurona pre-sináptica. Por tal motivo en este trabajo nos dimos a la tarea de caracterizar el eflujo de glutamina procedente de las células gliales de Bergmann cuando existe un estímulo de glutamato. Encontrando que SNAT3 un miembro del sistema N de captura de glutamina es el responsable de la liberación de glutamina en las células gliales de Bergmann. También describimos que el gradiente de sodio inducido por la captura de glutamato por parte de GLAST es el que induce la liberación de glutamina por parte de SNAT3. Se demostró que estos transportadores no solo tienen una interacción funcional sino que también existe una interacción física entre ellos la cual es regulada por sus sustratos.

El óxido nítrico es producido por la neurona post-sináptica en respuesta a un estímulo de glutamato, el cual activa los receptores NMDA, este evento conlleva a la producción de óxido nítrico por parte de la enzima óxido nítrico sintetasa. Este oxido nítrico eventualmente llega a las células gliales y desencadena distintos efectos. En este trabajo demostramos que el óxido nítrico induce una regulación positiva sobre la actividad de los transportadores de glutamato al incrementar su translocación a membrana. Esto tiene como consecuencia un aumento en la captura de glutamato, este efecto es dependiente del intercambiador Na+/Ca2+ y la vía GMPc/PKG.

En la última parte de este proyecto analizamos el efecto del metilfenidato un fármaco comúnmente utilizado para el tratamiento de desórdenes del espectro autista. Aunque este medicamento tiene su efecto principal sobre el sistema dopaminérgico existen reportes que también afecta a neuronas glutamatérgicas. Nosotros decidimos evaluar el efecto de esta droga sobre la captura de glutamato de células gliales de Bergmann. Encontrando que el metilfenidato incrementa la captura de glutamato de manera dependiente de tiempo y dosis. Este aumentó en la captura es dependiente de la traducción de GLAST y depende en gran medida también de la acción de PKG.

Los resultados mostrados en esta tesis apoyan la noción de la sinapsis tripartita, en donde los astrocitos poseen un papel activo en la neurotransmisión y no solo fungen como soporte para las neuronas, ya que en esta tesis se demostró que las células gliales de Bergmann responden de manera activa a la actividad de las neuronas.

ABSTRACT

Glutamate the major excitatory neurotransmitter in the central nervous system is involved in different cognitive processes such as learning and memory. Glutamate can induce neuronal death if their concentrations are not properly regulated, Exitatori aminino acid transportes are the responsible for regulating the extracellular concentrations of this amino acid, 5 subtypes are known: GLAST, GLT-1, EAAC-1, EAAT -4, EAAT-5. GLAST and GLT-1 have preferential astrocyte expression and are responsible for removal 80%of glutamate released in the synaptic cleft. These glutamate transporters also has a key role in glutamate / glutamine shuttle and because of its high importance many studies have focused on this transporters, but to this date is unknown the responsible protein of returning glutamate as glutamine to presynaptic neuron. Therefore in this study we took the task of characterizing glutamine efflux from Bergmann glial cells in the event of glutamate stimulus. Finding that SNAT3 a member of system N is responsible of Bergmann glial cells glutamine release. We also describe that increase of intracellular by GLAST induce SNAT3 release of glutamine. It was shown that these carriers have not only a functional interaction but also a physical interaction which is regulated by its substrates.

Nitric oxide is produced by the postsynaptic neuron in response to stimulation of glutamate, which activates NMDA receptors, this event leads to the production of nitric oxide by the enzyme nitric oxide synthase. This nitric oxide eventually reaches glial cells and triggers different effects. In this work we demonstrate that nitric oxide induces GLAST activity upregulation. This result in an increase in the glutamate uptake, this effect is NCX and cGMP \PKG pathway dependent.

In the last part of this project we analyze the effect of methylphenidate a drug commonly used to treat autism spectrum disorders. While this drug has its main effect on the dopaminergic system there are reports that appoint an affects over glutamatergic neurons. We decided to evaluate the effect of this drug on the Bergmann glial cells glutamate uptake. Finding that methylphenidate increase glutamate uptake in a time and dose dependent event. This uptake increased is GLAST translation and PKG dependent depends.

The results shown in this thesis support the notion of tripartite synapses, where astrocytes have an active role in neurotransmission and not just serve as support to the neurons, this thesis demonstrated that Bergmann glial cells respond to the neurons activity.

CAPÍTULO 1: INTRODUCCIÓN GENERAL Y LIBERACIÓN DE GLUTAMINA DE CÉLULAS GLIALES DE BERGMANN

GLUTAMATO

El glutamato (Glu) es el principal neurotransmisor excitador del sistema nervioso central (SNC) en vertebrados [1-3]. Desde la década de los 50 se conocía el efecto excitatorio del Glu sobre las neuronas, pero debido a sus altas concentración y su distribución generalizada en el cerebro [4], no fue hasta la década de 1970 [5] cuando se reconoció como neurotransmisor. Hoy en día se sabe que el Glu participa en distintos procesos fisiológicos y cognitivos, tales como el aprendizaje y la memoria; igualmente se conoce la función que el Glu desempeña en el desarrollo del SNC, particularmente en la formación y eliminación de sinapsis, la migración y la diferenciación celular tanto de neuronas como de astrocitos [1].

En el sistema nervioso central el Glu es sintetizado al añadir un grupo amino al intermediario del ciclo de los ácidos tricarboxilicos α-cetoglutarato por la enzima glutamato deshidrogenasa o al remover un grupo amino de la glutamina a través de la enzima glutaminasa (PAG). Es importante resaltar que el metabolismo del Glu involucra tanto a neuronas como a células gliales [6, 7].

El Glu ejerce sus acciones al activar receptores específicos de membrana que se han dividido en dos grandes grupos de acuerdo a su mecanismo de transducción de señales. En ese contexto los receptores a Glu se han clasificado en metabotrópicos (mGluRs) e ionotrópicos (iGluRs)[8]. Los primeros son proteínas de siete segmentos transmembranales acopladas a proteínas G, mientras que los receptores inotrópicos son canales iónicos dependientes de ligando.

RECEPTORES DE GLUTAMATO METABOTRÓPICOS

Los receptores mGluRs son receptores activados por Glu y son esenciales para la actividad sináptica[9]. Estos pertenecen a la clase C de la famila de receptores acoplados a proteína G (GPCR), en esta familia también encontramos receptores que son activados por GABA, calcio y sabores dulce y umami [1, 9], pero en lo que concierne a la superfamilia de mGluRs consta de 12 miembros codificados por 8 genes. Estos receptores poseen un domino de unión a ligando extracelular de gran tamaño denominado "*Region flytrap Venus*"[10] y también posee un dominio transmembranal de siete segmentos helicoidales con un sitio de regulación alostérico para los moduladores sintéticos, en conjunto la "Region flytrap Venus" es responsable de la activación de la proteína G (Figura 1). Los mGluRs se pueden clasificar en tres grupos dependiendo de su estructura y actividad fisiológica.

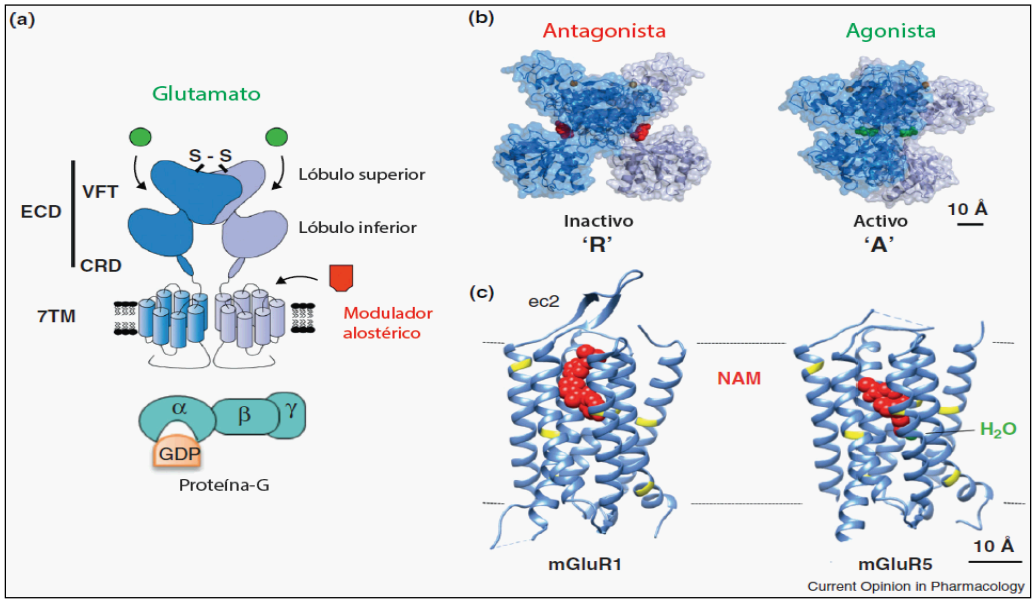

Figura 1 Organización estructural de los receptores metabotrópicos de glutamato y estructuras cristalinas de los dominios de unión de ligando. (a) Ilustración de un dímero mGluR estabilizado por puentes bisulfuro. (b) Dímero ECD en reposo (r; unidos a un antagonista rojo) y conformación activa (a; unidos a un agonista en verde). (c) Estructura de los 7 segmentos transmembranales de los receptores mGluR1 y 5 en complejo con los sitios alostericos de regulación negativa. Los residuos más conservados de observan en amarillo[9]. (ECD: dominio de unión de ligando extracelular, VFT: dominio flytrap venus, CRD: dominio rico en cisteína, 7TM: 7 segmentos transmembranales, NAM: modulador alosterico negativo)

El grupo I está formado por receptores acoplados a proteínas Gq e incluye los receptores mGluR1a-c y mGluR5a-b involucrados en la activación de fosfolipasa C (PLC). La PLC cataliza la conversión de L-3-fosfatidilmioinositol-4,5-bifosfato (PIP2) a inositol-1,4,5-trifosfato (IP3) y diacilglicerol (DAG). Los productos de esta reacción repercuten en la activación de la PKC y la liberación de Ca^{2+} desde el retículo endoplasmico respectivamente[11]. Estos receptores responden a quiscualato y al acido 1-amino-ciclopentano-trans-1,3-dicarboxilico (t-ACPD) además de glutamato.

El grupo II está formado por mGluR2 y mGluR3, que se acoplan a proteínas Gi (esta inhibe a la adenilato ciclasa) reduciendo los niveles de AMPc; responden al agonista (2s, 1'R, 2'R, 3'R)-2-(2,3-dicarboxiciclopropil) glicina (L-CCG-1) y t-ACPD [12].

El grupo III está constituido por los receptores mGLuR4a-b y mGluR6, mGluR7 y mGluR8 y están acoplados a la proteína Gi. Estos receptores también inhiben a la adenilato ciclasa y se caracterizan por ser sensibles a L-2-amino-4-fosfonobutirato (L-AP4) y L-serina-O-fosfato [13].

RECEPTORES IONOTRÓPICOS DE GLUTAMATO

Los receptores ionotropicos de glutamato (iGluRs) se caracterizan por formar un canal iónico que se abre en respuesta a la interacción con un ligando. Se clasifican en tres grupos según su agonista específico: N-metil-D-aspartato (NMDA) que es permeable a Ca^{2+} y Na^{+}. Los receptores de tipo α-amino-3-hidroxi-5-metil-4-isoxazol-propionato (AMPA) son permeables a Ca^{2+} si carecen de la subunidad 2 y permeables a Na^{+} si la poseen. Por último tenemos a los receptores tipo ácido kaínico (KA) que permean a Ca^{2+} y/o Na^{+} dependiendo de las subunidades que lo conforman.

La organización topológica revela cierta similitud entre los iGluRs, como es el caso de la región S1 que forma el domino carboxilo terminal y la región S2 la cual forma una asa reentrante que se ubica entre los dominios transmembranales 3 y 4, estos dos dominios juntos (S1 y S2) forman el sitio de unión al ligando, Adicionalmente en el carboxilo terminal poseen un sitio de

regulación para el transporte de iones a través de la membrana, el cual cuando es fosforilado inhibe el transporte, a este fenómeno se le conoce como desensibilización [14].

Recientemente Avalon y Stern Bach aportaron evidencia de un ensamblaje secuencial de canales tetraméricos de iGluRs como dímeros de dímeros. Primero se forma una dimerización de las subunidades mediada principalmente por la interacción entre dominios N-terminal compatibles (dímeros de monómeros). Esta primera dimerización es seguida por una segunda dimerización más débil entre dímeros, la cual se forma por la compatibilidad de los dominios de unión al ligando y de los dominios transmembranales de las subunidades, permitiendo así la obtención del tetrámero funcional de los iGluRs [15].

La formación de los tetrámeros de los iGluRs deriva de las interacciones combinadas entre los dominios transmembrana junto con las interacciones entre el domino N-terminal y los dominios S1S2 [16].

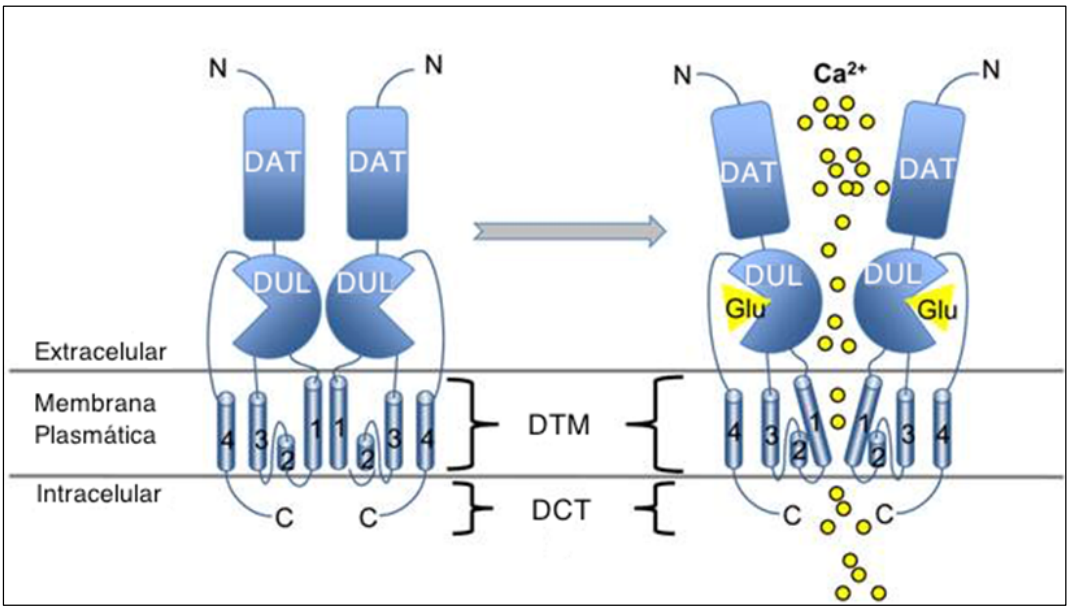

FIGURA 2. Estructura y activación de los iGluRs. Todos los iGluRs comparten la misma estructura básica: Empiezan con el dominio amino terminal (DAT) el cual es seguido por el domino de unión al ligando (DUL), por cuatro dominios transmembranales (DTM, enumerados del 1 al 4) y un dominio carboxilo terminal (DCT). En el Panel A se muestra la conformación natural de los iGluRs en estado de reposo. Solo se muestran dos subunidades, pero la molécula completa consiste en cuatro subunidades las cuales se arreglan de tal forma que crean un canal a través de la membrana plasmática. Ya que se une el Glu (Panel B), ocurre un cambio conformacional en el DTM 1 que permite que se abra el canal por el cual entra el Ca^{2+} o el Na^{+} a la célula por difusión. Modificado de Willard y Koochekpour, 2013 [17].

RECEPTORES AMPA

Estos receptores como su nombre lo indica reconocen y son activados por AMPA, pero también pueden ser activados por el KA aunque con una menor afinidad. Estos receptores están formados por las subunidades GluR1 a 4 que poseen cerca de 900 aminoácidos, comparten alrededor del 70% de identidad y son permeables tanto a sodio como potasio. En general estos receptores son impermeables a Ca^{2+}, pero la ausencia de la subunidad GluR2 hace posible la entrada de iones Ca^{2+} a través de los receptores AMPA [15].

La ausencia de la subunidad GluR2 no es la única manera en que los receptores AMPA puedan permear Ca^{2+}. La falta de edición del aminoácido 607 glutamina (Gln) por arginina en el RNAm produce que los receptores AMPA sean permeables a Ca^{2+}. Dicha edición es realizada por la acción de la adenosina desaminasa, enzima que retira un grupo amino de la adenosina, transformándola en inosina la cual es interpretada como guanosina, por lo tanto el codón de CAG que codifica para glutamina es leído como CGG que codifica para arginina. Esta edición se presenta en el 99.9% de los casos en el organismo adulto por lo que se concluye que la expresión de la subunidad GluR2 dicta la selectividad de los receptores AMPA [18].

RECEPTORES KA

Los receptores KA son activados como su nombre lo indica por el ácido kaínico un análogo del Glu, los cuales están formados por las subunidades GluR5 a 7 y las subunidades KA-1 y KA-2. La afinidad de estos receptores por el KA varía dependiendo de las subunidades que lo conformen y se dividen en dos grupos los de baja afinidad, lo que se refleja en una K_m de 50 nM y están formados por las subunidades GluR5, GluR6 y GluR7 y los receptores de alta afinidad que están formados por las subunidades KA-1 y KA-2 que interaccionan con las subunidades GluR5 y GluR7 y presentan una K_m de 5 nM [15].

Los receptores KA presentan homología en un 35-40% con los receptores AMPA. Las subunidades GluR5-7 presentan 75-80% de identidad entre ellas y se constituyen de alrededor

de 900 aminoácidos, mientras que KA-1 y KA-2 poseen cerca de 970 aminoácidos con un 70% de identidad entre ellas [13].

El sitio de edición Q/R referido en GluR2, también está presente en GluR5 y GluR6, en esta última existen otros cambios de isoleucina por valina y otro de tirosina por cisteína, en todos los casos favorecen la permeabilidad a Ca^{2+}; así los homodímeros GluR6 son permeables a este ión.

RECEPTORES NMDA

Los receptores NMDA se caracterizan por responder de manera lenta en comparación con los receptores AMPA y KA [19]. La respuesta lenta al Glu se debe a que estos receptores se inactivan en presencia de magnesio (Mg^{2+}) y requieren una despolarización de la membrana para liberar esse ion y permitir de esta manera su activación. Esta despolarización es aportada por el efecto de los receptores AMPA y KA que poseen una respuesta rápida al estímulo con Glu [19].

Los receptores NMDA son altamente permeables a Ca^{2+}, Na^{+} y K^{+}; están conformados como heterómeros que contienen las subunidades NR1 y NR2 (NR2A-NR2D), y en algunos casos la subunidad NR3 (NR3A y NR3B). Las subunidades NR2 comparten 38-53% de identidad en su secuencia de aminoácidos y cerca del 72% de homología con NR1. Las subunidades NR3 comparten aproximadamente 50% de identidad aminoacídica, y cerca del 27% con las subunidades NR1 y NR2. Las subunidades NR2 son funcionales si se expresan conjuntamente con las NR1. Cada subunidad consta de 938 aminoácidos. En cuanto al sitio de edición del RNA mensajero (mRNA) Gln/Arg, los receptores NMDA presentan Asn, lo que controla la permeabilidad a Ca^{2+} y el bloqueo por Mg^{2+}. Cuando el residuo Asn es reemplazado por Gln se reduce tanto la permeabilidad a Ca^{2+} como el bloqueo por Mg^{2+}, mientras que el cambio de Asn por Arg abate ambas características [13]. Los receptores NMDA requieren de co-agonismo por glicina o D-serina, los cuales se unen a la subunidad NR1, mientras que el Glu se une a la subunidad NR2 [20].

TRANSPORTADORES DE GLU

La captura del neurotransmisor es uno de los aspectos más importantes en la transmisión sináptica, tal es el grado de importancia que la existencia de un sistema de captura específico es uno de los requisitos para que una sustancia deba de cumplir para que sea considerada como neurotransmisor. En el caso del Glu, su remoción es llevada a cabo por proteínas transportadoras que usan el gradiente electroquímico a través de la membrana plasmática[21].

Los transportadores de Glu se expresan tanto en neuronas como en células gliales. Algunos de esos se encuentran en membrana plasmática y otros intracelularmente. Los transportadores de Glu se clasifican en dos tipos: transportadores de Glu independientes de Na^+ o de baja afinidad con una K_m>500µM y transportadores de Glu acoplados a Na^+ y K^+ de alta afinidad con una K_m=1-100µM, también llamados transportadores de aminoácidos excitadores (EAATs) [21].

Existe un sistema de nomenclatura general para los sistemas de transporte de membrana. De acuerdo con este esquema los sistemas de transportadores dependientes de Na^+ se nombran con letras mayúsculas (A, L, ASC, X, por nombrar algunos), mientras que los sistemas independientes de Na^+ se nombran con letras minúsculas. El código de una letra utilizado para los transportadores de aminoácidos dicarboxílicos es X. La carga del aminoácido transportado se indica con + o – superíndice. Las letras A, G o C subíndices describen al sustrato preferencial aspartato, Glu o cisteína respectivamente. Por lo que en el cerebro los transportadores de Asp/Glu dependientes de Na^+ son referidos como X-AG, mientras que los intercambiadores de Glu-cisteina independientes de Na^+ son llamados x+CG[21].

Los transportadores de Glu de baja afinidad poseen valores de afinidad bajos (cercanos a 500 µM) por su ligando[22] y es un sistema independiente de Na^+ y es inhibido por D-Glu y L-homocisteico. Se ha sugerido que este sistema de captura está diseñado para suplir las demandas metabólicas de aminoácidos en las células cerebrales, pero la investigación al respecto es limitada y poco se sabe acerca de ellos.

Se han clonado 5 tipos de EAATs en el humano. Estos transportadores poseen una localización celular específica y la localización de estas dentro del SNC. Los transportadores EAAT1 y EAAT2

se encuentran predominantemente en glía y son los trasportadores más abundantes en el SNC, estos son los responsables de capturar alrededor del 80% del Glu, en este sistema. Los transportadores EAAT3, EAAT4 y EAAT5 tiene una expresión preferencial en neuronas y solo capturan el 20% del Glu extracelular.

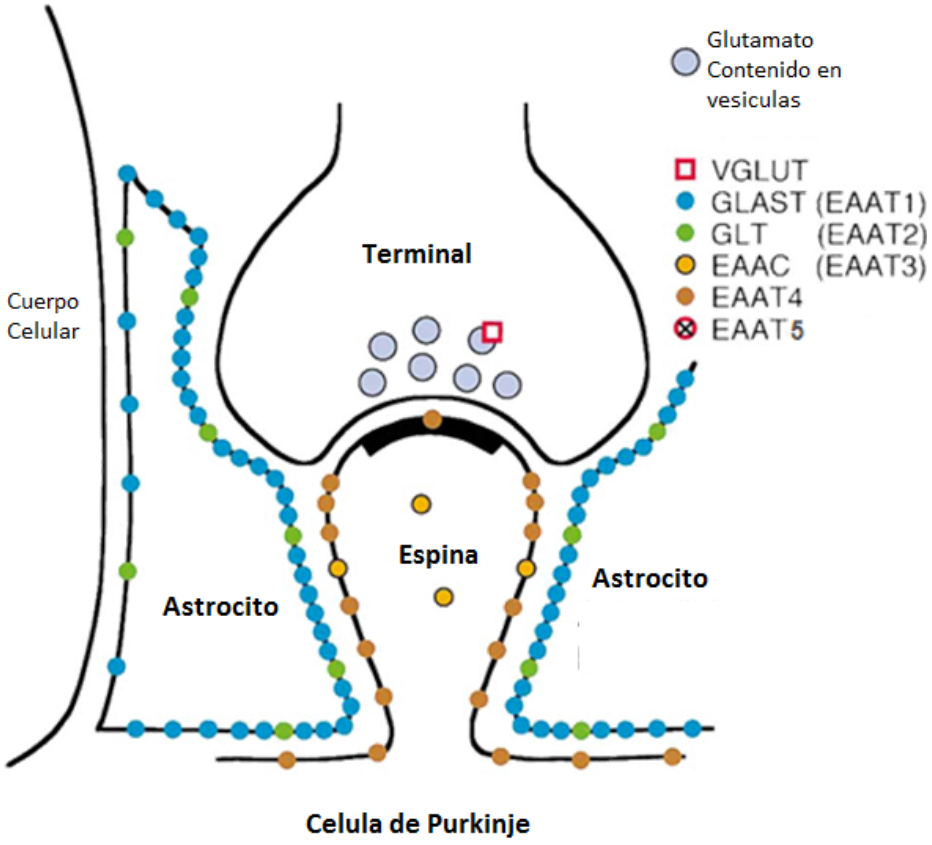

Figura 3. Esquema detallado de la localización de los transportadores de Glu en la sinapsis glutamatérgica [21]

Los transportadores de Glu se encuentran altamente regulados, principalmente por la fosforilación de proteínas accesorias lo cual modula el tráfico de los transportadores desde compartimientos intracelulares hacia la membrana plasmática y su endocitosis [21]. En células gliales de Bergmann (CGB) y astrocitos, la regulación de los transportadores de Glu parece ser tanto dependiente como independiente de los mGluRs e iGluRs, mediante la activación de cascadas de señalización que implican proteínas tales como la proteína cinasa dependiente de Ca^{2+} y diacilglicerol (PKC)[23] y la proteína cinasa dependiente de AMP cíclico (PKA)[24].

EL proceso de captura del Glu por los transportadores es un proceso electrogénico generado por el gradiente iónico de Na^+ y K^+, mientras el K^+ es esencial para el transporte, el Na^+ es necesario para la unión del Glu con el transportador. La estequiometria del transporte es: 1 molécula de Glu es transportada junto con 3 iones Na^+ y un protón (H^+), mientras que el ion K^+ es transportado fuera de la célula [21]. Este proceso también puede ocurrir de manera inversa y se le conoce como transporte reverso.

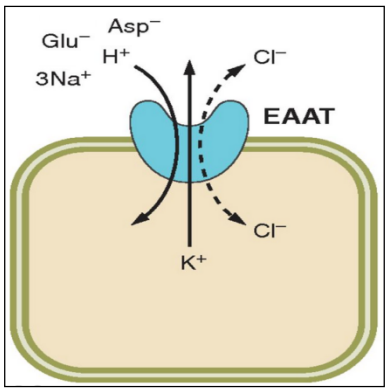

Figura 4. Estequiometria del influjo iónico acoplado al transporte de glutamato. Los EAATs están acoplados a un cotrasporte de $3Na^+$ y $1H^+$ seguido de un antiporte de $1K^+$

TRANSPORTADORES DE GLUTAMINA

La Gln es el aminoácido más abundante en el SNC y está involucrada en muchos procesos biosintéticos. Distintos transportadores de membrana que difieren en el mecanismo de transporte, regulan la homeostasis de Gln al coordinar su absorción, reabsorción y liberación en distintos tejidos. Estos transportadores pertenecen a distintas familias proteicas, son redundantes y ubicuos. Su clasificación, originalmente se basó en sus propiedades funcionales, recientemente ha sido asociado a la nomenclatura SLC (Familia de transportadores de solutos). Mucho de los estudios de estos transportadores se han realizado en sistemas de expresión heterólogos, debido a su complejidad.

La función de los transportadores de Gln está asociada a su forma de transportar y su acople a Na^+ y H^+. La mayoría de los transportadores no son específicos a Gln sino que pueden transportar otros aminoácidos neutros. Se han clasifican en 4 sistemas de transportadores ASC, L, N, y A.

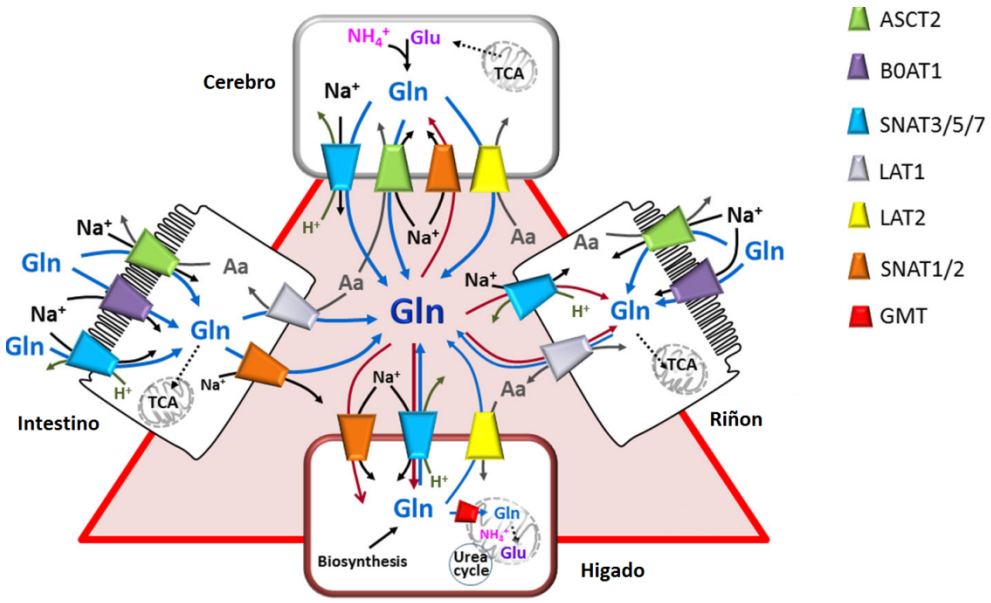

Figura 5. Sistema de Transportadores de Glutamina. Distribución simplificada de la expresión de los distintos transportadores de Gln[25]

SISTEMA ASC

La familia de transportadores ASC (alanina, serina y cisteína) posee dos miembros ASCT1 y ASCT2 que son codificados por los genes SLC1A4 y SLC1A5 respectivamente. Aunque ambos transportadores son expresados en el sistema nervioso central, ASCT2 es de expresión exclusiva glial mientras que ASCT1 se expresa preferentemente en neuronas [26]. El ASCT2 se expresa en astrocitos y posee una mayor afinidad para transportar Gln el ASCT1[27].

El sistema de transportadores ASC, tiene una funcionalidad optima a pH 8[28], tanto ASCT1 y 2 son intercambiadores obligados de aminoácidos dependientes de un gradiente de Na^+ pero insensibles a las concentraciones de K^+[29], esa insensibilidad a las concentraciones de K^+ es clave para que estos transportadores solo funcionen como intercambiador y no induzcan un flujo neto de aminoácidos [30, 31].

El sistema ASC se encuentra expresado de manera abundante en etapas tempranas del desarrollo en el sistema nervioso central, por lo cual se especula que cumple con un rol de importancia durante estas etapas [32]. Aunque la información disponible sobre su regulación es

escasa se sabe que la misma Gln tiene un papel en la regulación de este transportador[33]. Como es común en los transportadores la principal forma de regulación es la translocación de membrana, las señales de translocación son iniciadas por insulina y IGF al activar a sus receptores correspondientes. Lo cual lleva a la activación de PI3K y esta a su vez activa a PKB y SGK[33]. La translocación de membrana de estos transportadores es dependiente de PI3K y la estabilidad es dependiente de Rho GTPasa [34].

SISTEMA L

Entre los sistemas de transportadores de Gln el primero en ser descrito fue el sistema L. Este sistema tiene una preferencia a capturar leucina y es el único sistema de transporte de Gln independiente de Na^+ y pH. Este sistema está compuesto por dos integrantes LAT1 y LAT2. Estas proteínas comparten el 50% de homología entre ellas, LAT1 es una proteína de 507 aminoácidos y LAT2 de 535 aminoácidos. Se expresan principalmente en riñón, placenta, cerebro, bazo, ovarios y testículos [35, 36].

De igual manera que el sistema ASC el sistema L funciona intercambiando nucleótidos, con ello equilibra las concentraciones de Gln y otros aminoácidos en las pozas celulares [37].

Los transportadores LAT1 y LAT2 necesitan formar heterodimeros con 4F2hc para facilitar su translocación a membrana, esta unión obligada no repercute en su afinidad por sus sustratos, ni parece tener algún efecto sobre su regulación [38]. Aunque estos dos transportadores de aminoácidos funcionan de manera muy similar poseen una diferencia en cuanto a la preferencia de sustratos, mientras LAT1 prefiere aminoácidos neutros voluminosos LAT2 prefiere los aminoácidos pequeños. Las constantes de afinidad de LAT1 por sus sustratos varían de 5 a 50 µM mientras que la K_M de LAT2 por sus sustratos van desde 0.2 a 1mM [37]. De igual manera su regulación es distinta mientras LAT1 es regulado a la alta en situaciones de altos niveles de insulina de manera dependiente de mTORC1 [39], LAT2 es regulada positivamente por inducción de citosinas pro inflamatorias de manera dependiente de mTORC1 [40]. LAT2 también puede ser regulado por EGF de manera dependiente de ERK1/2 [41].

SISTEMA A

El sistema A de captura de Gln fue descrito en 1965 y fue definido como la porción de transportadores bloqueados por el ácido α-(metil) isobutirico (MeAIB) [36, 42]. El sistema A está conformado por tres proteínas que son SNAT1, 2 y 4. Aunque la expresión del sistema A es ubicua, los transportadores SNAT1 y 2 tienen una expresión preferencial en el cerebro [43]. SNAT1 es altamente expresado en el cerebelo, tálamo, bulbo olfatorio, en menor medida se expresa en la corteza cerebral y el estriado. SNAT2 tiene una alta expresión en el bulbo olfatorio e hipocampo y una moderada expresión en el tálamo, corteza cerebral y el estriado. Estos transportadores se expresan principalmente en las terminales presinápticas de neuronas [44].

El mecanismo de transporte de este sistema es electrogénico, transporta un ion Na^+ por cada aminoácido transportado, la disminución de pH inhibe la su capacidad de transporte, pero no es necesario el antiporte de H^+ para catalizar el flujo de aminoácidos [45]. SNAT1 posee una K_M por Gln de 498 μM mientras que SNAT2 posee una K_M por glutamina de 1.65 mM [46]. Es importante señalar que estos transportadores pueden exportar o importar su sustrato dependiendo de las concentraciones de Na^+ intra y extra-celular[46].

La regulación de estas proteínas no se ha caracterizado completamente, en el caso de SNAT1 se sabe que su expresión es estimulada por PKA [47]. SNAT2 se regula por deprivación de sustrato ocasionando un aumento de su actividad y expresión [48].

SISTEMA N

El sistema N de transportadores de Gln difiere mucho al resto de transportadores, ya que este sistema posee una pequeña gama de sustratos que puede transportar la cual se limita a Gln, Asp e His, todos estos sustratos contiene nitrógeno en sus respectivas cadenas laterales, lo que dista mucho a los demás sistemas, que poseen un alto grado de promiscuidad en cuanto al tipo de sustrato que pueden transportar [49].

Los transportadores SNAT3, SNAT5 y SNAT7 son los integrantes del Sistema N. SNAT3 se expresa principalmente en el hígado, musculo esquelético, riñón, páncreas y en el cerebro [50, 51].

SNAT5 se expresa en el estómago, cerebro, hígado, pulmones, colon riñón y en el intestino delgado[52]. Por último la expresión de SNAT7 es ubicua se expresa en todos los tejidos[53]. En el caso particular del SNC, la expresión de los transportadores SNAT3 y SNAT5 se exclusiva de las células gliales [25, 54].

En términos generales el transporte de Gln por parte del sistema N esta acoplado al influjo de dos iones Na^+ y un H^+. SNAT3 y SNAT5 son los únicos miembros de este sistema que pueden tolerar el remplazo del ion Na^+ por el ion Li^+[49, 53]. El pH óptimo para su realizar el transporte de aminoácidos neutros oscila entre 6 a 8 [55]. La afinidad por su sustrato de este sistema oscila entre 0.7-1.5mM, y siendo transportadores de la súper familia SLC, su regulación es dada principalmente por translocación a membrana. En el caso de SNAT3 se ha descrito que en S52 posee un sito consenso de fosforilación para PKCα el cual modula su inserción a membrana, este sitio de fosforilación solo tiene efecto sobre su translocación de membrana y en lo absoluto afecto su afinidad por su sustrato. Debido a que este transportador depende de la concentración Na+ para llevar acabo su transporte a aminoácidos, es capaz de capturar o liberar Gln en función de la concentración intracelular o extracelular que se presenten.

Sistema ASC	Sistema A	Sistema L	Sistema N
Depende de Na^+	Depende de Na^+	Independiente de Na+	Depende de Na+ Antiporte H^+
Prefiere aminoácidos de cadena corta	Prefiere aminoácidos de cadena corta	Prefiere aminoácidos voluminosos y de cadena ramificada	Transporta Gln, Asn, His
Sensibles a cambios de pH	Sensibles a cambios de pH	Insensible a cambios de pH	Sensibles a cambios de pH
Thr, Ala, Ser, Cys,	Reconoce a MeAIB, Pro	Leu, Ile, Phe	
Intercambiador de aminoácidos	Transportador de aminoácidos	Intercambiador de aminoácidos	Transportador de aminoácidos
ASCT1 (Neurona), ASCT2(Glia)	SNAT1, SNAT2, SNAT4 (Neurona)	LAT1, LAT2 (Neurona y glia)	SNAT3, SNAT5 (Glia)

Tabla1. Sistemas de captura de Gln. Tabla en que se resumen las principales cualidades de los cuatro sistemas de captura de Gln

CÉLULAS GLIALES

Las células gliales son las células más abundantes del SNC en una relación de 10:1 con respecto a las neuronas. A pesar de su abundancia esta estirpe celular había sido relegada a una función pasiva, de mantenimiento de la neurotransmisión y regulación del microambiente neuronal. Investigaciones recientes han demostrado que las células gliales también participan activamente en las funciones cerebrales y procesamiento de la información [56].

Estas células las podemos subdividir en 3 grupos principales dentro del SNC: oligodendrocitos, microglia y astrocitos. Esta clasificación se fundamenta en diferencias morfológicas, ubicación y función que desempeñan [57].

Los oligodendrocitos son células que envuelven los axones de las neuronas del SNC mediante una capa rica en lípidos denominada mielina, la cual acelera la conducción de impulsos eléctricos durante la neurotransmisión. En el sistema nervioso periférico (SNP) existen células gliales con la misma función denominadas células de Schwann [56].

Las células de microglia se caracterizan por tener un cuerpo celular pequeño (≤3 µm de diámetro), además no provienen de una estirpe neuronal. La función más importante de estas células es actuar como fagocitos al eliminar las células muertas y desechos del SNC. También están implicadas en la remodelación de la sinapsis durante el desarrollo del sistema nervioso y se ha sugerido que participan en la regulación del ambiente iónico de las neuronas.

Los astrocitos se caracterizan morfológicamente por proyectar una gran cantidad de procesos. Se ha encontrado que los astrocitos cumplen una amplia variedad de funciones. Contribuyen a la homeostasis en el cerebro proporcionando energía a las neuronas, ya sea en forma de glucosa o lactato y suministrando sustancias necesarias para la neurotransmisión, de igual manera también proporcionan una barrera física entre la conexión sináptica de neuronas vecinas. Los astrocitos son los responsables de terminar la acción de los neurotransmisores liberados por las neuronas al remover al neurotransmisor del espacio extracelular. Por estos y otras funciones astrocíticas, se cree que modulan la función sináptica mediante comunicación bidireccional con las neuronas [56].

CÉLULAS GLIALES DE BERGMANN

La glía de Bergmann es un tipo de glía radial que podemos encontrar en un individuo adulto en el cerebelo. Estas células no sufren la denominada transformación astrocítica posterior al nacimiento[58]. Los procesos de estas células rodean las sinapsis glutamatérgica establecida entre las fibras paralelas y las células de Purkinje.

Debido a que las células de Purkinje integran gran cantidad de señales generadas en la corteza del cerebelo, las células gliales de Bergmann (CGB) adquieren una importancia central para la salida de información en este sistema.

Las CGB pueden responder de manera activa al Glu debido a que presentan receptores inotrópicos del tipo NMDA (NMDAR1 y NMDAR2), KA (iGluR5-7) y AMPA (iGlu1, iGlu3 e iGlu4). También expresan receptores metabotrópicos del Grupo I (mGluR1 y mGluR5) y del Grupo III (mGluR4, 6 y 7) [59]. Estas células expresan de manera casi exclusiva al transportador de Glu/Aspartato (GLAST) [60].

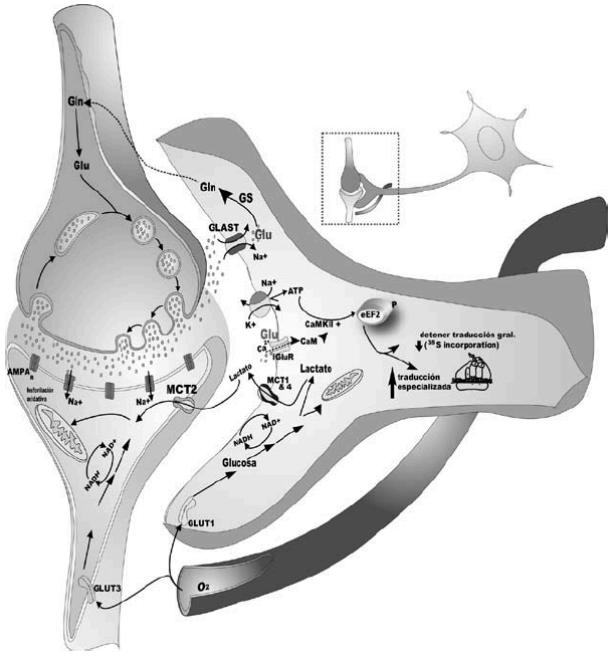

Figura 6. Arquitectura de las sinapsis establecidas por las células de purkinje y las fibras paralelas, se observa que rodeando de esta sinapsis se encuentra las CGB [58].

EL GLUTAMATO Y SU EFECTO SOBRE LAS CÉLULAS GLIALES DE BERGMANN

La activación de los receptores glutamatérgicos cambia la fisiología celular a corto, mediano y largo plazo. En CGB se ha demostrado que el Glu a tiempos cortos provoca un influjo de iones que regulan múltiples procesos celulares, a mediano plazo se regulan las modificaciones post-traduccionales como fosforilación, acetilación, entre otras [61], además de la regulación traduccional; en estudios recientes se demostró que a los 15 minutos del tratamiento con Glu, este incrementa siete veces el tiempo de transito ribosomal [62], disminuyendo así la síntesis global de proteínas, esto favorece la traducción de proteínas con mRNAs con estructuras complejas en su 5'UTR tales como la glutamina sintetasa.

En CGB se ha demostrado que el Glu regula la transcripción de diversos genes, entre los cuales se encuentran kbp*, oct-2,* y glast [61, 63, 64]; en células gliales se demostró que estímulos prolongados con Glu, provocan un aumento en la expresión del transportador GLAST, y una disminución de la expresión del transportador de Glu 1 (GLT-1). Adicionalmente se ha demostrado una regulación positiva en la secreción de neurotrofinas, principalmente el factor neurotrófico derivado de cerebro (BDNF), dependiente de Glu [65].

CICLO GLUTAMATO/GLUTAMINA

La neurotransmisión glutamatergica excitadora se caracteriza por la liberación sináptica de Glu, que es predominantemente capturada por los astrocitos y es convertida en Gln, la cual subsecuentemente es transferida de regreso a la neurona glutamatergica. Este proceso involucra a los transportadores de Glu de alta afinidad, a la glutamina sintetiza así como a los transportadores de Gln por parte de los astrocitos y por parte de la neurona tenemos la participación de la glutaminasa activada por fosfatos (PAG) [21, 66].

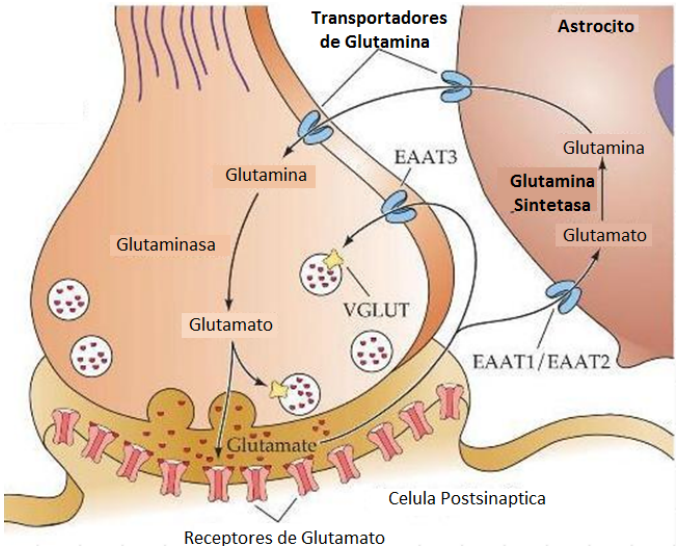

Figura7. Esquema simplificado del Ciclo Glutamato/Glutamina. Se muestra una terminal sináptica y los distintos pasos para el reciclamiento del Gln, se excluye el ciclo del TCA.

Es importante enfatizar que el ciclo Glu/Gln no opera con una estequiometria 1:1, esto porque el Glu puede ser oxidado en astrocitos y metabolizado en el ciclo de Krebs en orden de obtener energía adicionalmente de ser convertido a Gln[7, 67, 68]. Aunado a esto, parte de la Gln también puede ser oxidada en las neuronas después de ser convertido a Gln e ingresar al ciclo del TCA como α-cetoglutarato. Para la completa oxidación a CO_2 del esqueleto de carbono del Glu, es necesaria la salida del ciclo del TCA en el paso de malato a oxalacetato, para ser convertido a piruato y subsecuentemente reentrar en forma de acetil-CoA. Esta parte del reciclamiento del piruato se ha reportado en el cerebro de ratas. Bajos niveles de reciclamiento de piruvato se han reportado en astrocitos y neuronas en cultivo celular [69]. Cabe mencionar que en el desarrollo se han reportado niveles elevados de reciclamiento de piruvato y es relevante resaltar que este proceso se ve incrementado en casos de hipoglucemia[70].

En el ciclo Glu/Gln existe una gran información acerca de la participación de los transportadores de Glu y de la glutamina sintetasa así como las vías alternas por las cuales se puede metabolizar el Glu. Para la evidencia de los transportadores de Gln su participación y su identidad aún son desconocidas, por lo cual en este trabajo nos enfocamos primeramente a caracterizar, la función y mecanismo por el cual los transportadores de Gln llevan a cabo el reciclamiento del Glu.

JUSTIFICACIÓN

Existe evidencia de la importancia de la Gln en la neurotransmisión, a pesar de esto hasta la fecha no se ha caracterizado el transporte de Gln, en las células gliales de Bergmann

OBJETIVO GENERAL

Caracterizar la captura de Gln dependiente del sistema N (SNAT3/5) en células gliales de Bergmann

OBJETIVOS ESPECÍFICOS

- Demostrar le expresión de SNAT3 en células gliales de Bergmann
- Caracterizar el sistema de captura de Gln en CGB
- Estudiar la relación entre la captura de Asp y la captura de Gln
- Caracterizar el proceso de eflujo de Gln en células gliales de Bergmann
- Identificar la interacción de SNAT3 con otras proteínas
- Analizar el efecto de Glu y Gln en la interacción proteína-proteína de SNAT3

MATERIALES Y MÉTODOS

MATERIAL BIOLÓGICO

Embriones de pollo de 10 días donados por Avi-Mex S.A. de C.V. se mantuvieron en incubación a 37°C hasta la elaboración del cultivo primario de CGB. Los experimentos se llevaron a cabo de acuerdo a las normas internacionales sobre el uso ético de animales.

REACTIVOS

Los reactivos para la elaboración del cultivo primario se compraron a Gibco Invitrogen. Los reactivos para geles de acrilamida/bisacrilamida e inmunodetección en fase solida se adquieren de Bio-Rad (Hercules, CA). Los anticuerpos anti-GLAST y KBP policlonales se produjeron y caracterizaron en el laboratorio. Los anticuerpos anti-SNAT3 fueron comprado en Santa Cruz, CA, USA, el anticuerpo anti-calbindina fue comprada de Sigma-Aldrich, St. Louis, MO USA. Se usaron a una dilución 1:1000. Los anticuerpos anti-conejo policlonal conjugado y acoplado a peroxidasa se compraron al Laboratorios Amersham Biosciences (Buckinghamshire, UK). Todos los reactivos utilizados para la realización de las técnicas son de Sigma (St. Louis, Mo, USA) o Tocris-Cookson (St. Louis, Mo, USA). [^{3}H]-L-Gln (50.3Ci/mmol actividad específica), [^{3}H]-D-Asp (11.3Ci/mmol actividad específica) fueron compradas de Perkin Elmer (Waltham, MA, USA).

CULTIVOS PRIMARIOS DE CÉLULAS DE BERGMANN

Los cultivos primarios de glía de Bergmann son preparados de acuerdo al protocolo descrito por Ortega y colaboradores (Ortega et al. 1991) a partir de cerebelos de pollo de 14 días diseccionados y homogenizados enzimática y mecánicamente, sembrados a una densidad aproximada de 8X10^5 células/mL, utilizando por pozo 3.5mL de Medio Opti-MEM® (Medio modificado del suero mínimo de Eagle) (GIBCOTM) suplementado con 2.5% de suero fetal bovino (GIBCOTM) y 50µg/ml de gentamicina. Se incuba a 37°C en una atmosfera con 5% de

CO^2, hasta que la monocapa de células alcanza una confluencia de 80-95%. La pureza de los cultivos es evaluada por la expresión de la proteína de unión a kainato (KBP), que es específica de glía de Bergmann (Somogyi et al., 1989)

EXTRACTOS DE PROTEÍNAS DE CÉLULAS GLIALES DE BERGMANN

Antes de cualquier tratamiento, la monocapa de CGB se le cambió el medio por una solución reguladora de ensayo (HEPES 25 mM, NaCl 130 mM, KCl 5.4 mM, $MgCl_2$ 0.8 mM, Na_2HPO_4 1 mM glucosa 33.3 mM, CaCl2 1.8 mM; pH=7.4 ajustado con TRIS base 1 M) durante 2 horas. Después de que las células fueron tratadas con un estímulo de Glu (1 mM) a diferentes tiempos (0, 5, 10, 15, 30, 60 minutos) o a diferentes concentraciones (0.0001 mM, 0.001 mM, 0.01 mM, 0.1 mM, 1 mM), las células fueron cosechadas mecánicamente, en PBS con inhibidores de fosfatasas y proteasas (Tris-HCl 20 mM pH 7.4 con 2 mM de EGTA, 316 mM NaCl, 2mM de Na_3Vo_4, 0.5 mM de PMSF, 50 µg/ml de aprotinina y 50 µg/ml de leupectina).

Posteriormente se procedió a la lisis celular, en este punto se ocuparon dos métodos, uno para la obtención de extractos totales y otro para la obtención de extractos membranales. Para los extractos totales después de los pasos anteriores, se centrifugaron a 13,000 rpm por 5 min, se retiró el sobrenadante y se resuspendió en una solución de lisis celular (RIPA 500ml, EGTA, 1mM de EDTA, 1mM de PMSF, 20mM de $NaVO_4$, 0.1% NP-40, 0.25% NaDOX, 50µg/ml de aprotinina y 50µg/ml de leupectina). Los extractos se cuantificaron por el método de Bradford (Bradford, 1976).

Para obtener los extractos membranales, nuevamente se centrifugó a 13,000 rpm por 5 min, paso seguido se resuspendió en una solución de TRIS-HCl 50 mM pH 7.5 más inhibidores de proteasas y fosfatasas (Tris 50 mM, NaF 20 mM, NaMoO 10 mM, $NaVO_4$ 1 mM, 50 µg/ml de aprotinina y 50µg/ml de leupectina), luego se congeló a -70°C toda la noche. Al día siguiente se descongelaron las muestras y se realizó la cuantificación de proteínas por el método de Bradford (Bradford, 1976), después se centrifugaron las muestras por 5 min a 13,000 rpm, el sobrenadante fue descartado y la pastilla fue resuspendida en 200 µl de buffer de fosfatos 0.5

M pH 7.0, 20% glicerol (p/V), Tritón X-100 1% (p/v) con 0.1 mM de PMSF y 1.0 mM de EDTA. Se agitó por 2 horas, para luego centrifugarlo nuevamente a 13,000rpm por 5 min y obtener de esta manera el sobrenadante el cual contenía a las proteínas de membrana.

Teniendo los extractos membranales o totales de las células, se resuspendieron en solución reguladora de muestra (Tris-HCl 0.5M pH 6.8, SDS 6%, 50mM de β-mercaptoetanol, 50mM de Ditrioteitol, 3% de azul de bromofenol y 30% de glicerol) y se colocaron en baño de agua a ebullición por 5 minutos.

INMUNODETECCIÓN EN FASE SÓLIDA

Los extractos totales normalizados por el contenido de proteína se desnaturalizaron y diluyeron 1:3 en buffer de muestra (187.5 mM Tris-HCl pH6.8, 6% dodecil sulfato de sodio (SDS), 30% glicerol, 5% ß-mercapto etanol, 0.03% azul de bromofenol, 2mM DTT Ditiotreitol) y se hirvieron en baño maría durante 5 minutos. Los extractos así preparados se analizaron por electroforesis en geles de poliacrilamida al 6-10% en presencia de dodecil fosfato de sodio (SDS-PAGE) y se transfirieron a una membrana de nitrocelulosa en cámara húmeda (Bio-Rad). Los blots se tiñeron con rojo de Ponceau para confirmar que el contenido de proteína fuera igual en todos los carriles. Las membranas se destiñeron dando dos lavados con agua bidestilada y un tercero con PBS. Los sitios irrelevantes se cubrieron por incubación de las membranas durante una hora a temperatura ambiente con solución de bloqueo: TBS (0.2 M Tris-HCl y 1.36 M NaCl), 5% de leche en polvo semidescremada y 0.1% Tween 20. Después de un breve lavado con TBS-T las membranas se incubaron con el anticuerpo primario indicado en cada figura a una dilución de 1:1000 en solución de anticuerpos (TBS, 0.25% BSA, 0.1% Tween-20 y 0.01% Timerosal) durante toda la noche a 4°C. Las membranas se lavaron tres veces con solución TBS/Tween en un agitador orbital y se incubaron durante 2 horas con anticuerpo secundario acoplado a peroxidasa de rabano en una dilución 1:4000 a temperatura ambiente. Las membranas así tratadas se lavaron 2 veces con TBS/Tween. Después de lavar las membranas, se adicionaron a las membranas el reactivo de quimioluminicencia Amersham como sustrato de la peroxidasa de

rábano, la cual cataliza la oxidación de luminol en presencia de peróxido de hidrógeno emitiendo luz. Las bandas relevantes se detectaron por auto radiografía y se examinó la intensidad de la señal. Se realizaron los análisis densitométricos con ayuda del programa ID Image Analysis Software (Kodak Coorporation, USA) y los datos se analizaron con el Software GraphPad, Prism (San Diego, CA, USA).

ENSAYOS DE LIBERACIÓN DE [^{3}H]-L-GLN

A monocapas confluentes de CGB sembradas en cajas de cultivo celular de cajas Petri P60, se les cambió el medio extracelular por 1 mL de medio de ensayo (HEPES 25mM, NaCl 130 mM, KCl 5.4 mM, $MgCl_2$ 0.8 mM, Na_2HPO_4 1 mm glucosa 33.3 mM, CaCl2 1.8 mM; pH=7.4 ajustado con TRIS base 1M) con 0.4 µL de [^{3}H]-L-Gln, por un lapso de tiempo de una hora se dejó incubar las células en el ensayo. Transcurrida la hora por diez min se dieron lavados cada minuto con 1 mL de medio de ensayo para remover el exceso de radiactividad en el medio. Después de los diez primeros lavados se cambió el medio de ensayo diez veces más pero en esta ocasión fue cada dos minutos, todas las fracciones hasta este punto fueron desechadas. Cuando se desechó la décima muestra, se colectó el sobrenadante cada dos minutos durante quince ocasiones, en la quinta a la décima se colocó el estímulo, se colectó el sobrenadante cada 2 min cinco veces más después del estímulo, para posteriormente lisar las muestras con NaOH 0.1 N. A cada una de las fracciones recolectadas se les agregó 8 µL de líquido de centelleo y 50 µL de ácido acético, y se llevaron a un contador de centelleo.

ENSAYOS DE CAPTURA DE [^{3}H]-L-GLN

Monocapas confluentes de CGB sembradas en cajas de cultivo celular de 24 pozos se lavaron tres veces para remover las células no adheridas con 0.5 mL de solución de ensayo. La captura de [^{3}H]-L-Gln se inició en el tiempo cero por la adición de 0.250 mL de solución de ensayo que contenía 0.4 µL de [^{3}H]-L-Gln y los competidores a una concentración establecida si fue el caso.

Cuando se utilizaron inhibidores, se adicionaron 30 minutos antes de empezar con los ensayos de captura de [^{3}H]-L-Gln. La captura se terminó por aspiración del medio radiactivo y se lavó cada pozo por 15 seg con 250 µL de la solución de ensayo. Las células de los pozos se expusieron por dos horas a 37°C en 250 µL de NaOH 0.1 M y se les agregaron 50 µL de ácido acético y 5 mL de solución de centelleo. Se detectó la radioactividad en un contador de centelleo Beckmann 7800LS. Los experimentos se realizaron por cuadruplicados.

ENSAYOS DE CAPTURA DE [^{3}H]-D-ASP

Monocapas confluentes de CGB sembradas en cajas de cultivo celular de 24 pozos se lavaron tres veces para remover las células no adheridas con 0.5 mL de solución de ensayo. La captura de [^{3}H]-D-Asp se inició en el tiempo cero por la adición de 0.250 mL de solución de ensayo que contenía 0.4 µL de [^{3}H]-D-Asp y el estímulo a una concentración establecida si fue el caso. Cuando se utilizaron inhibidores, se adicionaron 30 minutos antes de empezar con los ensayos de captura de [^{3}H]-D-Asp. La captura se terminó por aspiración del medio radiactivo y se lavó cada pozo por 15 seg con 0.25 ml de la solución de ensayo. Las células de los pozos se expusieron por dos horas a 37°C en 250 µL de NaOH 0.1 M y se les agregaron 50 µL de ácido acético y 5 mL de solución de centelleo. Se detectó la radioactividad en un contador de centelleo Beckmann 7800LS. Los experimentos se realizaron por cuadruplicados.

ENSAYOS DE INFLUJO DE $^{45}Ca^{2+}$ EN CÉLULAS GLIALES DE BERGMANN

Monocapas confluentes de CGB sembradas en pozos de 24 se lavaron tres veces para remover las células no adheridas con 0.5 mL de solución de ensayo. El influjo inducido por glutamato o [^{3}H]-D-Asp se inició en el tiempo cero por la adición de 0.5 mL de solución de ensayo, conteniendo glutamato o D-Aspartato a la concentración deseada. Cuando se probaron los inhibidores, se adicionaron 30 minutos antes de empezar con los ensayos de influjo de $^{45}Ca^{2+}$. La reacción se detuvo por aspiración del medio radioactivo y el lavado de cada pozo por 15

segundos con 0.5 mL de la solución de ensayo fría. Las células de los pozos se expusieron por dos horas a 37°C a 250 µL de NaOH 0.1 M y se les agregó 50 µL de ácido acético y 5 mL de solución de centelleo. Y se detectó la radioactividad en un contador de centelleo Beckmann 7800LS. Los experimentos se realizaron al menos tres veces con cuatro repeticiones cada uno.

INMUNOPRECIPITACIÓN DE PROTEÍNAS

Después de realizar los extractos proteicos, estos se colocaron (500 µg de proteína) a interactuar con anticuerpos acoplados a perlas de G-agarosa (100 µL) por un periodo de 8 horas, en un volumen total de reacción de 500 µL. Este acople se realizó en PBS estéril. Las perlas de agarosa se acoplaron con anterioridad al anticuerpo, durante 4 horas 3µL de perlas de agarosa por 1µL de anticuerpo en un volumen total de 100 µL. Después del acople de proteínas con el anticuerpo acoplado a agarosa, se centrifugo a 13,000 RPM por 10 min, se resuspendió en buffer ripa y se repitió el proceso 3 veces. Por ultimo a la pastilla que quedo en el tubo se agregó buffer de ensayo y se hirvió la muestra, en este punto se procedió a realizar una detección en fase sólida.

INMUNOFLUORESCENCIAS

Cultivos primarios de CGB se crecieron en cubreobjetos de vidrio tratados con poli-L-lisina (0.01 mg/mL). Las células se fijaron al exponerse a metanol durante 10 min a -20˚C y se lavaron dos veces con PBS con 0.5% de Triton X-100 (solución de lavado). Para evitar unión inespecífica se incubar los cubreobjetos con 1% de albumina de suero bovino en PBS (solución de bloqueo) durante una hora. Las células se incubaron durante una hora con los anticuerpos primarios anti-SNAT3 en solución de bloqueo a 25˚C. Después las células se lavaron tres veces con solución de lavado y se incubaron con anticuerpos secundarios acoplados a fluoresceína a una dilución 1:100 en solución de bloqueo. Después de lavar tres veces el anticuerpo secundario no unido,

las preparaciones se montaron con Vectashield (Vector Laboratories, Burlingame, CA, EU) y se examinaron con un microscopio de fluorescencia invertido (Zeiss Axioscope 40, Gottingen, Alemania).

INMUNOHISTOQUIMICAS

Cerebelos de pollo de P0 se disectaron y colocaron inmediatamente en PBS frio. El tejido se lavó con PBS frio para remover la sangre y se colocó en PBS con parafolmadehido 4% (pH 7.4) durante una hora. Pasada esta hora el fijador se cambió por nuevo y se dejó el tejido en este a 4˚C durante 48h. Los cerebelos fueron crioprotejidos sucesivamente en 10%, 20% y 30% de sacarosa en PBS y se cortaron sagitalmente a 50 µm usando un criostrato (Microm International GmbH, Walldorf, Alemania). Para la inmunohistoquimica, los tejidos se lavaron abundantemente en PBS para remover el exceso de aldehídos y después se incubaron en una solución de peróxido de hidrogeno al 1.8% durante 10 min para remover la actividad peroxidasa endógena. La unión inespecífica de los anticuerpos se bloqueó al incubar las secciones en solución de bloqueo (3% de suero de cabra en PBS conteniendo 0.3% de Triton) durante 1h a 25˚C. Las secciones se incubaron durante 48h con los siguientes anticuerpos primarios: anti-calbindina (1:5000), anti-KBP (1:2500), y anti-SNAT3 (1:2500) en solución de bloqueo a 4˚C. Las secciones se lavaron tres veces en PBS y se colocaron los anticuerpos secundarios biotinilados (1:1000, Vector Laboratories, Inc. Burlingame, Ca, EU) durante 3 h, para calbindina se usó anti-mouse, para KBP anti-rabbit y para SNAT3 anti-cobayo. Pasadas las 3h las secciones se incubaron con peroxidasa de rabano acoplada a avidina (1:250, Vector Labs). Los complejos anticuerpos-peroxidasa se revelaron con una solución que contenía 0.05% diaminobenzidina, sulfato de niquel (10 mg/mL; Fisher Scientific, Pittsburg, PA, EU), cloruro de cobalto (10 mg/mL; Fisher Scientific), y 0.01% de peróxido de hidrogeno, lo que produce un precipitado negro-purpura. Las secciones se montaron en cubreobjetos preparados con gelatina, dehidratados y limpiados en Hemo-De (Fisher Scientific); después se colocaron con Permount. Las secciones se analizaron en un microscopio BX41 Olympus.

ANÁLISIS ESTADÍSTICO

Los datos se expresaron como el promedio ± el error estándar. Se realizó un análisis de varianza de una via (ANOVA) para determinar las diferencias significativas entre condiciones. Cuando el análisis indicó una diferencia estadísticamente significativa (a un nivel de 0.05), se realizó una prueba de análisis Dunnett para determinar que condición presentaba una diferencia significativa con respecto al control con el software Prism (GraphPath).

RESULTADOS

EXPRESIÓN DE LOS TRANSPORTADORES DE GLUTAMINA EN CÉLULAS DE GLÍA DE BERGMANN

Como primer paso para caracterizar la posible interacción entre la captura de Glu y la liberación de Gln, decidimos explorar la naturaleza bioquímica de la captura de Gln en CGB. Debido a que los transportadores de Gln descritos en células gliales los únicos que pueden funcionar bidireccionalmente pertenecen a la familia N, nos concentramos en este sistema particularmente en el SNAT3, porque se ha descrito que este transportador se expresa en altos niveles en los días post-natal 7 en el cerebelo de rata[71, 72], lo cual correspondería a 14 días de desarrollo embrionario en pollo (estadio medio de desarrollo del cerebelo) [72]. Para tener una visión general de la expresión de SNAT3 en CGB, realizamos una inmunohistoquímica de cerebelos de pollo en estadio P0 utilizando un anticuerpo específico contra-SNAT3 junto con marcadores específicos de células tales como calbindina, KBP y GLAST/EAAT1 para la identificación las capas de la corteza cerebelar.

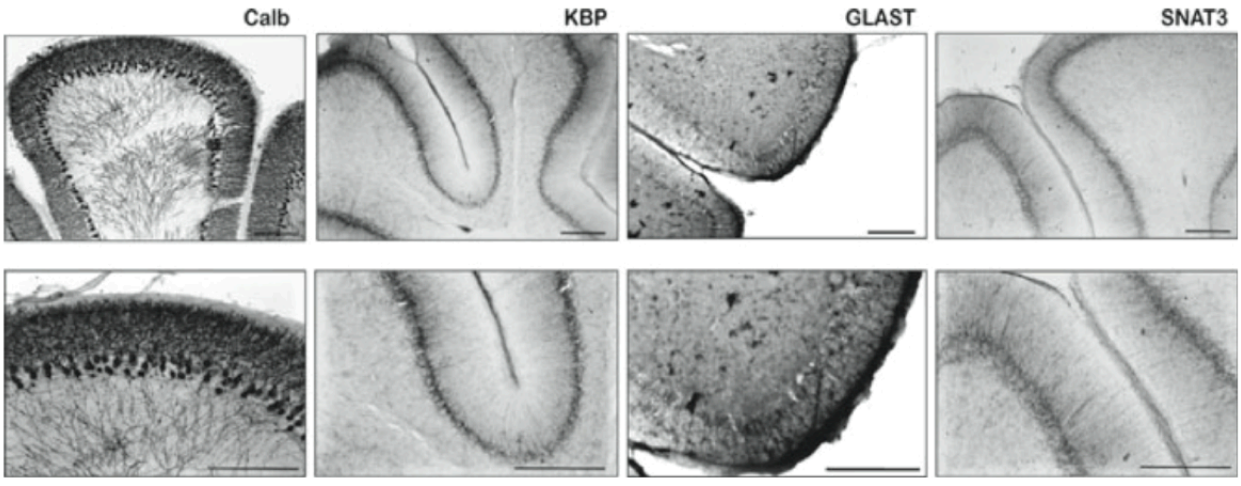

Figura8. Expresión de SNAT3 en cerebelo de pollo. Caracterización Inmunohistoquimica de secciones de cerebelo de pollo. Se ocupó calbindina (Calb) para marcar a las células de Purkije, proteína de unión a kainato (KBP) y GLAST para marcar a células de glía de Bergmann. Tamaño de barra 50 µm.

En la Figura8 se observa la localización de las células de Purkinje y sus arborizaciones después de la inmunotinción con calbindina un marcador específico de las células de Purkinje. Las CGB se localizaron gracias al uso de los anticuerpos anti-KBP y GLAST/EAAT1. KBP es expresado exclusivamente por las CGB en cerebelo de pollo[73] y GLAST/EAAT1 es el transportador de glutamato de mayor expresión en las células gliales del cerebelo [74, 75]. La inminotincion de SNAT3 se encontró principalmente en el borde apical de la capa molecular lo cual corresponde a los pies terminarles de CGB así también en los procesos de estas células, de manera muy similar al marcaje detectado con KBP, por el contrario la tinción encontrada por calbindina difiere totalmente a la observada por SNAT3. Junto con la detección de SNAT3 en cerebelo de pollo se decidió hacer una inmunofloresencia en cultivo celular, la cual muestra la expresión de SNAT3 tanto en membrana como en citoplasma. Por último se realizó una inmunodetección de fase solida detectando una banda de 60kDa la cual corresponde a SNAT3. EN conjunto estos resultados muestran que SNAT3 se expresa en CGB tanto in situ como en el cultivo primario.

A)

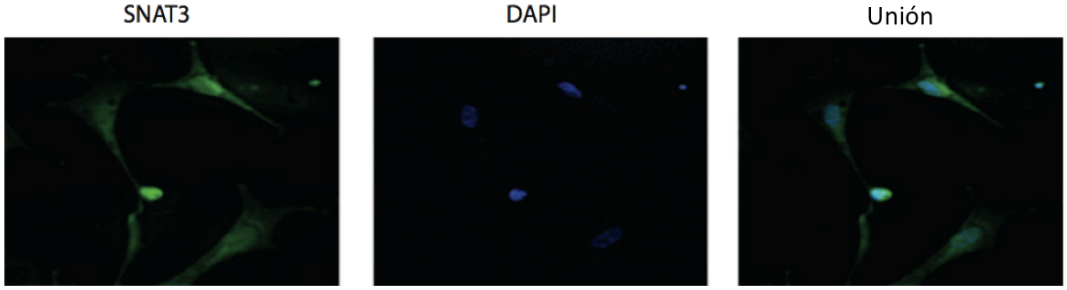

B)

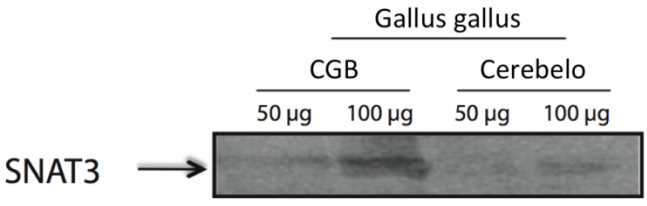

Figura9. Expresión de SNAT3 en cultivo de células de glía de Bergmann. A) Células teñidas con el anticuerpo anti-SNAT3 (verde), núcleos de color azul teñidos con DAPI. B) Extractos totales de proteínas de cultivo de CGB y cerebelos, fueron probadas en detección en fase solida con anticuerpos ati-SNAT3.

CARACTERIZACIÓN DE LA CAPTURA DE GLN EN CULTIVO CELULAR DE GLÍA DE BERGMANN

Para establecer un acople funcional entre la captura de Glu y la liberación de Gln es necesario conocer los parámetros cinéticos de la captura de Gln en nuestro cultivo. Debido a que el sistema N es el único sistema de captura de Gln que puede funcionar con Li^+, decidimos usar una solución de ensayo la cual se remplaza el NaCl por LiCl. Como se muestra en la Figura 10 existe una dependencia de tiempo en la acumulación de Gln aun en la solución de ensayo a la que se le remplazó el NaCl por LiCl. Incrementando las concentraciones de Gln, logramos determinar los parámetros cinéticos de la captura de Gln. Como se describe en la Figura11, el componente tolerante al Li^+ muestra una K_m de 2.925mM y una V_{max} de 1.818 µmol/min*mg. Adicionalmente, realizamos experimentos de competencia con distintos aminoácidos con el fin de determinar qué porcentaje total de la Gln capturada por CGB pertenecen al sistema N. Usando MeAIB, el inhibidor del Sistema A, alanina como competidor del Sistema ASC, A y N; para el sistema N usamos histidina y una mescla de leucina y treonina como competidor para los sistemas ASC y L. Como se observa en la Figura12, His reduce aproximadamente el 40% de la captura de Gln en CGB, de manera similar a lo que se observa en los ensayos de captura de Gln con medio al cual se remplazó el Na^+ por el Li^+. Estos resultados sugieren que el 40% de la captura de Gln en CGB es mediada por el Sistema N, mientras que el resto de la captura pertenece a los sistemas ASC y L.

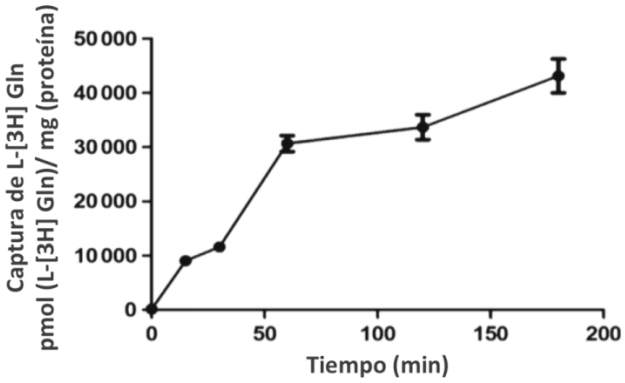

Figura10. Captura dependiente de tiempo**.** Curso temporal de la captura de Gln, la solución de captura posee LiCl en lugar de NaCl.

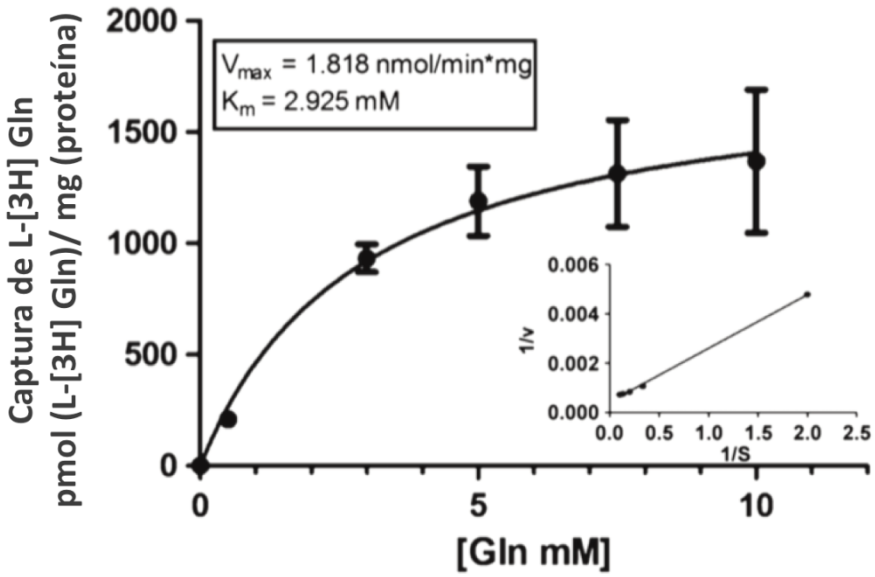

Figura11. Parámetros cinéticos del sistema N. Se ocuparon concentraciones crecientes de Gln no marcada con una concentración fija de 0.5µCi/mL con el fin de determinar los parámetros cinéticos (K_m y V_{max}).

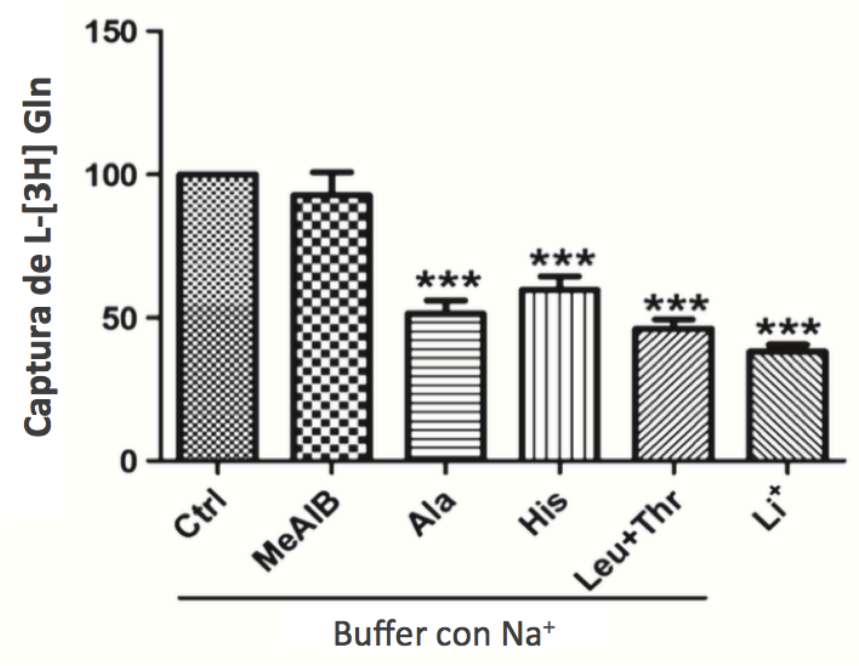

Figura12. Inhibición de los distintos sistemas de captura de Gln en CGB. Efecto de diferentes aminoácidos en la captura de Gln, se ocuparon concentraciones de 10mM de Ala, His, Leu y Thr. Para el MeAIB se usó concentración de 0.5mM

ACOPLE FUNCIONAL ENTRE GLAST Y SNAT3

La captura de Glu en CGB es llevada a cabo por GLAST [76], igual que el Glu el Asp también es transportado por GLAST de una manera electrogénica con un flujo neto de Na^+. Bajo estas circunstancias, es probable que la captura de Gln, la cual depende del gradiente de Na^+ se vea inhibida. La Figura 13 muestran que el Asp en concentraciones de 60 y 120 µM, previenen la captura de Gln. Como era esperado este efecto es dosis dependiente con una IC_{50} de 0.873µM (Figura 14). Este resultado es un efecto mediado por un transportado y en ningún momento denota la afinidad del transportador por su sustrato. Este resultado nos llevó a evaluar la liberación de Gln al medio extracelular consecuencia de un transporte reverso de SNAT3 inducido por estímulos de Glu o Asp en CGB. Como se muestra en la Figura 15, existe un incremento en las concentraciones extracelulares de Gln resultado de la liberación de Gln en estímulos con Glu. Es importante señalar que exposición a 50 µM o 1 mM de Asp, también indujo una liberación de Gln. En contraste, el agonista de los receptores AMPA y KA, no produjo ninguna liberación significativa de Gln. Estos resultados sugieren que la captura de Glu está ligada a la liberación de Gln.

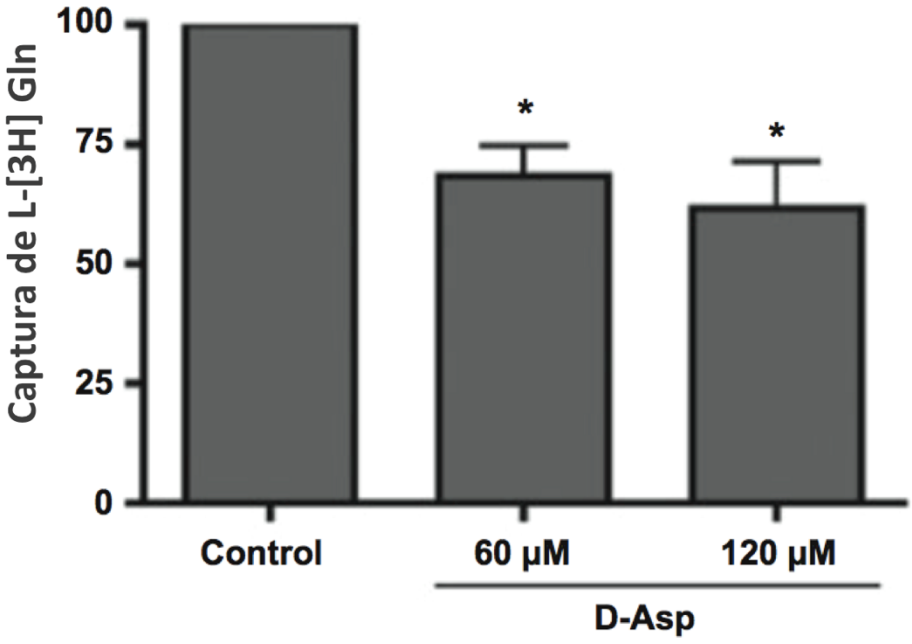

Figura13. Efecto de la activación de los transportadores de Glu en la captura de Gln. Efecto de dos diferentes concentraciones de Asp (60 y 120 µM) en la captura de Glu en CGB

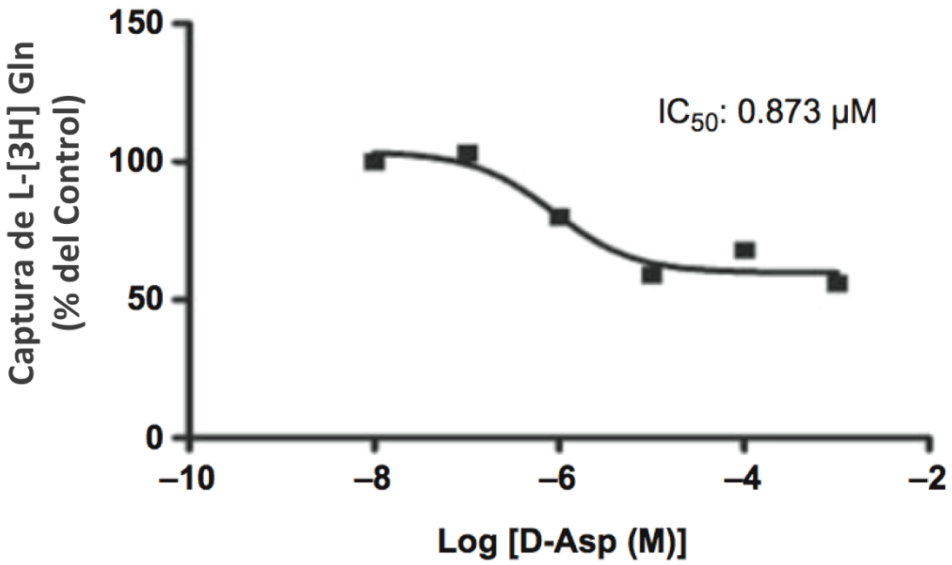

Figura14. IC_{50} de los transportadores de Gln por estímulos con Asp. Se determina el valor de IC_{50} de Asp sobre la captura de Gln en CGB

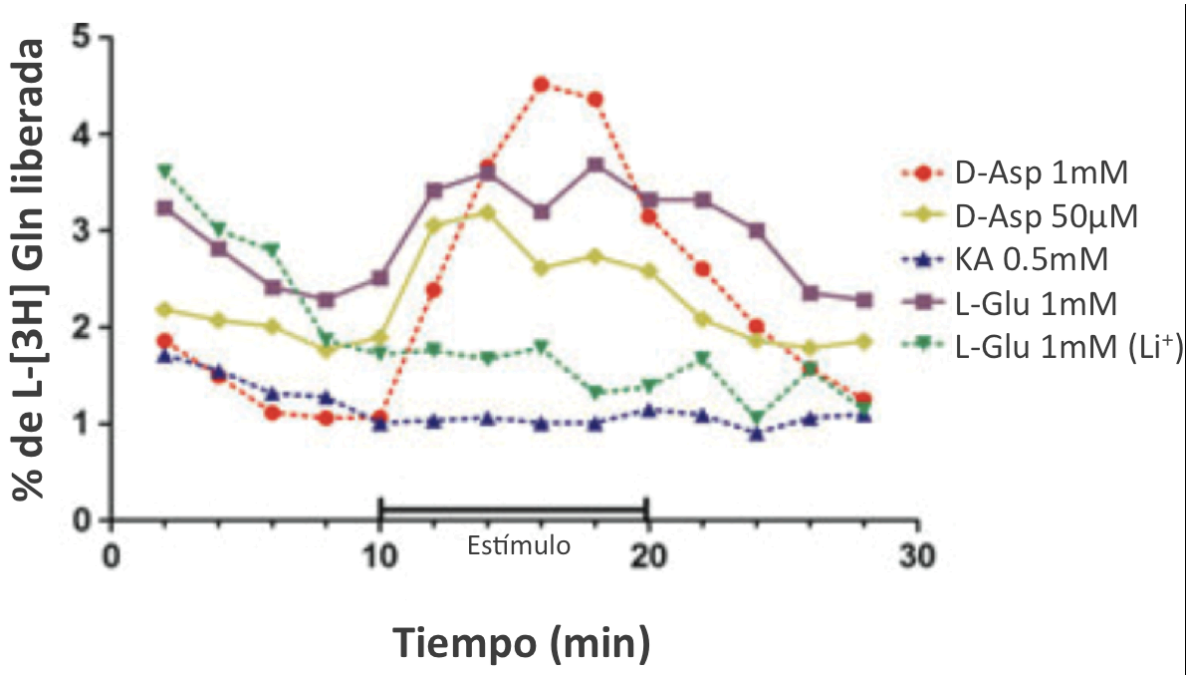

Figura15. Ensayos de liberación de Gln. Las CGB fueron cargadas con 0.5µCi/ml de [^{3}H]-L- Gln. Se colectaron 15 fracciones, las fracciones 5 a la 10 fueron las correspondientes a los estímulos.

INTERACCIÓN FÍSICA ENTRE GLAST Y SNAT3

Los resultados anteriores sugieren una posible interacción física entre GLAST y SNAT3. Para probar esta hipótesis, realizamos un ensayo de Inmunoprecipitación acoplada a una detección en fase solida. En la Figura16 se muestra la Inmunoprecipitación de extractos proteicos de CGB con el anticuerpo ant-GLAST y la Inmunoprecipitación en fase sólida utilizando el anticuerpo anti-SNAT3, lo cual nos permite establecer la presencia del complejo formado por estas dos proteínas en CGB. De igual manera la inmunoprecipitación con SNAT3 contiene a la proteína GLAST. Partiendo del hecho de que SNAT3 interactúa con GLAST decidimos probara si la actividad de GLAST era capaz de modificar esta interacción. Con este fin, expusimos CGB a concentraciones de 1mM de Glu y/o 2mM de Gln. Como se describe en la Figura5, Glu pero no Gln favorece la interacción física de SNAT3/GLAST. Nuestro siguiente paso fue probar si la actividad de estos transportadores alteraba esta interacción. Con este fin expusimos nuestro cultivo celular a concentraciones de 60uM de Asp y 200uM de Gln, o a una combinación de estos. Como se observa en la Figura17 el Asp induce la asociación de GLAST/SNAT3, mientras que Gln reduce el efecto de Asp.

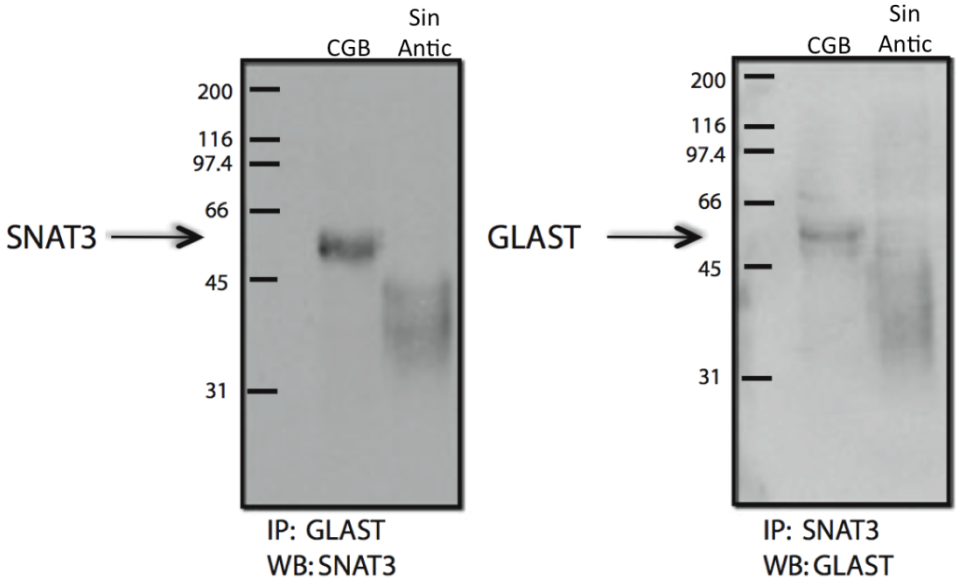

Figura16. Interacción entre SNAT3 y GLAST. Extractos de CGB fueron inmunoprecipitados contra GLAST y analizados en inmunodetección de fase solida contra SNAT3, el experimento inverso también se realizó.

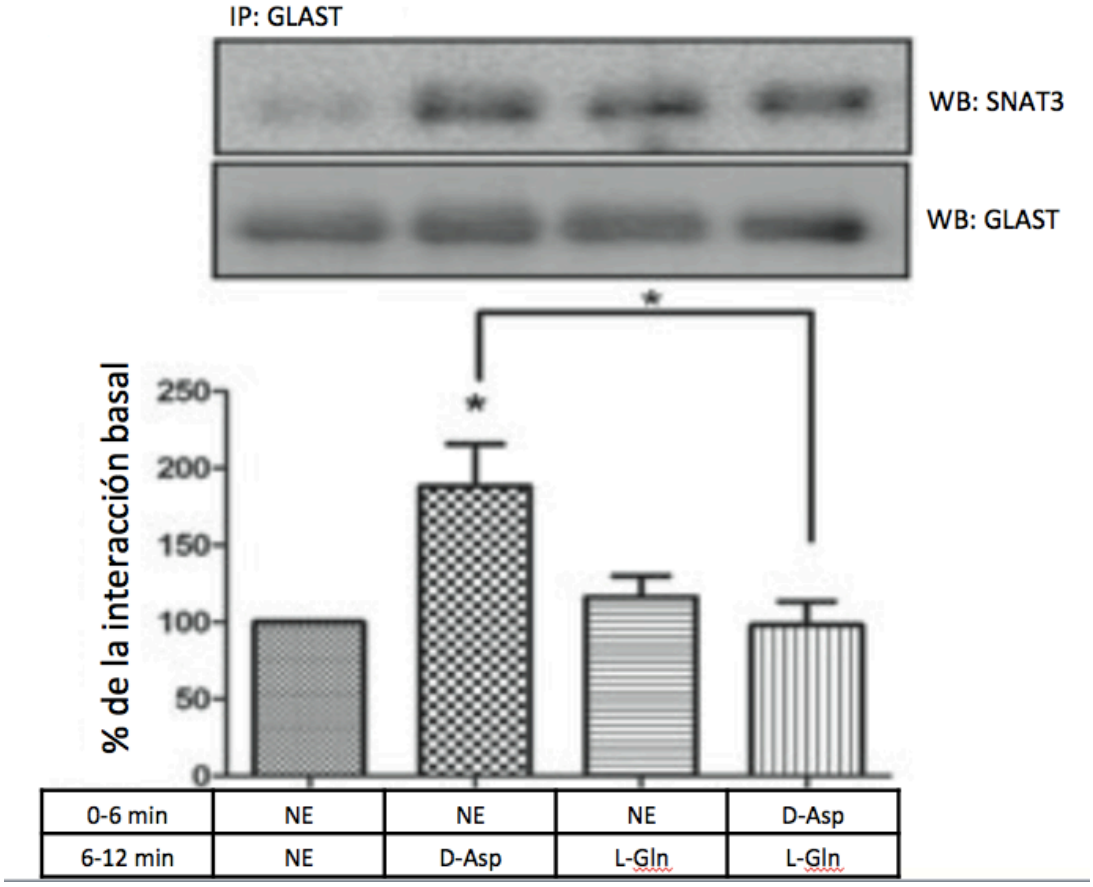

Figura17. Regulación de la interacción entre SNAT3 y GLAST. CGB fueron expuestas a concentraciones de Asp (1mM) y Gln(2mM). Posteriormente se realizó unainmunoprecipitación contra GLAST y una inmunodetección de fase sólida contra SNAT3.

DISCUSIÓN

Desde hace más de veinte años, investigaciones en el campo de la neurociencia han soportado y fundamentado el concepto de sinapsis tripartita [77, 78]. En la sinapsis glutamatérgica, la principal función de las células gliales es reciclar el neurotransmisor [79]. La lanzadera Glu/Gln es una evidencia sólida de la capacidad de respuesta de las células de glía a la actividad sináptica, ya que estas células pueden modificar sus funciones celulares tales como la expresión de GS y su actividad. Otro ejemplo es el estrecho acople energético que existe entre las células gliales y las neuronas que se conoce como lanzadera astrocito/neurona lactato [80]. Más aun las CGB poseen receptores a Glu y estos se activan en cada evento de despolarización que sucede en la sinapsis entre las fibras paralelas y las células de Purkinje[81].

En la primera sección de esta tesis, nos enfocamos en caracterizar la captura/liberación de Gln en CGB en el contexto de la neurotransmisión glutamatergica. Con lo cual el primer paso antes de hacer una caracterización bioquímica de los transportadores de Gln, era establecer la expresión de transportadores que pudieran funcional en sentido reverso. Debido a que el sistema N de transportadores de Gln es el único que se expresa en células gliales y es capaz de funciona bidireccionalmente, acortamos la búsqueda a SNAT3 ya que de los dos integrantes SNAT3 es el que presenta una mayor expresión en etapas prenatales, pero esto no excluye la expresión de SNAT5 [82]. En las Figura8, 9 y 10, demostramos la expresión de SNAT3 en CGB tanto in situ como en el cultivo celular. Es importante recalcar que la expresión tanto de SNAT3, GLAST y KBP que se detectada por inmunohistoquimica (Figura8) es muy similar entre ellas, denotando que estas proteínas se expresan en las CGB, debido a que los tres anticuerpos fueron generados en conejos, por lo cual esto nos impidió hacer doble marcaje.

Cuando medimos los valores cinéticos par SNAT3 en nuestro cultivo primario y obtuvimos valores en el orden mM, nos dio confianza que efectivamente estábamos trabajando con el transportador SNAT3. Se podría argumentar que los valores de Km reportados por otros grupos de trabajo son de alrededor de 1mM [49, 83, 84] para SNAT3 y el valor que nosotros obtuvimos es ligeramente superior (2.9mM), pero hay que tomar en cuenta que los valores obtenidos por esos grupos fueron en sistemas heterologos a diferencia de nosotros que lo obtuvimos de un

cultivo primario. Aunado a eso nosotros utilizamos un medio con el remplazo del Na^+ por Li^+, aunque en este punto no podemos discernir qué es lo que pudo causar esta leve discrepancia en el valor de la Km sin el cambio del Na^+ por Li^+ o el hecho de no usar un sistema de expresión heterólogo o simplemente las diferencias en cuanto a especies ya que nosotros usamos como modelo de estudio células provenientes de pollo mientras que en otros estudios se utilizan células o proteínas propias de rata o ratón. En este punto no es posible descartar la participación de SNAT5 de la captura o liberación de Gln.

Uno de los puntos importantes en el efecto de la liberación de Gln es porque el Asp es capaz de inducir una liberación de Gln de manera más eficiente (Figura15). Una posible explicación es que el Glu no solo activa transportadores sino que también a receptores mientras que el Asp solo es capaz de activar a los transportadores en este caso específico a GLAST. Este resultado favorece nuestra hipótesis del acople entre GLAST y SNAT3.

El hecho de que GLAST y SNAT3 estén asociados, sugiere de que SNAT3 necesita el influjo de Na^+ proveniente de la captura de Glu por parte GLAST para funcionar en modo reverso. Como se muestra en la Figura13 el hecho de que la captura de Gln se vea afectada por la presencia de Glu en el medio extracelular y que la disminución de la captura de Gln es dependiente de la concentración de Glu (Figura14), nos sugiere claramente que la captura de Glu y la liberación de Gln están acoplados íntimamente.

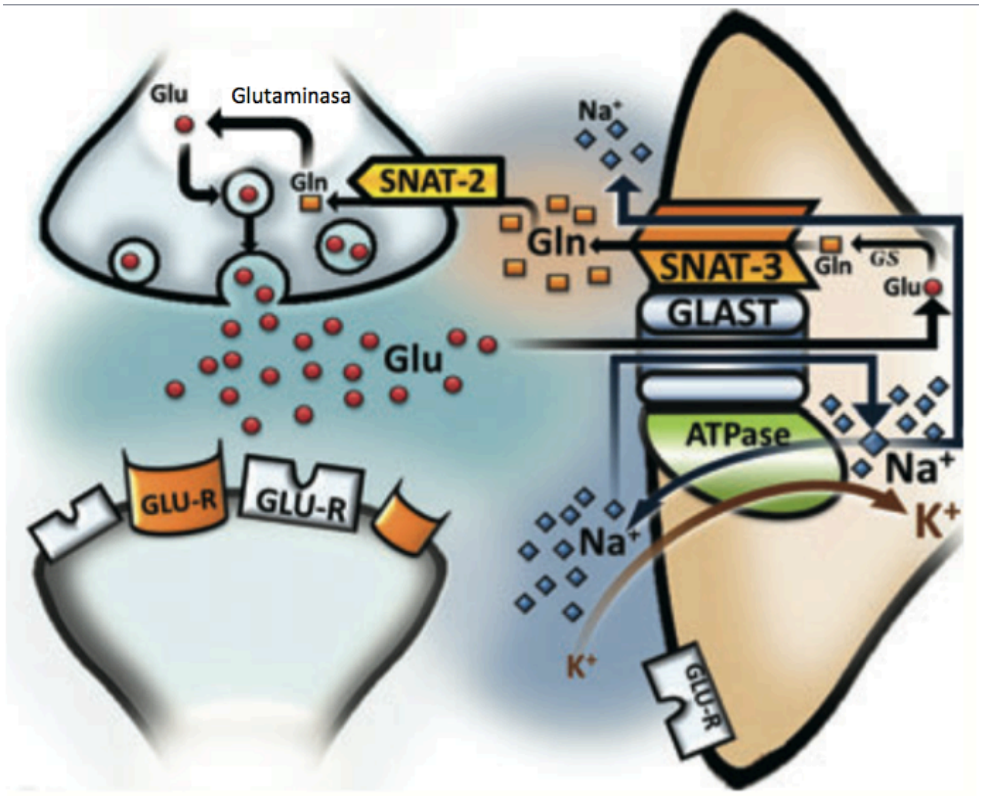

Figura18. Esquema representativo del complejo formado por GLAST/SNAT3. EL Glu liberado por las fibras paralelas es capturado por la CGB a través de GLAST, este influjo de Glu es acompañado por 3 iones Na^+, el incremento en Na^+ sirve como fuerza motriz para que SNAT3 pueda funcionar en modo reverso y expulsar la Gln al medio extracelular, para su posterior recaptura por la neurona y pueda rellenar sus vesículas sinápticas con Glu el cual obtendrá de convertir a la Gln recién capturada.

CAPÍTULO 2: REGULACIÓN DE GLAST EN CÉLULAS GLIALES DE BERGMANN POR LA VÍA DEL ÓXIDO NÍTRICO/GMPC

INTRODUCCIÓN

Desde el descubrimiento del factor relajante de endotelio (EDRF) y que se demostró que este factor es el óxido nítrico (ON) [85, 86], muchos científicos han descrito diversas funciones biológicas de esta molecular, y su rol en distintos fenómenos fisiológico distribuidos en distintos sistemas, entre estos tenemos al sistema nervioso[87, 88]. Su importancia fue tal en los últimos 20 años que en 1992 el ON fue nombrada molécula del año y desde ese momento el estudio y entendimiento de los mecanismo que involucran al ON han ido en aumento sobretodo en el sistema nervioso.

El ON un radical libre que se produce por algunas células a partir de los aminoácidos arginina (Arg) y citrulina (Cit) [89], es una molécula muy reactiva y posee una vida media muy corta, lo cual la hizo virtualmente invisible hasta su descubrimiento. El ON activa ala guanilato ciclasa soluble (sGC) lo cual induce un incremento en los niveles de 3',5' Guanosín monofosfato cíclico (GMPc), estos niveles elevados inducen la activación de PKG [90, 91]. Aunque el ON activa distintas cascadas de fosforilación gracias a su habilidad a reaccionar con el Fe(II) contenido en los grupos hemo de las proteínas como es el caso de GCs. También puede actuar nitrosilando proteínas en sus residuos de cisteína, lo cual tiene un impacto en la función de proteínas, estabilidad y localización.

ON es una molécula gaseosa capas de señalizar creada en la mayoría de los casos por la encima óxido nítrico sintetasa (NOS). Además del uso de Arg y Ca^{2+} calmodulina, NOS también requiere moléculas de oxígeno, NADP reducido, cofactores derivados de flavina (FMN y FAD), tetrahidrobiopterina (BH4) y Cit [92]. Generalmente NOS requiere unirse a proteínas como el

receptor NMDA a través de sus dominios de unión PDZ, así como de otras moléculas adaptadoras como PSD95, el complejo Ca^{2+}-calmodulina que le sirven de soporte estructural para la producción de ON.

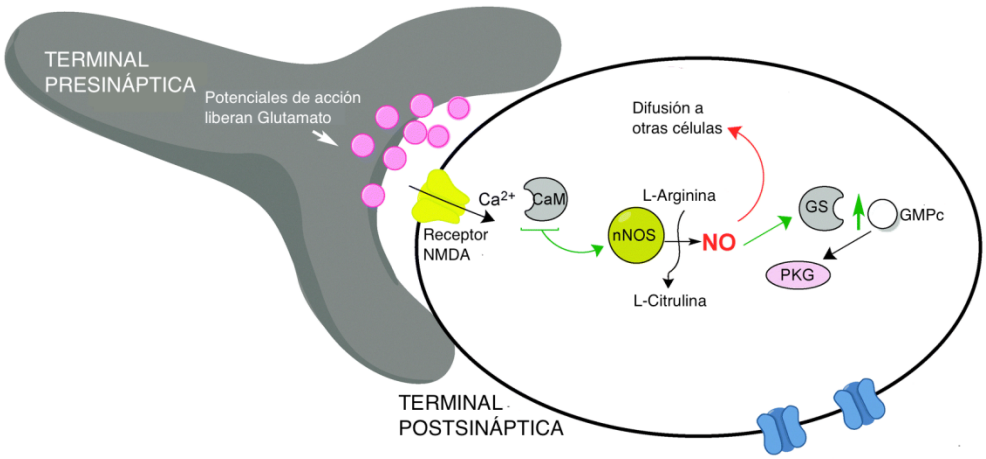

Figura 19. Vía del óxido nítrico/GMPc. La liberación de Glu provoca la entrada de Ca2+ en la neurona post-sináptica a través de la apertura de los receptores NMDA, el Ca^{2+} se une a la Calmodulina (CaM), el complejo Ca^{2+}/Calmodulina activa entonces a la sintetasa de óxido nítrico neuronal (nNOS). La enzima nNOS utiliza como substrato L-Arginina para producir L-Citrulina y óxido nítrico (NO), el cual difunde a traves de la membrana plasmática y del citoplasma. El NO reacciona con el sitio activo de la enzima guanilato ciclasa (GS) y estimula la producción de GMP cíclico (GMPc). Después, el GMPc interactúa con la proteína cinasa dependiente de GMPc (PKG), la cual forsforila múltiples substratos y participa en la propagación de la señal (Modificado de Mukherjee 2014 [93])

La activación de los receptores NMDA en el cerebro inducen la actividad de NOS y la producción de ON lo que lleva a elevar los niveles de GMPc en el cerebro. Este efecto ha sido claramente demostrado en el cerebelo donde el incremento de GMPc se ha visto no únicamente en las células de Purkinje sino también en la CGB [94-96].

En diversos estudios han mostrado que el ON regula la liberación de neurotrasmisor y diferentes aspectos de la dinámica sináptica, tales como la diferenciación de la especialización sináptica, dinámica de microtúbulos, arquitectura y organización de las proteínas presentes en la sinapsis así como la modulación de efectos sinápticos como plasticidad sináptica [97-100].

A pesar de que existe una fuerte evidencia el efecto del ON en el cerebelo y sobretodo en las CGB, poco es sabido de su efecto sobre estas. Dada que la producción de ON y los incrementos de GMPc están asociados a altos niveles de actividad sináptica nosotros decidimos estudiar la captura de Glu por parte de las CGB cuando existe la producción de ON, para lo cual usamos el bien caracterizado modelo de estudio de nuestro laboratorio (el cultivo de CGB) y lo sometimos a estímulos con nitro prusiato de sodio un donador de ON.

JUSTIFICACIÓN

Existe evidencia de la importancia del ON en la neurotransmisión, a pesar de esto hasta la fecha no se ha caracterizado el efecto de este, sobre células gliales de Bergmann en el contexto del ciclo Glu/Gln

OBJETIVO GENERAL

Caracterizar el efecto del óxido nítrico en la captura de Glu de células gliales de Bergmann

OBJETIVOS ESPECÍFICOS

- Estudiar el efecto del óxido nítrico en la captura de Glu en células gliales de Bergmann
- Demostrar la participación de la vía Guanilato ciclasa /PKG en el efecto inducido por el óxido nítrico
- Determinar las constantes cinéticas de la captura de glutamato de celular gliales de bergmann al ser estimuladas con óxido nítrico
- Identificar si el efecto es debido a un aumento de transportadores en la membrana o a una mayor eficiencia de los transportadores
- Analizar la participación del intercambiador Na^{+}/Ca^{2+} en el efecto inducido por el óxido nítrico

RESULTADOS

Con el estudio de la captura de Gln en CGB logramos tener un mayor entendimiento acerca del ciclo glutamato/glutamina y su regulación. Con la idea general de descubrir que otros factores influyen en la regulación del reciclamiento del neurotransmisor Glu, decidimos estudiar el efecto del óxido nítrico sobre la captura de glutamato. Como se describió en la introducción la producción de óxido nítrico por parte de la neurona está íntimamente ligada a la activación de los receptores NMDA y la producción de este gas está asociado al incremento en los niveles de GMPc en CGB pero hasta el momento es poco claro el efecto que tiene sobre el ciclo glutamato glutamina, por tal motivo decidimos evaluar si existía algún efecto sobre la captura de Glu una parte crucial en el ciclo de este importante neurotransmisor.

LA ACTIVACIÓN DE ON/GMPC INCREMENTA LA CAPTURA DE ASP EN BGC

Al exponer las CGB al donador de ON nitro prusiato de sodio (SNP), observamos un incremento en la captura de Asp (Figura20). Existen dos posibles mecanismos biológicos de dicho efecto: la nitración de proteínas o la activación de la proteína GCs acompañado de un incremento intracelular de GMPc. Usando el análogo pobremente metabolisable de GMPc el dbGMPc obtuvimos resultados muy similares a los observados con SNP (Figura21). Cuando inhibimos a la GCs con azul de metileno bloqueamos el efecto inducido por SNP (Figura22). En conjunto estos resultados indican que la vía del ON/GMPc está implicada en el incremento de la captura de Glu en CGB.

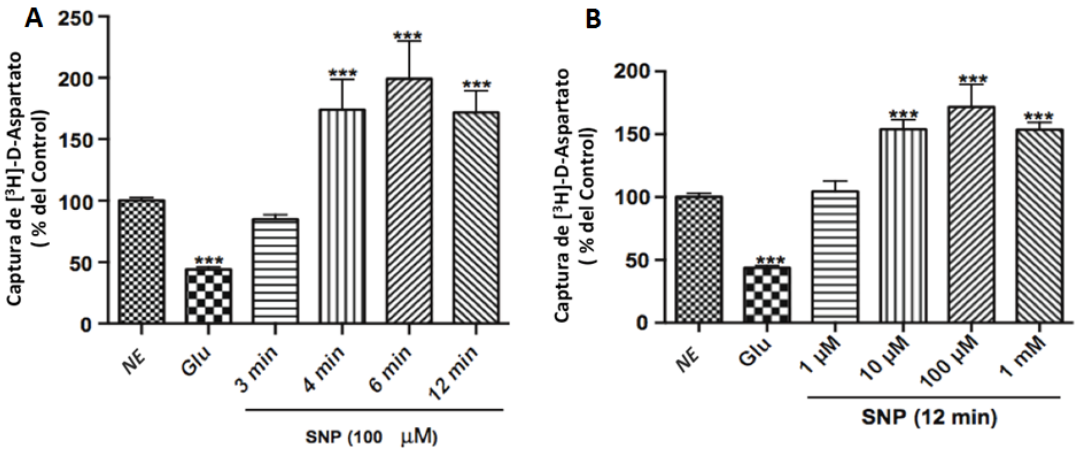

Figura 20. Efecto del SNP en la captura de [3H]-D-Asp. **A)** CGB fueron preincubadas con SNP a una concentración 100µM, por los tiempos indicados de tiempo o B) incubadas por 12 min con concentraciones crecientes de SNP, después de eso la captura de [3H]-D-Asp por 30 min se llevó acabo**.**

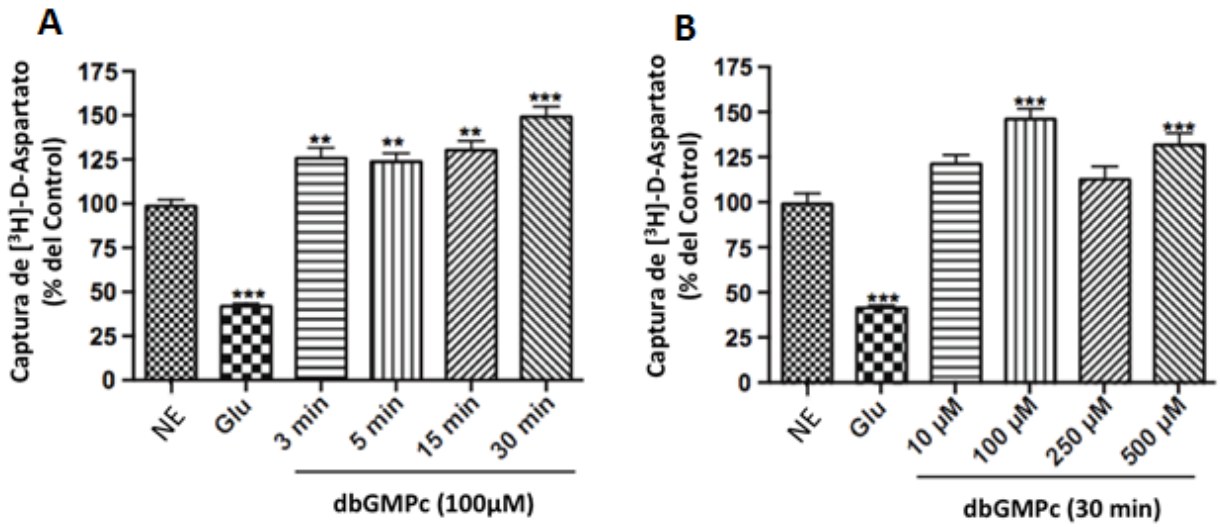

Figura 21. Efecto del dbGMPc en la captura de [3H]-D-Asp. A) CGB fueron preincubadas con dbGMPc a una concentración 100µM, por los tiempos indicados de tiempo o B) incubadas por 30 min con concentraciones crecientes de dbGMPc, después de eso la captura de [3H]-D-Asp por 30 min se llevó acabo**.**

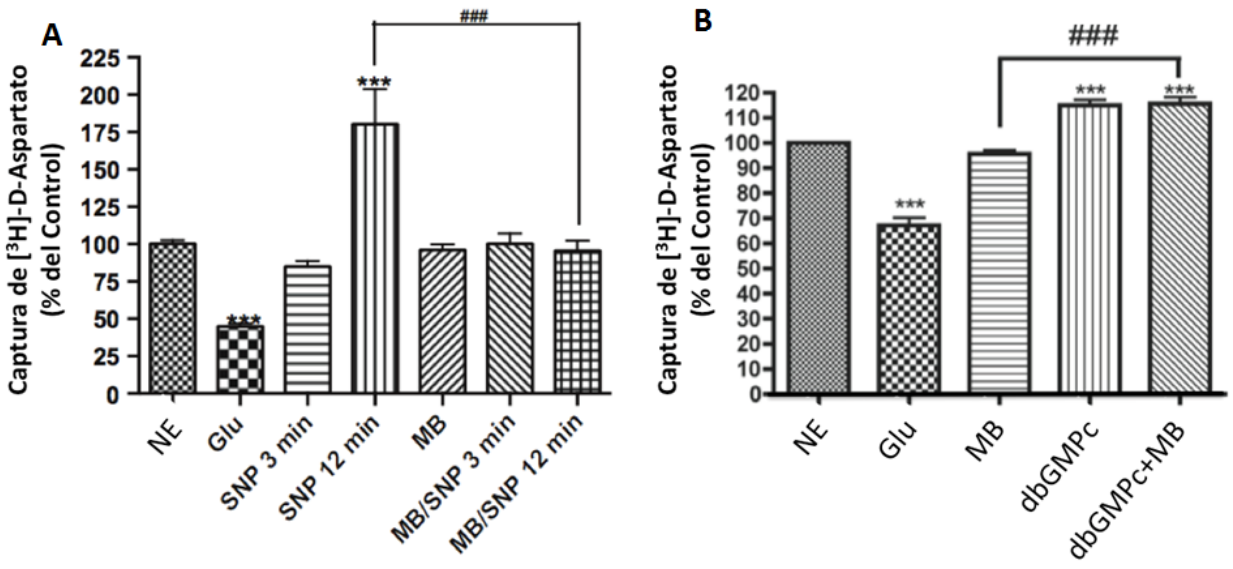

Figura 22. Participación de la GCs en el incremento en la actividad de GLAST dependiente de ON. CGB se trataron con 100 µM SNP durante 3 o 12 min A) o con 100µM dbGMPc durante 30 min B) en presencia o ausencia del inhibidor de GCs, azul de metileno (MB). La captura de [3H]-D-Asp se realizó durante 30 min como se describe en la sección de Métodos.

LA VIA ON/GMPC REGULA LA ACTIVIDAD DE GLAST

Para probar la participación de GLAST en el incremento en la captura de Glu mediado por ON, decidimos remplazar el NaCl por cloruro de colina debido a que el transportador GLAST depende Na^+ para llevar acabo la captura de Glu. Como se muestra en la Figura23 el efecto inducido por SNP es abolido sin la participación de GLAST.

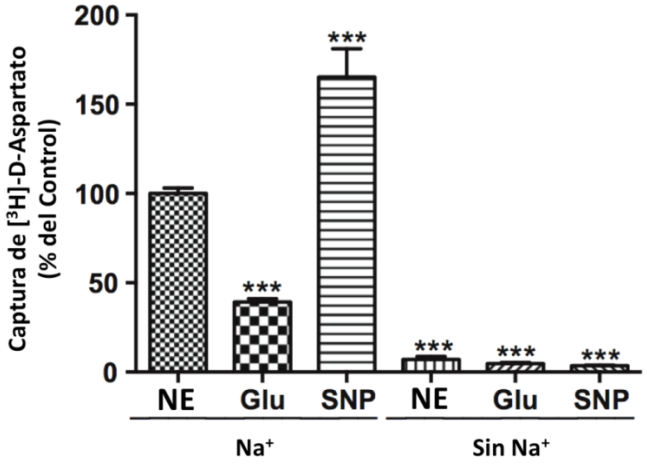

Figura 23. Importancia del sodio en la captura de Glu. CGB fueron tratadas con 1mM Glu durante 30 min o con 100 µM SNP durante 12 min en solución de ensayo con Na^+, pasada esta incubación se realizó la captura de [3H]-D-Asp durante 30 min en presencia o ausencia de Na^+.

Como siguiente punto decidimos examinar los cambios en los valores cinéticos inducidos por la vía ON/GMPc sobre la captura de Glu mediada por GLAST. Como se observa en la Figura24 el aumento en V_{max} pero no en K_m sugieren un aumento en el número total de transportadores en membrana. Como se demostró anteriormente este efecto es bloqueado cuando utilizamos azul de metileno un inhibidor de GCs. Para corroborar que efectivamente hay un incremento en el número de transportadores totales en la membrana realizamos experimentos de unión de ligando radiactivo utilizando soluciones con y sin Na^+ y Ca^{2+}. Como se muestra en la Figura25 el SNP incrementa el número de transportadores en la membrana plasmática, de una manera dependiente de Ca^{2+}.

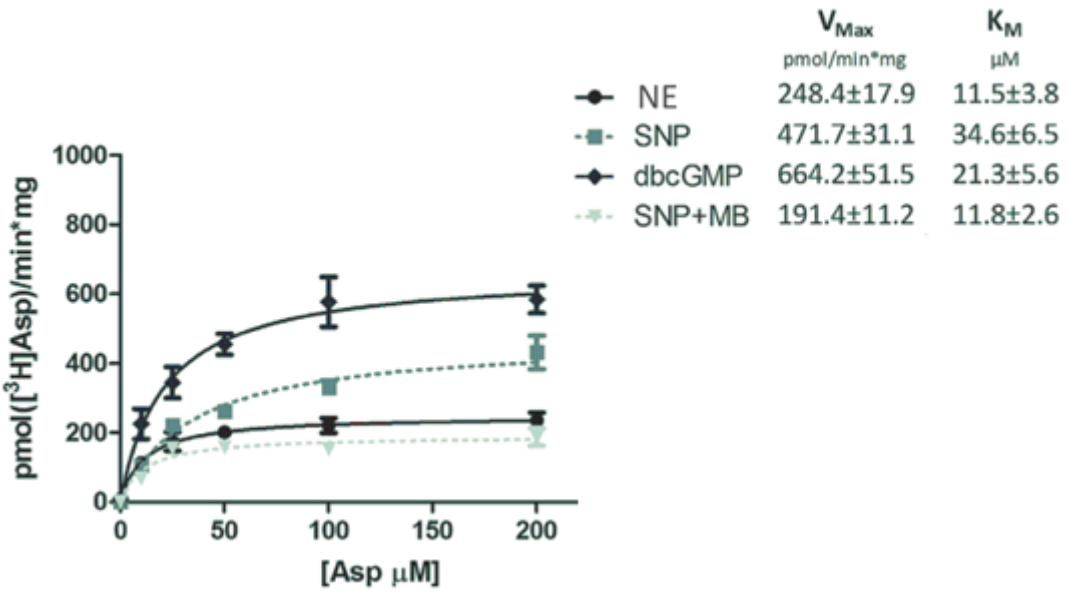

Figura 24. Constantes cinéticas de la captura de Glu en CGB. CGB se pre-incubaron con 100 µM SNP durante 12 min en presencia y ausencia del inhibidor de GCs, MB; o con 100 µM dbGMPc durante 30 min y se realizó la captura de [3H]-D-Asp con concentraciones crecientes de D-Asp no marcado (10, 25, 50, 100 y 200 µM) por 30 min.

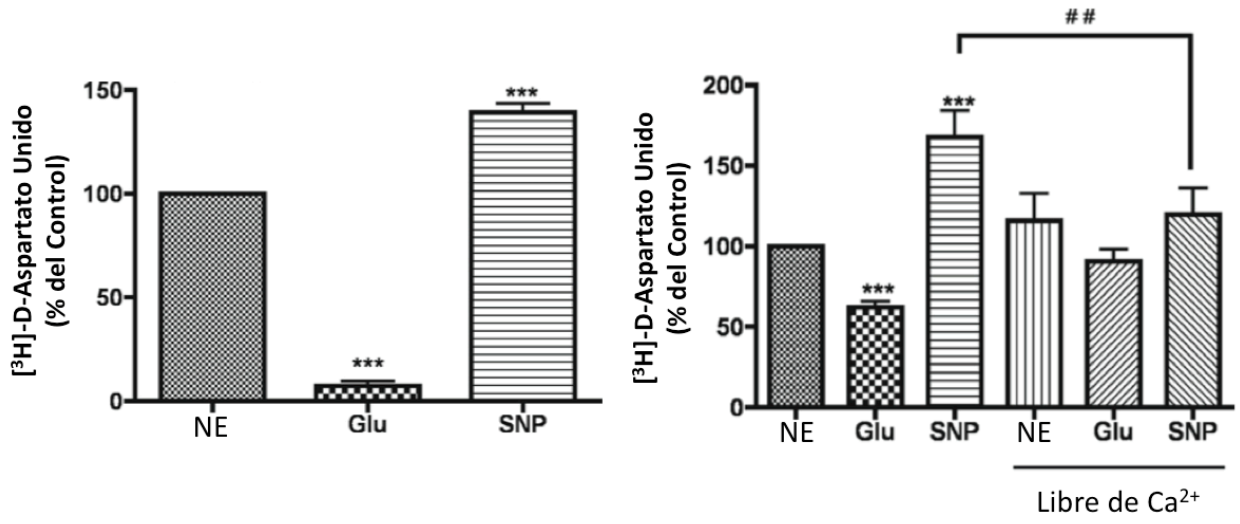

Figura 25. Ensayos de unión de [3H]-D-Asp en CGB. Células confluentes se estimularon con 1 mM Glu durante 30 min o con 100 µM SNP en presencia y ausencia de Na^+ (Panel A) y de Ca^{2+} (Panel B) según se indica. Después se realizó un ensayo de unión de [3H]-D-Asp a 4˚C.

EL ÓXIDO NÍTRICO INDUCE INFLUJOS DE CA2+ VIA PKG EN CGB

El hecho de que el dbGMPc mimetice el efecto del ON, sugiere que el siguiente paso en la vía de señalación que conlleva al aumento en la captura de Glu involucra a PKG. Para probar esta hipótesis, inhibimos a PKG con un inhibidor específico Rp-8-Br-PET-GMPc antes de estimular con SNP a las CGB. Como se muestra en la Figura26, el inhibidor de PKG bloquea el efecto inducido por SNP, demostrando de esta manera la participación de esta cinasa en la cascada de señalización inducida por ON.

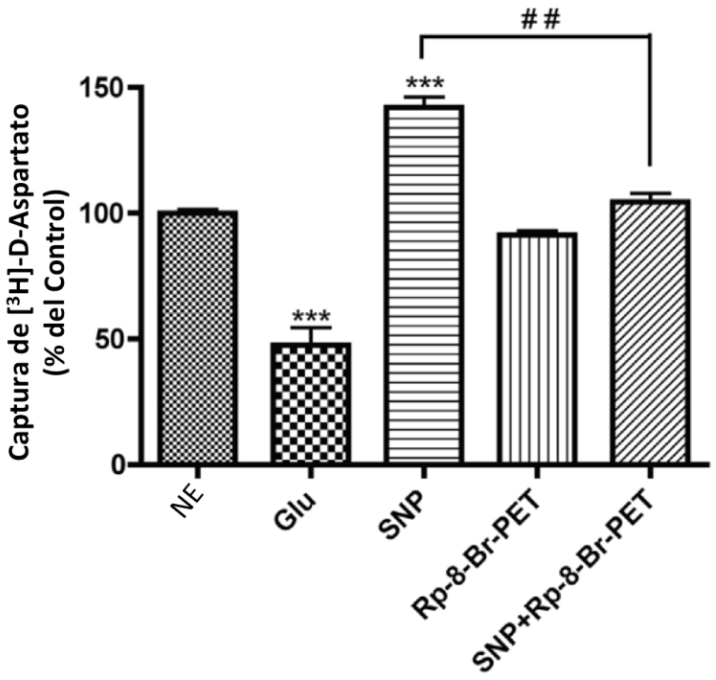

Figura 26. Participación de PKG en efecto del ON. CGB se estimularon con 100 µM SNP durante 12 min en presencia o ausencia del inhibidor de PKG, Rp-8-Br-PET-cGMPS a 10 µM durante 30 min. La captura de [3H]-D-Asp se realizó durante 30 min como se describe en la sección de Métodos

Se ha reportado que tanto el SNP induce incrementos en los niveles de GMPc de manera dependiente de Ca^{2+} [101]. De manera independiente Kitao y colaboradores demostraron que SNP y GMPc inducen un influjo de Ca^{2+} a través del modo reverso del intercambiador Na^{+}/Ca^{2+} (NCX) en astrocitos [102]. Por lo tanto decidimos analizar la participación de Ca^{2+} y el NCX en el efecto de SNP observado en CGB. Utilizando un medio de ensayo sin Ca^{2+} y el inhibidor específico para NCX, KB-R7943, determinamos que el efecto del SNP es dependiente de Ca^{2+} y que la participación del NCX es necesaria (Figura27).

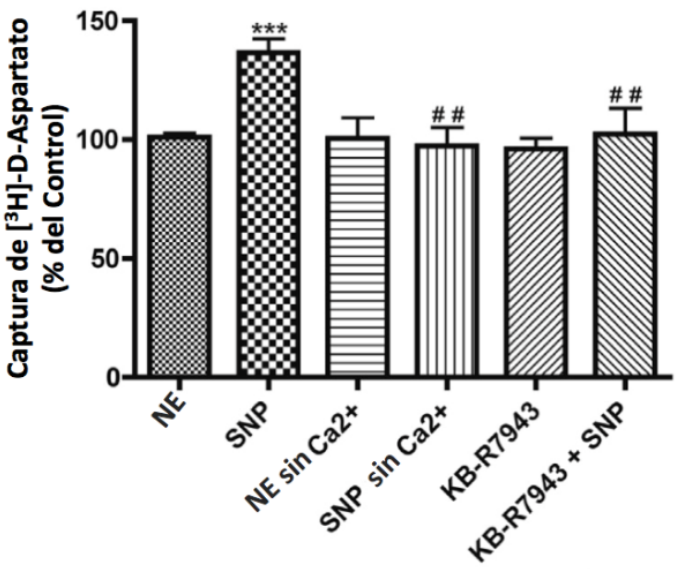

Figura 27. Papel del NCX en el efecto del ON. CGB se trataron con 100 µM SNP durante 12 min en presencia o ausencia de Ca2+; o se pre-incubaron con el inhibidor del NCX, KB-R7943 a una concentración de 15 µM durante 30 min y después se trataron con SNP. La captura de [3H]-D-Asp se realizó como se describe en la sección de métodos.

Como último punto decidimos probar si el influjo de Ca^{2+} proveniente del NCX era dependiente de PKG, con eso en mente realizamos ensayos de captura de Ca^{2+}. Como se muestra en la Figura28 el efecto en el incremento de la captura de Ca^{2+} producido por SNP es bloqueado por el inhibidor de PKG, indicando que PKG es necesario para activar el modo reverso del NCX e inducir el incremento en los niveles intracelular de Ca^{2+}. En conjunto estos resultados sugieren que el efecto de ON involucra la activación del modo reverso de NCX inducida por PKG, lo cual lleva al incremento en el número de transportadores en membrana.

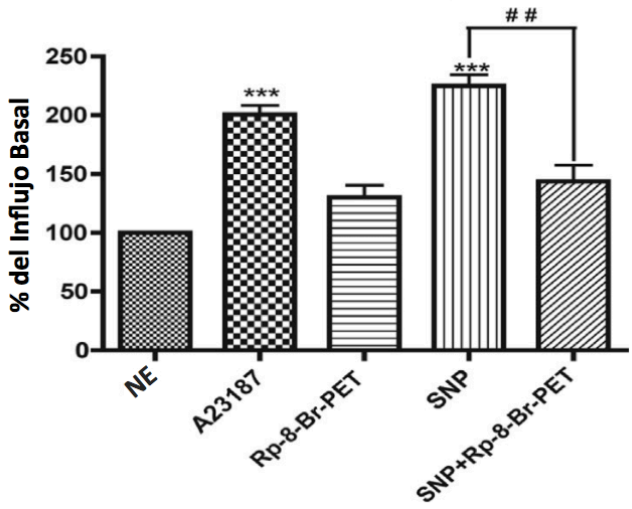

Figura 28. Influjo de Ca^{2+} inducido por ON/PKG en CGB. Cultivos confluentes de CGB se pre-incubaron con el inhibidor de PKG, Rp-8-Br-PET-cGMPS a 10 µM durante 30 min según se indica en la figura, y después se incubaron con 100 µM SNP. El influjo de [$^{45}Ca^{2+}$] se realizó durante 3 min. El ionoforo de Ca^{2+}, A23187 se usó a 10 µM como control positivo.

DISCUSIÓN

La captación de Glu por parte de los astrocitos no es un evento estático, por el contrario existen distintos eventos moleculares que pueden regular la actividad de los transportadores de Glu y Gln. Uno de los principales reguladores y más estudiados estímulos que las CGB es el Glu, el cual regula su propia captura, como lo describieron Gonzales y Ortega en el 2000.

En un esfuerzo por avanzar en el entendimiento de las funciones de las células gliales en la sinapsis decidimos analizar el posible efecto del ON en la captura de Glu. Describimos que la exposición de SNP o dbGMPc aumenta la captura de Glu por parte de GLAST. En la Figura20 podemos notar que el efecto de SNP es transitorio mientras que dbGMPc induce un efecto sostenido, esto podría deberse al hecho que el dbGMPc es pobremente degradado por las fosfodiesterasas. Tanto el efecto del SNP y dbGMPc se ve reflejado en el aumento en el valor de V_{max} (Figura24), lo que nos indica que el aumento en la captura de Glu es debido al aumento en el número de transportadores en la membrana. Aunque los valores obtenidos de V_{max} con SNP y dbGMPc varían considerablemente, se podría deber al efecto transitorio del SNP que contrasta con un efecto más duradero por parte del dbGMPc.

Especulando un poco es probable que *in vivo*, durante los periodos de alta actividad eléctrica en la capa molecular del cerebelo, ocurra un incremento de los niveles de ON de forma dependiente de Glu por la activación de la NOS, este ON puede difundir y activar en CGB a la CGs y por consecuencia incrementaría los niveles de GMPc lo que finalmente activaría a PKG. El proceso descrito anteriormente tendría como consecuencia el aumento del número de transportadores GLAST en membrana, incrementando la capacidad de las células gliales de unir Glu y por ende modular el potencial excitatorio post-sináptico [103] [104]. Apoyando esta hipótesis tenemos el hecho que el efecto inducido por SNP, el incremento en la captura de Glu es despues de 4 min, mientras que el efecto por parte del Glu, reducción de la captura de Glu es después de 30min. El blanco directo PKG hasta el momento sigue siendo desconocido. Es poco probable que PKG actué directamente sobre GLAST, debido a que hasta la fecha no se ha podido describir una función regulatoria sobre los sitos de fosforilación de esta proteína [105]. Interesantemente todos los efectos reportados son dependientes del influjo de Ca^{2+} mediado

por NCX (Figuras 25, 26, 27 y 28). En este punto uno podría especular que los efectos observados son mediados por un reacomodo del citoesqueleto, una estructura estrechamente regulada por fosforilaciones inducidos por influjos de Ca^{2+}.

En resumen, el Glu pone en marcha un compleja regulación de señales bioquímicas que regulan el intercambio y por lo tanto la disponibilidad de Glu en la terminal pre sináptica, involucrando no únicamente a las neuronas sino también a las células gliales.

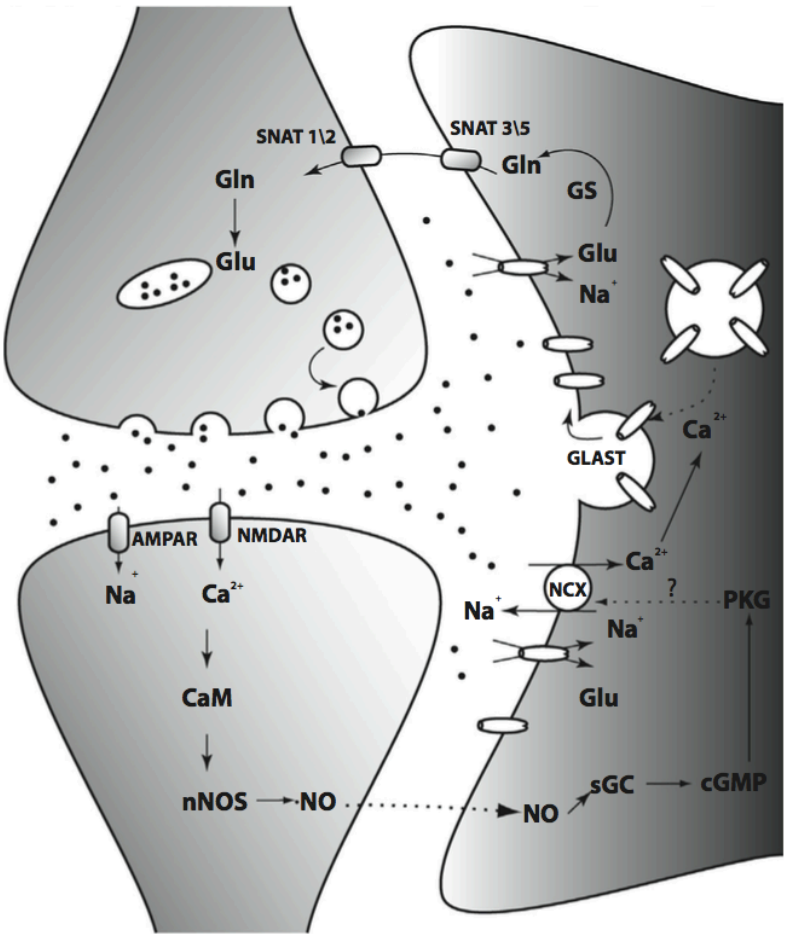

Figura 29. Modelo del efecto del ON en la captura de Glu en CGB. Cuando las células granulares son depolarizadas, la liberación de Glu activa a sus receptores ionotrópicos en las células de Purkinje, llevando a la síntesis y liberación del ON, el cual difunde a través de las membranas y activa a la enzima GCs en las CGB, resultando en un incremento en los niveles de GMPc y la consecuente activación de PKG. La activación de PKG repercute en la activación del NCX permitiendo un influjo de Ca^{2+} a las CGB, el incremento en las concentraciones intracelulares de Ca^{2+} favorece el movimiento de las vesículas que contienen a GLAST/EAAT1 a la membrana plasmática y de esta manera facilitando su inserción a la membrana, provocando un aumento en la captura de Glu.

CAPÍTULO 3: METILFENIDATO REGULA LA ACTIVIDAD DE GLAST EN CÉLULAS GLIALES DE BEGMANN

INTRODUCCIÓN

Los desórdenes del espectro autista son un grupo de enfermedades del desarrollo que incluyen el desorden de Asperger, Autismo y los trastornos generalizados del desarrollo, los cuales comparten características como la insolvencia de habilidades de interacción social[106, 107]. Las características y el origen de estos padecimientos son muy diversos, ya que múltiples factores contribuyen a esta etiología, los principales factores son inmunológicos, ambientales y genético [107-109]. No solo la etiología es muy diversa sino también los síntomas y el comportamiento inadaptado de los paciente es muy variado. Los síntomas parecidos a déficit de atención e hiperactividad son muy comunes en pacientes con autismo, presentes en más de un tercio de los pacientes con este padecimiento. Este comportamiento generalmente es tratado con el uso de medicamentos estimulantes tales como el Metilfenidato (MPH) [110, 111].

A pesar del uso regular del MPH en padecimientos como el Autismo y otros trastornos del desarrollo, sus efectos son muy variables así como su eficacia y efectos adversos.

METILFENIDATO

Los efectos del MPH están claramente reportados con un aumento en los efectos de la dopamina (DA). Se ha caracterizado que el MPH incrementa los niveles extracelulares de DA en el corteza prefrontal, estriado núcleo accumbens y que incrementa también los niveles de así también norepinefrina (NE) en la corteza prefrontal pero no en el estriado y el núcleo accumbens[112]. También se ha encontrado que en estimula a neuronas piramidales al incrementar las concentraciones de catecolaminas[112]. En estudios realizados en humanos se ha demostrado que las concentraciones máximas alcanzadas en el cerebro después de una dosis

de MPH se alcanzan alrededor de 1 a 1.5 horas, momento en el cual los efectos de dicho fármaco comienzan a ser visibles[113].

Se ha demostrado que MPH bloquea los transportadores de DA lo que conlleva a un aumento en la señal inducida por DA, al activar a los receptores D1 en la post-sinapsis. También MPH puede actúa indirectamente evitando desensibilización D2 en los dominós pre-sinápticos, de las neuronas DA. Los efectos del MPH también se han asociado a la activación de los receptores α2 noradrenergicos (agonista)[114]. Existe evidencia que señala que el MPH también puede bloquear a los transportadores de NE de manera similar a la de los transportadores de DA (NET, Ki=0.10 µM, DAT, Ki=0.06µM) [115], varios investigadores sugieres que parte del efecto del MPH es mediado por el sistema noradrenergico [115-117].

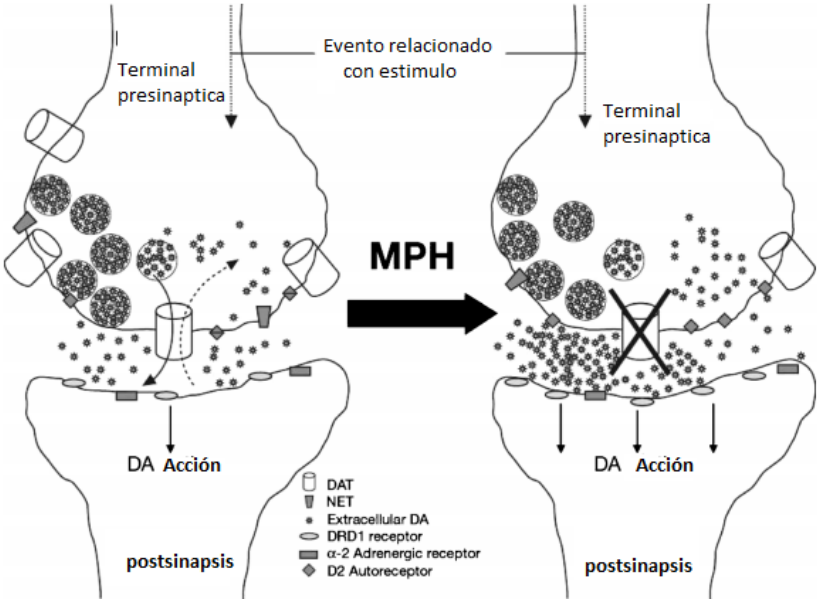

Figura 30. Modelo de acción del MPH sobre el sistema dopaminergico, La figura de la izquierda describe una sinapsis dopaminergica común a la derecha encontramos una neurona bajo el efecto del MPH. Se postula que el efecto del MPH es debido a un incremento de los niveles extracelulares de DA por diversos mecanismos, incluido el bloqueo de los transportadores de DA, evita la desensibilización de los receptores D2 en la presinapsis y la activación de los receptores D1 en la postsinapsis, lo que tiene como resultado final una amplificación de la señal de DA.

Aun menos conocido está el efecto sobre el sistema glutamatergico, en el cual hay un efecto de potenciación sobre la respuesta de los receptores NMDA. En este efecto se ha visto implicado el proteína Sigma-1 (σ1), este receptor se describió como un sub-tipo de receptor opioide. Este

receptor se encuentra generalmente en la post-sinapsis específicamente en la membrana del retículo endoplasmático y en la membrana plasmática. La activación de este receptor modula la entrada de calcio a través de la membrana plasmática (vía canales de K^+, receptores NMDA, canales de Ca^{2+} dependientes de voltaje) [118, 119].

JUSTIFICACIÓN

Debido al pobre entendimiento de los efectos del MPH el sistema glutamatergico y la importancia de este sistema sobre funciones superiores, es importante entender más afondo distintos mecanismos relacionados con el efecto de este estimulante.

OBJETIVO GENERAL

Caracterizar el efecto del MPH sobre la captura de Glu de células gliales de Bergmann

OBJETIVOS ESPECÍFICOS

- Determinar el efecto del Metilfenidato en la captura de Glu
- Determinar las constantes cinéticas de la captura de Glu en presencia de Metilfenidato
- Caracterizar la vía de señalización implicada en el efecto de Metilfenidato en la captura de Glu

RESULTADOS

Los resultados anteriores nos llevaron a un mayor entendimiento de la regulación del ciclo Glu/Gln y de sus distintos componentes tales como los transportadores de Glu y Gln, los cuales juegan un papel preponderante en la neurotransmisión glutamatergica. Con el conocimiento generado en los últimos años en el laboratorio ye hemos caracterizado el ciclo Glu/Gln en condiciones fisiológicas, sin embargo diversos grupos al igual que nosotros [120, 121] hemos propuesto los transportadores de Glu como blancos terapéuticos para el tratamiento de enfermedades neurológicas. Con esto en mente decidimos evaluar el efecto del MPH, un fármaco comúnmente utilizado en enfermedades del espectro autista así como tratamientos de déficit de atención, en la función de los transportadores de Glu en las CGB.

EL METILFENIDATO INDUCE UN AUMENTO EN LA CAPTURA DE GLU EN CGB.

La posibilidad que el MPH tenga un efecto sobre el sistema de neurotransmisión glutamatergico ha sido sugerido desde algún tiempo [121-123], a pesar de este hecho, los efectos sobre las CGB no han sido caracterizadas. Por tal motivo decidimos probar si el MPH era capaz de modular una función perfectamente caracterizada de las CGB, la captura de Glu.

Como lo muestra la Figura31, cuando el cultivo de CGB es tratado con MPH a una concentración de 100uM, existe un incremento en la captura de Asp después de 2h de tratamiento y el efecto se mantiene hasta las 12h. Con el fin de caracterizar el efecto desde una perspectiva farmacológica, decidimos exponer el cultivo celular de diferentes concentraciones de MPH (1, 10, 100, 1000 µM) por 1 y 4 h. Como se muestra el panel A y C de la Figura31, el efecto del MPH se presenta después de las 2 h de estímulo en dosis de 100 y 1000 µM.

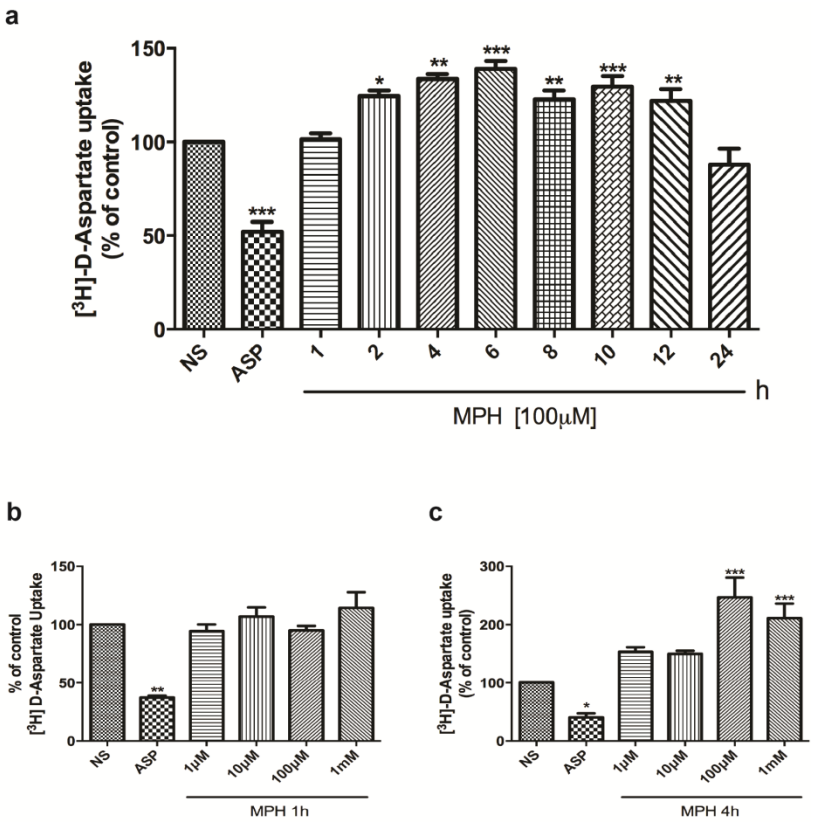

Figura 31. El MPH aumenta la actividad de GLAST. CGB se pre-incubaron con MPH a una concentración de 100 μM por el tiempo indicado (1, 2, 4, 6, 10, 12 o 24 h) (Panel A), o pre-incubados por 1 h (Panel B) o 4 h (Panel C) con concentraciones crecientes de MPH (1, 10, 100 o 1000 μM), la captura de [3H]-D-Asp se realizó durante 30 min. Como control del experimento las células se pre-incubaron durante 30 min con Glu 1mM.

MPH INDUCE UN INCREMENTO DEL TRANSPORTADOR GLAST EN LA MEMBRANA.

Con los resultados anteriores podemos inferir que existe un incremento en la actividad de GLAST, este efecto puede ser el resultado de un incremento en el número de transportadores de membrana o un cambio en la afinidad del transportador hacia su sustrato. Con el propósito de determinar este punto decidimos hacer un análisis de Michaelis-Menten de la captura de Glu en CGB tratadas con MPH. Como se muestra en la Figura32a, existe un incremento en el valor de Vmax cuando las células son tratados con MPH en comparación con las no tratadas (NS= 102.8±13.7 pmol/min*mg, MPH= 206.4±41.7 pmol/min*mg) lo cual no sucede con el valor

de la afinidad en el cual prácticamente no existe diferencia estadísticamente significativa alguno (Km= NS: 8.946±5.2 µM, MPH: 15.62±10.8 µM). Estos resultados sugieren que existe un incremento en el número de transportadores en la membrana. Con el objetivo de confirmar este resultado, medimos el número de transportadores de membrana a través de experimentos de unión de ligando radiactivo. Como se muestra en la Figura32b, el MPH incrementa el número de sitios de unión del Asp en membrana, un índice del número de moléculas de GLAST presentes en ese compartimento. Si realmente MPH está relacionado con el recambio de GLAST en membrana, el re-arregló del citoesqueleto es necesario, con eso en mente decidimos utilizar citocalasina B para bloquear el rearreglo del citoesqueleto y por ende en efecto del MPH. En la Figura32c se muestra como el pretratamiento de 30min con citocalasina B es suficiente para inhibir el efecto del MPH.

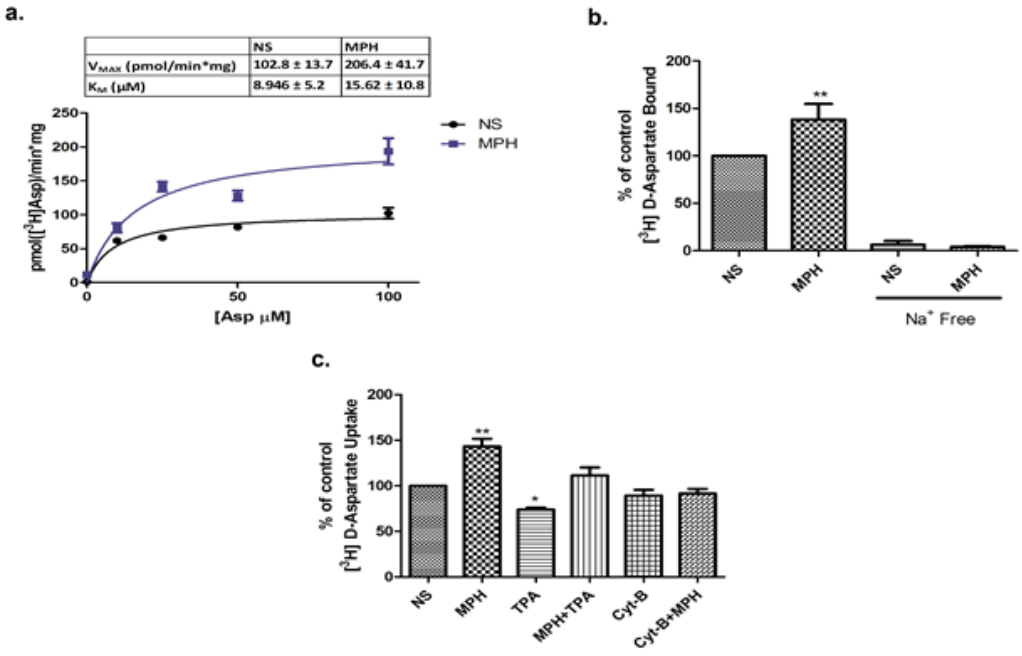

Figura 32. MPH incrementa la cantidad de moléculas de GLAST disponibles en la membrana plasmática. Panel A: CGB se pre-incubaron con MPH 100 µM (n) o con el vehículo (NS) (Ÿ) durante 4h y la captura de [3H]-D-Asp se realizó con concentraciones crecientes de D-Asp no marcado (0, 10, 25, 50 y 100 µM) durante 30 min. Panel B: Monocapas de CGB se estimularon con 100µM MPH durante 4 h en presencia o ausencia de Na+, según lo indica la figura. Después se realizó un ensayo de unión de [3H]-D-Asp a 4˚C. Panel C: CGB se pre-incubaron con 50 µM Citocalasina B, un inhibidor de la polimerización de los filamentos de actina, durante 30 min, después en el mismo medio se agregó 100 µM de MPH o del vehículo por 4h; la captura de [3H]-D-Asp se realizó durante 30 min a temperatura ambiente.

VÍAS DE SEÑALIZACIÓN IMPLICADAS EN EL AUMENTO DE LA CAPTURA DE GLU INDUCIDAS POR MPH

Resultados previos de nuestro en nuestro grupo de trabajo han demostrado que tanto la señalización a través de PKC y a través PKG son capases de regular la actividad de GLAST. En el caso de PKC, esta proteína induce una regulación negativa de la actividad de GLAST e incluso disminuye la expresión de su gen[23]. En contraste, la vía GMPc/PKG aumenta la actividad de GLAST de una manera muy similar a lo descrito por MPH [124]. Con esto en mente, decidimos pre-exponer al cultivo celular a los bloqueadores de PKC (Bis I) y de PKG (Rp-8-Br-PET-GMPc) y al activador de PKC (TPA) antes del tratamiento con MPH. Como se muestra en la Figura33 el inhibidor de PKG disminuyó ligeramente el efecto del MPH aunque no de manera significativa. Cuando ocupamos el bloqueador de PKC no se obtuvo ninguna respuesta en el efecto del MPH, sin embargo cuando ocupamos TPA se detectó un ligero efecto en el incremento de la captura de Glu inducido por MPH. En este punto no podemos descartar la posible participación tanto de PKG o PKC en la vía de señalización del MPH.

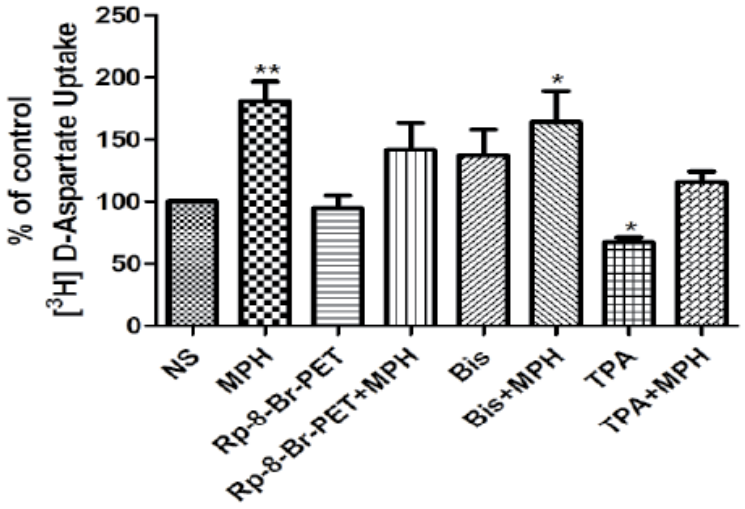

Figura 33. Papel de las cinasas PKC y PKG en el incremento de la actividad de GLAST dependiente de MPH. CGB fueron tratadas con 100 µM MPH durante 4 h en presencia o ausencia de los siguientes moduladores: el inhibidor de PKG, Rp-8-Br-PET a una concentración 10 µM, el inhibidor de PKC, Bisindolilmaleimida I a una concentración de 2 µM, o el activador de PKC, TPA a una concentración de 100 nM, los moduladores de las cinasas se colocaron 30 min antes de los tratamientos con MPH. La captura de [3H]-D-Asp se realizó durante 30 min.

Dado el hecho que el efecto del MPH es relativamente lento, su efecto se observa después de las 2 h, decidimos explorar la participación de la síntesis de proteínas en el efecto del MPH. Con este fin, preincubamos a las células con CHX un inhibidor de la síntesis de proteínas. Como se muestra en la Figura34, los tratamientos con CHX previenen el efecto del MPH, sugiriendo que MPH incrementa la tasa de traducción de GLAST. Para confirmar este puto decidimos medir los niveles totales de GLAST a distintos periodos de tiempo. Como se muestra en la Figura35A existe un claro incremento de GLAST en las células después de la exposición con MPH. Como último punto decidimos evaluar la posibilidad de que el aumento de la proteína GLAST esté involucrado un efecto a nivel de la transcripción para lo cual utilizamos ACT-D un inhibidor de la transcripción, como se muestra en la Figura34 el inhibidor no tiene ningún efecto sobre el efecto de MPH, para corroborar esto decidimos medir el RNAm de glast como se muestra en Figura35B, no se observa ningún cambio en los niveles del mensajero con lo cual corroboramos que la transcripción no está relacionada en el efecto del MPH pero si hay un aumento en la eficacia de la traducción de GLAST.

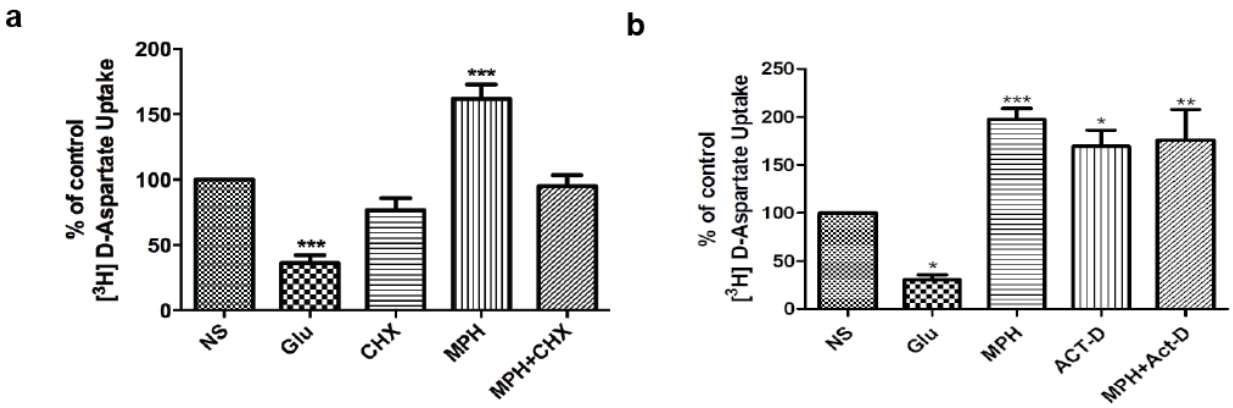

Figura 34. MPH incrementa la traducción de GLAST. CGB se pre-incubaron con 100 µM MPH durante 4h en presencia o ausencia del inhibidor de la síntesis de proteínas, cicloheximida (CHX) a una concentración de 1mM (Panel A) o en presencia o ausencia del inhibidor de la transcripción, Actinomicina D (ACT-D) a una concentración de 10 µg/mL (Panel B), la captura de [3H]-D-Asp se realizó durante 30 min. Como control del experimento CGB se pre-incubaron con 1mM de Glu durante 30 min.

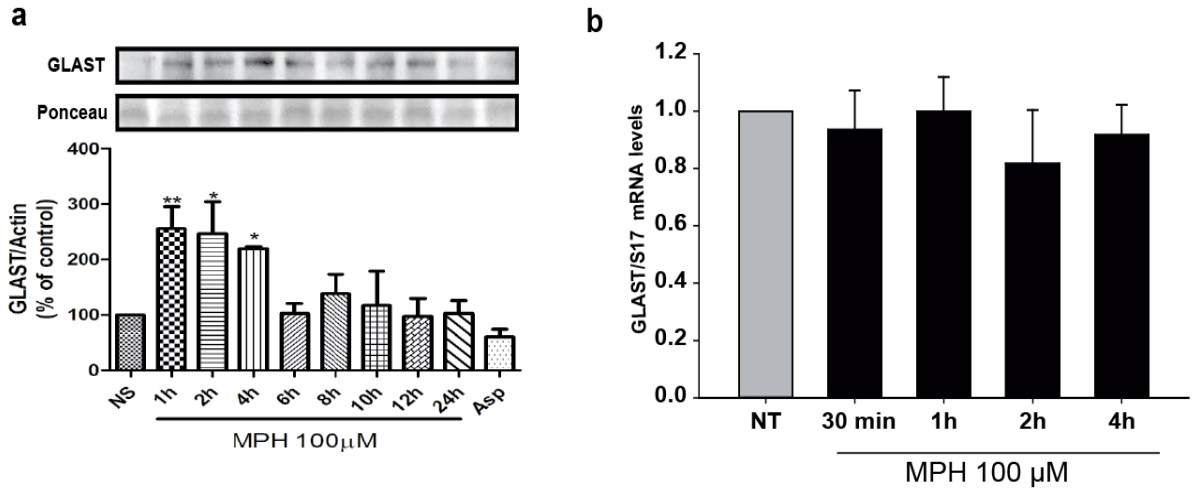

Figura 35. MPH incrementa los niveles proteicos de GLAST sin modificar los niveles de su RNAm. Panel A: Ensayos de RT-PCR cuantitativa se realizaron en cultivos primarios de CGB tratados o no con 100 µM MPH por los tiempos indicados, después de los tratamientos las células se cosecharon y colectaron. El RNAm se analizó utilizando cebadores específicos para Glast como se describe en la sección de métodos. Los niveles del RNAm de la proteína ribosomal S17 se utilizaron para normalizar. Panel B: Monocapas confluentes de CGB se expusieron a 100 µM MPH por los tiempos indicados. GLAST se detectó vía Inmunodetección en fase solida utilizando anticuerpos anti-GLAST 1:1000. Los niveles proteicos de Actina se utilizaron para normalizar. Tratamientos con 1mM D-Asp se utilizaron como control del experimento.

DISCUSIÓN

Después de trabajar en cuestiones fisiológicas, sobre distintos aspectos en la regulación del ciclo Glu/Gln. Decidimos realizar una aproximación a hacia una patología como es el caso del Autismo, debido a que los pacientes con autismo poseen una desregulación del en los niveles de Glu en sangre periférica [125]. De igual manera datos no publicados en el laboratorio muestran que los pacientes poseen una menor cantidad de GLT-1 y Glutamina Sintetasa. Debido a que hemos caracterizado a fondo el reciclamiento de Glu en nuestro modelo de estudio la CGB, las cuales juegan un papel primordial en regular los niveles extracelulares de Glu a través de GLAST y evitar la excitotoxicidad de las neuronas de Purkije, las cuales se ha demostrado que son un componente clave en padecimientos neurológicos [126, 127]. Nuestro modelo de estudio cobra una gran importancia cuanto lo ponemos en el contexto en el que la excitotoxicidad, la principal causa de la reducción en la densidad de células de Purkinje, por tal motivo es de suma importancia entender el efecto de medicamentos como el MPH pueden impactar los ciclos de regulación glutamatergica.

El MPH es una de las drogas más usadas para estimular el SNC, normalmente prescrita para tratar padecimientos como déficit de atención/desorden de hiperactividad, depresión, obesidad y desordenes del espectro autista. Aunque ha sido generalmente aceptado que MPH bloquea los transportadores de dopamina y por lo tanto incrementa los niveles intrasinapticos de dopamina [128], es claro que los efectos del MPH no se restringen a los transportadores de dopamina. Con esto en mente decidimos investigar una posible interacción entre el MPH con el sistema glutamatérgico, debido a que se ha descrito que esta droga es capaz de incrementar la respuesta de los receptores ionotrópicos glutamatergicos en neuronas dopaminergicas [129, 130]. Nosotros pensamos que si la cantidad de dopamina puede ser regulada por los receptores ionotrópicos glutamatérgicos en las neuronas dopaminérgicas, entonces es posible que el MPH pueda regular la disponibilidad de este neurotransmisor en la sinapsis, disponibilidad que es regulada por transportadores de glutamato específicos de células gliales.

Al exponer a nuestras células a concentraciones de 100 μM de MPH, observamos un incremento en la actividad de GLAST. Este efecto fue tiempo y dosis dependiente, fue un

fenómeno lento en comparación de los efectos antes descritos tales como el óxido nítrico o el mismo glutamato, este efecto inicio después de 2 horas y duro hasta 12 horas. El análisis de los parámetros cinéticos nos indica que el incremento en la actividad de GLAST es debido a un aumento del número de transportadores en membrana. Confirmamos este resultado a través del ensayo de unión de radio ligando, detectando un aumento en los sitios de unión específicos en tratamientos con MPH.

En este punto el incremento del número de Trasportadores en membrada es evidente, por lo tanto decidimos bloquear el movimiento del citoesqueleto utilizando citocalasina B. Como era de esperar, el efecto del MPH fue bloqueado completamente, lo que nos indica que necesariamente se requiere del movimiento del citoesqueleto para mover las vesículas que contiene a GLAST.

El siguiente paso que decidimos abordar fue, explorar las posibles rutas de señalización involucradas en el efecto de MPH. Primero decidimos analizar dos rutas de señalización implicadas en la regulación de GLAST las cuales ya hemos caracterizado con anterioridad. Aunque no hay evidencia concluyente, es probable la tanto PKC y PKG estén involucradas en el efecto de MPH. Interesantemente, mientras PKG está involucrado en el efecto del MPH, PKC bloquea dicho efecto. Para clarificar estos puntos es necesario realizar estudios más minuciosos.

El hecho de que CHX pero no actinomicina D bloquearan el efecto de MPH, no señala que hay un incremento en la traducción del mensajero de GLAST, junto con un incremento en el movimiento de GLAST a la membrana plasmática. Algo ligeramente diferente a lo reportado anteriormente cuando se trataba únicamente de la translocación del transportador tanto en el caso de un efecto inducido por ON o Glu. Lo que nos habré la puerta para futuras investigaciones con este fármaco y sus posibles implicaciones en el sistema de reciclaje del Glu.

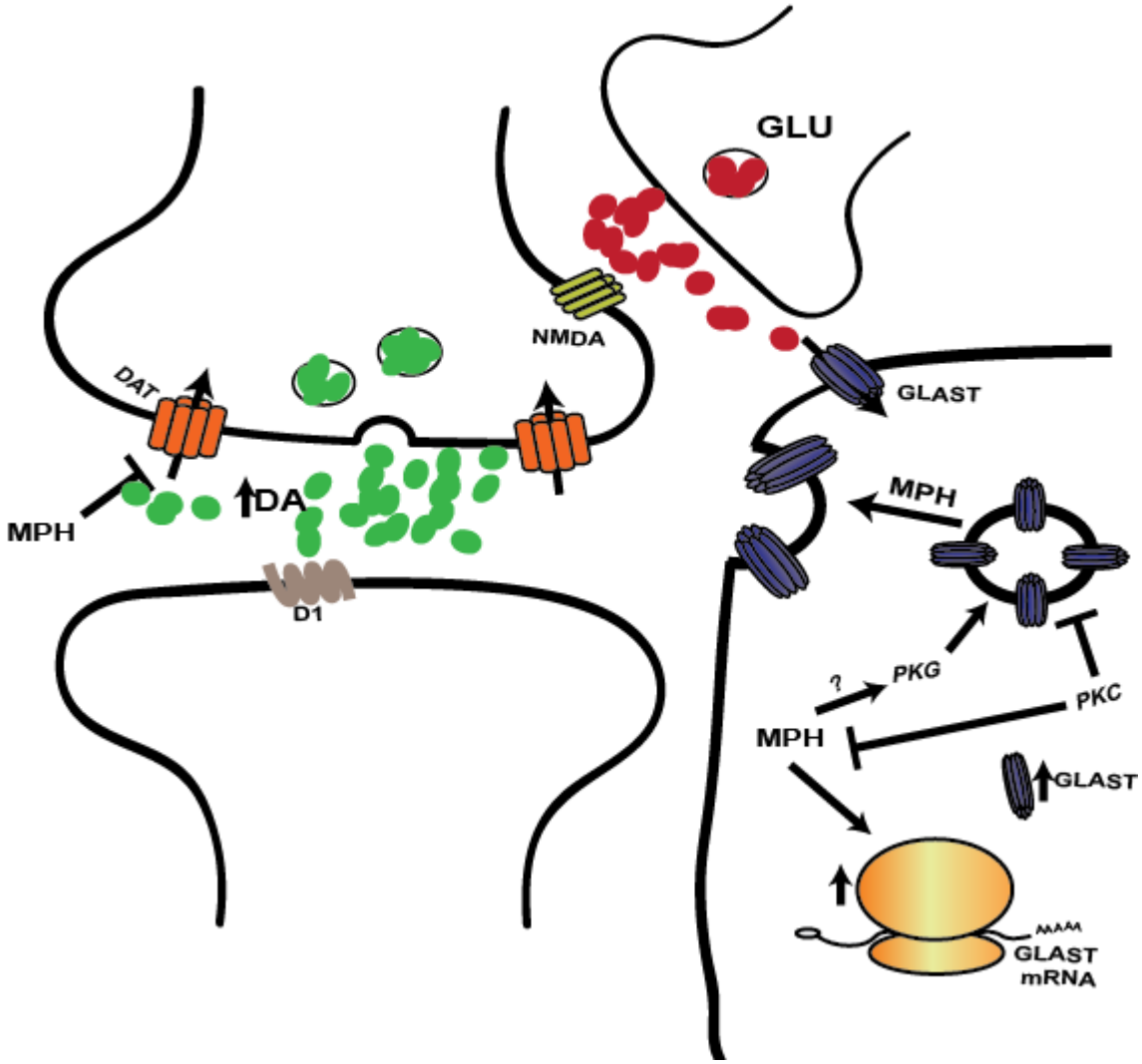

Figura 36. Modelo del efecto del MPH en la actividad de GLAST en CGB. El MPH regula la captura de glutamato a dos niveles, aumenta la traducción del RNAm de GLAST y aumenta la translocación de GLAST a la membrana plasmática, con una aparente participación de las cinasas PKG y PKC. Este modelo ilustra que además de regular a los transportadores de dopamina, el MPH también tiene como blanco a los transportadores de Glu en las células gliales, regulando la transmisión dopaminérgica así como la glutamatérgica.

CONCLUSIONES

- El Sistema N se expresa en células gliales de Bergmann y representa el 30% de la captura total de Gln
- SNAT3 y GLAST tienen un acople físico y funcional el cual es regulado por sus sustratos
- El óxido nítrico incrementa la translocación de GLAST a la membrana plasmática de células gliales de Bergmann a través de la vía GCs/GMPc/PKG
- La actividad del NCX es necesaria para la translocación de GLAST inducida por óxido nítrico
- El MPH aumenta la captura de Glu en células gliales de Bergmann incrementando el número de transportadores en la membrana plasmática
- Las cinasas PKG y PKC modulan el efecto del MPH en células gliales de Bergmann
- La CHX abate el efecto del MPH en células gliales de Bergmann

BIBLIOGRAFÍA

1. Watkins JC, Evans RH. Excitatory amino acid transmitters. Annu Rev Pharmacol Toxicol. 1981; **21**: 165-204.
2. Oja SS, Piha RS. Changes in the concentration of free amino acids in the rat brain during postnatal development. Life Sci. 1966; **5**(10): 865-70.
3. Stone TW. Glutamate as the neurotransmitter of cerebellar granule cells in the rat: electrophysiological evidence. Br J Pharmacol. 1979; **66**(2): 291-6.
4. Curtis DR, Watkins JC. Acidic amino acids with strong excitatory actions on mammalian neurones. J Physiol. 1963; **166**: 1-14.
5. Meldrum BS. Glutamate as a neurotransmitter in the brain: review of physiology and pathology. J Nutr. 2000; **130**(4S Suppl): 1007S-15S.
6. Sonnewald U, Westergaard N, Hassel B, Muller TB, Unsgard G, Fonnum F, et al. NMR spectroscopic studies of 13C acetate and 13C glucose metabolism in neocortical astrocytes: evidence for mitochondrial heterogeneity. Dev Neurosci. 1993; **15**(3-5): 351-8.
7. McKenna MC. The glutamate-glutamine cycle is not stoichiometric: fates of glutamate in brain. J Neurosci Res. 2007; **85**(15): 3347-58.
8. Hollmann M, Heinemann S. Cloned glutamate receptors. Annu Rev Neurosci. 1994; **17**: 31-108.
9. Rondard P, Pin JP. Dynamics and modulation of metabotropic glutamate receptors. Curr Opin Pharmacol. 2015; **20**: 95-101.
10. Moepps B, Fagni L. Mont Sainte-Odile: a sanctuary for GPCRs. Confidence on signal transduction of G-protein-couple receptors. EMBO Rep. 2003; **4**(3): 237-43.
11. Ribeiro FM, Paquet M, Cregan SP, Ferguson SS. Group I metabotropic glutamate receptor signalling and its implication in neurological disease. CNS Neurol Disord Drug Targets. 2010; **9**(5): 574-95.
12. Nakanishi S, Nakajima Y, Masu M, Ueda Y, Nakahara K, Watanabe D, et al. Glutamate receptors: brain function and signal transduction. Brain Res Brain Res Rev. 1998; **26**(2-3): 230-5.
13. Ozawa S, Kamiya H, Tsuzuki K. Glutamate receptors in the mammalian central nervous system. Prog Neurobiol. 1998; **54**(5): 581-618.
14. Goudet C, Magnaghi V, Landry M, Nagy F, Gereau RWt, Pin JP. Metabotropic receptors for glutamate and GABA in pain. Brain Res Rev. 2009; **60**(1): 43-56.
15. Madden DR. The structure and function of glutamate receptor ion channels. Nat Rev Neurosci. 2002; **3**(2): 91-101.
16. Jin R, Singh SK, Gu S, Furukawa H, Sobolevsky AI, Zhou J, et al. Crystal structure and association behaviour of the GluR2 amino-terminal domain. EMBO J. 2009; **28**(12): 1812-23.
17. Willard SS, Koochekpour S. Glutamate, glutamate receptors, and downstream signaling pathways. Int J Biol Sci. 2013; **9**(9): 948-59.
18. Bassani S, Valnegri P, Beretta F, Passafaro M. The GLUR2 subunit of AMPA receptors: synaptic role. Neuroscience. 2009; **158**(1): 55-61.
19. Yang CR, Svensson KA. Allosteric modulation of NMDA receptor via elevation of brain glycine and D-serine: the therapeutic potentials for schizophrenia. Pharmacol Ther. 2008; **120**(3): 317-32.
20. Madden K. NMDA receptor antagonists and glycine site NMDA antagonists. Curr Med Res Opin. 2002; **18 Suppl 2**: s27-31.
21. Danbolt NC. Glutamate uptake. Prog Neurobiol. 2001; **65**(1): 1-105.
22. Johnston GAR. Glutamate uptake and its possible role in neurotransmitter inactivation. Wiley, Chichester, UK. 1981: 77-87.
23. Lopez-Bayghen E, Ortega A. Glutamate-dependent transcriptional regulation of GLAST: role of PKC. J Neurochem. 2004; **91**(1): 200-9.

24. Dias RB, Ribeiro JA, Sebastiao AM. Enhancement of AMPA currents and GluR1 membrane expression through PKA-coupled adenosine A(2A) receptors. Hippocampus. 2012; **22**(2): 276-91.
25. Pochini L, Scalise M, Galluccio M, Indiveri C. Membrane transporters for the special amino acid glutamine: structure/function relationships and relevance to human health. Front Chem. 2014; **2**: 61.
26. Broer S, Brookes N. Transfer of glutamine between astrocytes and neurons. J Neurochem. 2001; **77**(3): 705-19.
27. Kanai Y, Hediger MA. The glutamate/neutral amino acid transporter family SLC1: molecular, physiological and pharmacological aspects. Pflugers Arch. 2004; **447**(5): 469-79.
28. Utsunomiya-Tate N, Endou H, Kanai Y. Cloning and functional characterization of a system ASC-like Na+-dependent neutral amino acid transporter. J Biol Chem. 1996; **271**(25): 14883-90.
29. Zerangue N, Kavanaugh MP. ASCT-1 is a neutral amino acid exchanger with chloride channel activity. J Biol Chem. 1996; **271**(45): 27991-4.
30. Zhang Y, Kanner BI. Two serine residues of the glutamate transporter GLT-1 are crucial for coupling the fluxes of sodium and the neurotransmitter. Proc Natl Acad Sci U S A. 1999; **96**(4): 1710-5.
31. Kavanaugh MP, Bendahan A, Zerangue N, Zhang Y, Kanner BI. Mutation of an amino acid residue influencing potassium coupling in the glutamate transporter GLT-1 induces obligate exchange. J Biol Chem. 1997; **272**(3): 1703-8.
32. Wu VW, Nishiyama N, Schwartz JP. A culture model of reactive astrocytes: increased nerve growth factor synthesis and reexpression of cytokine responsiveness. J Neurochem. 1998; **71**(2): 749-56.
33. Palmada M, Speil A, Jeyaraj S, Bohmer C, Lang F. The serine/threonine kinases SGK1, 3 and PKB stimulate the amino acid transporter ASCT2. Biochem Biophys Res Commun. 2005; **331**(1): 272-7.
34. Avissar NE, Sax HC, Toia L. In human entrocytes, GLN transport and ASCT2 surface expression induced by short-term EGF are MAPK, PI3K, and Rho-dependent. Dig Dis Sci. 2008; **53**(8): 2113-25.
35. Fotiadis D, Kanai Y, Palacin M. The SLC3 and SLC7 families of amino acid transporters. Mol Aspects Med. 2013; **34**(2-3): 139-58.
36. Fraga S, Pinho MJ, Soares-da-Silva P. Expression of LAT1 and LAT2 amino acid transporters in human and rat intestinal epithelial cells. Amino Acids. 2005; **29**(3): 229-33.
37. del Amo EM, Urtti A, Yliperttula M. Pharmacokinetic role of L-type amino acid transporters LAT1 and LAT2. Eur J Pharm Sci. 2008; **35**(3): 161-74.
38. Bode BP. Recent molecular advances in mammalian glutamine transport. J Nutr. 2001; **131**(9 Suppl): 2475S-85S; discussion 86S-7S.
39. Walker DK, Drummond MJ, Dickinson JM, Borack MS, Jennings K, Volpi E, et al. Insulin increases mRNA abundance of the amino acid transporter SLC7A5/LAT1 via an mTORC1-dependent mechanism in skeletal muscle cells. Physiol Rep. 2014; **2**(3): e00238.
40. Kurayama R, Ito N, Nishibori Y, Fukuhara D, Akimoto Y, Higashihara E, et al. Role of amino acid transporter LAT2 in the activation of mTORC1 pathway and the pathogenesis of crescentic glomerulonephritis. Lab Invest. 2011; **91**(7): 992-1006.
41. Hamdi MM, Mutungi G. Dihydrotestosterone stimulates amino acid uptake and the expression of LAT2 in mouse skeletal muscle fibres through an ERK1/2-dependent mechanism. J Physiol. 2011; **589**(Pt 14): 3623-40.
42. Handlogten ME, Barber EF, Bracy DS, Kilberg MS. Amino acid-dependent inactivation of glucagon-induced System A transport activity in cultured rat hepatocytes. Mol Cell Endocrinol. 1985; **43**(1): 61-9.
43. Conti F, Melone M. The glutamine commute: lost in the tube? Neurochem Int. 2006; **48**(6-7): 459-64.
44. Wiedenmann B, Franke WW. Identification and localization of synaptophysin, an integral membrane glycoprotein of Mr 38,000 characteristic of presynaptic vesicles. Cell. 1985; **41**(3): 1017-28.

45. Reimer RJ, Chaudhry FA, Gray AT, Edwards RH. Amino acid transport system A resembles system N in sequence but differs in mechanism. Proc Natl Acad Sci U S A. 2000; **97**(14): 7715-20.
46. Varoqui H, Zhu H, Yao D, Ming H, Erickson JD. Cloning and functional identification of a neuronal glutamine transporter. J Biol Chem. 2000; **275**(6): 4049-54.
47. Ogura M, Taniura H, Nakamichi N, Yoneda Y. Upregulation of the glutamine transporter through transactivation mediated by cAMP/protein kinase A signals toward exacerbation of vulnerability to oxidative stress in rat neocortical astrocytes. J Cell Physiol. 2007; **212**(2): 375-85.
48. Palii SS, Chen H, Kilberg MS. Transcriptional control of the human sodium-coupled neutral amino acid transporter system A gene by amino acid availability is mediated by an intronic element. J Biol Chem. 2004; **279**(5): 3463-71.
49. Kilberg MS, Handlogten ME, Christensen HN. Characteristics of an amino acid transport system in rat liver for glutamine, asparagine, histidine, and closely related analogs. J Biol Chem. 1980; **255**(9): 4011-9.
50. Chaudhry FA, Reimer RJ, Krizaj D, Barber D, Storm-Mathisen J, Copenhagen DR, et al. Molecular analysis of system N suggests novel physiological roles in nitrogen metabolism and synaptic transmission. Cell. 1999; **99**(7): 769-80.
51. McGivan JD, Bungard CI. The transport of glutamine into mammalian cells. Front Biosci. 2007; **12**: 874-82.
52. Nakanishi T, Hatanaka T, Huang W, Prasad PD, Leibach FH, Ganapathy ME, et al. Na+- and Cl--coupled active transport of carnitine by the amino acid transporter ATB(0,+) from mouse colon expressed in HRPE cells and Xenopus oocytes. J Physiol. 2001; **532**(Pt 2): 297-304.
53. Hagglund MG, Sreedharan S, Nilsson VC, Shaik JH, Almkvist IM, Backlin S, et al. Identification of SLC38A7 (SNAT7) protein as a glutamine transporter expressed in neurons. J Biol Chem. 2011; **286**(23): 20500-11.
54. Deitmer JW, Broer A, Broer S. Glutamine efflux from astrocytes is mediated by multiple pathways. J Neurochem. 2003; **87**(1): 127-35.
55. Mackenzie B, Erickson JD. Sodium-coupled neutral amino acid (System N/A) transporters of the SLC38 gene family. Pflugers Arch. 2004; **447**(5): 784-95.
56. Allen NJ, Barres BA. Neuroscience: Glia - more than just brain glue. Nature. 2009; **457**(7230): 675-7.
57. Kandel ER, Schwartz JH, Jessell TM. Principles of neural science. 4th ed. ed. New York ; London: McGraw-Hill, Health Professions Division; 2000.
58. Lopez-Bayghen E, Ortega A. [Glial cells and synaptic activity: translational control of metabolic coupling]. Rev Neurol. 2010; **50**(10): 607-15.
59. Lopez-Bayghen E, Rosas S, Castelan F, Ortega A. Cerebellar Bergmann glia: an important model to study neuron-glia interactions. Neuron Glia Biol. 2007; **3**(2): 155-67.
60. Espinoza-Rojo M, Lopez-Bayghen E, Ortega A. GLAST: gene expression regulation by phorbol esters. Neuroreport. 2000; **11**(12): 2827-32.
61. Aguirre G, Rosas S, Lopez-Bayghen E, Ortega A. Valproate-dependent transcriptional regulation of GLAST/EAAT1 expression: involvement of Ying-Yang 1. Neurochem Int. 2008; **52**(7): 1322-31.
62. Barrera I, Flores-Mendez M, Hernandez-Kelly LC, Cid L, Huerta M, Zinker S, et al. Glutamate regulates eEF1A phosphorylation and ribosomal transit time in Bergmann glial cells. Neurochem Int. 2010; **57**(7): 795-803.
63. Aguirre A, Lopez-Bayghen E, Ortega A. Glutamate-dependent transcriptional regulation of the chkbp gene: signaling mechanisms. J Neurosci Res. 2002; **70**(1): 117-27.
64. Mendez JA, Lopez-Bayghen E, Ortega A. Glutamate activation of Oct-2 in cultured chick Bergmann glia cells: involvement of NFkappaB. J Neurosci Res. 2005; **81**(1): 21-30.

65. Taylor S, Srinivasan B, Wordinger RJ, Roque RS. Glutamate stimulates neurotrophin expression in cultured Muller cells. Brain Res Mol Brain Res. 2003; **111**(1-2): 189-97.
66. Kvamme OJ, Olesen F, Samuelson M. Improving the interface between primary and secondary care: a statement from the European Working Party on Quality in Family Practice (EQuiP). Qual Health Care. 2001; **10**(1): 33-9.
67. McKenna MC, Tildon JT, Stevenson JH, Huang X. New insights into the compartmentation of glutamate and glutamine in cultured rat brain astrocytes. Dev Neurosci. 1996; **18**(5-6): 380-90.
68. Yudkoff M, Daikhin Y, Lin ZP, Nissim I, Stern J, Pleasure D. Interrelationships of leucine and glutamate metabolism in cultured astrocytes. J Neurochem. 1994; **62**(3): 1192-202.
69. Cerdan S, Kunnecke B, Seelig J. Cerebral metabolism of [1,2-13C2]acetate as detected by in vivo and in vitro 13C NMR. J Biol Chem. 1990; **265**(22): 12916-26.
70. Waagepetersen HS, Qu H, Hertz L, Sonnewald U, Schousboe A. Demonstration of pyruvate recycling in primary cultures of neocortical astrocytes but not in neurons. Neurochem Res. 2002; **27**(11): 1431-7.
71. Rodriguez A, Ortega A, Berumen LC, Garcia-Alcocer MG, Gimenez C, Zafra F. Expression of the System N transporter (SNAT5/SN2) during development indicates its plausible role in glutamatergic neurotransmission. Neurochem Int. 2014; **73**: 166-71.
72. Boulland JL, Rafiki A, Levy LM, Storm-Mathisen J, Chaudhry FA. Highly differential expression of SN1, a bidirectional glutamine transporter, in astroglia and endothelium in the developing rat brain. Glia. 2003; **41**(3): 260-75.
73. Somogyi P, Eshhar N, Teichberg VI, Roberts JD. Subcellular localization of a putative kainate receptor in Bergmann glial cells using a monoclonal antibody in the chick and fish cerebellar cortex. Neuroscience. 1990; **35**(1): 9-30.
74. Ottersen OP, Landsend AS. Organization of glutamate receptors at the synapse. Eur J Neurosci. 1997; **9**(11): 2219-24.
75. Ottersen OP, Chaudhry FA, Danbolt NC, Laake JH, Nagelhus EA, Storm-Mathisen J, et al. Molecular organization of cerebellar glutamate synapses. Prog Brain Res. 1997; **114**: 97-107.
76. Ruiz M, Ortega A. Characterization of an Na(+)-dependent glutamate/aspartate transporter from cultured Bergmann glia. Neuroreport. 1995; **6**(15): 2041-4.
77. Araque A, Parpura V, Sanzgiri RP, Haydon PG. Tripartite synapses: glia, the unacknowledged partner. Trends Neurosci. 1999; **22**(5): 208-15.
78. Haydon PG, Blendy J, Moss SJ, Rob Jackson F. Astrocytic control of synaptic transmission and plasticity: a target for drugs of abuse? Neuropharmacology. 2009; **56 Suppl 1**: 83-90.
79. Bak LK, Schousboe A, Waagepetersen HS. The glutamate/GABA-glutamine cycle: aspects of transport, neurotransmitter homeostasis and ammonia transfer. J Neurochem. 2006; **98**(3): 641-53.
80. Magistretti PJ. Role of glutamate in neuron-glia metabolic coupling. Am J Clin Nutr. 2009; **90**(3): 875S-80S.
81. Balakrishnan S, Bellamy TC. Depression of parallel and climbing fiber transmission to Bergmann glia is input specific and correlates with increased precision of synaptic transmission. Glia. 2009; **57**(4): 393-401.
82. Cubelos B, Gonzalez-Gonzalez IM, Gimenez C, Zafra F. Amino acid transporter SNAT5 localizes to glial cells in the rat brain. Glia. 2005; **49**(2): 230-44.
83. Chaudhry FA, Krizaj D, Larsson P, Reimer RJ, Wreden C, Storm-Mathisen J, et al. Coupled and uncoupled proton movement by amino acid transport system N. EMBO J. 2001; **20**(24): 7041-51.
84. Broer A, Deitmer JW, Broer S. Astroglial glutamine transport by system N is upregulated by glutamate. Glia. 2004; **48**(4): 298-310.
85. Furchgott RF, Zawadzki JV. The obligatory role of endothelial cells in the relaxation of arterial smooth muscle by acetylcholine. Nature. 1980; **288**(5789): 373-6.

86. Palmer RM, Ferrige AG, Moncada S. Nitric oxide release accounts for the biological activity of endothelium-derived relaxing factor. Nature. 1987; **327**(6122): 524-6.
87. Newman EA. Glial cell regulation of neuronal activity and blood flow in the retina by release of gliotransmitters. Philos Trans R Soc Lond B Biol Sci. 2015; **370**(1672).
88. Yuste JE, Tarragon E, Campuzano CM, Ros-Bernal F. Implications of glial nitric oxide in neurodegenerative diseases. Front Cell Neurosci. 2015; **9**: 322.
89. Knowles RG, Palacios M, Palmer RM, Moncada S. Formation of nitric oxide from L-arginine in the central nervous system: a transduction mechanism for stimulation of the soluble guanylate cyclase. Proc Natl Acad Sci U S A. 1989; **86**(13): 5159-62.
90. Deguchi T, Yoshioka M. L-Arginine identified as an endogenous activator for soluble guanylate cyclase from neuroblastoma cells. J Biol Chem. 1982; **257**(17): 10147-51.
91. Arnold WP, Mittal CK, Katsuki S, Murad F. Nitric oxide activates guanylate cyclase and increases guanosine 3':5'-cyclic monophosphate levels in various tissue preparations. Proc Natl Acad Sci U S A. 1977; **74**(8): 3203-7.
92. Wiesinger H. Arginine metabolism and the synthesis of nitric oxide in the nervous system. Prog Neurobiol. 2001; **64**(4): 365-91.
93. Mukherjee P, Cinelli MA, Kang S, Silverman RB. Development of nitric oxide synthase inhibitors for neurodegeneration and neuropathic pain. Chem Soc Rev. 2014; **43**(19): 6814-38.
94. Ferrendelli JA, Chang MM, Kinscherf DA. Elevation of cyclic GMP levels in central nervous system by excitatory and inhibitory amino acids. J Neurochem. 1974; **22**(4): 535-40.
95. de Vente J, Bol JG, Steinbusch HW. Localization of cGMP in the cerebellum of the adult rat: an immunohistochemical study. Brain Res. 1989; **504**(2): 332-7.
96. De Vente J, Bol JG, Berkelmans HS, Schipper J, Steinbusch HM. Immunocytochemistry of cGMP in the Cerebellum of the Immature, Adult, and Aged Rat: the Involvement of Nitric Oxide. A Micropharmacological Study. Eur J Neurosci. 1990; **2**(10): 845-62.
97. Allen BW, Demchenko IT, Piantadosi CA. Two faces of nitric oxide: implications for cellular mechanisms of oxygen toxicity. J Appl Physiol (1985). 2009; **106**(2): 662-7.
98. Tschetter WW, Alam NM, Yee CW, Gorz M, Douglas RM, Sagdullaev B, et al. Experience-enabled enhancement of adult visual cortex function. J Neurosci. 2013; **33**(12): 5362-6.
99. Wang V, Chuang TC, Hsu YD, Chou WY, Kao MC. Nitric oxide induces prion protein via MEK and p38 MAPK signaling. Biochem Biophys Res Commun. 2005; **333**(1): 95-100.
100. Wang HG, Lu FM, Jin I, Udo H, Kandel ER, de Vente J, et al. Presynaptic and postsynaptic roles of NO, cGK, and RhoA in long-lasting potentiation and aggregation of synaptic proteins. Neuron. 2005; **45**(3): 389-403.
101. Linden DJ, Dawson TM, Dawson VL. An evaluation of the nitric oxide/cGMP/cGMP-dependent protein kinase cascade in the induction of cerebellar long-term depression in culture. J Neurosci. 1995; **15**(7 Pt 2): 5098-105.
102. Kitao T, Takuma K, Kawasaki T, Inoue Y, Ikehara A, Nashida T, et al. The Na+/Ca2+ exchanger-mediated Ca2+ influx triggers nitric oxide-induced cytotoxicity in cultured astrocytes. Neurochem Int. 2010; **57**(1): 58-66.
103. Tzingounis AV, Wadiche JI. Glutamate transporters: confining runaway excitation by shaping synaptic transmission. Nat Rev Neurosci. 2007; **8**(12): 935-47.
104. Takayasu Y, Iino M, Ozawa S. Roles of glutamate transporters in shaping excitatory synaptic currents in cerebellar Purkinje cells. Eur J Neurosci. 2004; **19**(5): 1285-95.
105. Conradt M, Stoffel W. Inhibition of the high-affinity brain glutamate transporter GLAST-1 via direct phosphorylation. J Neurochem. 1997; **68**(3): 1244-51.
106. Geschwind DH. Advances in autism. Annu Rev Med. 2009; **60**: 367-80.
107. Muhle R, Trentacoste SV, Rapin I. The genetics of autism. Pediatrics. 2004; **113**(5): e472-86.

108. Wills S, Cabanlit M, Bennett J, Ashwood P, Amaral D, Van de Water J. Autoantibodies in autism spectrum disorders (ASD). Ann N Y Acad Sci. 2007; **1107**: 79-91.
109. Dalton P, Deacon R, Blamire A, Pike M, McKinlay I, Stein J, et al. Maternal neuronal antibodies associated with autism and a language disorder. Ann Neurol. 2003; **53**(4): 533-7.
110. Aman MG. Treatment planning for patients with autism spectrum disorders. J Clin Psychiatry. 2005; **66 Suppl 10**: 38-45.
111. Esbensen AJ, Greenberg JS, Seltzer MM, Aman MG. A longitudinal investigation of psychotropic and non-psychotropic medication use among adolescents and adults with autism spectrum disorders. J Autism Dev Disord. 2009; **39**(9): 1339-49.
112. Bymaster FP, Katner JS, Nelson DL, Hemrick-Luecke SK, Threlkeld PG, Heiligenstein JH, et al. Atomoxetine increases extracellular levels of norepinephrine and dopamine in prefrontal cortex of rat: a potential mechanism for efficacy in attention deficit/hyperactivity disorder. Neuropsychopharmacology. 2002; **27**(5): 699-711.
113. Volkow ND, Fowler JS, Wang G, Ding Y, Gatley SJ. Mechanism of action of methylphenidate: insights from PET imaging studies. J Atten Disord. 2002; **6 Suppl 1**: S31-43.
114. Andrews GD, Lavin A. Methylphenidate increases cortical excitability via activation of alpha-2 noradrenergic receptors. Neuropsychopharmacology. 2006; **31**(3): 594-601.
115. Han DD, Gu HH. Comparison of the monoamine transporters from human and mouse in their sensitivities to psychostimulant drugs. BMC Pharmacol. 2006; **6**: 6.
116. Kim CH, Hahn MK, Joung Y, Anderson SL, Steele AH, Mazei-Robinson MS, et al. A polymorphism in the norepinephrine transporter gene alters promoter activity and is associated with attention-deficit hyperactivity disorder. Proc Natl Acad Sci U S A. 2006; **103**(50): 19164-9.
117. Kuczenski R, Segal DS. Locomotor effects of acute and repeated threshold doses of amphetamine and methylphenidate: relative roles of dopamine and norepinephrine. J Pharmacol Exp Ther. 2001; **296**(3): 876-83.
118. Itzhak Y. Repeated methamphetamine-treatment alters brain sigma receptors. Eur J Pharmacol. 1993; **230**(2): 243-4.
119. Takahashi S, Miwa T, Horikomi K. Involvement of sigma 1 receptors in methamphetamine-induced behavioral sensitization in rats. Neurosci Lett. 2000; **289**(1): 21-4.
120. Cvetanovic M. Decreased expression of glutamate transporter GLAST in bergmann glia is associated with the loss of Purkinje neurons in the spinocerebellar ataxia type 1. Cerebellum. 2015; **14**(1): 8-11.
121. Martinez-Lozada Z, Guillem AM, Flores-Mendez M, Hernandez-Kelly LC, Vela C, Meza E, et al. GLAST/EAAT1-induced glutamine release via SNAT3 in Bergmann glial cells: evidence of a functional and physical coupling. J Neurochem. 2013; **125**(4): 545-54.
122. Zhang CL, Feng ZJ, Liu Y, Ji XH, Peng JY, Zhang XH, et al. Methylphenidate enhances NMDA-receptor response in medial prefrontal cortex via sigma-1 receptor: a novel mechanism for methylphenidate action. PLoS One. 2012; **7**(12): e51910.
123. Ortega A, Eshhar N, Teichberg VI. Properties of kainate receptor/channels on cultured Bergmann glia. Neuroscience. 1991; **41**(2-3): 335-49.
124. Balderas A, Guillem AM, Martinez-Lozada Z, Hernandez-Kelly LC, Aguilera J, Ortega A. GLAST/EAAT1 regulation in cultured Bergmann glia cells: role of the NO/cGMP signaling pathway. Neurochem Int. 2014; **73**: 139-45.
125. Shinohe A, Hashimoto K, Nakamura K, Tsujii M, Iwata Y, Tsuchiya KJ, et al. Increased serum levels of glutamate in adult patients with autism. Prog Neuropsychopharmacol Biol Psychiatry. 2006; **30**(8): 1472-7.
126. Palmen SJ, van Engeland H, Hof PR, Schmitz C. Neuropathological findings in autism. Brain. 2004; **127**(Pt 12): 2572-83.

127. Courchesne E. Brainstem, cerebellar and limbic neuroanatomical abnormalities in autism. Curr Opin Neurobiol. 1997; **7**(2): 269-78.
128. Mergy MA, Gowrishankar R, Davis GL, Jessen TN, Wright J, Stanwood GD, et al. Genetic targeting of the amphetamine and methylphenidate-sensitive dopamine transporter: on the path to an animal model of attention-deficit hyperactivity disorder. Neurochem Int. 2014; **73**: 56-70.
129. Prieto-Gomez B, Vazquez-Alvarez AM, Martinez-Pena JL, Reyes-Vazquez C, Yang PB, Dafny N. Methylphenidate and amphetamine modulate differently the NMDA and AMPA glutamatergic transmission of dopaminergic neurons in the ventral tegmental area. Life Sci. 2005; **77**(6): 635-49.
130. Di Miceli M, Gronier B. Psychostimulants and atomoxetine alter the electrophysiological activity of prefrontal cortex neurons, interaction with catecholamine and glutamate NMDA receptors. Psychopharmacology (Berl). 2015; **232**(12): 2191-205.

ANEXOS

Neurochemistry International 59 (2011) 1133–1144

Contents lists available at SciVerse ScienceDirect

Neurochemistry International

journal homepage: www.elsevier.com/locate/nci

Brain-derived neurotrophic factor and its receptors in Bergmann glia cells

Irais Poblete-Naredo [a], Alain M. Guillem [a], Claudia Juárez [b], Rossana C. Zepeda [b], Leticia Ramírez [a], Mario Caba [b], Luisa C. Hernández-Kelly [a,c], José Aguilera [c], Esther López-Bayghen [a], Arturo Ortega [a,*]

[a] Departamento de Genética y Biología Molecular, Centro de Investigación y de Estudios Avanzados del Instituto Politécnico Nacional, Apartado Postal 14-740, México D.F. 07000, Mexico
[b] Centro de Investigaciones Biomédicas, Universidad Veracruzana, Apartado Postal 114, Xalapa, Veracruz 91000, Mexico
[c] Institut de Neurociénces i Department de Bioquímica i Biología Molecular, Universitat Autònoma de Barcelona, Cerdanyola del Vallès, Spain

ARTICLE INFO

Article history:
Received 7 June 2011
Received in revised form 27 September 2011
Accepted 9 October 2011
Available online 14 October 2011

Keywords:
BDNF
Bergmann glia
Transcriptional control

ABSTRACT

Brain-derived neurotrophic factor is an abundant and widely distributed neurotrophin expressed in the Central Nervous System. It is critically involved in neuronal differentiation and survival. The expression of brain-derived neurotrophic factor and that of its catalytic active cognate receptor (TrkB) has been extensively studied in neuronal cells but their expression and function in glial cells is still controversial. Despite of this fact, brain-derived neurotrophic factor is released from astrocytes upon glutamate stimulation. A suitable model to study glia/neuronal interactions, in the context of glutamatergic synapses, is the well-characterized culture of chick cerebellar Bergmann glia cells. Using, this system, we show here that BDNF and its functional receptor are present in Bergmann glia and that BDNF stimulation is linked to the activation of the phosphatidyl-inositol 3 kinase/protein kinase C/mitogen-activated protein kinase/Activator Protein-1 signaling pathway. Accordingly, reverse transcription-polymerase chain reaction (RT-PCR) experiments predicted the expression of full-length and truncated TrkB isoforms. Our results suggest that Bergmann glia cells are able to express and respond to BDNF stimulation favoring the notion of their pivotal role in neuroprotection.

1. Introduction

Neurotrophins are low molecular weight proteins that promote survival, development and neuronal differentiation. To date, this family of factors is composed of four members identified as nerve growth factor (NGF), brain-derived neurotrophic factor (BDNF), neurotrophin-3 (NT-3) and neurotrophin 4-5 (NT-4/5). BDNF is a small basic protein highly conserved among different species (Barde et al., 1982; Hofer et al., 1990). It is widely distributed and in fact, is the most abundant neurotrophin expressed in the Central Nervous System (CNS) (Leibrock et al., 1989; Maisonpierre et al., 1990). BDNF is critical during development and brain plasticity-related processes (Alonso et al., 2005; Kovalchuk et al., 2002).

Even though BDNF was initially described as a factor from neuronal origin, it has also been identified in microglia, oligodendrocytes, astrocytes, radial glial cells, immune cells and some peripheral tissues (Aharoni et al., 2005; Maisonpierre et al., 1990; Murer et al., 2001; Stadelmann et al., 2002). Glial BDNF synthesis has been described in cultured cells from different brain areas including cortex, cerebellum, forebrain, retina and olfactory bulb (Harada et al., 2002; Lipson et al., 2003; Miklic et al., 2004; Runyan and Phelps, 2009; Seki et al., 2005; Wu et al., 2004). BDNF levels in retinal Müller cells are higher than those of NGF and NT-3 (Taylor et al., 2003; Wu et al., 2004). Furthermore, BDNF production by astrocytes *in vivo* has been extensively associated with cellular stress or pathological conditions such as transient ischemia (Tokumine et al., 2003), multiple sclerosis (Stadelmann et al., 2002) or Alzheimer's disease (Burbach et al., 2004), suggesting a glial neuroprotective role by the production and release of neurotrophic factors.

The activity of BDNF is mediated through its binding to different receptors: TrkB ($p145^{TrkB}$) or high-affinity receptor, a member of the tropomyosin receptor kinase family; and $p75^{NTR}$ or low-affinity receptor, a member of the tumor necrosis factor family of receptors (Barbacid, 1995). The binding of BDNF to TrkB triggers receptor dimerization, tyrosine trans-phosphorylation and activation of intracellular signaling cascades and effectors including the mitogen-activated protein kinase (MAPK), phosphatidylinositol 3-kinase (PI3K) and phospholipase C-γ1 (PLCγ1) (Patapoutian and Reichardt, 2001). Moreover, TrkB is also present in a truncated isoform called tTrkB ($p95^{TrkB}$) that lacks the tyrosine kinase domain and is devoid of catalytic activity (Allen et al., 1994; Klein et al., 1990a,b). In a simplified scenario, neurons express the full-length form, while astrocytes only possess the truncated TrkB isoform (Rose et al., 2003). $p75^{NTR}$ is involved mainly in the migrating effects of pro-BDNF on cerebellar granule cells (Xu et al., 2011).

* Corresponding author. Tel.: +52 5 55061 3800x5316; fax: +52 5 55061 3800x5317.
E-mail address: arortega@cinvestav.mx (A. Ortega).

0197-0186/$ - see front matter © 2011 Elsevier B.V. All rights reserved.
doi:10.1016/j.neuint.2011.10.002

Most of BDNF physiological actions are based on its capacity to modulate gene transcription. In fact, BDNF regulated genes are involved in the regulation of synaptic function, metabolism, and the expression of ion channels and receptor subunits (Gokce et al., 2009). Among the inducible transcription factors regulated by BDNF, the activator protein 1 (AP-1) and the cAMP responsive element binding protein (CREB) have been established as common targets (Okamoto et al., 2003; Sanchez-Huertas and Rico, 2011). In cortical glial cells, the BDNF-dependent activation of such transcription factors has also been described (Roback et al., 1995).

Bergmann glia cells (BGC) are specialized glial cells that do not undergo the *so-called* astrocytic conversion and surround excitatory and inhibitory synapses in the molecular layer of the cerebellum. BGC carry out important roles in cerebellar development, neuronal viability and synaptic modulation. During cerebellar development, granule cells migrate from the external granular cell layer along BGC fibers into the internal molecular layer (Bellamy, 2006; Wilson et al., 2010). The clearance of glutamate from the synaptic cleft, relies on high-affinity sodium-dependent glutamate/aspartate transporters expressed in BGC membranes preventing glutamate-dependent neuronal death (Rothstein et al., 1994). It has been recently assumed that the expression of glutamate receptors and transporters in BGC enable them to modulate synaptic transmission (Bellamy, 2006). It has also been reported that BGC responds to a variety of growth factors that regulate their development (Lin et al., 2009; Martinez et al., 2011) or their activity (Gamboa and Ortega, 2002; Poblete-Naredo et al., 2009).

In the present study we have investigated the expression of BDNF, its high affinity receptor (TrkB) as well as BDNF-activated pathways in BGC. Our results indicate that BGC express and respond to BDNF. Given the strategic localization and cytoarchitecture of BGC cells, it is possible that BGC represent a source of neurotrophic factors. Manipulation of the availability of neurotrophic factors in glia cells might be a promising strategy in the treatment of human neurological diseases.

2. Materials and methods

2.1. Materials

Cell culture reagents were obtained from Gibco (Gaithersburg, MD, USA). Plastic ware was purchased from Costar (Cambridge, MA, USA). Trizol reagent, DNase I Amp Grade, MMLV reverse transcriptase, DNA polymerase and oligo (dT) were purchased from Invitrogen Corporation (Carlsbad, CA, USA). The antibodies used were anti-BDNF (Alomone Labs, Jerusalem, Israel), anti-calbindin (Sigma–Aldrich, St. Louis, MO, USA), anti-kainate binding protein (KBP) anti-serum (produced in our laboratory); anti-phospho Akt1/2/3 (Ser-473; sc-7985-R), anti-Akt1/2 (H-136; sc-8312), anti-ERK1 (K-23; sc-94) and anti-phospho ERK1/2 (E-4; sc-7383) were from Santa Cruz Biotechnology, Inc. (Santa Cruz, CA, USA). BDNF was purchased from Sigma (St. Louis, MO, USA). The inhibitors wortmannin and 2-(2-amino-3-methoxyphenyl)-4H-1-benzopyran-4-one (PD98059) were from Tocris Cookson Ltd. (Bristol, UK) and bisindolylmaleimide (BisI) from Sigma. Horseradish peroxidase-linked anti-rabbit antibodies, and the enhanced chemiluminescence reagent (ECL), were obtained from Amersham Biosciences (Buckinghamshire, UK). All other chemicals were purchased from Sigma (St. Louis, MO, USA).

2.2. Cell culture and stimulation protocol

Primary cultures of cerebellar BGC were prepared from 14-day-old chick embryos as described previously (Ortega and Teichberg, 1990) with minor modifications. Briefly, chick embryos were killed by decapitation and cerebella were cut into small pieces in Puck's medium. The tissue was transferred to a new Puck's medium containing 0.125% trypsin and 0.1% DNase and incubated for 15 min at 37 °C to dissociate the tissue into cells. The supernatant was removed by decantation and the pellet was dissolved in dissociation media containing Opti-MEM, 2.5% fetal calf serum, 0.1% DNase and gentamicin (50 μg/mL). After trituration of the pellet by aspiration through fired Pasteur pipettes and a 21-gauge needle, the cell suspension was left to settle down for 10 min. The cell supernatant was collected and centrifuged at 3000 rpm for 10 min, followed by solubilization of the cell pellet in the aforementioned dissociation media without DNase. Viable cells were counted by Trypan Blue exclusion and plated in 60 mm diameter plastic culture dishes. By using this protocol the 95% of cells are BGC as demonstrated by immunocytochemistry with the BGC marker, KBP (Somogyi et al., 1990). Furthermore, no specific immunostaining of these cultures with anti-neurofilament antibodies has been detected and ion fluxes experiments together cell volume measurements have clearly demonstrated that the cultured cells are indeed Bergmann glia (Ortega et al., 1991). Cells were used on the 4th to 5th day after culture. Before any treatment, cell monolayers were switched to serum-free media for 8–12 h and treated as indicated. Inhibitors were added 30 min before any treatment. Unless otherwise stated, cells were stimulated in serum-free culture media for the indicated times.

2.3. Staining procedures

BGC primary cultures were grown on poly-L-lysine-treated (0.01 mg/ml) glass coverslips following the procedure described above. Cells were fixed by exposure for 10 min to methanol at −20 °C and washed twice with PBS containing 0.5% Triton X-100 (washing solution). Non-specific binding was prevented by incubation with 1% BSA in PBS (blocking solution) for 1 h. Cells were exposed 1 h to the primary antibodies anti-BDNF or anti-KBP in blocking solution at room temperature. Then, cells were washed three times with washing solution and incubated with a 1:100 dilution of the fluorescent-labeled secondary antibodies dissolved in blocking solution. After washing out secondary antibodies, cell preparations were mounted with Vectashield (Vector Laboratories, Burlingame, CA, USA) and examined with an inverted fluorescence microscope (Zeiss Axioscope 40).

For immunohistochemistry, P0 chick cerebella was removed and placed immediately in cold PBS. The tissue was washed once in cold PBS to remove blood and placed in 4% paraformaldehyde in phosphate buffer (PB, pH 7.4) for one hour. The fixative was changed once and the tissue was left at 4 °C during 48 h. The cerebella were cryoprotected successively in 10%, 20% and 30% sucrose in PB and sagittally sectioned at 50 μm with a cryostat (Microm International GmbH). For immunohistochemistry, tissue was washed profusely in PB buffer to remove excess aldehydes and then incubated 10 min in 1.8% hydrogen peroxide solution to remove endogenous peroxidase activity. Non-specific antibody binding was blocked by incubating the sections in blocking solution (3% goat serum in PB buffer containing 0.3% Triton, PBT) for 1 h at room temperature. Sections were incubated for 48 h at 4 °C with mouse anti-calbindin (1:5000) antibody in blocking solution. The primary antibody was washed out rinsing the sections three times in buffer PBT. The tissue was placed in biotinylated anti-mouse secondary antibody (1:200; Vector Laboratories, Inc., Burlingame, CA) for 1 h, followed by 1 h incubation with the avidin–biotinylated horseradish peroxidase complex (1:250; Vector Labs). The antibody-peroxidase complex was stained with 0.05% diaminobenzidine (DAB; Polysciences) and 0.01% hydrogen peroxide producing a brown precipitate. After the stopping the reaction by rinsing the sections in buffer PB, the tissue was incubated with the rabbit primary antibodies anti-KBP

(1:5000) or anti-BDNF (1:5000; Alomone Laboratories, Jerusalem, Israel) in blocking solution, and the same procedure described previously was followed for the incubation with anti-rabbit secondary antibody. The antibody-peroxidase complexes were revealed with a solution containing 0.05% 3,3′-diaminobenzidine (DAB), nickel sulfate (10 mg/mL; Fisher Scientific), cobalt chloride (10 mg/mL; Fisher Scientific) and 0.01% hydrogen peroxide, which produced a black-purple precipitate. Sections were mounted onto gelatin-subbed slides, dehydrated, and cleared in Hemo-De (Fisher Scientific); then cover slips were collocated with Permount. Fluorescent immunolabeling was performed as described above but using goat anti-mouse TRITC as the secondary antibody for calbindin, or goat anti-rabbit FITC (Zymed, San Francisco, CA, USA) secondary antibody for KBP or BDNF immunostaining. The sections were analyzed in an Olympus BX41 microscope.

2.4. Reverse transcriptase-polymerase chain reaction (RT-PCR)

Total RNA was isolated from confluent BGC monolayers using the Trizol method. Two μg of total RNA was treated with 1 U deoxyribonuclease I (DNase I, Amp Grade) to digest contaminating DNA. First-strand cDNA was synthesized using 1 μg DNA-digested RNA with 200 U of Moloney murine leukemia virus-reverse transcriptase (MMLV-RT, Invitrogen). PCR was performed using specific primers directed to the coding region of chick *bdnf* (*chBDNFup* 5′-*GCAGTCAAGTGCCTTTG*-3′, *chBDNFlw* 5′-*GAGCCCACTATCTTCCCC*-3′) and chick trkB (*chTrkBF* 5′-*CTTCAGCTGGACAACCCTAC*-3′, *chTrkBRK*$^{+}$ 5′-*TGGAAGTCCT TGCGGGCATT*-3′ and *chTrkBRK*$^{-}$ 5′-*AACAGCCCCTCTCTCATCTT*-3′) (Zhou et al., 2004). PCR conditions were 2 μl cDNA, 2.5 U Taq DNA polymerase, 0.2 mM dNTPs and 2.0 mM $MgCl_2$ (BDNF) or 1.5 mM $MgCl_2$ (TrkB). Cycling conditions for BDNF were 94 °C for 30 s, 60 °C for 1 min and 68 °C for 1 min, by 25 cycles. For TrkB, the cycling conditions were 95 °C for 1 min, 58 °C for 1 min and 72 °C for 10 min, by 27 cycles. PCR products were resolved in 1.5% agarose gels stained with ethidium bromide and examined with a UV-transilluminator (BioRad).

2.5. SDS–polyacrylamide gel electrophoresis and Western blots

Whole-cell extracts from cultured BGC were prepared by scraping the cells in PBS buffer with protease and phosphatase inhibitors (1 mM PMSF, 10 mM Na_2MoO_4, 25 mM NaF, 1 mM Na_3VO_4). After centrifugation at 13,000 rpm for 5 min, the cell pellet was dissolved in RIPA buffer (50 mM Tris–HCl, pH 7.5; 150 mM NaCl; 1 mM EDTA; protease and phosphatase inhibitors and 5 μg/ml leupeptin and aprotinin). An small aliquot was saved for protein concentration determination by the Bradford's method (Bradford, 1976) and the rest of the sample was solubilized with 2% Triton X-100 and 0.2% SDS, and vortexed 1 h at 4 °C. Cell debris was discarded by centrifugation for 5 min at 13,000 rpm. Equal amounts of protein (approximately 50 μg) were diluted in Laemmli's sample buffer, boiled for 5 min and analyzed through polyacrylamide gel electrophoresis (SDS–PAGE). Proteins were transferred to nitrocellulose membranes and stained with Ponceau S solution to confirm equal loading of proteins. The blots were soaked in PBS to remove Ponceau staining and incubated with the primary antibodies diluted in 0.25% bovine serum albumin, 0.1% Tween-20 in TBS buffer, followed by horseradish peroxidase-conjugated secondary antibodies. Finally, the proteins were revealed using an enhanced chemiluminescence kit (GE Healthcare) and exposed to X-ray films.

2.6. Nuclear extracts and electrophoretic mobility shift assays

AP-1, CREB, Nuclear factor E2-related factor (Nrf2) and recombination signal binding protein for immunoglobulin kappa J region (RBPJk) binding to their consensus nucleotide sequences were determined by electrophoretic mobility shift assays (EMSA) as previously described (Lopez-Bayghen et al., 1996). Briefly, BDNF-treated and control cells were harvested in Tris–Dulbecco buffer pH 7.4 containing 1 mM PMSF, and centrifuged 5 min at 13,000 rpm. Nuclear extracts were obtained by dissolving the cell pellet in 400 μl ice-cold buffer A (10 mM HEPES pH 7.9, 10 mM KCl, 0.1 mM EDTA, 0.1 mM EGTA, 1 mM DTT, 1 mM PMSF and protease inhibitor cocktail) and the homogenate was incubated on ice for 20 min. 25 μl of a 10% NP-40 solution was added to the samples and vigorously mixed for 10 min. After centrifugation at 9000 rpm for 1 min, the supernatant was discarded, and the nuclear pellet was dissolved in a buffer C (20 mM HEPES pH 7.9, 400 mM NaCl, 0.1 mM EDTA, 0.1 mM EGTA, 1 mM DTT, 1 mM PMSF and protease inhibitor cocktail). Following protein concentration determination, nuclear extracts were incubated on ice with 500 ng of poly[dI-dC] as non-specific competitor (GE Healthcare), and 1 ng of [^{32}P]-end labeled double stranded oligonucleotides:

AP-1(SV40) 5′-CTAGTTCCGGCTGAGTCATCAAGC-3′,
CREB 5′-CTAGAGAGATTGCCTGACGTCAGAGAGCTAG-3′
Nrf2 5′-GCAGAATGCTGAGTCACGGTGGAA-3′
RBPJk 5′-CTAGGGTGTAAACACGCCGTGGGAAAAAATTTAT-3′

The reaction mixtures were incubated for 20 min on ice and electrophoresed through 8% polyacrylamide gels with low ionic strength 0.5% TBE buffer. The gels were dried and exposed to autoradiographic films. For competition assays, the reaction mixtures were pre-incubated with the non-labeled probes for 15 min before adding the labeled oligonucleotides.

2.7. Transient transfections and reporter assays

TRE-CAT and CRE-CAT contain the structural gene for chloramphenicol acetyltransferase (CAT) under the control of the Herpes virus thymidine kinase (HSV-TK) promoter and five SV40 AP-1 sites cloned upstream for TRE-CAT or five CRE elements for CRE-CAT (Rutberg et al., 1999). pGL2-hARE-LUC contains the NQO-hARE site (antioxidant response element from NAD(P)H:quinone oxidoreductase gene) cloned in the pGL2-Basic vector was kindly donated by Dr. Phil Jaiswal University of Maryland, School of Medicine (Dhakshinamoorthy and Jaiswal, 2000). Transient transfection assays were performed in 80% confluent BGC cultures using a calcium phosphate protocol with the indicated amount of purified plasmids. Under such conditions, the transfection efficacy was close to 50% determined by a transfection control (β-gal). Treatments were done 4 h post-transfection and cell harvesting for reporter assays was performed 24 h post-transfection. Protein lysates were obtained as follows: cells were harvested in cold PBS buffer, lysed with one freeze–thaw cycle and centrifuged at 12,000*g* for 1 min. Equal amounts of protein lysates (80 μg) were incubated with 0.25 μCi of [^{14}C]-chloramphenicol (50 mCi/mmol)(Amersham Biosciences, Buckinghamshire, UK) and 0.8 mM Acetyl-CoA (Sigma–Aldrich Co.) at 37 °C. Acetylated forms were separated by thin-layer chromatography and quantified using a Typhoon radioactive image analyzer and the ImageQuant software (GE Healthcare). CAT activities were expressed as the acetylated fraction corrected for the activity in the pCAT-Basic vector and are expressed as relative activities to non-treated control cell lysates. The luciferase activity was determined using the Luciferase Assay System (Promega). 24 h post-transfection, cells were processed for luciferase measurement. Briefly, protein lysates were obtained from cells harvested in cold PBS and lysed in 100 μl of Reporter Lysis Buffer (Promega). Equal amounts of protein lysates (~70 μg) were incubated with luciferase assay reagent. Light

detection was performed in a FluoroSkan Ascent FL 374 (Labsystems) and activity values were normalized to protein content.

2.8. Statistical analysis

Data are expressed as the mean ± standard error of at least three independent experiments. One-way analysis of variance (ANOVA) was performed to determine the statistical significance between conditions and the post hoc Newman–Keuls comparison test was used to elucidate, which conditions were significantly different from each other (Prism, GraphPad Software, San Diego, CA).

3. Results

3.1. Bergmann glia cells express BDNF and its TrkB receptor

To gain insight into BDNF expression in BGCs, we performed immunolabeling of P0 chick cerebella with an anti-BDNF specific antibody along with staining for specific cell markers to identify the layers of the cerebellar cortex. Fig. 1A and B illustrates the localization of the Purkinje cell bodies and their arborizations after immunolabeling with the Purkinje's cell marker, calbindin. BGC localization was done with the BGC marker, KBP that decorated the molecular cell layer surrounding the Purkinje's cell bodies, and the cerebellar pial surface. BDNF immunostaining was abundantly found in the Purkinje cell bodies as well as in the pial border lining the molecular cell layer similar to the KBP labeling. Note that the pial cerebellar surface corresponds to BGC terminal end-feet (Bellamy and Ogden, 2006; Yamada and Watanabe, 2002). Double immunolabeling calbindin/KBP and calbindin/BDNF shows that calbindin does not co-localize with BDNF nor KBP in the cerebellar pial border, clearly suggesting that BGC express BDNF within its glial fibers, concentrated particularly in its most distal portion. Immunofluorescence staining was performed to gain higher resolution. Fig. 1B reveals again that BDNF and KBP are expressed in the pial portion of the cerebellar cortex, demonstrating that BGC express BDNF *in vivo*. Several attempts were made to co-localize BDNF and KBP in Bergmann glia, although none of them were successful, the main problem being that the available anti-BDNF antibodies that cross-react with chicken BDNF are from rabbit origin, the same as the available anti-KBP antibodies.

As previously suggested, astroglial cells are able to take up, store and deliver BDNF from the extracellular space (Rubio, 1997), hence BDNF localization in glia do not necessarily imply its synthesis by this cell type. Consequently, to verify BDNF synthesis in BGC, primary BGC cultures were obtained from 14-day old chick embryos and the expression of BDNF mRNA and protein was investigated. To this end, total RNA was isolated from BGC

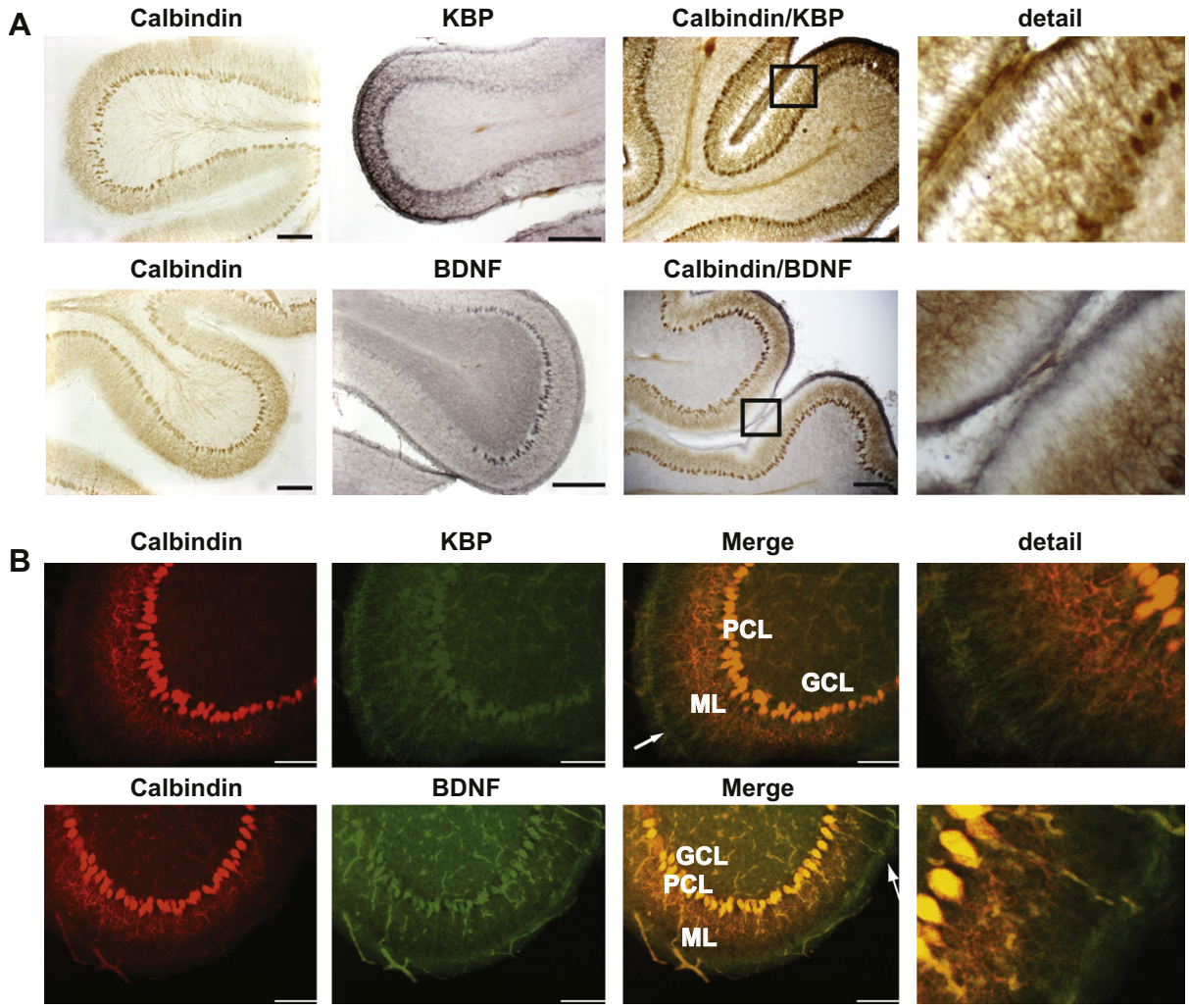

Fig. 1. BDNF expression in cerebellum. BDNF reactivity in chick cerebellar sections (A) immunocytochemistry and (B) immunofluorescence staining. Calbindin is the selected marker for Purkinje cells and KBP is the marker for Bergmann glial cells. ML: molecular layer, PCL, Purkinje cell layer; GL, granular layer. Images were obtained in a fluorescence microscope using different objective. Bar size: 100 μ. Amplified images were added in the right panel to show data in detail (squares).

monolayers and treated with DNase, since both primers align in the unique coding exon. As clearly shown in Panel A of Fig. 2, the expected 462 bp amplicon was obtained. The expression of the cognate BDNF receptor, the full-length TrkB, and its truncated isoform (tTrkB) was also explored in primary BGC cultures. The *trkB* amplification by RT-PCR using the pair of primers *chTrkBF* and *chTrkBRK*$^{+}$, gave rise to a product that is consistent with the predicted full-length *trkB* from chick origin (Garner et al., 1996) (Fig. 2A). Moreover, the restriction profile after digestion with *Sca*I and *Bmp*I endonucleases produced the predicted fragments size (data not shown). Truncated *trkB* isoforms were also detected using the pair or primers *chTrkBF* and *chTrkBRK*$^{-}$, and three amplification products of the expected size (450, 525 and 600 pb) (Garner et al., 1996) were obtained (Fig. 2A). Both, the *trkB* and the 600 pb truncate *trkB* amplification products were sequenced, confirming the identity of both fragments (not shown). BDNF protein expression was assessed by Western blot using total BGC protein extracts. As depicted in panel B of Fig. 2, very intense immunoreactive bands were obtained at the expected molecular weight for the monomeric BDNF protein as well as a less intense band corresponding to the proBDNF form located at approximately 36 kDa. The specificity of the antibody was confirmed with the successfully competition of the 14 kDa band with the antigenic peptide (data not shown). Accordingly, BGC immunofluorescence revealed BDNF expression in KBP-positive cells (Fig. 2 panel C). All together, these results suggest that BGC are able to express

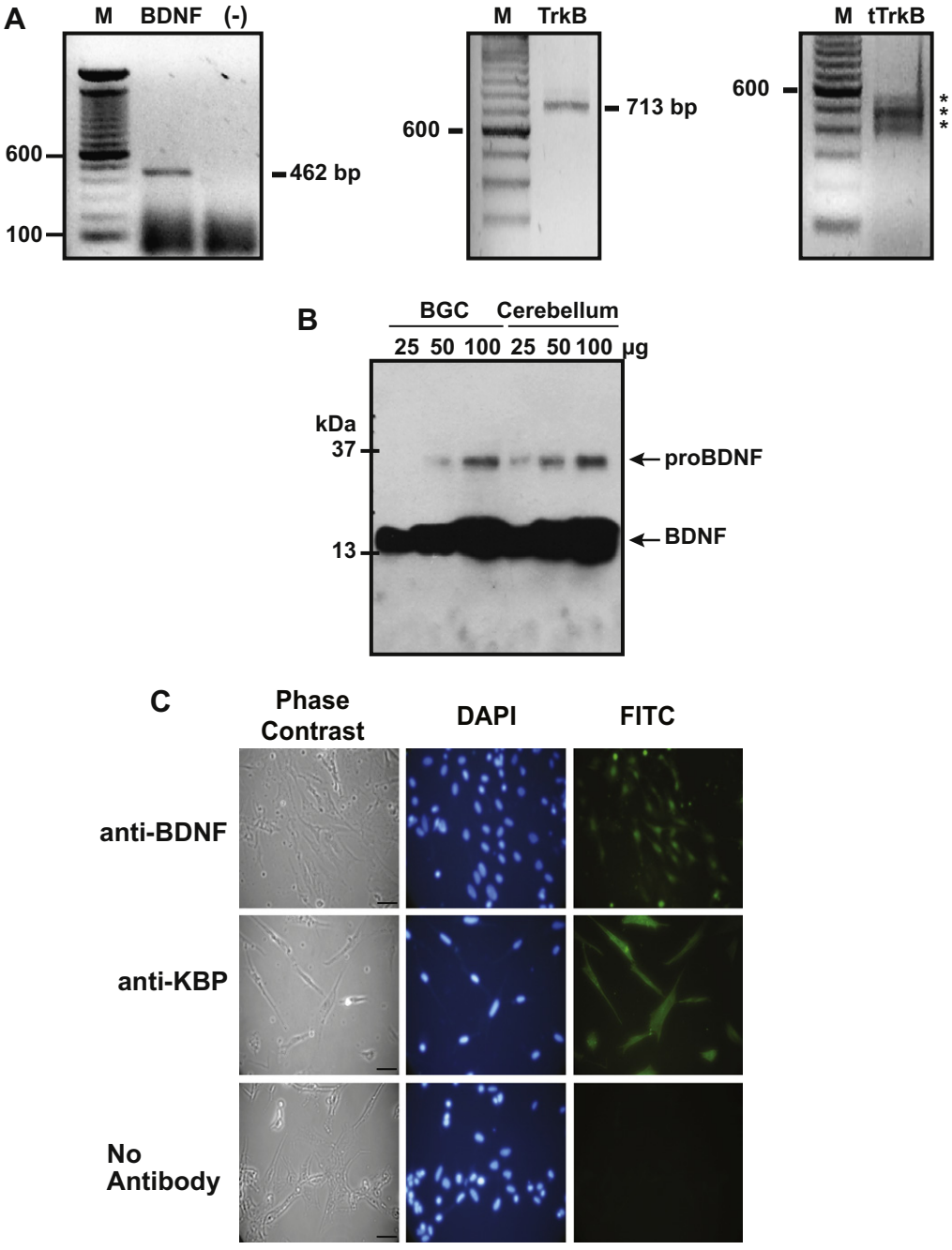

Fig. 2. BDNF, TrkB and tTrkB expression in BGC. Panel A: Total DNase-treated RNA obtained from chick primary BGC cultures was amplified by RT-PCR with specific primers (indicated in Section 2) for BDNF, TrkB and tTrkB mRNAs. (−) Negative control, without retro transcriptase. M, 100 bp ladder. Panel B: BDNF immunodetection using anti-BDNF and total extracts from BGC primary cultures and E14 chick cerebellum (protein µg are indicated). Panel C: BGC primary cultures were stained with the indicated antibodies. Nuclei were counter-stained with DAPI. Images were obtained using an inverted fluorescence microscope (40× objective) and the scale bar denotes 100 µ.

BDNF *in vivo* and *in vitro* and are also prone to BDNF stimulation due to the synthesis of *trkB* mRNA.

3.2. Bergmann glia express functional TrkB receptors

Previous studies have reported the exclusive expression of the truncated TrkB isoform in astroglial cells (Condorelli et al., 1995; Frisen et al., 1993; Rudge et al., 1994) being the full-length *trkB* mRNA only identified by RT-PCR (Roback et al., 1995). As we detected the expression of *trkB* mRNA in BGC, it was interesting to determine its functionality upon exogenous BDNF administration. To this end, the Tyr 204 phosphorylation pattern of p42/p44 mitogen-activated protein kinase (MAPK) and Ser 473 phosphorylation of protein kinase B (PKB)/Akt were explored in BDNF-treated cells. As reported in panel A of Fig. 3, a time-dependent increase in p42/p44 and PKB/Akt phosphorylation and therefore activation, was found upon stimulation of BGC monolayers with BDNF (50 ng/ml) in serum-free media.

Alternatively, the well-characterized induction of the DNA-binding activity of inducible transcription factors after BDNF stimulation (Patapoutian and Reichardt, 2001) was examined. Electrophoretic mobility shift assays (EMSA) were performed with nuclear cell extracts from BGC control (NT) or BDNF stimulated cells, incubated with end-labeled [^{32}P]-AP-1 (SV40), CREB, Nrf2 and RBPJk probes. As shown in Fig. 3 (panel B) AP-1 and Nrf2 binding activity were significantly increased upon a 30 min BDNF stimulation, whereas CREB binding was increased only after a 4 h treatment. In contrast, RBPJk binding remained constant under the same treatment conditions. The MAPK and PI3K/Akt phosphorylation and the modulation of AP-1, Nrf2 and CREB DNA-binding, show that BGC are fully responsive to BDNF stimulation by the expression of the full-length TrkB receptor.

3.3. BDNF stimulates the AP1 and Nrf2 transcriptional activity

The kinetics of the BDNF-dependent increase in AP-1 DNA-binding was determined and results are depicted in panel A of

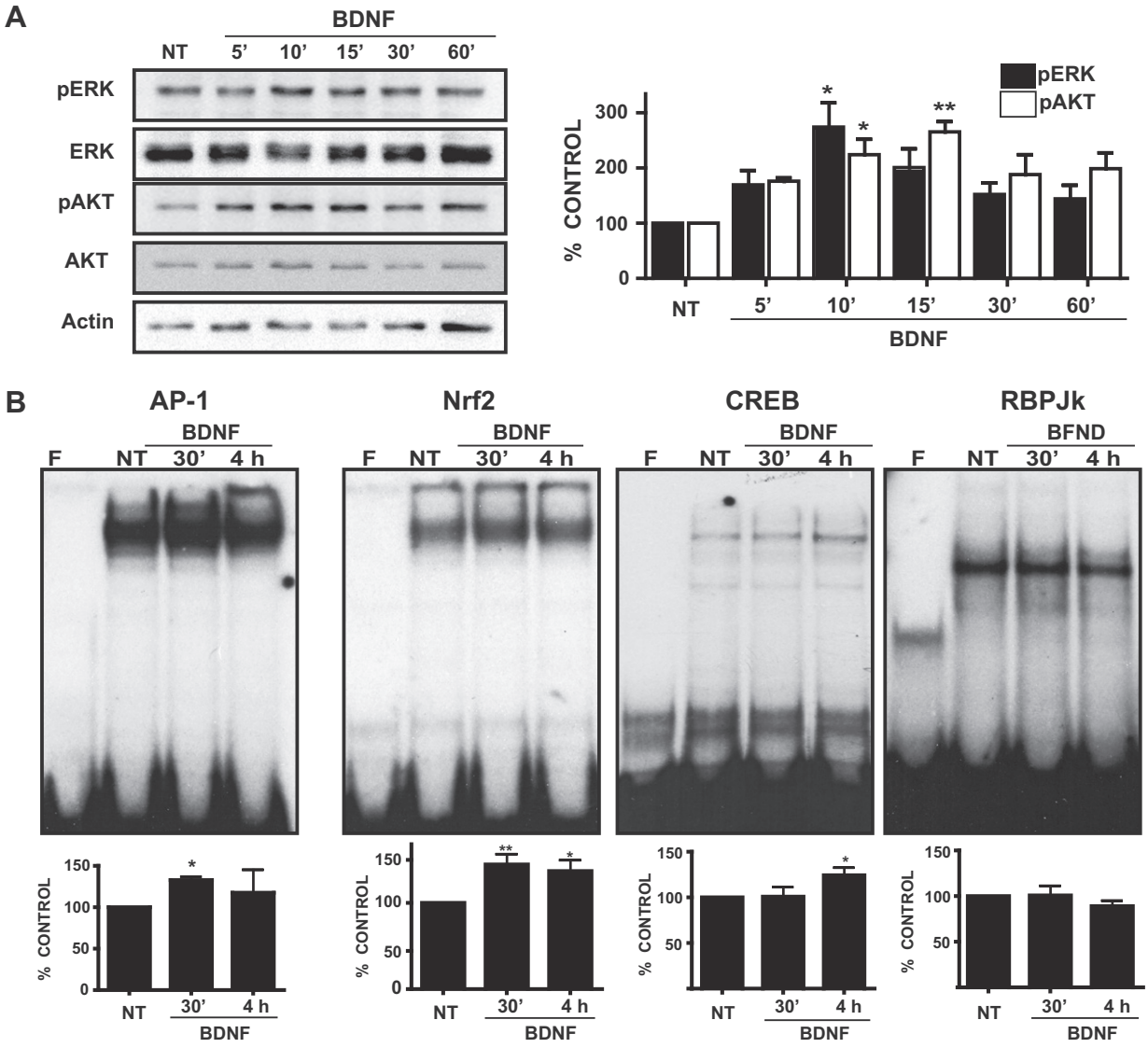

Fig. 3. BDNF activates MAPK and Akt/PKB signaling cascades and induces an increased transcription factor-DNA binding in BGC. Panel A: BDNF treatment was applied for the indicated times and the ERK and Akt/PKB phosphorylation levels assessed. In the graph, quantitative analysis performed from densitometric data, represents the relative density respect to non-stimulated control; mean values ± SE from at least three independent experiments. Panel B: DNA-binding activity was evaluated with nuclear extracts (20–40 μg) from chick Bergmann glial cells treated with BDNF (50 ng/μl for 30 min and 4 h). ^{32}P en-labeled oligonucleotides for AP-1, Nrf2, CREB and RBPJκ were tested. NT, control untreated cells. F, free probe. In all cases, statistical analysis was performed comparing against non-stimulated cell using a non-parametric one-way ANOVA (Kruskal–Wallis test) and Dunn's pos hoc test ($^{*}p < 0.05$; $^{**}p < 0.001$).

Fig. 4. As early as 30 min of BDNF exposure results in a significant increase in AP-1 DNA, increase that persists at least for 4 h returning to its basal levels after 6 h stimulation. As expected, the BDNF effect was dose-dependent with a maximal response observed with 25–50 ng/ml BDNF, corroborating a receptor-mediated effect. The kinetics of Nrf2 DNA-binding was also established (Fig. 4A). Similar to AP-1, the increase in Nrf2 DNA binding upon BDNF is present after a 30 min exposure and the effect lasts for at least 4 h.

The physiological significance of the increased AP-1 DNA binding was determined with transcriptional assays using a chloramphenicol-acetyl-transferase reporter vector under the control of the TRE promoter (TRE-CAT). Taking into consideration that AP-1 mediated transcription is activated by glutamatergic stimulation in BGC glutamate treatment was used as a positive control (Sanchez and Ortega, 1994). As shown in Fig. 4 panel B, BDNF stimulated the AP1-dependent transcription in the same extent as glutamate does (twofold). Also note the dose dependency of the effect, which as, one would expect, is relevant in terms of transcriptional control, since a Nrf2 driven reporter gene augments its transcriptional activity after the treatment with 50 ng/ml of BDNF (Fig. 4, panel B). In contrast, neither CREB DNA binding nor CREB-mediated transcription were significantly augmented by the BDNF treatment (Fig. 4). Taken together, these results provide evidence that the BDNF mediated increase in DNA-binding activity of AP-1 and Nrf2 correlates with a raise in transcriptional activity driven by these transcription factors.

3.4. BDNF-activated AP-1 and Nrf2 DNA-binding and transcriptional activity are mediated by the PKC signaling pathway

To gain insight into the signaling pathway involved in the BDNF nuclear effects, we used selective inhibitors. The results depicted in panel A of Fig. 5 shows that the inhibition of the PI3K pathway with wortmannin (100 nM) does not have any effect over BDNF activation of AP-1 or Nrf2. However, the use of bisindolylmaleimide BisI (1 μM), a protein kinase C (PKC) signaling pathway inhibitor, or the inhibition of the MAPK pathway with PD98059 (50 μM) reverted both AP-1 and Nrf2 binding activities. Transcriptional assays corroborated that PKC and MAPK pathway are involved in BDNF transcriptional effects. Experiments done with sub-maximal BisI or PD98059 doses (0.1 and 5 μM, respectively) demonstrate that both pathways operate separately (panel B of Fig. 5). Taken together, the results described thus far demonstrate that Bergmann glia express BDNF and its functional receptor.

4. Discussion

4.1. BDNF expression in Bergmann glia

Astroglial cells are active participants in neurotransmission, neurogenesis, synaptic plasticity, learning and memory; and constitute and an important source of trophic factors that support

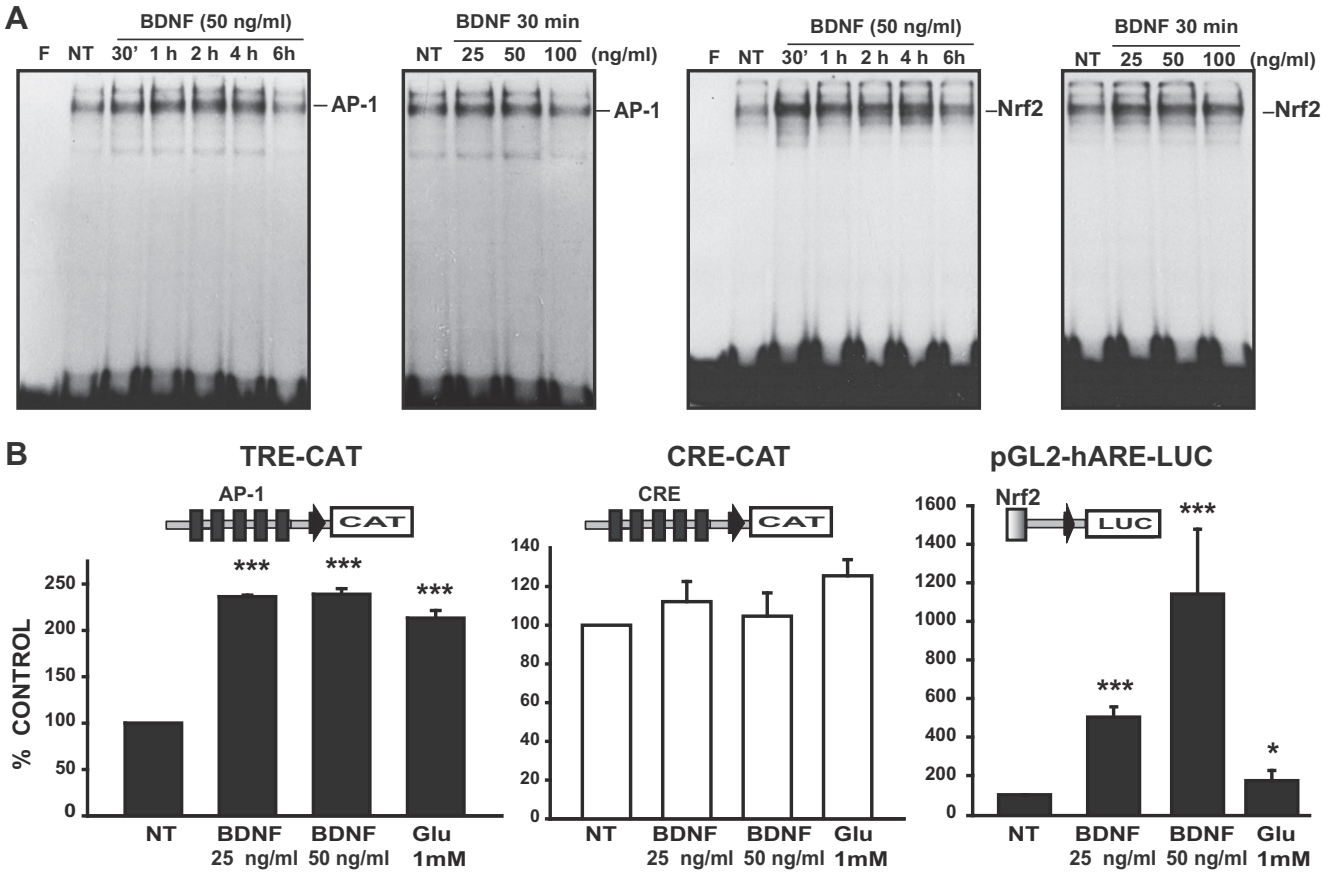

Fig. 4. AP-1 and Nrf2 DNA binding and transcriptional activity in BDNF treated-BGC: time and dose-dependent induction. Nuclear extracts from BGC treated with BDNF (50 ng/μl) for indicated times or with increasing concentrations for 30 min, were tested with the labeled AP-1 or Nrf2 probes in gel shift assays. A typical autoradiogram is shown (from three experiments). Panel B: TRE-CAT and CRE-CAT constructs as well as the Nrf2 responsive construct, pGL2-h-ARE-LUC, were transfected in BGC monolayers; 16 h post transfection, cells were exposed to the indicated BDNF concentrations for 4 h. Glu (1 mM, 4 h) was used as an activation control. The transcriptional activity was determined as described in Section 2. Results are mean values ± the standard error from at least six independent experiments. Statistical analysis was performed comparing against data from non-stimulated cells using a non-parametric one-way ANOVA (Kruskal–Wallis test) and Dunn's pos hoc test; ($^{*}p < 0.05$; $^{***}p < 0.001$).

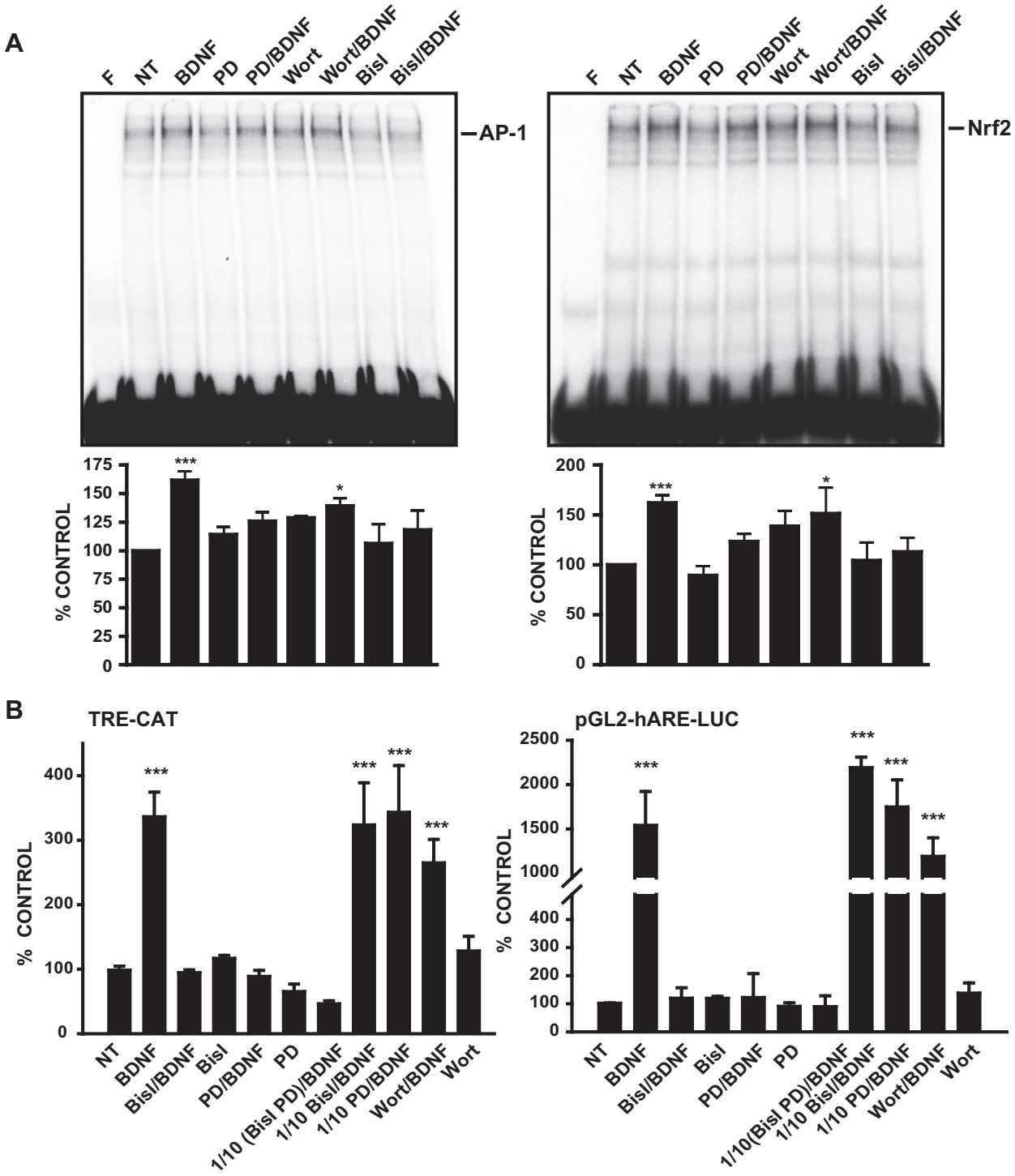

Fig. 5. BDNF signaling in BGC: activation of AP-1 and Nrf2. Panel A: Gel shift assays were performed using nuclear extracts from BGC primary cultures pre-treated for 30 min with the MEK inhibitor, PD98059 (50 μM, PD); the PI3K inhibitor, wortmannin (100 nM, Wort) or the PKC inhibitor, bisindolylmaleimide (1 μM, BisI); and then treated with BDNF (50 ng/ml) for one hour. Representative assays from three independent experiments are shown. Data from densitometry were graphs plotted and shown below each image. Panel B: The TRE-CAT and Nrf2 constructs were transfected in BGC monolayers; 16 h post transfection cells were pre-exposed (30 min) to the same inhibitors used in panel A after what, BDNF treatment (50 ng/ml) was applied for 4 h. Sub-effective doses were: PD98059 5 μM (1/10PD); 0.1 μM, BisI (1/10 BisI); applied together or separated (as indicated). Relative activities from both reporter constructs were obtained harvesting 24 h after treatment. Results are the mean values ± the standard error of at least five independent experiments. Statistical analysis was performed comparing against data obtained from non-stimulated cells using a non-parametric one-way ANOVA (Kruskal–Wallis test) and Dunn's pos hoc test; $^{**}p < 0.01$; $^{***}p < 0.001$.

neuronal survival (de Melo Reis et al., 2008a,b; Jordan et al., 2008; Taylor et al., 2007). BDNF is an essential neurotrophin involved in the survival of different neuronal populations (Hofer and Barde, 1988; Knusel et al., 1991; Lindholm et al., 1993; Schecterson and Bothwell, 1992; Zirrgiebel et al., 1995), and plays a central role in brain plasticity-related processes (Cunha et al., 2010). The first attempts to establish BDNF distribution suggested that astrocytes did not express this neurotrophin (Hofer et al., 1990). Nevertheless, with the use of more sensitive techniques such as quantitative polymerase chain reaction (qPCR) the presence of the BDNF

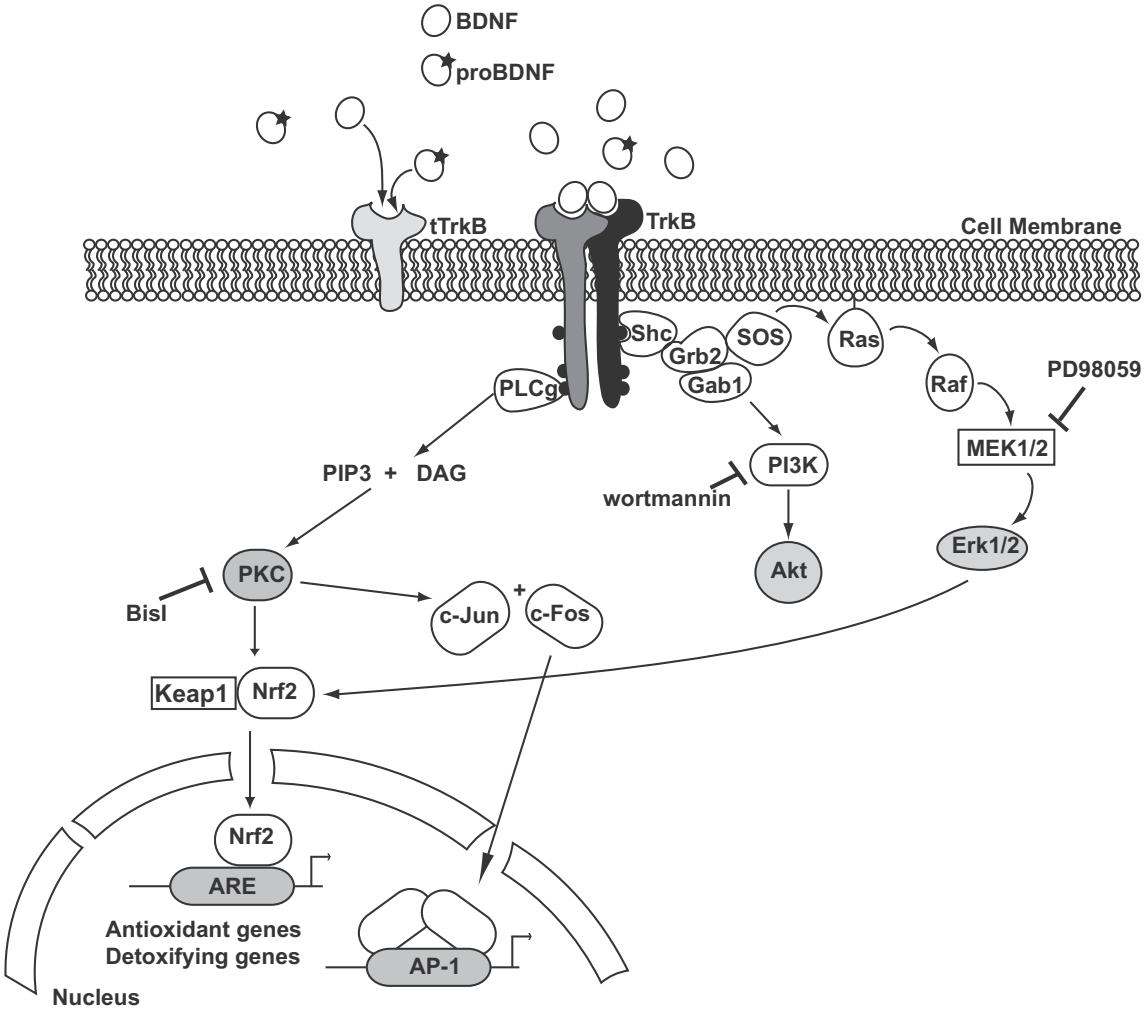

Fig. 6. Current model for BDNF signaling in cultured Bergmann glia cells. BDNF binds to Trk resulting in the docking of PLCg (Phospholipase Cg); IP3 and DAG (diacylglycerol) are produced and PKC activated. PI3K and Akt/PKB are also activated through Gab1 while Erk1/2 activation is p21ras-dependent. PKC activation results also in augmentation in AP-1 and Nrf2 DNA-binding and an increase in transcription. Pro-BDNF presumably binds truncated TrkB.

transcript (Koyama et al., 2005; Saha et al., 2006) and protein (Miklic et al., 2004; Seki et al., 2005; Taylor et al., 2003; Wu et al., 2004) was reported in astrocytes. More recently, the role of glial cells in supporting neuronal survival by its BDNF production and release has been studied in the context of cholinergic neurons (Jean et al., 2008), in mesencephalon cells (Imamura et al., 2008), hippocampus (Kimoto et al., 2009), retina (Seki et al., 2005) and cortex (Juric et al., 2008).

In the present communication, we show that BGC express BDNF at the mRNA and protein levels in a well-defined cell culture model: chick cerebellar Bergmann glia cells. It is worth to mention that this culture has been characterized since 1991 (Ortega et al., 1991) and has been extensively used throughout the years (Lopez-Bayghen et al., 2007). A recent transcriptional profiling study supports the expression of BDNF in Bergmann glia (Koirala and Corfas, 2010). The PCR product obtained with the reported set of *chbdnf* primers was of the expected size and matches previous studies in chick parasympathetic neurons (Zhou et al., 2004). Sequencing data confirmed the identity of the amplicon as *chbdnf*. A false positive result due to DNA contamination is unlikely since PCR amplification of DNase-treated samples without the reverse transcriptase step did not give any visible product.

BDNF was detected with specific antibodies either via immunostaining procedures as well as Western blots. Immunoreactive bands were detected by SDS–PAGE from BGC extracts with an apparent molecular weight of 14 and 36 kDa, in accordance to the molecular weight of the monomeric BDNF and proBDNF, respectively (Barker, 2009). Furthermore, immunolabeling of BGC cultures corroborated BDNF staining in KBP-positive cells. Even though glial cells are capable to uptake neurotrophins and pro-neurotrophins from the extracellular space by their truncated TrkB receptor (Alderson et al., 2000; Rubio, 1997), the fact that BDNF is detected in an almost pure BGC culture makes this suggestion unlikely. Moreover, the identification of the BDNF mRNA strongly suggests an *in situ* synthesis of BDNF within BGC.

In the cerebellar cortex, BDNF mRNA is present in the granular cell layer (Hofer et al., 1990; Rocamora et al., 1993; Wetmore et al., 1990). Surprisingly, BDNF displays a rather divergent expression patterns in this structure. For example, in the mice, BDNF is localized in the Purkinje cell body and dendrites with a low immunoreactivity signal in granule cells (Schwartz et al., 1997). In contrast, monkey cerebellum displays a very low BDNF immunoreactivity in the Purkinje cells but a strong labeling in granule cells and even in some fibers that run through the molecular layer (Zhang et al., 2007). The discrepancy among BDNF mRNA and protein localization might be explained in terms of the ability of neurotrophic factors to travel in a retrograde/anterograde mode, opening the possibility that the identification of BDNF in any cell lineage might

not correspond to a *bona fide in situ* synthesis. In this contribution, using histological preparations from P0 chick cerebella, BDNF was localized to the Purkinje cell soma, in accordance to Schwartz et al. (1997), as well as lining the pial cerebellar surface (Fig. 1) (Schwartz et al., 1997). Taking into consideration that BGC extend in a radial fashion from the Purkinje cell layer to the pial portion of the cerebellum, where their end feet are located (Yamada and Watanabe, 2002), we suggest that BDNF staining at the pial surface correspond to BGC-derived BDNF. However, it is also possible that BDNF localization at the pial surface could also correspond to endocytosed and redistributed BDNF from neighboring cells. It can be argued that co-localization of BDNF and KBP or even BDNF and GFAP might be necessary to claim BDNF expression in Bergmann glia. Nevertheless, as already stated, available anti-BDNF antibodies that recognize the protein of avian origin are from rabbit origin, the same as the anti-KBP anti-sera. In regard of GFAP labeling of chick Bergmann glia, note that previous work from our group demonstrate that chick Bergmann glia are barely decorated with anti-GFAP antibodies and that in fact, vimentin is the best intermediate filament marker for these cells (Ortega et al., 1991). In any event, a detailed assessment of BDNF mRNA in chick cerebellar tissue should be considered to trace better conclusions (Lessmann et al., 2003).

4.2. Bergmann glia as a BDNF target

The expression of BDNF in our culture system opened the possibility of the expression of its receptors and the existence of an autocrine loop, even though that granule cells and Purkinje cells release this neurotrophin (Xu et al., 2011). As already pointed out, TrkB expression in glial cells is controversial and the current view is that the ratio between full length TrkB and its truncated isoform, tTrkB depends on the differentiation state of the cells, being the full length isoform the predominant in radial glia (Climent et al., 2000; Roback et al., 1995).

Exogenous BDNF application in BGC triggers the canonical TrkB signaling pathways p42/p44 MAPK, PI3K/Akt, and PKC (Patapoutian and Reichardt, 2001). One could argue that the described effects might be mediated by proBDNF, which as depicted in panel B of Fig. 2 is present in our culture system. This suggestion is unlikely since it has been shown that proBDNF signaling is carried out mainly by p75 neurotrophin receptor (p75NTR) and sortilin, proteins that apparently are not present in Bergmann glia (Koirala and Corfas, 2010). No evident participation of an increase in intracellular Ca^{2+} from the intracellular or the extracellular compartment could be established in agreement to BDNF signaling in neuronal cultures (Zhou et al., 2004). Apparently, PKC and MAPK signaling cascades mediate BDNF transcriptional control, at least in BGC, given the fact that their specific inhibitors, BisI and PD98059 prevent AP-1 and Nrf2-dependent transcription and that when these inhibitors are used at sub-maximal doses their effects are additive. Interestingly, while the BDNF promoted the increase in AP-1/DNA binding and transcriptional activity that has been documented in astroglial cells (Okamoto et al., 2003), Nrf2 activation through this neurotrophin has not been reported before.

Nrf2 is involved in the transcriptional control of genes that maintain the so-called *redox homeostasis*. This transcription factor belongs to the cap'n collar proteins and form heterodimers with members of the AP-1 family in some cases. Nrf2-mediated transcriptional activation is a process that involves its dissociation from the Nrf2 inhibitor iNrf2 (also called Keap1), a dimeric protein that anchors to the cytoskeleton and sequester Nrf2 in the cytoplasm promoting its proteasomal degradation (Singh et al., 2010). Nrf2 release from its inhibitor is a PKC-dependent effect. Nrf2 is a PKC substrate, in fact, phorbol esters induce the transcription of ARE-containing genes (Bloom and Jaiswal, 2003; Huang et al., 2002; Numazawa et al., 2003). Indeed, BGC display a higher Nrf2 expression than granular neurons and present ARE-mediated transcriptional activation by the antioxidant compound t-BHQ (Ahlgren-Beckendorf et al., 1999).

It is tempting to speculate that the genes that are transcriptionally regulated by BDNF in BGC are involved in the continuous neuronal/glia dialogue, fundamental for proper synaptic function. A working model is schematized in Fig. 6, work currently in progress in our labs is aimed at the characterization of signal transduction mechanisms triggered by BDNF in BGC that could possibly regulate the transcription of genes involved in the continuous glia/neuronal dialogue.

Acknowledgements

This work was supported by grants from Conacyt-Mexico to A.O. (79502 and 123625) and to E.L.B. (155518/2011). I.P.-N. and L.R. are supported by Conacyt/SNI-Mexico fellowship. The technical assistance of Luis Cid, Miriam Huerta and Blanca Ibarra is acknowledged.

References

Aharoni, R., Eilam, R., Domev, H., Labunskay, G., Sela, M., Arnon, R., 2005. The immunomodulator glatiramer acetate augments the expression of neurotrophic factors in brains of experimental autoimmune encephalomyelitis mice. Proc. Natl. Acad. Sci. USA 102, 19045–19050.

Ahlgren-Beckendorf, J.A., Reising, A.M., Schander, M.A., Herdler, J.W., Johnson, J.A., 1999. Coordinate regulation of NAD(P)H:quinone oxidoreductase and glutathione-S-transferases in primary cultures of rat neurons and glia: role of the antioxidant/electrophile responsive element. Glia 25, 131–142.

Alderson, R.F., Curtis, R., Alterman, A.L., Lindsay, R.M., DiStefano, P.S., 2000. Truncated TrkB mediates the endocytosis and release of BDNF and neurotrophin-4/5 by rat astrocytes and schwann cells in vitro. Brain Res. 871, 210–222.

Alonso, M., Bekinschtein, P., Cammarota, M., Vianna, M.R., Izquierdo, I., Medina, J.H., 2005. Endogenous BDNF is required for long-term memory formation in the rat parietal cortex. Learn Mem. 12, 504–510.

Allen, S.J., Dawbarn, D., Eckford, S.D., Wilcock, G.K., Ashcroft, M., Colebrook, S.M., Feeney, R., MacGowan, S.H., 1994. Cloning of a non-catalytic form of human trkB and distribution of messenger RNA for trkB in human brain. Neuroscience 60, 825–834.

Barbacid, M., 1995. Neurotrophic factors and their receptors. Curr. Opin. Cell Biol. 7, 148–155.

Barde, Y.A., Edgar, D., Thoenen, H., 1982. Purification of a new neurotrophic factor from mammalian brain. EMBO J. 1, 549–553.

Barker, P.A., 2009. Whither proBDNF? Nat. Neurosci. 12, 105–106.

Bellamy, T.C., 2006. Interactions between Purkinje neurones and Bergmann glia. Cerebellum 5, 116–126.

Bellamy, T.C., Ogden, D., 2006. Long-term depression of neuron to glial signalling in rat cerebellar cortex. Eur. J. Neurosci. 23, 581–586.

Bloom, D.A., Jaiswal, A.K., 2003. Phosphorylation of Nrf2 at Ser40 by protein kinase C in response to antioxidants leads to the release of Nrf2 from INrf2, but is not required for Nrf2 stabilization/accumulation in the nucleus and transcriptional activation of antioxidant response element-mediated NAD(P)H:quinone oxidoreductase-1 gene expression. J. Biol. Chem. 278, 44675–44682.

Bradford, M.M., 1976. A rapid and sensitive method for the quantitation of microgram quantities of protein utilizing the principle of protein-dye binding. Anal. Biochem. 72, 248–254.

Burbach, G.J., Hellweg, R., Haas, C.A., Del Turco, D., Deicke, U., Abramowski, D., Jucker, M., Staufenbiel, M., Deller, T., 2004. Induction of brain-derived neurotrophic factor in plaque-associated glial cells of aged APP23 transgenic mice. J. Neurosci. 24, 2421–2430.

Climent, E., Sancho-Tello, M., Minana, R., Barettino, D., Guerri, C., 2000. Astrocytes in culture express the full-length Trk-B receptor and respond to brain derived neurotrophic factor by changing intracellular calcium levels: effect of ethanol exposure in rats. Neurosci. Lett. 288, 53–56.

Condorelli, D.F., Salin, T., Dell' Albani, P., Mudo, G., Corsaro, M., Timmusk, T., Metsis, M., Belluardo, N., 1995. Neurotrophins and their trk receptors in cultured cells of the glial lineage and in white matter of the central nervous system. J. Mol. Neurosci. 6, 237–248.

Cunha, C., Brambilla, R., Thomas, K.L., 2010. A simple role for BDNF in learning and memory? Front. Mol. Neurosci. 3, 1.

de Melo Reis, R.A., Cabral-da-Silva, M.C., de Mello, F.G., Taylor, J.S., 2008a. Muller glia factors induce survival and neuritogenesis of peripheral and central neurons. Brain Res. 1205, 1–11.

de Melo Reis, R.A., Ventura, A.L., Schitine, C.S., de Mello, M.C., de Mello, F.G., 2008b. Muller glia as an active compartment modulating nervous activity in the

vertebrate retina: neurotransmitters and trophic factors. Neurochem. Res. 33, 1466–1474.
Dhakshinamoorthy, S., Jaiswal, A.K., 2000. Small maf (MafG and MafK) proteins negatively regulate antioxidant response element-mediated expression and antioxidant induction of the NAD(P)H: quinone oxidoreductase1 gene. J. Biol. Chem. 275, 40134–40141.
Frisen, J., Verge, V.M., Fried, K., Risling, M., Persson, H., Trotter, J., Hokfelt, T., Lindholm, D., 1993. Characterization of glial trkB receptors: differential response to injury in the central and peripheral nervous systems. Proc. Natl. Acad. Sci. USA 90, 4971–4975.
Gamboa, C., Ortega, A., 2002. Insulin-like growth factor-1 increases activity and surface levels of the GLAST subtype of glutamate transporter. Neurochem. Int. 40, 397–403.
Garner, A.S., Menegay, H.J., Boeshore, K.L., Xie, X.Y., Voci, J.M., Johnson, J.E., Large, T.H., 1996. Expression of TrkB receptor isoforms in the developing avian visual system. J. Neurosci. 16, 1740–1752.
Gokce, O., Runne, H., Kuhn, A., Luthi-Carter, R., 2009. Short-term striatal gene expression responses to brain-derived neurotrophic factor are dependent on MEK and ERK activation. PLoS One 4, e5292.
Harada, T., Harada, C., Kohsaka, S., Wada, E., Yoshida, K., Ohno, S., Mamada, H., Tanaka, K., Parada, L.F., Wada, K., 2002. Microglia-Muller glia cell interactions control neurotrophic factor production during light-induced retinal degeneration. J. Neurosci. 22, 9228–9236.
Hofer, M., Pagliusi, S.R., Hohn, A., Leibrock, J., Barde, Y.A., 1990. Regional distribution of brain-derived neurotrophic factor mRNA in the adult mouse brain. EMBO J. 9, 2459–2464.
Hofer, M.M., Barde, Y.A., 1988. Brain-derived neurotrophic factor prevents neuronal death in vivo. Nature 331, 261–262.
Huang, H.C., Nguyen, T., Pickett, C.B., 2002. Phosphorylation of Nrf2 at Ser-40 by protein kinase C regulates antioxidant response element-mediated transcription. J. Biol. Chem. 277, 42769–42774.
Imamura, K., Takeshima, T., Nakaso, K., Ito, S., Nakashima, K., 2008. Pramipexole has astrocyte-mediated neuroprotective effects against lactacystin toxicity. Neurosci. Lett. 440, 97–102.
Jean, Y.Y., Lercher, L.D., Dreyfus, C.F., 2008. Glutamate elicits release of BDNF from basal forebrain astrocytes in a process dependent on metabotropic receptors and the PLC pathway. Neuron Glia Biol. 4, 35–42.
Jordan, P.M., Cain, L.D., Wu, P., 2008. Astrocytes enhance long-term survival of cholinergic neurons differentiated from human fetal neural stem cells. J. Neurosci. Res. 86, 35–47.
Juric, D.M., Loncar, D., Carman-Krzan, M., 2008. Noradrenergic stimulation of BDNF synthesis in astrocytes: mediation via alpha1- and beta1/beta2-adrenergic receptors. Neurochem. Int. 52, 297–306.
Kimoto, H., Eto, R., Abe, M., Kato, H., Araki, T., 2009. Alterations of glial cells in the mouse hippocampus during postnatal development. Cell. Mol. Neurobiol. 29, 1181–1189.
Klein, R., Conway, D., Parada, L.F., Barbacid, M., 1990a. The trkB tyrosine protein kinase gene codes for a second neurogenic receptor that lacks the catalytic kinase domain. Cell 61, 647–656.
Klein, R., Martin-Zanca, D., Barbacid, M., Parada, L.F., 1990b. Expression of the tyrosine kinase receptor gene trkB is confined to the murine embryonic and adult nervous system. Development 109, 845–850.
Knusel, B., Winslow, J.W., Rosenthal, A., Burton, L.E., Seid, D.P., Nikolics, K., Hefti, F., 1991. Promotion of central cholinergic and dopaminergic neuron differentiation by brain-derived neurotrophic factor but not neurotrophin 3. Proc. Natl. Acad. Sci. USA 88, 961–965.
Koirala, S., Corfas, G., 2010. Identification of novel glial genes by single-cell transcriptional profiling of Bergmann glial cells from mouse cerebellum. PLoS One 5, e9198.
Kovalchuk, Y., Hanse, E., Kafitz, K.W., Konnerth, A., 2002. Postsynaptic induction of BDNF-mediated long-term potentiation. Science 295, 1729–1734.
Koyama, Y., Tsujikawa, K., Matsuda, T., Baba, A., 2005. Endothelin increases expression of exon III- and exon IV-containing brain-derived neurotrophic factor transcripts in cultured astrocytes and rat brain. J. Neurosci. Res. 80, 809–816.
Leibrock, J., Lottspeich, F., Hohn, A., Hofer, M., Hengerer, B., Masiakowski, P., Thoenen, H., Barde, Y.A., 1989. Molecular cloning and expression of brain-derived neurotrophic factor. Nature 341, 149–152.
Lessmann, V., Gottmann, K., Malcangio, M., 2003. Neurotrophin secretion: current facts and future prospects. Prog. Neurobiol. 69, 341–374.
Lin, Y., Chen, L., Lin, C., Luo, Y., Tsai, R.Y., Wang, F., 2009. Neuron-derived FGF9 is essential for scaffold formation of Bergmann radial fibers and migration of granule neurons in the cerebellum. Dev. Biol. 329, 44–54.
Lindholm, D., Dechant, G., Heisenberg, C.P., Thoenen, H., 1993. Brain-derived neurotrophic factor is a survival factor for cultured rat cerebellar granule neurons and protects them against glutamate-induced neurotoxicity. Eur. J. Neurosci. 5, 1455–1464.
Lipson, A.C., Widenfalk, J., Lindqvist, E., Ebendal, T., Olson, L., 2003. Neurotrophic properties of olfactory ensheathing glia. Exp. Neurol. 180, 167–171.
Lopez-Bayghen, E., Rosas, S., Castelan, F., Ortega, A., 2007. Cerebellar Bergmann glia: an important model to study neuron-glia interactions. Neuron Glia Biol. 3, 155–167.
Lopez-Bayghen, E., Vega, A., Cadena, A., Granados, S.E., Jave, L.F., Gariglio, P., Alvarez-Salas, L.M., 1996. Transcriptional analysis of the 5'-noncoding region of the human involucrin gene. J. Biol. Chem. 271, 512–520.
Maisonpierre, P.C., Belluscio, L., Squinto, S., Ip, N.Y., Furth, M.E., Lindsay, R.M., Yancopoulos, G.D., 1990. Neurotrophin-3: a neurotrophic factor related to NGF and BDNF. Science 247, 1446–1451.
Martinez, R., Eller, C., Viana, N.B., Gomes, F.C., 2011. Thyroid hormone induces cerebellar neuronal migration and Bergmann glia differentiation through epidermal growth factor/mitogen-activated protein kinase pathway. Eur. J. Neurosci. 33, 26–35.
Miklic, S., Juric, D.M., Carman-Krzan, M., 2004. Differences in the regulation of BDNF and NGF synthesis in cultured neonatal rat astrocytes. Int. J. Dev. Neurosci. 22, 119–130.
Murer, M.G., Yan, Q., Raisman-Vozari, R., 2001. Brain-derived neurotrophic factor in the control human brain, and in Alzheimer's disease and Parkinson's disease. Prog. Neurobiol. 63, 71–124.
Numazawa, S., Ishikawa, M., Yoshida, A., Tanaka, S., Yoshida, T., 2003. Atypical protein kinase C mediates activation of NF-E2-related factor 2 in response to oxidative stress. Am. J. Physiol. Cell Physiol. 285, C334–342.
Okamoto, H., Shino, Y., Hashimoto, K., Kumakiri, C., Shimizu, E., Shirasawa, H., Iyo, M., 2003. Dynamic changes in AP-1 transcription factor DNA binding activity in rat brain following administration of antidepressant amitriptyline and brain-derived neurotrophic factor. Neuropharmacology 45, 251–259.
Ortega, A., Eshhar, N., Teichberg, V.I., 1991. Properties of kainate receptor/channels on cultured Bergmann glia. Neuroscience 41, 335–349.
Ortega, A., Teichberg, V.I., 1990. Phosphorylation of the 49-kDa putative subunit of the chick cerebellar kainate receptor and its regulation by kainatergic ligands. J. Biol. Chem. 265, 21404–21406.
Patapoutian, A., Reichardt, L.F., 2001. Trk receptors: mediators of neurotrophin action. Curr. Opin. Neurobiol. 11, 272–280.
Poblete-Naredo, I., Angulo, C., Hernandez-Kelly, L., Lopez-Bayghen, E., Aguilera, J., Ortega, A., 2009. Insulin-dependent regulation of GLAST/EAAT1 in Bergmann glial cells. Neurosci. Lett. 451, 134–138.
Roback, J.D., Marsh, H.N., Downen, M., Palfrey, H.C., Wainer, B.H., 1995. BDNF-activated signal transduction in rat cortical glial cells. Eur. J. Neurosci. 7, 849–862.
Rocamora, N., Garcia-Ladona, F.J., Palacios, J.M., Mengod, G., 1993. Differential expression of brain-derived neurotrophic factor, neurotrophin-3, and low-affinity nerve growth factor receptor during the postnatal development of the rat cerebellar system. Brain Res. Mol. Brain Res. 17, 1–8.
Rose, C.R., Blum, R., Pichler, B., Lepier, A., Kafitz, K.W., Konnerth, A., 2003. Truncated TrkB-T1 mediates neurotrophin-evoked calcium signalling in glia cells. Nature 426, 74–78.
Rothstein, J.D., Martin, L., Levey, A.I., Dykes-Hoberg, M., Jin, L., Wu, D., Nash, N., Kuncl, R.W., 1994. Localization of neuronal and glial glutamate transporters. Neuron 13, 713–725.
Rubio, N., 1997. Mouse astrocytes store and deliver brain-derived neurotrophic factor using the non-catalytic gp95trkB receptor. Eur. J. Neurosci. 9, 1847–1853.
Rudge, J.S., Li, Y., Pasnikowski, E.M., Mattsson, K., Pan, L., Yancopoulos, G.D., Wiegand, S.J., Lindsay, R.M., Ip, N.Y., 1994. Neurotrophic factor receptors and their signal transduction capabilities in rat astrocytes. Eur. J. Neurosci. 6, 693–705.
Runyan, S.A., Phelps, P.E., 2009. Mouse olfactory ensheathing glia enhance axon outgrowth on a myelin substrate in vitro. Exp. Neurol. 216, 95–104.
Rutberg, S.E., Adams, T.L., Olive, M., Alexander, N., Vinson, C., Yuspa, S.H., 1999. CRE DNA binding proteins bind to the AP-1 target sequence and suppress AP-1 transcriptional activity in mouse keratinocytes. Oncogene 18, 1569–1579.
Saha, R.N., Liu, X., Pahan, K., 2006. Up-regulation of BDNF in astrocytes by TNF-alpha: a case for the neuroprotective role of cytokine. J. Neuroimmune Pharmacol. 1, 212–222.
Sanchez-Huertas, C., Rico, B., 2011. CREB-Dependent Regulation of GAD65 Transcription by BDNF/TrkB in Cortical Interneurons. Cereb. Cortex 21, 777–788.
Sanchez, G., Ortega, A., 1994. AMPA/KA receptor induced AP-1 DNA binding activity in cultured Bergmann glia cells. Neuroreport 5, 2109–2112.
Schecterson, L.C., Bothwell, M., 1992. Novel roles for neurotrophins are suggested by BDNF and NT-3 mRNA expression in developing neurons. Neuron 9, 449–463.
Schwartz, P.M., Borghesani, P.R., Levy, R.L., Pomeroy, S.L., Segal, R.A., 1997. Abnormal cerebellar development and foliation in BDNF-/- mice reveals a role for neurotrophins in CNS patterning. Neuron 19, 269–281.
Seki, M., Tanaka, T., Sakai, Y., Fukuchi, T., Abe, H., Nawa, H., Takei, N., 2005. Muller Cells as a source of brain-derived neurotrophic factor in the retina: noradrenaline upregulates brain-derived neurotrophic factor levels in cultured rat Muller cells. Neurochem. Res. 30, 1163–1170.
Singh, S., Vrishni, S., Singh, B.K., Rahman, I., Kakkar, P., 2010. Nrf2-ARE stress response mechanism: a control point in oxidative stress-mediated dysfunctions and chronic inflammatory diseases. Free Radic. Res. 44, 1267–1288.
Somogyi, P., Eshhar, N., Teichberg, V.I., Roberts, J.D., 1990. Subcellular localization of a putative kainate receptor in Bergmann glial cells using a monoclonal antibody in the chick and fish cerebellar cortex. Neuroscience 35, 9–30.
Stadelmann, C., Kerschensteiner, M., Misgeld, T., Bruck, W., Hohlfeld, R., Lassmann, H., 2002. BDNF and gp145trkB in multiple sclerosis brain lesions: neuroprotective interactions between immune and neuronal cells? Brain 125, 75–85.

Taylor, A.R., Gifondorwa, D.J., Newbern, J.M., Robinson, M.B., Strupe, J.L., Prevette, D., Oppenheim, R.W., Milligan, C.E., 2007. Astrocyte and muscle-derived secreted factors differentially regulate motoneuron survival. J. Neurosci. 27, 634–644.

Taylor, S., Srinivasan, B., Wordinger, R.J., Roque, R.S., 2003. Glutamate stimulates neurotrophin expression in cultured Muller cells. Brain Res. Mol. Brain Res. 111, 189–197.

Tokumine, J., Kakinohana, O., Cizkova, D., Smith, D.W., Marsala, M., 2003. Changes in spinal GDNF, BDNF, and NT-3 expression after transient spinal cord ischemia in the rat. J. Neurosci. Res. 74, 552–561.

Wetmore, C., Ernfors, P., Persson, H., Olson, L., 1990. Localization of brain-derived neurotrophic factor mRNA to neurons in the brain by in situ hybridization. Exp. Neurol. 109, 141–152.

Wilson, P.M., Fryer, R.H., Fang, Y., Hatten, M.E., 2010. Astn2, a novel member of the astrotactin gene family, regulates the trafficking of ASTN1 during glial-guided neuronal migration. J. Neurosci. 30, 8529–8540.

Wu, H., Friedman, W.J., Dreyfus, C.F., 2004. Differential regulation of neurotrophin expression in basal forebrain astrocytes by neuronal signals. J. Neurosci. Res. 76, 76–85.

Xu, Z.Q., Sun, Y., Li, H.Y., Lim, Y., Zhong, J.H., Zhou, X.F., 2011. Endogenous proBDNF is a negative regulator of migration of cerebellar granule cells in neonatal mice. Eur. J. Neurosci. 33, 1376–1384.

Yamada, K., Watanabe, M., 2002. Cytodifferentiation of Bergmann glia and its relationship with Purkinje cells. Anat. Sci. Int. 77, 94–108.

Zhang, H.T., Li, L.Y., Zou, X.L., Song, X.B., Hu, Y.L., Feng, Z.T., Wang, T.T., 2007. Immunohistochemical distribution of NGF, BDNF, NT-3, and NT-4 in adult rhesus monkey brains. J. Histochem. Cytochem. 55, 1–19.

Zhou, X., Nai, Q., Chen, M., Dittus, J.D., Howard, M.J., Margiotta, J.F., 2004. Brain-derived neurotrophic factor and trkB signaling in parasympathetic neurons: relevance to regulating alpha7-containing nicotinic receptors and synaptic function. J. Neurosci. 24, 4340–4350.

Zirrgiebel, U., Ohga, Y., Carter, B., Berninger, B., Inagaki, N., Thoenen, H., Lindholm, D., 1995. Characterization of TrkB receptor-mediated signaling pathways in rat cerebellar granule neurons: involvement of protein kinase C in neuronal survival. J. Neurochem. 65, 2241–2250.

ASN NEURO RESEARCH ARTICLE

ASN NEURO 4(5):art:e00095.doi:10.1042/AN20120022

Glutamate transporter-dependent mTOR phosphorylation in Müller glia cells

Ana María López-Colomé*, Zila Martínez-Lozada†, Alain M Guillem†, Edith López* and Arturo Ortega†1

*División de Neurociencias, Instituto de Fisiología Celular, Universidad Nacional Autónoma de México, México D.F., México

†Departamento de Genética y Biología Molecular, Centro de Investigación y de Estudios Avanzados del Instituto Politécnico Nacional, Apartado Postal 14-740, México D.F. 07000, México

Cite this article as: López-Colomé AM, Martínez-Lozada Z, Guillem AM, López E and Ortega A (2012) Glutamate transporter-dependent mTOR phosphorylation in Müller glia cells. ASN NEURO 4(5):art:e00095.doi:10.1042/AN20120022

ABSTRACT

Glu (glutamate), the excitatory transmitter at the main signalling pathway in the retina, is critically involved in changes in the protein repertoire through the activation of signalling cascades, which regulate protein synthesis at transcriptional and translational levels. Activity-dependent differential gene expression by Glu is related to the activation of ionotropic and metabotropic Glu receptors; however, recent findings suggest the involvement of Na^+-dependent Glu transporters in this process. Within the retina, Glu uptake is aimed at the replenishment of the releasable pool, and for the prevention of excitotoxicity and is carried mainly by the GLAST/EAAT-1 (Na^+-dependent glutamate/aspartate transporter/excitatory amino acids transporter-1) located in Müller radial glia. Based on the previous work showing the alteration of GLAST expression induced by Glu, the present work investigates the involvement of GLAST signalling in the regulation of protein synthesis in Müller cells. To this end, we explored the effect of D-Asp (D-aspartate) on Ser-2448 mTOR (mammalian target of rapamycin) phosphorylation in primary cultures of chick Müller glia. The results showed that D-Asp transport induces the time- and dose-dependent phosphorylation of mTOR, mimicked by the transportable GLAST inhibitor THA (threo-β-hydroxyaspartate). Signalling leading to mTOR phosphorylation includes Ca^{2+} influx, the activation of $p60^{src}$, phosphatidylinositol 3-kinase, protein kinase B, mTOR and $p70^{S6K}$. Interestingly, GLAST activity promoted AP-1 (activator protein-1) binding to DNA, supporting a function for transporter signalling in retinal long-term responses. These results add a novel receptor-independent pathway for Glu signalling in Müller glia, and further strengthen the critical involvement of these cells in the regulation of glutamatergic transmission in the retina.

Key words: excitatory amino acid, gene expression regulation, signalling.

INTRODUCTION

Glu (glutamate), the main excitatory neurotransmitter in the radial signalling pathway of the vertebrate retina (Massey and Miller, 1990), regulates proliferation, migration and survival of neuronal progenitors and immature neurons (Guerrini et al., 1995). It also plays a key role in the regulation of gene expression required for physiological adaptive processes, including synaptic plasticity (Thomas and Huganir, 2004; Wang et al., 2007).

The ability of Glu to drive a diversity of functions relates to its interaction with a wide variety of receptor subtypes and transporters that act independently or in combination to attain differential responses. Glutamatergic activity is mediated by iGluRs (ionotropic receptors) and mGluRs (G-protein-coupled metabotropic receptors). The superfamily of iGluRs includes the Na^+- or Ca^{2+}-permeable cation channels NMDA (*N*-methyl-D-aspartate), AMPA (α-amino-3-hydroxy-5-methylisoxazole-4-propionic acid) and KA (kainite) receptors. Eight mGluRs, linked to the activation of second messenger cascades, have been identified (Michaelis, 1998), coupled to the stimulation of phospholipase C and the release of intracellular Ca^{2+} (Group I), or to the inhibition of adenylyl cyclase (Groups II and III) (Coutinho and Knopfel, 2002).

Glia cells respond to neurotransmitters through the activation of specific receptors and intracellular pathways,

[1] To whom correspondence should be addressed (email arortega@cinvestav.mx).

Abbreviations: AMPA, α-amino-3-hydroxy-5-methylisoxazole-4-propionic acid; AP-1, activator protein-1, EAAT1-5, excitatory amino acids transporters 1-5; 4E-BP, 4E-binding protein; GLAST, Na^+-dependent glutamate/aspartate transporter; iGluR, ionotropic receptor; KA, kainite; MGC, Müller glia cells; mGluRs, G-protein-coupled metabotropic receptors; mTOR, mammalian target of rapamycin; NMDA, *N*-methyl-D-aspartate; PBS, phosphate-buffer saline; PDC, L-*trans*-pyrrolidine-2,4-dicarboxylic acid; PKB/Akt, protein kinase B; $p70^{S6K}$, 70 kDa S6 ribosomal kinase; RTK, receptor tyrosine kinase; Src, non-receptor tyrosine kinase $p60^{src}$; T3MG, ($\pm$)-threo-3-methylglutamic acid; THA, threo-β-hydroxyaspartate.

which directly or indirectly modify the neuronal activity (Fields and Stevens-Graham, 2002). Among its functions, MGC (Müller glia cells), the main type of retinal glia, are responsible for potassium homoeostasis, lactate supply to neurons, pH regulation and neurotransmitter removal (Hollander et al., 1991; Lopez-Colome and Romo-de-Vivar, 1991; Rauen and Kanner, 1994; Lopez et al., 1997; Bringmann et al., 2009).

Owing to their close apposition to synaptic contacts in both plexiform layers of the retina, MGC are exposed to synaptically released Glu, and are involved in the recycling of Glu through the Glu/glutamine neuron–glia shuttle, which provides Glu supply to the presynaptic terminals. Also along this line, the activation of Glu receptors in Müller cells feeds back on to neurons by triggering the release of neuroactive compounds (Uchihori and Puro, 1993; Lopez-Colome et al., 1995; Lopez et al., 1998; Lopez-Bayghen et al., 2006).

mTOR (mammalian target of rapamycin), now officially known as mechanistic TOR, is a protein kinase involved in the regulation of a wide range of cellular processes including protein synthesis, gene transcription, the cell cycle and autophagy (Proud, 2007; Laplante and Sabatini, 2012), and it has been implicated in cancer and other diseases, as well as in the control of lifespan and aging (Blagosklonny, 2010). mTOR forms the catalytic core of two different complexes: mTOR complex 1 (mTORC1) and mTOR complex 2 (mTORC2) that differ in composition; while complex 1 contains raptor, complex 2 is composed of rictor, Sin1 and protor. Both complexes contain mLST8 (Wang and Proud, 2011). mTORC1 but not mTORC2 is inhibited by a low concentration of the macrolide rapamycin; in an over-simplified scenario, mTORC1 mediates the mTOR effects that are rapamycin-sensitive. An accepted index of mTOR activation is Ser-2448 phosphorylation as the result of a signalling cascade involving PI3K (phosphoinositide 3-kinase), PDK1 (phosphoinositide-dependent kinase 1), mTORC2 and PKB/Akt (protein kinase B), which can phosphorylate mTORC1 (Foster and Fingar, 2010). Phosphorylated mTORC1 acts on $p70^{S6K}$ (70 kDa S6 ribosomal kinase), 4E-BP (4E-binding protein), eEF2K (eukaryotic elongation factor 2 kinase) and eEF1A (eukaryotic elongation factor 1A), increasing translation. It should be noted that $p70^{S6K}$ also phosphorylates mTOR at Ser-2448, which is assumed to be an additional level of mTOR regulation (Rosner and Hengstschlager, 2010).

Glu concentration at the synaptic cleft requires tight regulation in order to avoid excitotoxic neuronal death (Mattson, 2003; Olney, 2003). Such regulation is accomplished through the removal of Glu by a family of Na^+-dependent transporters expressed in neurons and glia (Danbolt, 2001). To date, five subtypes of transporters known as EAAT1–5 (excitatory amino acids transporters 1–5) have been reported. The glia transporters EAAT-1 [GLAST (Na^+-dependent glutamate/aspartate transporter)] and EAAT-2 (GLT-1) are responsible for more than 90% of the Glu uptake in the brain. In the retina, although the expression of EAAT-4 has been reported (Fyk-Kolodziej et al., 2004), GLAST, located in Müller cells, is the predominant transporter responsible for Glu reuptake (Gadea et al., 2004).

Evidence has accumulated suggesting that Glu transporters might be involved in intracellular signalling. In fact, Glu and transportable blockers down-regulate Glu uptake in a receptor-independent manner (Gonzalez and Ortega, 2000; Gadea et al., 2004). Furthermore, the coupling of GLAST/EAAT-1 activity to the Na^+/K^+ ATPase in astrocytes (Gegelashvili et al., 2007; Rose et al., 2009) and to the promotion of mTOR phosphorylation in cerebellar glia (Zepeda et al., 2008) has also been reported.

Dysfunction of EAATs is specifically involved in excitotoxic neuronal death under pathological neurodegenerative conditions and ischaemic stroke injury, characterized by the elevation of extracellular Glu. Hence, the characterization of signalling mechanisms activated by transporter function may provide tools for the modulation of EAAT function under pathological conditions.

In order to provide evidence for GLAST/EAAT-1-mediated Glu signalling in the vertebrate retina, we analysed transporter-dependent mTOR phosphorylation in primary cultures of chick MGC. Our results show that GLAST activity triggers Ca^{2+} influx, and increases mTOR phosphorylation and AP-1 (activator protein-1) DNA-binding activity, suggesting that Glu imbalance could alter the translation of proteins involved in gene regulation in the retina.

MATERIALS AND METHODS

Materials

Tissue culture reagents were obtained from GE Healthcare. Wortmannin, amiloride [3,5-diamino-6-chloro-*N*-(diaminomethylene)pyrazine-2-carboxamide], PP2 {4-amino-5-(4-chlorophenyl)-7-(dimethylethyl)pyrazolo[3,4-*d*]pyrimidine}, W7 [N-(6-aminohexyl)-5-chloro-1-naphthalenesulfonamide], AMPA, KA acid, NMDA, CNQX (6-cyano-7-nitroquinoxaline-2,3-dione), DL-TBOA (DL-threo-b-benzyloxyaspartic acid), THA (threo-β-hydroxyaspartate), D-Asp and Glu were all obtained from Tocris-Cookson. $^{45}Ca^{2+}$ and [α^{32}P]dATP was from PerkinElmer. Polyclonal anti-phospho-mTOR (Ser-2448) and anti-mTOR antibodies (05-235) were purchased from Cell Signalling Technology. Anti-phospho-$p60^{src}$ (Tyr-527) was obtained from Abcam. Horseradish peroxidase-linked anti-rabbit antibodies and the enhanced chemiluminescence reagent (ECL) were obtained from Amersham Biosciences. PDC (L-*trans*-pyrrolidine-2,4-dicarboxylic acid), T3MG [(±)-threo-3-methylglutamic acid] and all other chemicals were purchased from Sigma.

Cell culture and stimulation protocol

Primary cultures of retina MGC were prepared from 7-day-old chick embryos as previously described (Lopez-Colome

et al., 1993). The cells were plated in 6- or 24-well plastic culture dishes in OptiMEM containing 4% foetal bovine serum, 2 mM glutamine and gentamicin (50 μg/ml) and used on the 10th to the 12th day in the culture. Before any treatment, confluent monolayers were serum-deprived with 0.5% bovine serum albumin in OptiMEM for 30 min and then treated as indicated. Inhibitors were included 30 min prior to agonist addition. Glu and its analogues were added to the medium for the indicated time periods; following treatment, the medium was replaced by 0.5% albumin/OptiMEM.

SDS/PAGE and Western blots

Cells from confluent monolayers were harvested in PBS (phosphate-buffered saline) (10 mM K_2HPO_4/KH_2PO_4, 150 mM NaCl, pH 7.4) containing phosphatase inhibitors (10 mM NaF, 1 mM Na_2MoO_4 and 1 mM Na_3VO_4). The cells were lysed with RIPA buffer (50 mM Tris/HCl, 1 mM EDTA, 150 mM NaCl, 1 mM PMSF, 1 mg/ml aprotinin, 1 mg/ml leupeptin, 1% NP-40, 0.25% sodium deoxycolate, 10 mM NaF, 1 mM Na_2MoO_4 and 1 mM Na_3VO_4, pH 7.4). Cell lysates were denatured in Laemmli's buffer, and proteins resolved by SDS/PAGE (6–10% gel) and electroblotted on to nitrocellulose membranes. Blots were stained with Ponceau S to confirm that protein content was equal in all lanes. Membranes were soaked in PBS to remove the Ponceau S and incubated in 50 mM Tris/HCl, pH 7.4, and 150 mM NaCl (TBS) containing 5% dried skimmed milk and 0.1% Tween 20 for 60 min to block the excess of non-specific protein binding sites. The membranes were then incubated overnight at 4°C with the primary antibodies indicated in each Figure, followed by the corresponding secondary antibodies. Immunoreactive polypeptides were detected by chemiluminescence and exposed to X-ray films. Densitometric analyses were performed and data were analysed with Prism from GraphPad Software.

$^{45}Ca^{2+}$ Influx

Confluent MGC monolayers seeded in 24-well plates were washed three times to remove all non-adhering cells with 0.5 ml aliquots of solution A containing 25 mM Hepes/Tris, 130 mM NaCl, 5.4 mM KCl, 1.8 mM $CaCl_2$, 0.8 mM $MgCl_2$, 33.3 mM glucose and 1 mM NaH_2PO_4 at pH 7.4. The Glu- or D-Asp-induced $^{45}Ca^{2+}$ influx was initiated at $t=0$ by the addition of 0.5 ml of solution A containing 1.5 μCi of $^{45}Ca^{2+}$/ml solution A, Glu or D-Asp at a given concentration. When tested, inhibitors or modulators were included 30 min prior to the addition of $^{45}Ca^{2+}$. The reaction was stopped by aspirating the radioactive medium and washing each well within 15 s with 0.5 ml aliquots of an ice-cold solution A. The cells were digested in 0.5 ml of 1 M NaOH for 2 h at 37°C. The radioactivity contained in each fraction was determined using a Beckmann 7800LS scintillation counter in the presence of a scintillation cocktail. All experiments were performed in triplicate.

EMSAs (electrophoretic mobility-shift assays)

After the stimulation period, the cells were shifted to complete culture media for 1 h and nuclear extracts were prepared as described previously (Zepeda et al., 2008). All the buffers contained a protease inhibitor cocktail to prevent nuclear factor proteolysis. Protein concentration was measured using the Bradford method. Nuclear extracts (approximately 20 μg) from control or treated MGC were incubated on ice with 500 ng of poly[(dI-dC)] as non-specific competitor (LG Healthcare) and 1 ng of [^{32}P]-end labelled double-stranded AP-1 (SV40) oligonucleotide: 5′-CTAGTTCC-GGCTGAGTCATCAAGC-3′

The reaction mixtures were incubated for 20 min on ice, and the proteins were separated by electrophoresis in SDS/PAGE (6% gels) in a low ionic strength 0.5X TBE buffer. The gels were vacuum-dried and exposed to an auto-radiographic film overnight.

Statistical analysis

Data are expressed as the mean (average) ± standard error (S.E.). A one-way analysis of variance (ANOVA) (Kruskal–Wallis test) and Dunn's post-hoc test were performed to determine significant differences between conditions with the Prism software.

RESULTS

Glu- and D-Asp-induced mTOR phosphorylation in MGCs

mTOR is a fundamental kinase involved in translational control, the fine-tuning process of gene expression. As Glu is known to modify this process, we investigated a possible Glu transport-mediated change in mTOR phosphorylation pattern in retinal MGC. As depicted in Figure 1(A), inclusion of 1 mM Glu induced a fast time-dependent increase in Ser-2448 mTOR phosphorylation, reaching a maximal value at 15 min. No apparent changes in mTOR levels were observed in this condition. The results presented in Figure 1(B) show that a time-dependent increase in mTOR phosphorylation by Glu was also induced by 1 mM D-Asp. The return of mTOR phosphorylation to basal levels in both conditions suggests a Glu- or D-Asp-dependent $p70^{S6K}$ dephosphorylation that through a feedback loop would decrease mTOR Ser-2448 phosphorylation (Harrington et al., 2004; Um et al., 2004; Rosner and Hengstschlager, 2010).

Exposure of MGC cultures to increasing concentrations of D-Asp for 15 min reveals a clear dose-dependency with an apparent EC_{50} of 15.2 μM (Figure 1C), indicating the specificity of the effect. It should be noted that this value is only indicative of a receptor/transporter-mediated effect,

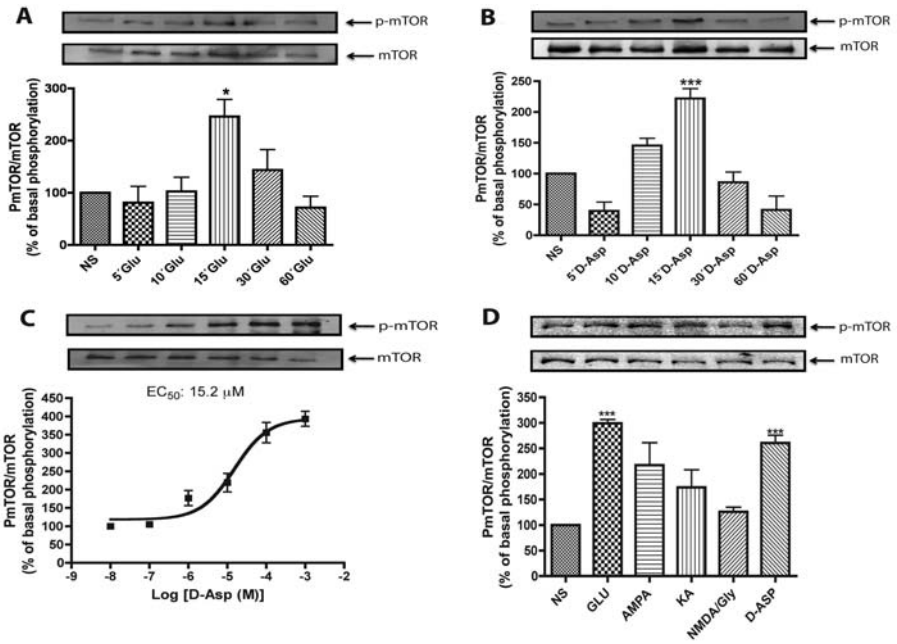

Figure 1 **D-Asp induces Ser-2448 mTOR phosphorylation**

(**A**) MGC were treated with 1 mM Glu for the indicated time periods, and the level of total and Ser-2448 phosphorylated mTOR were analysed by Western blot as described in the Materials and methods section. (**B**) Confluent MGC monolayers were treated with 1 mM D-Asp for the indicated time periods. The level of mTOR phosphorylation was determined as described for (**A**). (**C**) Müller glia cultures were exposed for 15 min to increasing D-Asp concentrations; the EC_{50} was calculated from the densitometric analysis using the Prism program (GraphPad). (**D**) Cells were incubated for 15 min with vehicle (NS), Glu (1 mM) or the Glu analogues AMPA (1 mM), KA (1 mM), NMDA (1 mM) plus 10 μM glycine (NMDA/Gly), and D-Asp (1 mM). The results are presented as the mean ±S.E. of at least three independent experiments. In each panel, a representative Western blot is shown. Statistical analysis was performed comparing against non-stimulated cells using a non-parametric one-way ANOVA (Kruskal–Wallis test) and Dunn's post-hoc test (*$P<0.05$, ***$P<0.001$).

as it does not take into consideration the amplification inherent to signalling cascades (Kholodenko, 2006).

In order to discard the contribution of Glu receptors to the observed effects, the cells were treated with 1 mM of the specific ionotropic receptor agonists: AMPA, KA and NMDA plus glycine (10 μM). A discrete non-significant increase in mTOR phosphorylation by AMPA and KA was detected (Figure 1D), suggesting that the transporter activity is responsible for most, if not all, of the Glu-induced mTOR phosphorylation.

In order to confirm these results, MGC were treated for 30 min, prior to D-Asp or THA addition, with 50 μM of the non-NMDA iGluR antagonist CNQX (Figure 2A), the NMDA receptor antagonist MK-801, the group I mGluR antagonist LAP5, or with CPCCOEt, the group II/III mGluR antagonist (Figures 2B and 2C). The results showed that Glu receptor antagonists failed to block the increase in mTOR phosphorylation induced by D-Asp or THA, further supporting the fact that the effect of Glu on mTOR is mainly transporter-mediated. Moreover, as D-Asp does not activate Glu receptors, the lack of a statistically significant difference between the Glu- and D-Asp-induced effects further indicates that mTOR phosphorylation is transporter-mediated.

GLAST/EAAT-1-dependent mTOR phosphorylation

In order to directly confirm that the D-Asp-induced increase in mTOR phosphorylation relies on GLAST/EEAT-1 transport activity, the effect of transportable and non-transportable GLAST inhibitors was analysed. As shown in Figure 3(A), D-Asp-induced increase in mTOR phosphorylation was mimicked by 100 μM of the transportable inhibitors THA and PDC. In contrast, the non-transportable inhibitor TBOA (100 μM) had no effect. As the expression of EAAT-4 in MGC has been recently reported (Fyk-Kolodziej et al., 2004), we evaluated the involvement of this transporter in mTOR phosphorylation. As clearly shown in Figure 3(B), pretreatment with the specific EAAT-4 blocker T3MG did not alter the D-Asp response, ruling out the participation of EAAT-4.

If, indeed, the effect of D-Asp and THA is mediated by GLAST activity, it should be abolished in the Na^+-free medium. As clearly shown in Figure 3(C), mTOR phosphorylation was completely prevented by substituting choline chloride for NaCl, clearly demonstrating the involvement of Na^+-dependent transport in this process. In order to provide evidence for transporter-mediated mTOR activation, we

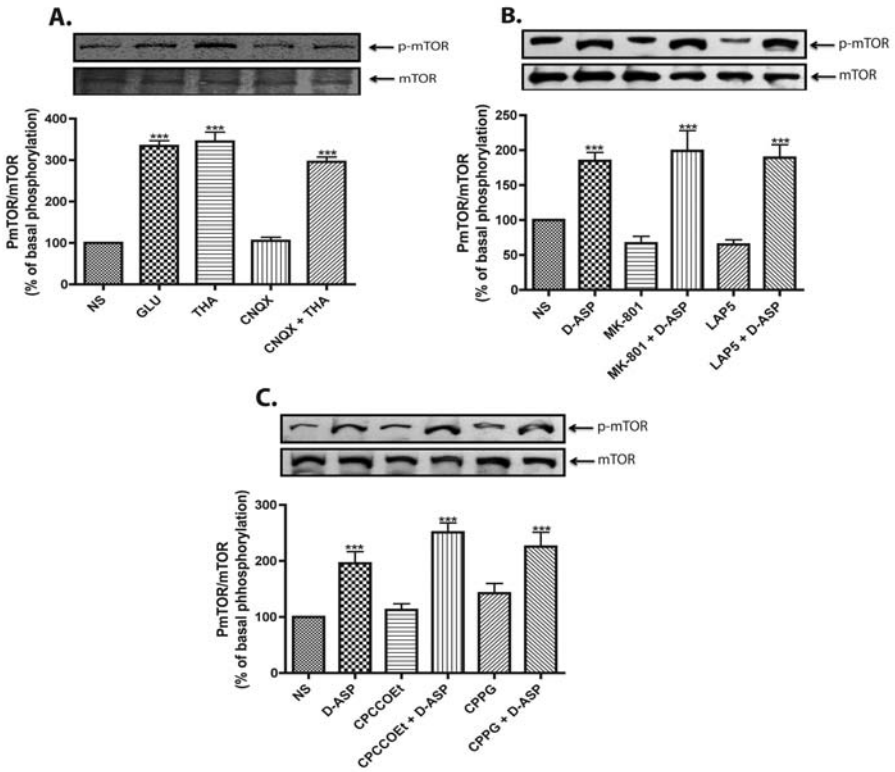

Figure 2 **D-Asp-induced mTOR phosphorylation is GLAST activity-dependent**
In all panels phosphorylated mTOR was detected as described for Figure 1. (**A**) MGC monolayers were incubated for 15 min with Glu (1 mM), THA (100 μM), the AMPA receptor antagonist CNQX (50 μM), and CNQX plus THA, in this case CNQX was added 30 min prior to THA treatment (100 μM, 15 min). MGC cultures were pre-exposed to NMDA receptor antagonists MK-801 (5 μM) or LAP5 (10 μM) (**B**) and to metabotropic Glu receptors antagonists, for group I CPCCOEt (100 μM) and for group II/III CPPG (300 μM) (**C**), 30 min prior to D-Asp treatment (1 mM, 15 min). Data are expressed as the mean ±S.E. of at least three independent experiments. Representative Western blots are shown for each condition. Statistical analysis was performed comparing against non-stimulated cells using a non-parametric one-way ANOVA (Kruskal–Wallis test) and Dunn's post-hoc test (*$P<0.05$, ***$P<0.001$).

explored the phosphorylation of one of its substrates, 4E-BP; the results are shown in Figure 4(D). Exposure of the cultured cells to D-Asp or THA results in a rapamycin-sensitive increase in 4E-BP phosphorylation.

GLAST-induced mTOR phosphorylation is Ca^{2+}-dependent

Intracellular Na^+ increase driven by GLAST may activate Na^+/Ca^{2+} exchange, leading to an increase in intracellular Ca^{2+} concentration. In order to assess the Ca^{2+}-dependence of the GLAST response, the cells were treated with D-Asp or THA in Ca^{2+}-free medium supplemented with 500 μM EDTA. As shown in Figure 4(A), removal of extracellular Ca^{2+} fully prevented the GLAST effect on mTOR phosphorylation. These results demonstrate that GLAST-mediated mTOR phosphorylation requires Ca^{2+} influx. As a possible mechanism linking transporter activity to Ca^{2+} entry, the activation of the Na^+/Ca^{2+} exchanger by GLAST-mediated Na^+ influx was explored using the inhibitors amiloride and KB-R7943. The results in Figure 4(B) show that both compounds prevented D-Asp-induced mTOR phosphorylation. Since calmodulin is the main Ca^{2+} intracellular receptor, its possible participation in GLAST induction of Ca^{2+}-dependent mTOR activation was explored. The results in Figure 4(C) show that 25 μM of the calmodulin antagonist W7 fully prevented the D-Asp response. Collectively, these data indicate that the D-Asp increase in mTOR phosphorylation is achieved through the entry of Na^+ as a result of GLAST activity and the consequent activation of the Na^+/Ca^{2+} exchanger, which, in turn, increases the intracellular Ca^{2+} that binds to calmodulin.

GLAST-induced $^{45}Ca^{2+}$ influx

To further confirm this conclusion, confluent MGC cultures were exposed to a 1 mM D-Asp solution containing 1 μCi/ml $^{45}Ca^{2+}$ for various time periods. As shown in Figure 5(A), D-Asp induced a fast time-dependent influx of $^{45}Ca^{2+}$, which saturated at 3 min. As expected, removal of extracellular Na^+ ions prevents the D-Asp-induced $^{45}Ca^{2+}$ influx (Figure 5B). A fixed 10 μM concentration of the Ca^{2+}ionophore A23187, as well as THA and PDC, also evoked significant entry of the

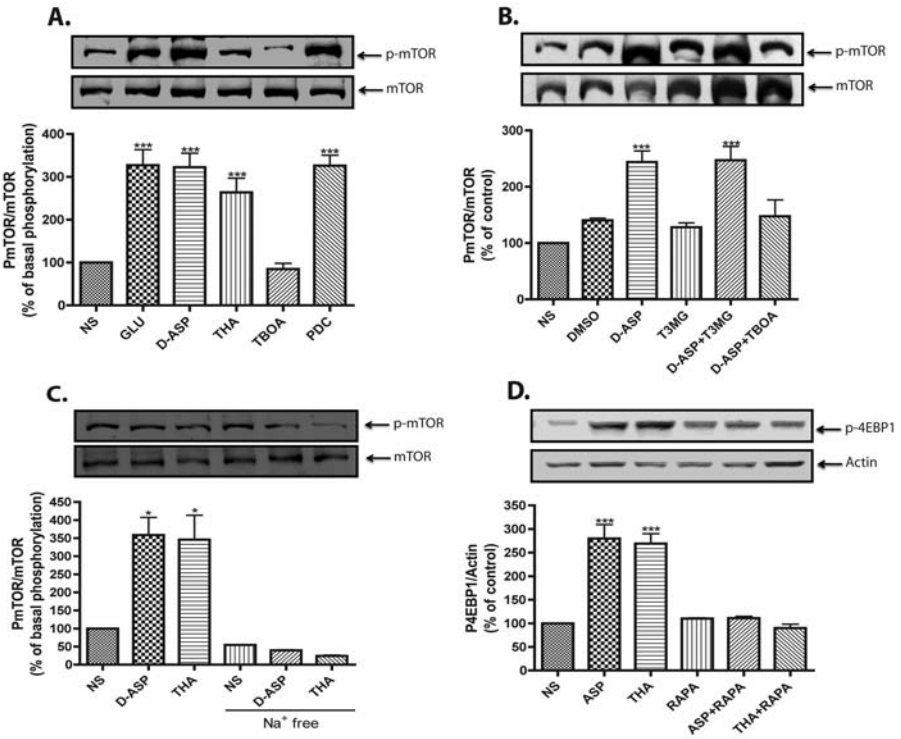

Figure 3 **D-Asp-induced mTOR phosphorylation is transport-dependent event**

(**A**) MGC monolayers were incubated for 15 min with vehicle (NS), Glu (1 mM), D-Asp (1 mM) or EAAT blockers, THA (100 μM), TBOA (100 μM) and PDC (100 μM), and the levels of Ser-2448 phosphorylated mTOR and total mTOR were detected via Western blots. (**B**) Cultured cells were treated with EAAT-4 blocker T3MG (200 μM) or TBOA (100 μM) for 30 min, prior to the addition of 1 mM D-Asp for 15 min, DMSO (0.01%) was used as a vehicle control. (**C**) MGC monolayers were exposed to vehicle (NS), D-Asp (1 mM) or THA (100 μM), in complete or Na^+-free assay buffer and then the phosphorylation of mTOR was analysed. (**D**) Levels of Thr 70 phosphorylated 4E-BP were detected after treatment with 1 mM D-Asp or 100 μM THA in the presence or absence of 100 nM rapamicin (RAPA) for 30 min; actin was used as loading control. Data are expressed as the mean ± S.E. of at least three independent experiments. Representative Western blots are shown for each condition. Statistical analysis was performed comparing against non-stimulated cells using a non-parametric one-way ANOVA (Kruskal–Wallis test) and Dunn's post-hoc test (*$P<0.05$, ***$P<0.001$).

radioactive ion (Figure 5C). In contrast, the non-transportable GLAST inhibitor TBOA did not induce $^{45}Ca^{2+}$ influx (Figure 5D). The EAAT-4 blocker T3MG failed to prevent the D-Asp-evoked response (Figure 5E). Furthermore, the Na^+/Ca^{2+} exchanger specific inhibitor KB-R7943 prevented the D-Asp-triggered increase in $^{45}Ca^{2+}$ influx (Figure 5F), clearly indicating a transporter-induced effect. To rule out the participation of the L-type voltage-gated Ca^{2+} channels (VGCC), confluent MGC cultures were pre-incubated with 10 μM nifedipine and the effect of D-Asp measured. As shown in Figure 5(G), pre-incubation with nifedipine did not modify the D-Asp-dependent Ca^{2+} influx.

Intracellular signalling involved in GLAST-mediated mTOR phosphorylation

To establish the molecular signalling cascade involved in GLAST-mediated mTOR phosphorylation, we first explored the participation of PI3K, known to act upstream of mTOR in several systems. Pretreatment of MGC for 15 min with 10 nM of the PI3K inhibitor wortmannin, completely prevented the increase in mTOR phosphorylation induced by either D-Asp or THA (Figure 6A).

The phosphorylation of membrane phosphatidylinositol at the C3-OH position of the inositol ring by PI3K is known to anchor proteins containing PH (pleckstrin homology) domains (Harrington et al., 2004), such as PKB. The results in Figure 6(B) demonstrate that 100 nM of the PKB inhibitor PKBI-IV was capable of preventing the GLAST-mediated effect, indicating the involvement of PKB, downstream of PI3K, in GLAST-dependent mTOR phosphorylation.

Activation of PI3K involves the docking of the regulatory subunit of PI3K to a phosphorylated tyrosine residue (Vanhaesebroeck and Alessi, 2000). We evaluated the possible involvement of the Src (non-receptor tyrosine kinase $p60^{src}$) in GLAST signalling. As clearly shown in Figure 6(C), MGC pretreatment with 10 nM of the specific Src inhibitor PP2, prevented the D-Asp effect on mTOR. Since Src activation requires Tyr-527 in a dephosphorylated state, we examined the phosphorylation level of this residue in D-Asp-stimulated MGC and showed that, indeed, D-Asp treatment sharply reduced Tyr-527 $p60^{src}$ phosphorylation levels (Figure 6D). This result

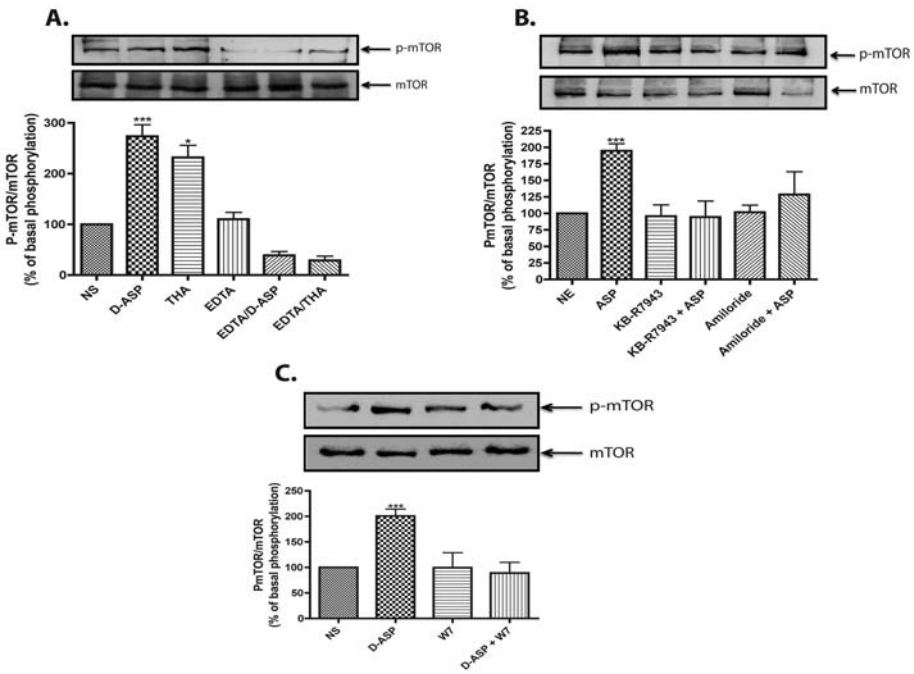

Figure 4 **D-Asp-induced mTOR phosphorylation is a Na^+/Ca^{2+} exchanger-dependent event**
mTOR phosphorylation was detected as for Figure 1. (**A**) Monolayers were incubated in normal or Ca^{2+}-free medium supplemented with EDTA (500 μM, 30 min), and then treated with D-Asp (1 mM) or THA (100 μM) for 15 min. (**B**) MGC were stimulated with D-Asp (1 mM, 15 min) in the presence or absence of the Na^+/Ca^{2+} exchanger inhibitors amiloride (10 μM) or KB-R7943 (15 μM) added 30 min prior to D-Asp treatment. (**C**) MGC monolayers were pretreated (30 min) with the calmodulin antagonist, W7 (25 μM) prior treatment with D-Asp (1 mM, 15 min). The results are the mean ± S.E. of at least three independent experiments. In each panel a representative Western blot is shown. Statistical analysis was performed comparing against non-stimulated cells using a non-parametric one-way ANOVA (Kruskal–Wallis test) and Dunn's post-hoc test (*$P<0.05$, ***$P<0.001$).

suggested the participation of an RTK (receptor tyrosine kinase) upstream of Src in GLAST-mediated mTOR phosphorylation. In order to explore this possibility, the effect of the RTK inhibitor genistein (25 μM) was tested. As expected, genistein was capable of preventing the effect of D-Asp (Figure 6D), suggesting a $p60^{src}$-dependent RTK *trans*-phosphorylation.

GLAST activity signalling-dependent transcriptional control

Glu stimulation has been linked to transcriptional control in glial cells (Lopez-Bayghen et al., 2006). Following the demonstration of GLAST-induced Ca^{2+}-dependent activation of the translation regulator mTOR, the possible induction of gene transcription by this process was analysed. We investigated if GLAST activity induced by D-Asp and THA results in increased DNA binding of the inducible transcription factor AP-1, known to be Ca^{2+}-dependent in MGC (Lopez-Colome et al., 1995). The results presented in Figure 7(A), clearly show that D-Asp as well as Glu and THA increase GLAST-mediated AP-1 DNA-binding activity in Müller cells. In order to explore the participation of Na^+/Ca^{2+} exchanger in transcriptional regulation, the effects of the Na^+/Ca^{2+} exchanger inhibitor (KB-R7943) and of the calmodulin antagonist W7 were determined. The results shown in Figure 7(B) clearly demonstrate that Na^+/Ca^{2+} exchanger and calmodulin participates in the transcriptional regulation mediated by GLAST.

DISCUSSION

Traditionally regarded as supportive and passive elements, glia cells have proven to be critically involved in glutamatergic transmission (Eulenburg and Gomeza, 2010). The participation of glia cells in the control of excitatory transmission through the so-called Glu/glutamine shuttle, which replenishes releasable Glu stores in neurons, has been recognized for more than 25 years (Shank and Campbell, 1984). Furthermore, an energetic neuronal dependence on astrocytes has also been described for glutamatergic synapses (Pellerin, 2008). In spite of the fact that most Glu receptors are expressed in glia cells (D'Antoni et al., 2008), the availability of Glu for inter-neuronal and neuron–glia

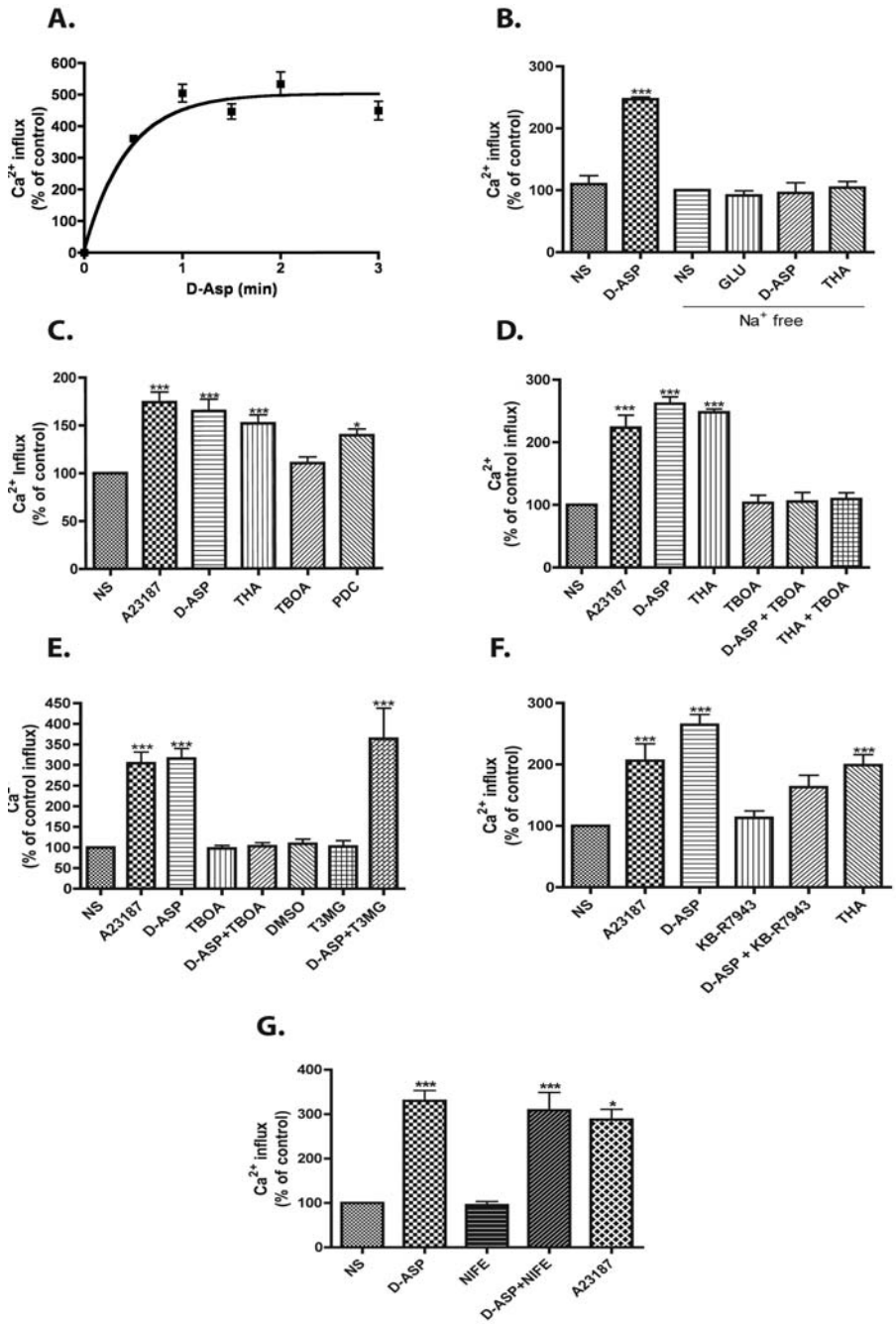

Figure 5 **GLAST activity induces $^{45}Ca^{2+}$ entry**

(**A**) MGC were incubated with 1 mM D-Asp at room temperature, and $^{45}Ca^{2+}$ uptake was measured at the indicated time periods (0, 0.5, 1, 1.5, 2 and 3 min). (**B**) Monolayers were incubated in complete or Na^+-free assay buffer and treatment with Glu (1 mM), D-Asp (1 mM) or THA (100 μM). (**C**) $^{45}Ca^{2+}$ influx was determined in the presence of 1 mM D-Asp, 100 μM THA, 100 μM TBOA or 100 μM PDC. The Ca^{2+} ionophore A23187 (10 μM) was used as a positive control. All drugs were included for 3 min. (**D**) Cells were pre-exposed for 30 min to the non-transportable Glu transport blocker TBOA 100 μM and then to D-Asp 1 mM and THA 100 μM, the influx time was 3 min. (**E**) MGC were incubated with TBOA (100 μM) or EAAT-4 blocker T3MG (200 μM) for 30 min prior the D-Asp treatment and then $^{45}Ca^{2+}$ uptake was measured. (**F**) Monolayers were pre-incubated (30 min) in presence or absence of KB-R7943 (15 μM) and treatment with D-Asp (1 mM). (**G**) MGC were pre-incubated for 30 min with the L-type VGCC blocker nifedipine (NIFE, 10 μM), and then exposed to 1 mM D-Asp. The Ca^{2+} ionophore A23187 10 μM was used as a positive control. The different drugs were present during the 3 min of $^{45}Ca^{2+}$ influx. Values represent the mean ± S.E. of at least three independent experiments performed in triplicate. Statistical analysis was performed comparing against non-stimulated cells using a non-parametric one-way ANOVA (Kruskal–Wallis test) and Dunn's post-hoc test (*$P<0.05$, ***$P<0.001$).

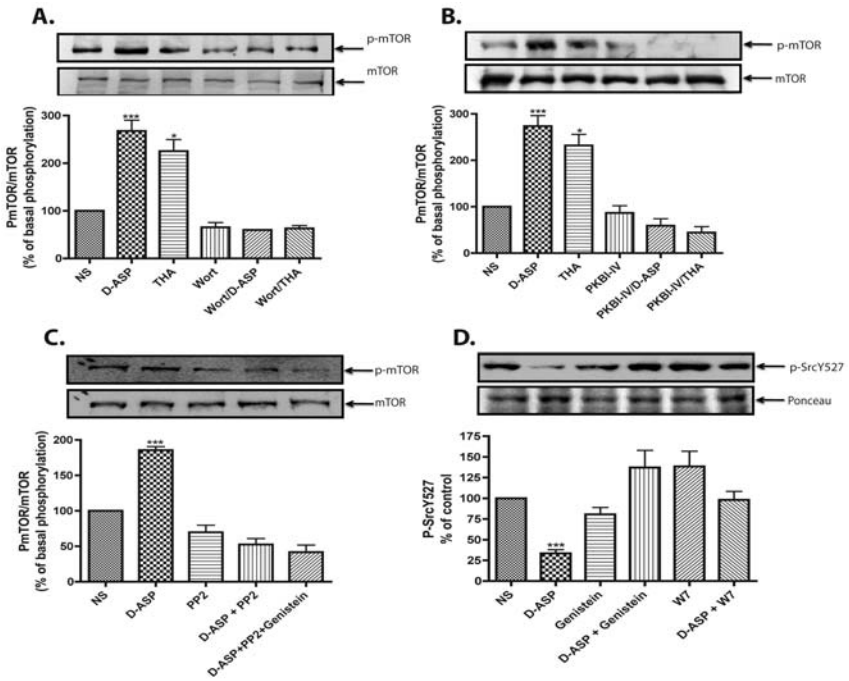

Figure 6 **D-Asp-induced mTOR phosphorylation is a PI3K-PKB/Akt pathway-dependent event**
MGC were pre-incubated for 30 min with 10 nM of the PI3K inhibitor wortmannin (Wort) (**A**), with 100 nM of the PKB inhibitor (PKBI-IV) (**B**), or the $p60^{src}$ inhibitor PP2 (10 nM) in the absence or presence of the RTK inhibitor genistein at 25 μM (**C**); and then treated with D-Asp (1 mM) or THA (100 μM). Levels of mTOR phosphorylation were detected as for Figure 1. (**D**) Levels of Tyr-527 phosphorylated $p60^{src}$ were detected after treatment with 1 mM D-Asp in the presence/absence of W7 (25 μM) or genistein (25 μM). Phospho-$p60^{src}$ levels were analysed by Western blot, Ponceau S was used as a loading control. The results are the mean ±S.E. of at least three independent experiments. In each panel, a representative Western blot is shown. Statistical analysis was performed comparing against non-stimulated cells using a non-parametric one-way ANOVA (Kruskal-Wallis test) and Dunn's post-hoc test (*$P<0.05$, ***$P<0.001$).

interactions relies on an efficient Glu uptake activity. It is therefore conceivable that transporters may contribute to Glu signalling, particularly in glia cells. In this context, we have described the regulation of Glu removal in radial glia cells by a transporter-mediated process involving the regulation of GLAST/EAAT-1 membrane expression (Gonzalez and Ortega, 2000; Gadea et al., 2004). More recently, the group of Hampson have demonstrated a direct coupling of Glu transporters to the Na,K-ATPase in glia cells (Rose et al., 2009). In such a scenario, it is tempting to speculate that intracellular signalling activated by Glu transporters could be linked to the long-term regulation of glia–neuronal reciprocal interactions in excitatory transmission.

The results from this study clearly show that the transport process itself triggers a signal transduction cascade involving the activation of $p60^{src}$, PI3K and PKB (Akt) linked to extracellular Ca^{2+} entry, which leads, not only to the promotion of translation by Ser-2448 phosphorylated mTOR, but also to transcriptional activity mediated by Ca^{2+}-dependent binding of inducible transcription factors, such as the AP-1. In this regard, the activation of CaMKII induces the phosphorylation/activation of RTKs which, in turn, allows PI3K membrane anchoring and activation (Wang and Proud, 2011). We show here, that Ca^{2+} entry promoted by GLAST activity induces a transient mTOR phosphorylation through $p60^{src}$/PI3K/Akt/mTOR/$p70^{S6K}$ signalling. It is quite possible that the Ca^{2+} signal activates phosphatase 2A that would dephosphorylate and inactivate $p70^{S6K}$, thus reducing mTOR Ser-2448 phosphorylation giving up the transient nature of the effect (Nunbhakdi-Craig et al., 2002). Furthermore, as CaMKII has been shown to activate the expression of *c-fos* through the MAPK MEK/ERK cascade in Müller glia, the proposed GLAST signalling cascade is supported by the increase in AP-1 binding (Abe and Saito, 2001; Takeda et al., 2002).

As mTOR has been regarded as a master regulator of protein synthesis (Foster and Fingar, 2010) and AP-1 DNA binding is critical for the transcriptional control of a number of genes (Shaulian, 2010), it is possible that the removal of Glu from the synaptic cleft is linked to gene expression regulation in glia cells. A working hypothesis is that specific genes, such as those coding for the Glu transporters, the Na^+/K^+-ATPase, glutamine synthetase or the neutral amino acid transporters could be the targets of GLAST-dependent gene expression regulation, and could participate actively in glia–neuronal coupling. Work currently in progress in our group is aimed at the identification of these genes. Taking into consideration that mTOR is not only a transducing molecule for mitogenic signals, but also for

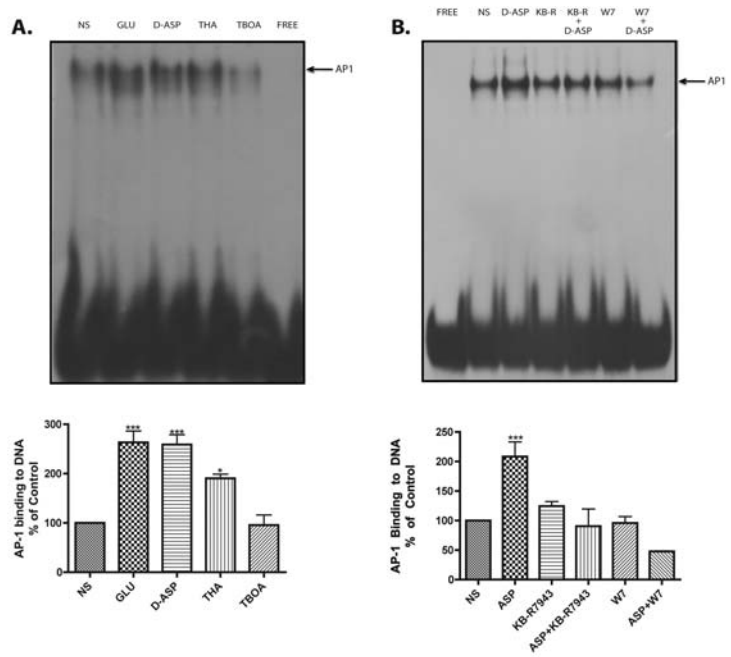

Figure 7 **GLAST activity signals to AP-1 DNA binding**

(**A**) EMSAs. Nuclear extracts were prepared from control or treated cells (Glu, D-Asp, THA or TBOA) and binding to the AP-1 consensus sequence was analysed as described in the Materials and methods section. (**B**) Nuclear extracts were prepared from cells pre-incubated 30 min with Na^+/Ca^{2+} exchanger inhibitor (KB-R7943, 15 μM) and with the calmodulin antagonist (W7, 25 μM), after that treated with D-Asp (1 mM, 90 min) the binding to the AP-1 consensus sequence was analysed. The results are the mean ± S.E. of at least three independent experiments. Statistical analysis was performed comparing against non-stimulated cells using a non-parametric one-way ANOVA (Kruskal–Wallis test) and Dunn's post-hoc test (*$P<0.05$, ***$P<0.001$).

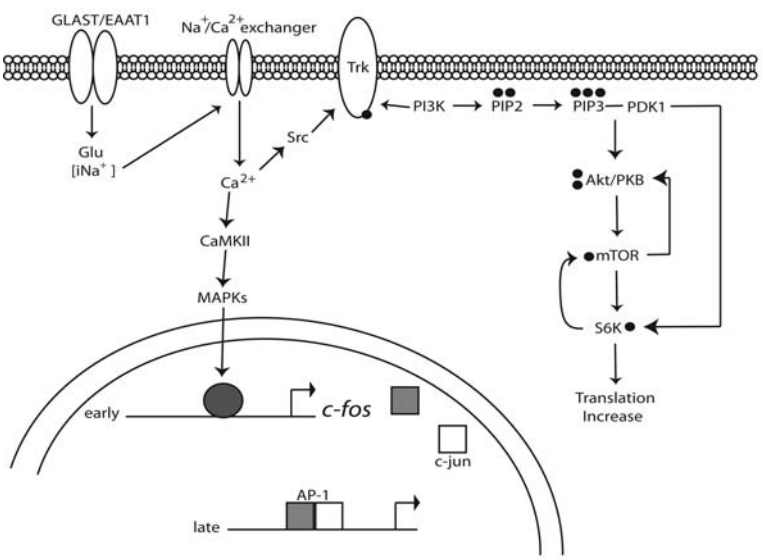

Figure 8 **Current model for GLAST signalling in MGC**

Glu uptake leads to an influx of Na^+ that activates the Na^+/Ca^{2+} exchanger, resulting in a net Ca^{2+} influx. The elevation of intracellular Ca^{2+} leads to the up-regulation of *c-fos* transcription and the promotion of AP-1 DNA-binding activity. On the other hand, Ca^{2+} entry results in $p60^{src}$ Tyr-527 dephosphorylation and Trk transactivation, the recruitment and activation of PI3K and Akt/PKB, which, in turn, results in mTOR phosphorylation and an increase in mRNA translation.

nutrient availability correlated with protein synthesis for housekeeping glial functions, transporter signalling to mTOR and gene expression could play a role in linking these responses (towards cell division).

The functional significance of signalling through the transporters compared with the cascades activated via Glu receptors, and the fact that both would lead to gene expression regulation in glia cells (Lopez-Bayghen et al., 2006), is elusive at this point. Yet, it is conceivable that the difference in the kinetics of activation, favoured by lower affinity of the transporters and their higher density (Danbolt, 2001), is the basis for a transporter-selective response at the level of transcriptional and/or translational control. Yet another possibility is that an activity-dependent differential distribution of transporters and receptors in detergent-resistant membrane domains and the inclusion or not of differential signalling partners constitutes the molecular basis of the existence of transporter-mediated signal transduction (Butchbach et al., 2004; Gonzalez et al., 2007; Hou et al., 2008).

In summary, we demonstrated here that Glu transport in MGC is linked to the activation of signal transduction cascades that lead to gene expression regulation. A description of our present findings is summarized in Figure 8. Our results further strengthen the pivotal role of glia cells in glutamatergic transmission in the retina.

ACKNOWLEDGEMENTS

The technical assistance of Luis Cid and Blanca Ibarra and the critical reading of the paper by Professor Angelina Rodríguez are acknowledged.

FUNDING

This work was supported by the Conacyt-Mexico [grant numbers 79502 and 123625 (to A.O.)], PAPIIT/UNAM [grant number IN201812 (to A.M.L.C.)]. Z.M.-L. and A.M.G. are supported by fellowships from Conacyt-Mexico.

REFERENCES

Abe K, Saito H (2001) Possible linkage between glutamate transporter and mitogen-activated protein kinase cascade in cultured rat cortical astrocytes. J Neurochem 76:217–223.

Blagosklonny MV (2010) Revisiting the antagonistic pleiotropy theory of aging: TOR-driven program and quasi-program. Cell Cycle 9:3151–3156.

Bringmann A, Pannicke T, Biedermann B, Francke M, Iandiev I, Grosche J, Wiedemann P, Albrecht J, Reichenbach A (2009) Role of retinal glial cells in neurotransmitter uptake and metabolism. Neurochem Int 54:143–160.

Butchbach ME, Tian G, Guo H, Lin CL (2004) Association of excitatory amino acid transporters, especially EAAT2, with cholesterol-rich lipid raft microdomains: importance for excitatory amino acid transporter localization and function. J Biol Chem 279:34388–34396.

Coutinho V, Knopfel T (2002) Metabotropic glutamate receptors: electrical and chemical signaling properties. Neuroscientist 8:551–561.

D'Antoni S, Berretta A, Bonaccorso CM, Bruno V, Aronica E, Nicoletti F, Catania MV (2008) Metabotropic glutamate receptors in glial cells. Neurochem Res 33:2436–2443.

Danbolt NC (2001) Glutamate uptake. Prog Neurobiol 65:1–105.

Eulenburg V, Gomeza J (2010) Neurotransmitter transporters expressed in glial cells as regulators of synapse function. Brain Res Rev 63:103–112.

Fields RD, Stevens-Graham B (2002) New insights into neuron–glia communication. Science 298:556–562.

Foster KG, Fingar DC (2010) Mammalian target of rapamycin (mTOR): conducting the cellular signaling symphony. J Biol Chem 285:14071–14077.

Fyk-Kolodziej B, Qin P, Dzhagaryan A, Pourcho RG (2004) Differential cellular and subcellular distribution of glutamate transporters in the cat retina. Vis Neurosci 21:551–565.

Gadea A, Lopez E, Lopez-Colome AM (2004) Glutamate-induced inhibition of D-aspartate uptake in Muller glia from the retina. Neurochem Res 29:295–304.

Gegelashvili M, Rodriguez-Kern A, Sung L, Shimamoto K, Gegelashvili G (2007) Glutamate transporter GLAST/EAAT1 directs cell surface expression of FXYD2/gamma subunit of Na, K-ATPase in human fetal astrocytes. Neurochem Int 50:916–920.

Gonzalez MI, Ortega A (2000) Regulation of high-affinity glutamate uptake activity in Bergmann glia cells by glutamate. Brain Res 866:73–78.

Gonzalez MI, Susarla BT, Fournier KM, Sheldon AL, Robinson MB (2007) Constitutive endocytosis and recycling of the neuronal glutamate transporter, excitatory amino acid carrier 1. J Neurochem 103:1917–1931.

Guerrini L, Blasi F, Denis-Donini S (1995) Synaptic activation of NF-kappa B by glutamate in cerebellar granule neurons *in vitro*. Proc Natl Acad Sci USA 92:9077–9081.

Harrington LS, Findlay GM, Gray A, Tolkacheva T, Wigfield S, Rebholz H, Barnett J, Leslie NR, Cheng S, Shepherd PR, Gout I, Downes CP, Lamb RF (2004) The TSC1-2 tumor suppressor controls insulin-PI3K signaling via regulation of IRS proteins. J Cell Biol 166:213–223.

Hollander H, Makarov F, Dreher Z, van Driel D, Chan-Ling TL, Stone J (1991) Structure of the macroglia of the retina: sharing and division of labour between astrocytes and Muller cells. J Comp Neurol 313:587–603.

Hou Q, Huang Y, Amato S, Snyder SH, Huganir RL, Man HY (2008) Regulation of AMPA receptor localization in lipid rafts. Mol Cell Neurosci 38:213–223.

Kholodenko BN (2006) Cell-signalling dynamics in time and space. Nat Rev Mol Cell Biol 7:165–176.

Laplante M, Sabatini DM (2012) mTOR Signaling. Cold Spring Harb Perspect Biol 4:2

Lopez T, Lopez-Colome AM, Ortega A (1997) NMDA receptors in cultured radial glia. FEBS Lett 405:245–248.

Lopez T, Lopez-Colome AM, Ortega A (1998) Changes in GluR4 expression induced by metabotropic receptor activation in radial glia cultures. Brain Res Mol Brain Res 58:40–46.

Lopez-Bayghen E, Cruz-Solis I, Corona M, Lopez-Colome AM, Ortega A (2006) Glutamate-induced octamer DNA binding and transcriptional control in cultured radial glia cells. J Neurochem 98:851–859.

Lopez-Colome AM, Romo-de-Vivar M (1991) Excitatory amino acid receptors in cultures of glial cells from the retina. Glia 4:431–439.

Lopez-Colome AM, Murbartian J, Ortega A (1995) Excitatory amino acid-induced AP-1 DNA binding activity in Muller glia. J Neurosci Res 41:179-184.

Lopez-Colome AM, Ortega A, Romo-de-Vivar M (1993) Excitatory amino acid-induced phosphoinositide hydrolysis in Muller glia. Glia 9:127–135.

Massey SC, Miller RF (1990) N-methyl-D-aspartate receptors of ganglion cells in rabbit retina. J Neurophysiol 63:16–30.

Mattson MP (2003) Excitotoxic and excitoprotective mechanisms: abundant targets for the prevention and treatment of neurodegenerative disorders. Neuromolecular Med 3:65–94.

Michaelis EK (1998) Molecular biology of glutamate receptors in the central nervous system and their role in excitotoxicity, oxidative stress and aging. Prog Neurobiol 54:369–415.

Nunbhakdi-Craig V, Machleidt T, Ogris E, Bellotto D, White CL, 3rd, Sontag E (2002) Protein phosphatase 2A associates with and regulates atypical PKC and the epithelial tight junction complex. J Cell Biol 158:967–978.

Olney JW (2003) Excitotoxicity, apoptosis and neuropyschiatric disorders. Curr Opin Pharmacol 3:101–109.

Pellerin L (2008) Brain energetics (thought needs food). Curr Opin Clin Nutr Metab Care 11:701–705.

Proud CG (2007) Cell signaling: mTOR, unleashed. Science 318:926–927.

Rauen T, Kanner BI (1994) Localization of the glutamate transporter GLT-1 in rat and macaque monkey retinae. Neurosci Lett 169:137–140.

Rose EM, Koo JC, Antflick JE, Ahmed SM, Angers S, Hampson DR (2009) Glutamate transporter coupling to Na,K-ATPase. J Neurosci 29: 8143–8155.

Rosner M, Hengstschlager M (2010) Evidence for cell cycle-dependent, rapamycin-resistant phosphorylation of ribosomal protein S6 at S240/244. Amino Acids 39:1487–1492.
Shank RP, Campbell GL (1984) Amino acid uptake, content, and metabolism by neuronal and glial enriched cellular fractions from mouse cerebellum. J Neurosci 4:58–69.
Shaulian E (2010) AP-1–The Jun proteins: Oncogenes or tumor suppressors in disguise? Cell Signal 22:894–899.
Takeda M, Takamiya A, Yoshida A, Kiyama H (2002) Extracellular signal-regulated kinase activation predominantly in Muller cells of retina with endotoxin-induced uveitis. Invest Ophthalmol Vis Sci 43:907–911.
Thomas GM, Huganir RL (2004) MAPK cascade signalling and synaptic plasticity. Nat Rev Neurosci 5:173–183.
Uchihori Y, Puro DG (1993) Glutamate as a neuron-to-glial signal for mitogenesis: role of glial N-methyl-D-aspartate receptors. Brain Res 613:212–220.
Um SH, Frigerio F, Watanabe M, Picard F, Joaquin M, Sticker M, Fumagalli S, Allegrini PR, Kozma SC, Auwerx J, Thomas G (2004) Absence of S6K1 protects against age- and diet-induced obesity while enhancing insulin sensitivity. Nature 431:200–205.
Vanhaesebroeck B, Alessi DR (2000) The PI3K-PDK1 connection: more than just a road to PKB. Biochem J 346:561–576.
Wang H, Gong B, Vadakkan KI, Toyoda H, Kaang BK, Zhuo M (2007) Genetic evidence for adenylyl cyclase 1 as a target for preventing neuronal excitotoxicity mediated by N-methyl-D-aspartate receptors. J Biol Chem 282:1507–1517.
Wang X, Proud CG (2011) mTORC1 signaling: what we still don't know. J Mol Cell Biol 3:206–220.
Zepeda RC, Barrera I, Castelan F, Soto-Cid A, Hernandez-Kelly LC, Lopez-Bayghen E, Ortega A (2008) Glutamate-dependent transcriptional regulation in bergmann glia cells: involvement of p38 MAP kinase. Neurochem Res 33:1277–1285.

Received 2 April 2012/27 June 2012; accepted 28 June 2012
Published as Immediate Publication 23 July 2012, doi 10.1042/AN20120022

Journal of Neurochemistry

JOURNAL OF NEUROCHEMISTRY | 2013 | 125 | 545–554 doi: 10.1111/jnc.12211

ORIGINAL ARTICLE

GLAST/EAAT1-induced Glutamine release via SNAT3 in Bergmann glial cells: evidence of a functional and physical coupling

Zila Martínez-Lozada,* Alain M. Guillem,* Marco Flores-Méndez,* Luisa C. Hernández-Kelly,* Carmelita Vela,† Enrique Meza,† Rossana C. Zepeda,† Mario Caba,† Angelina Rodríguez‡ and Arturo Ortega*

*Departamento de Genética y Biología Molecular, Centro de Investigación y de Estudios Avanzados del Instituto Politécnico Nacional, México D.F., México

†Centro de Investigaciones Biomédicas, Universidad Veracruzana, Xalapa, México

‡Facultad de Química, Centro Universitario Cerro de las Campanas, Universidad Autónoma de Querétaro, Querétaro, México

Abstract

Glutamate, the major excitatory transmitter in the vertebrate brain, is removed from the synaptic cleft by a family of sodium-dependent glutamate transporters profusely expressed in glial cells. Once internalized, it is metabolized by glutamine synthetase to glutamine and released to the synaptic space through sodium-dependent neutral amino acid carriers of the N System (SNAT3/slc38a3/SN1, SNAT5/slc38a5/SN2). Glutamine is then taken up by neurons completing the so-called glutamate/glutamine shuttle. Despite of the fact that this coupling was described decades ago, it is only recently that the biochemical framework of this shuttle has begun to be elucidated. Using the established model of cultured cerebellar Bergmann glia cells, we sought to characterize the functional and physical coupling of glutamate uptake and glutamine release. A time-dependent Na^+-dependent glutamate/aspartate transporter/EAAT1-induced System N-mediated glutamine release could be demonstrated. Furthermore, D-aspartate, a specific glutamate transporter ligand, was capable of enhancing the co-immunoprecipitation of Na^+-dependent glutamate/aspartate transporter and Na^+-dependent neutral amino acid transporter 3, whereas glutamine tended to reduce this association. Our results suggest that glial cells surrounding glutamatergic synapses may act as sensors of neuron-derived glutamate through their contribution to the neurotransmitter turnover.

Keywords: Bergmann glia, glutamate transporters, glutamate/glutamine shuttle, glutamine transporters.

J. Neurochem. (2013) **125**, 545–554.

Received June 18, 2012; revised manuscript received October 11, 2012; accepted February 15, 2013.

Address correspondence and reprint requests to Arturo Ortega, Ph.D., Departamento de Genética y Biología Molecular, Cinvestav-IPN, Apartado Postal 14-740, México DF 07000, México.
E-mail: arortega@cinvestav.mx

Abbreviations used: AMPA, α-amino-3-hydroxy-5-methylisoxazole-4-propionate; ANOVA, analysis of variance; BGC, Bergmann glial cells; BSA, bovine serum albumin; DAB, diaminobenzidine; D-Asp, D-Aspartate; DCG-IV, (1R,2R)-3-[(1S)-1-amino-2-hydroxy-2-oxoethyl]cyclopropoane-1,2-dicarboxylic acid; DHPG, (RS)-3,5-dihydroxyphenilglicine; DL-TBOA, DL-threo-b-Benzyloxyaspartic acid; DMEM, Dulbecco's modified Eagle's medium; DNQX, 6,7-Dinitroquinoxaline-2,3-dione; EAAT 1-5, excitatory amino acid transporters; ECL, enhanced chemiluminescence reagent; EDTA, ethylenediaminetetraacetic acid; GLAST, Na^+-dependent glutamate/aspartate transporter; Gln, glutamine; Glt-1, glutamate transporter-1; GS, glutamine synthetase; KA, kainate; KBP, kainate binding protein; L-AP4, L-(+)-2-amino-4-phosphonobutyric acid; L-Glu, L-glutamate; NMDA, N-methyl-D-aspartate; NP-40, Nonidet P-40; PBS, phosphate-buffer saline; PBT, phosphate-buffer saline containing 0.3% Triton; SDS-PAGE, sodium dodedecyl sulfate polyacrylamide gel electrophoresis; SNAT2-3-5, Na^+-dependent neutral amino acid transporter 2-3-5; TBS, Tris-buffered saline; THA, threo-β-hydroxyaspartate; trans-ACPD, (+/-)-1-aminocyclopentane-trans-1,3-dicarboxilic acid.

L-Glutamate (L-Glu) is the major excitatory amino acid neurotransmitter in the vertebrate brain. Membrane-specific L-Glu receptors expressed in neurons and glial cell mediate most, albeit not all, of its effects. Ionotropic receptors of the α-amino-3-hydroxy-5-methylisoxazole-4-propionate (AMPA), N-methyl-D-aspartate (NMDA), and kainate (KA) subtypes are proteins composed of different subunits (Sager *et al.* 2009). Metabotropic Glu receptors have been subdivided in terms of sequence similarity and signaling mechanisms in three groups. Signaling through these receptors is carried out by the phospholipase C and Ca^{2+} for Group I and inhibition of adenylate cyclase for Groups II and III (Wieronska and Pilc 2009).

L-Glu extracellular levels are tightly regulated through its uptake, mostly into glial cells, by a family of Na^+-dependent L-Glu transporters known as excitatory amino acid transporters of which EAAT-1, also known as Na^+-dependent glu/aspartate transporter (GLAST) and EAAT-2 or Glu transporter-1 (Glt-1) are mainly expressed in glia cells (Danbolt 2001). Once this amino acid has been removed, it is rapidly converted to L-glutamine (L-Gln) through the action of Gln synthetase (GS) (Shank and Campbell 1984). Neutral amino acid transporters mediate both the glial release and the neuronal uptake of L-Gln. Several transporter systems have been described for these amino acids, based not only in sequence identity but also on their kinetic properties (Dolinska *et al.* 2000, 2003; Hagglund *et al.* 2011). In general terms, it has been assumed that L-Gln release from astrocytes (Albrecht 1989). One of the transporters that carries out this release is the Na^+-dependent neutral amino acid transporter 3 (SNAT3), a member of System N, a family of L-Gln transporters capable of acting in a reversed fashion (Broer *et al.* 2004). In contrast, neuronal L-Gln uptake has been postulated to be carried out by members of System A transporters (SNAT2) (Jenstad *et al.* 2009), although this proposal has been questioned at least for neocortical neurons (Grewal *et al.* 2009).

Bergmann glial cells (BGC) extend their processes through the molecular layer of the cerebellar cortex surrounding excitatory and inhibitory synapses (Somogyi *et al.* 1990). The tripartite relationship between pre-synapse, post-synapse, and surrounding glia as a source of neuroactive substances like ATP and D-serine has also been acknowledged (Henneberger *et al.* 2010). Therefore, it has been postulated that BGCs are involved in neuronal communication and that they might even constitute a neuronal reservoir (Hansson and Ronnback 1995; Malatesta *et al.* 2003; Anthony *et al.* 2004). When cultured, BGC become an excellent model in which the molecular and cellular basis of glial–neuronal signaling can be analyzed in the context of glutamatergic transmission (Lopez-Bayghen *et al.* 2007). In such preparations, L-Glu acting through its receptors, changes gene expression at the transcriptional and translational levels (Gonzalez-Mejia *et al.* 2006; Rosas *et al.* 2007). In addition, it has become evident that plasma membrane L-Glu transporters are also involved in glutamatergic signaling. For example, it has been demonstrated that L-Glu uptake activity triggers glucose influx (Magistretti 2009) and increases GS activity (Lehmann *et al.* 2009) in astrocytes. Furthermore, in BGC cultures, GLAST/EAAT-1, the sole L-Glu transporter expressed in these cells (Regan *et al.* 2007) is linked to the mammalian target of rapamycin (mTOR) activation and thus protein expression regulation (Martinez-Lozada *et al.* 2011). With these evidences in mind, we decided to explore the putative role of L-Glu transporters in the regulation of L-Gln release. To reach this goal, we first characterized the L-[^{3}H] Gln uptake activity in our culture system and evaluated if GLAST/EAAT-1 substrates such as D-Aspartate (D-Asp) would induce a significant L-Gln release. Once we were able to detect such an effect, we hypothesized that both transporters are present in a macromolecular complex and that D-Asp treatment would be linked to the appearance of such complex. Indeed, we were able to detect a coupling between GLAST and SNAT3.

These results suggest that glia cells associated to glutamatergic synapses behave as L-Glu sensors and that these cells may control, to a greater extent than assumed before, excitatory transmission. Moreover, our findings strengthen the notion of the active participation of glia cells in synaptic transmission.

Materials and methods

Materials

Tissue culture reagents were obtained from GE Healthcare (Carlsbad, CA, USA). DHPG, 6,7-Dinitroquinoxaline-2,3-dione, AMPA, NMDA, DL-threo-b-Benzyloxyaspartic acid, threo-β-hydroxyaspartate and L-Glu were all obtained from Tocris-Cookson (St. Louis, MO USA). KA was obtained from Ocean Produce International (Shelburne, Nova Scotia, Canada). L-[^{3}H] Glutamic acid (specific activity 40 Ci/mmol) and L-[^{3}H] Glutamine (specific activity 50.3 Ci/mmol) were obtained from Perkin Elmer (Waltham, MA, USA). The AG 1X-8 anion exchange resin was purchased from Bio-Rad (Hercules, CA, USA). The antibodies used were anti- SNAT3 (Santa Cruz, CA, USA), anti-calbindin (Sigma-Aldrich, St. Louis, MO, USA), anti-kainate binding protein (KBP), and an anti-peptide (GLIQALVTALGTSSSSAT) GLAST anti-serum (produced and characterized in our laboratories). Specificity of the anti-peptide anti-GLAST antibodies was performed as follows. A 1 : 1000 dilution of the sera was pre-absorbed with 10 and 50 ng of the peptide for 30 min at 4°C and used for Western blot analysis of chick cerebellum and cultured Bergmann glia extracts (see below). Horseradish peroxidase-linked anti-mouse or anti-rabbit antibodies, and the enhanced chemiluminescence reagent, were obtained from Amersham Biosciences (Buckinghamshire, UK). All other chemicals were purchased from Sigma (St. Louis, MO, USA).

Cell culture and stimulation protocol

Primary cultures of cerebellar BGC were prepared from 14-day-old chick embryos as previously described (Ortega *et al.* 1991). Cells were plated in plastic culture dishes in Dulbecco's modified Eagle's medium (DMEM) containing 10% fetal bovine serum, 2 mM Gln, and gentamicin (50 μg/mL) and used on the fourth or fifth day after culture. Before any treatment, confluent monolayers were switched to non-serum DMEM media containing 0.5% bovine serum albumin for 30 min and then treated as indicated. Antagonists or inhibitors were added 30 min before agonists. The cells were treated with the L-Glu analogs added to culture medium for the indicated times; after that, medium was replaced with DMEM/0.5% albumin.

Staining procedures

BGC primary cultures were grown on poly-L-lysine-treated (0.01 mg/mL) glass coverslips following the procedure described above. Cells were fixed by exposure for 10 min to methanol at −20ºC and washed twice with phosphate-buffer saline (PBS) containing 0.5% Triton X-100 (washing solution). Non-specific binding was prevented by incubation with 1% bovine serum albumin in PBS (blocking solution) for 1 h. Cells were exposed 1 h to the primary antibodies anti-SNAT3 in blocking solution at 25°C. Then, cells were washed three times with washing solution and incubated with a 1 : 100 dilution of the fluorescent-labeled secondary antibodies dissolved in blocking solution. After washing out secondary antibody, cell preparations were mounted with Vectashield (Vector Laboratories, Burlingame, CA, USA) and examined with an inverted fluorescence microscope (Zeiss Axioscope 40, Gottingen, Germany).

For immunohistochemistry, P0 chick cerebella was removed and placed immediately in cold PBS. The tissue was washed once in cold PBS to remove blood and placed in 4% paraformaldehyde in PBS (pH 7.4) for one hour. The fixative was changed once and the tissue was left at 4°C during 48 h. The cerebella were cryoprotected successively in 10%, 20%, and 30% sucrose in PBS and sagittally sectioned at 50 μm with a cryostat (Microm International GmbH, Walldorf, Germany). For immunohistochemistry, tissue was washed profusely in PBS to remove excess aldehydes and then incubated 10 min in 1.8% hydrogen peroxide solution to remove endogenous peroxidase activity. Non-specific antibody binding was blocked by incubating the sections in blocking solution (3% goat serum in PBS containing 0.3% Triton, PBT) for 1 h at 25°C. Sections were incubated at 4°C for 48 h with primary antibodies; mouse anti-calbindin (1 : 5000), anti-KBP (1 : 2500), and anti-SNAT3 (1 : 2500) in blocking solution. The sections were washed three times in PB, and placed in biotinylated anti-mouse secondary antibodies (1 : 1000; Vector Laboratories, Inc., Burlingame, CA, USA) for 3 h (for calbindin), anti-rabbit secondary antibodies for KBP, and anti-guinea pig secondary antibodies for SNAT3. A 1 h incubation with the avidin-biotinylated horseradish peroxidase complex (1 : 250; Vector Labs) followed. The antibody-peroxidase complexes were revealed with a solution containing 0.05% diaminobenzidine, nickel sulfate (10 mg/mL; Fisher Scientific, Pittsburg, PA, USA), cobalt chloride (10 mg/mL; Fisher Scientific), and 0.01% hydrogen peroxide, which produced a black–purple precipitate. Sections were mounted onto gelatin-subbed slides, dehydrated, and cleared in Hemo-De (Fisher Scientific); then, cover slips were collocated with Permount. The sections were analyzed in an Olympus BX41 microscope.

L-[^{3}H]Gln Uptake and release

Confluent BGC monolayers seeded in 24-well plates were washed three times to remove all non-adhering cells with 0.5 mL aliquots of solution A containing 25 mM HEPES-Tris, 130 mM NaCl, 5.4 mM KCl, 1.8 mM $CaCl_2$. 0.8 mM $MgCl_2$, 33.3 mM glucose, and 1 mM NaH_2PO_4 at pH 7.4. When indicated, NaCl was replaced by LiCl. The time course of L-[^{3}H] Gln influx was initiated at $t = 0$ by the addition of 0.5 ml solution A containing 0.5 μCi/mL of L-[^{3}H] Gln solution A, 200 μM Gln. The reaction was stopped by aspirating the radioactive medium and washing each well within 15 s with 0.5 mL aliquots of an ice-cold solution A. For the determination of the kinetic parameters, the cold L-Gln concentration was modified to a final 0.5, 3, 5, 7.5, and 10 mM concentration and the uptake time was 30 min. The uptake was stopped as described above. The cells in the wells were then exposed for 2 h at 37°C to 0.5 mL NaOH and an aliquot of that solution counted in a Beckmann 7800LS scintillation counter. A minimum of three experiments in quadruplicates was done for each condition.

For the release experiments, BGC were seeded on 60 mm dishes and loaded for 3 h with 0.5 μCi/mL of L-[^{3}H] Gln in solution A. The medium was replaced every 2 min and a total of 15 fractions were collected. The various stimuli were added in fractions 6-10. The radioactivity associated to each fraction was determined by liquid scintillation counting and expressed as percentage of the total radioactivity in the experiment.

L-[^{3}H] Glutamine metabolism

The extent of L-[^{3}H] Gln remaining after the 3 h loading period and the percentage of L-[^{3}H] Gln released was determined by means of anion exchange separation of L-[^{3}H] Gln, using a AG 1X-8 200/400 resin essentially as described previously (Mongin *et al.* 2011). The system was standardized with L-[^{3}H] Glu and L-[^{3}H] Gln, that were eluted with HCl and H_2O, respectively.

Immunoprecipitation and Western blots

Cells from confluent monolayers were harvested with PBS (10 mM K_2HPO_4/KH_2PO_4, 150 mM NaCl, pH 7.4) containing protease inhibitors (1 mM phenylmethylsufonyl fluoride, 1 mg/mL aprotinin, 1 mg/mL leupeptin). Tissues or cells suspensions were lysed with RIPA buffer (50 mM Tris-HCl, 1 mM ethylenediaminetetraacetic acid, 150 mM NaCl, 1% Nonidet P-40, 0.25% sodium deoxycolate, pH 7.4). Cell lysates were pre-absorbed with 15 μL of protein G coupled to Sepharose 4B for 25 min at 4°C. The cleared lysates (1 mg of protein) were incubated with agarose-coupled anti-GLAST or anti-SNAT3 antibodies for 10 h, 4°C and then immunoblotted.

For Western blots, immunoprecipitates or cell lysates were denaturized in Laemmli's sample buffer, resolved through 10% sodium dodedecyl sulfate polyacrylamide gel electrophoresis and then electroblotted to nitrocellulose membranes. Blots were stained with Ponceau S stain to confirm that protein content was equal in all lanes. Membranes were soaked in PBS to remove the Ponceau S and incubated in Tris-buffered saline containing 5% dried skimmed milk and 0.1% Tween 20 for 60 min to block the excess of non-specific protein binding sites. Membranes were then incubated overnight at

4°C with the particular primary antibodies indicated in each figure, followed by the adequate secondary antibodies. Immunoreactive polypeptides were detected by chemiluminescence and exposed to X-ray films. Densitometric analyses were performed and data analyzed with the Prism, GraphPad Software (San Diego, CA, USA).

Statistical analysis

Data are expressed as the mean values (average) ± the standard error (SE). Statistical analyses were performed with a one-way ANOVA, and Tukey *post hoc* comparisons were considered statistically significant when $p \leq 0.05$.

Results

L-Gln transporter SNAT3 is expressed in cultured chick cerebellar BGC

As a first step in the characterization of a plausible coupling between L-Glu uptake and L-Gln release, we decided to explore the biochemical nature of L-Gln uptake activity in BGC. Taking into consideration that of the L-Gln transporters described thus far in glial cells, the N family is capable to function in a reverse mode, we concentrated in this system and particularly in SNAT3, because it has been described that the highest levels of this transporter are present from post-natal day 7 in the rat cerebella, which corresponds roughly to chick embryonic day 14 (middle stage of cerebellar development) (Boulland *et al.* 2003). To gain insight into SNAT3 expression in BGC, we performed immunolabeling of P0 chick cerebella with an anti-SNAT3 specific antibody along with staining for specific cell markers, calbindin, KBP, and GLAST/EAAT1 to identify the layers of the cerebellar cortex.

It is important to mention that the anti-GLAST/EAAT1 antibody used in this study was generated in our lab against a peptide sequence specific of the chick protein, that it is known to possess a divergent C-terminus from the rat, mouse, and human sequence (Espinoza-Rojo *et al.* 2000). The specificity of this anti serum is presented in Fig. 1a. Pre-absorption of a 1 : 1000 dilution of the antibodies with 50 ng of the peptide prevents completely the recognition of the characteristic 60 kDa band. Figure 1b illustrates the localization of the Purkinje cell bodies and their arborizations after immunolabeling with the Purkinje's cell marker, calbindin. BGC were localized through the use of anti-KBP antibodies, and by GLAST/EAAT1 immunoreactivity. KBP is expressed exclusively in chick cerebellum BGC (Somogyi *et al.* 1990) and GLAST/EAAT1 is the major cerebellar glia transporter (Ottersen *et al.* 1997). SNAT3 immunostaining was abundantly found in the pial border lining the molecular cell layer as well as in Bergmann glia processes, in a similar fashion as KBP labeling, in contrast to calbindin that strongly labels the Purkinje cell soma and arborizations. Note that the pial cerebellar surface corresponds to BGC terminal end-feet (Fig. 1b). Immunofluorescence experiments in our cultured cells demonstrate that SNAT3 is present in cultured BGC both in the cytoplasm and in the plasma membrane (Fig. 1c). Finally, in Fig. 1(d), the 60-kDa immunoreactive band that corresponds to SNAT3 was detected. Taken together, these results show that SNAT3 is present in Bergmann glia both *in situ* as well as in primary cultures.

Characterization of L-[^{3}H]Gln uptake activity in cultured Bergmann glia

To establish a functional coupling between L-Glu uptake and L-Gln release, we measured the kinetic parameters of L-[^{3}H] Gln uptake in our culture system. Since it is known that System N is the only L-Gln uptake system capable to function with Li^+, we decided to use a LiCl-containing solution A. The results are presented in Fig. 2. A time-dependence of L-[^{3}H] Gln accumulation in LiCl-buffer was observed (Fig. 2a). By increasing L-Gln concentrations, we were able to determine the kinetic parameters of L-[^{3}H] Gln uptake. As depicted in Fig. 2b, the Li^+-tolerant component displays a K_M of 2.925 mM and a V_{max} of 1.818 μmol/min*mg. In addition, we made an amino acid competition experiment, we used MeAIB, the specific inhibitor of system A, alanine as a competitor for System Asc, A and N; for system N we used histidine and the mix of leucine and threonine as competitors for systems Asc and L. As shown in Fig. 2c, His reduces approximately 50% of Gln uptake in BGC, which is similar to the amount of uptake that remains in Li^+ containing assay solution. Overall these results suggest that L-Gln transport in BGC is mediated in an approximate 40% by SNAT3.

Functional coupling of GLAST with SNAT3

In BGC, L-Glu uptake is carried out by GLAST/EAAT1 (Ruiz and Ortega 1995) and D-Asp is capable to be transported by this carrier in an electrogenic fashion, with a net Na^+ influx. Under such circumstances, we reasoned that the uptake of L-[^{3}H] Gln, that relies on the Na^+ gradient would have to be inhibited. The results are presented in Fig. 3a, D-Asp at saturating concentrations (60 and 120 μM), prevents L-[^{3}H] Gln uptake. As expected, this effect is dose dependent with an IC_{50} of 0.873 μM (Fig. 3b). It should be noted that this value is only indicative of a specific transporter mediated effect and by no means reflects the affinity of D-Asp toward GLAST/EAAT-1 as established by D-[^{3}H] Asp uptake experiments. It should be noted a common property of any signaling cascade is amplification (Seger and Krebs 1995). These results prompted us to evaluate if the exposure of L-[^{3}H]-Gln-loaded BGC to L-Glu or D-Asp resulted in an increase in the presence of radioactivity in the medium, consequence of a reversed transport of the tracer through SNAT3. Indeed this is the case, as depicted in Fig. 4: L-Glu treatment resulted in an induced L-[^{3}H] Gln release. The identity of the released material as L-[^{3}H] Gln was determined by ion exchange chromatography in a subset of experiments. Each fraction

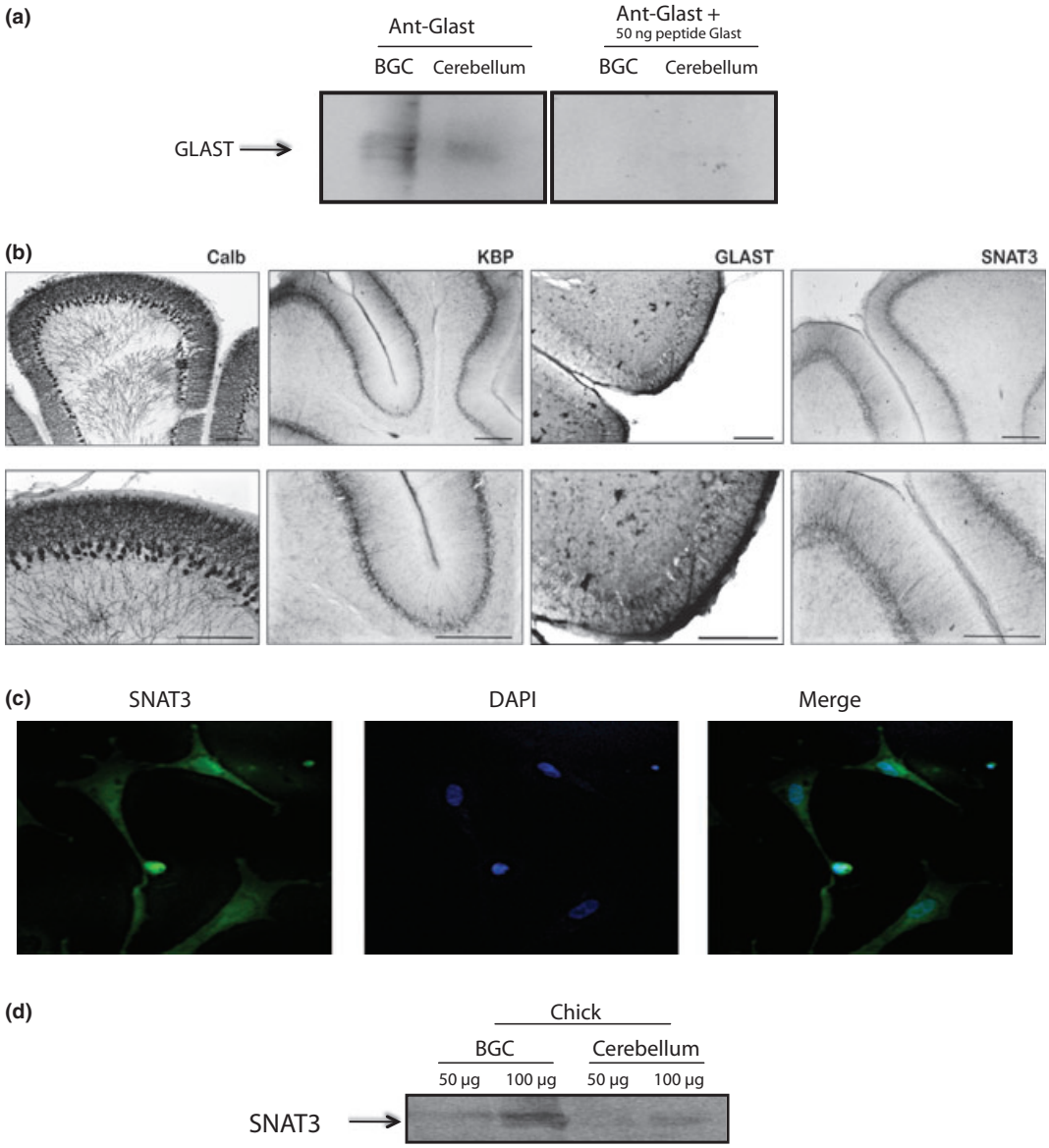

Fig. 1 Na^+-dependent neutral amino acid transporter 3 (SNAT3) expression in Bergmann glia. (a) Specificity of anti Na^+-dependent glutamate/aspartate transporter (GLAST)/EAAT1 anti-peptide antibodies. Total protein extracts from cultured chicken Bergmann glial cells (BGC) (50 µg) and cerebellum (75 µg) were assayed by Western blot with and without pre-absorption with 50 ng of the C-terminus chick GLAST peptide. (b) SNAT3 expression in chick cerebellum. Immunohistochemical characterization of chick cerebellar sections. Calbindin (Calb) labels Purkinje cells; kainate binding protein (KBP) and GLAST/EAAT1 are the BGC markers. Bar size: 50 µm. (c) Cells staining with anti-SNAT3 antibodies in cultured BGC (green). Nuclei were counterstained with DAPI (blue). (d) Total protein extracts from chick BGC cultures and cerebellum were assay by Western blot with anti-SNAT3 antibodies. A representative Western blot is shown.

collected *under the stimulus* (2 mL) of these experiments (three independent release experiments), as well as the final lysate, were added onto an activated 2 ml AG 1X-8 200/400 anion exchange column to separate L-[^{3}H] Gln from its metabolites. The column content was eluted with 2 ml volumes of H_2O, followed by three 2 ml volumes of 0.1 M HCl. Water elution removed uncharged L-[^{3}H] Gln, while subsequent acid elution extracted negatively charged metabolites such as L-Glu, α-ketoglutarate and other tricarboxylic acid intermediates (Mongin *et al.* 2011). The system was standardized with the application of a 150 µL aliquot of 10 µM L-[^{3}H] Glu aliquot and a 150 µL sample of 10 µM L-[^{3}H] Gln, that were eluted with HCl and H_2O, respectively. In all the fractions tested, roughly 70% of the radioactivity passed through the column as the L-[^{3}H] Gln standard. Moreover, this percentage was also found in the final cell

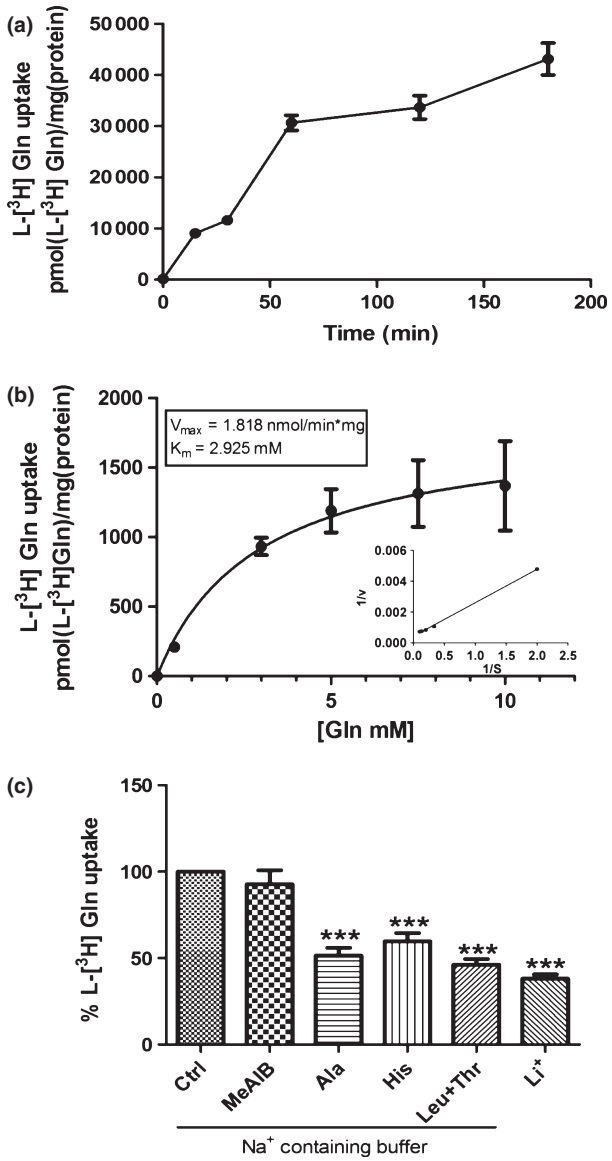

Fig. 2 System N kinetic parameters in cultured Bergmann glial cells (BGC). (a) Time course of L-[^{3}H] Gln uptake in BGC. The uptake was carried out in assay solution in which NaCl was replaced by LiCl (see Methods). A fixed amount of 0.5 μCi/mL L-[^{3}H] Gln, 200 μM L-Gln final concentration was present in the uptake assay for the indicated time periods. (b) L-[^{3}H] Gln uptake assay was performed with increasing L-Gln concentrations (0 mM, 0.5 mM, 3 mM, 5 mM, 7.5 mM, 10 mM). Transport kinetics V_{max} (μmol/min per mg protein) and K_M (mM) were determined by non-linear regression with the Prism 5 software (GraphPad) (c) Effect of different amino acids or the replacement of NaCl by LiCl on L-[^{3}H] Gln uptake in BGC. L-Gln was added at 200 μM concentration, the A-System specific substrate MeAIB was added at a 0.5 mM concentration, while other amino acids were added at a 10 mM concentration. Values represent mean ± SEM of a three independent experiments in quadruplicate, reproduced three times with similar results. Data were compared with non-stimulated of normal solution A by a Student's t-test (*** $p < 0.001$).

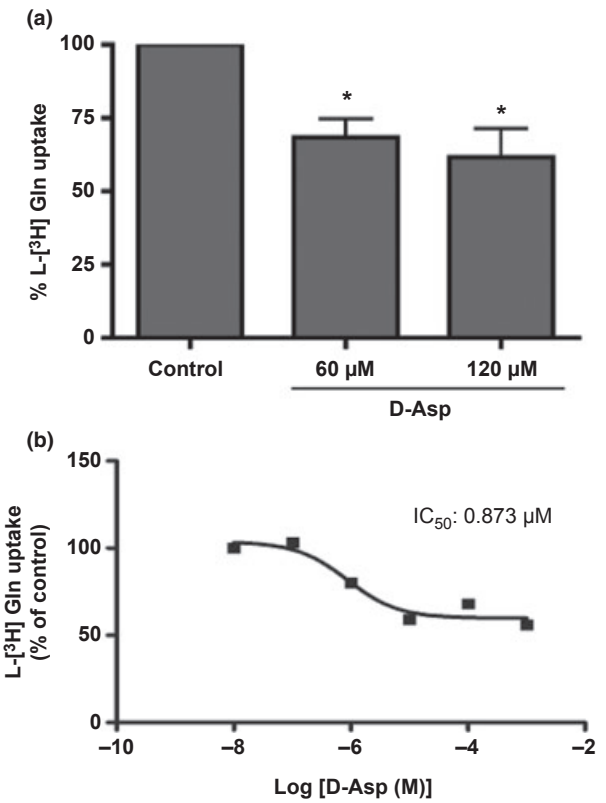

Fig. 3 Effect of D-Aspartate (D-Asp) in L-Gln uptake. (a) Effect of two different D-Asp concentrations (60 and 120 μM) in BGC L-[^{3}H] Gln uptake activity. Data were compared with non-stimulated cultures by a Student's t-test (*$p < 0.05$). (b) IC_{50} calculation of the D-Asp effect on L-[^{3}H] Glu uptake. Results are the mean ± SEM of three independent experiments. GraphPad Prism 5 was used to calculate the IC_{50} value.

extract, suggesting that most of the material released (> 70%) corresponds to L-Gln (Deitmer *et al.* 2003).

Note that exposure to either 50 μM or 1 mM D-Asp, also results in a stimulus-mediated release. In contrast, the AMPA receptors agonist, KA, did not evoke any significant L-[^{3}H] Gln release. These results suggest that L-Glu uptake is likely linked to L-Gln release.

Physical interaction between GLAST and SNAT3

The results described above were suggestive of a plausible physical interaction between GLAST and SNAT3. To test this possibility, we performed immunoprecipitation assays coupled to Western blot identification. The blots presented in Fig. 5a show that immunoprecipitation of BGC lysates with anti-GLAST antibodies and Western blot analysis with anti-SNAT3 antibodies enables us to detect the latter transporter in the immune complexes. As expected, SNAT3 immunoprecipitates contain GLAST. At this point, we decided to explore the possibility that GLAST activity would modulate its interaction with SNAT3. To this end, we exposed

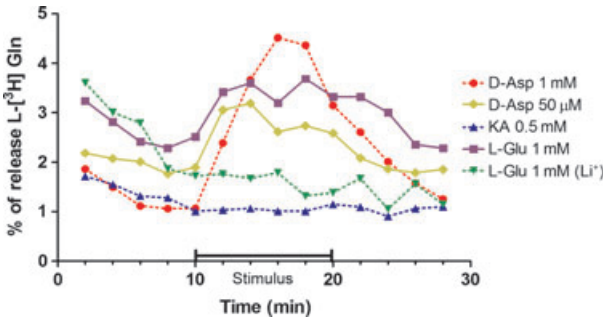

Fig. 4 L-glutamate (L-Glu) induces L-[^{3}H] Gln release from Bergmann glial cells (BGC). Cells were loaded with 0.5 μCi/mL of L-[^{3}H] Gln for 3 h. The media was removed and replaced every 2 min, a total of 15 fractions were collected. Fractions 1–5 and 11–14 contained solution A (see methods section), while in fractions 6–10 the following stimulus were added, D-Aspartate (D-Asp) 1 mM or 50 μM, kainate (KA) 0.5 mM, L-Glu 1 mM in sodium-containing or sodium-free assay buffer. Fraction 15 represents the cell lysates. The radioactivity associated to each fraction was determined by liquid scintillation counting and expressed as percentage of the total radioactivity in the experiment. A typical experiment is shown, reproduced three times with similar results.

confluent BGC cultures to 1 mM L-Glu and/or 2 mM L-Gln. As depicted in Fig. 5b, L-Glu but not L-Gln favor GLAST/SNAT3 physical interaction. We next explored if the transport activity of these two proteins would affect their putative association. To this end, we exposed the cultured cells to 60 μM D-Asp, 200 μM L-Gln, or a combination of both. The results are depicted in Fig. 5c: D-Asp induces GLAST/SNAT3 association (line 2), while L-Gln reduces the D-Asp effect (line 4). Note that 200 μM L-Gln induces a non-significative (compared to control) increase in GLAST/SNAT3 co-immunoprecipitation.

Discussion

Over the last decade, the concept of the tripartite synapse has been widely supported (Araque *et al.* 1999; Volterra and Meldolesi 2005; Halassa *et al.* 2007; Haydon *et al.* 2009). Glia cells express a battery of neurotransmitter receptors and transporters that enable them to respond to neuronal activity. Within glutamatergic synapses, the fundamental role of astrocytes in the recycling of the neurotransmitter has long been acknowledged (Bak *et al.* 2006). The L-Glu/Gln shuttle provides good evidence about the capacity of glial cells to respond to synaptic activity through the modification of their cellular functions such as GS expression and activity (Lehmann *et al.* 2009). Another example of a tight coupling of glia cells to glutamatergic synaptic activity is the astrocyte/neuron lactate shuttle (Magistretti 2009). Furthermore, depolarization of the cerebellar parallel fibers activates Bergmann glial L-Glu receptors and transporters (Balakrishnan and Bellamy 2009).

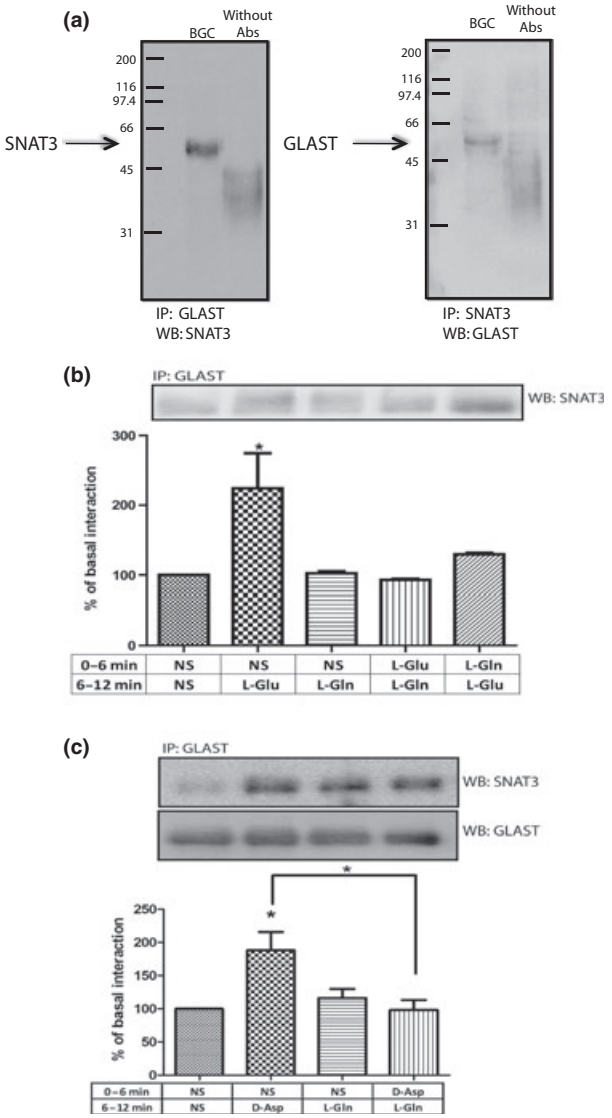

Fig. 5 Na^+-dependent neutral amino acid transporter 3 (SNAT3)/Na^+-dependent glutamate/aspartate transporter (GLAST) interaction in Bergmann glial cells (BGC). (a) BGC extracts were immunoprecipitated with anti-GLAST antibodies and the immunoprecipitate assayed by Western blot analysis with SNAT3 antibodies. The opposite experiment was done, total BGC proteins were immunoprecipitated with anti-SNAT3 and then subject to Western blot analysis with anti-GLAST serum. (b and c) BGC monolayers were exposed to the indicated stimulus; L-glutamate (L-Glu) 1 mM or L-Gln 2 mM (b), D-Asp 60 μM and L-Gln 200 μM (c). Total extracts were inmmunoprecipitated with anti-GLAST and then subjected to Western blot analysis with SNAT3 antibodies. Western blot anti-GLAST was used as loading control. (*$p < 0.05$) by a Student's *t*-test. A typical autoradiogram of three independent experiments is shown.

Using as a model system cultured BGC from chick cerebellum, we characterized several signaling cascades involved in L-Glu-dependent transcriptional regulation (Lopez-Bayghen *et al.* 2007). We have been able to demonstrate

that L-Glu signaling is also supported by the unique L-Glu transporter expressed in these cells, GLAST/EAAT1 (Martinez-Lozada *et al.* 2011). All these findings, as well as the lack of a complete biochemical characterization of the L-Glu/Gln shuttle, led us to explore a plausible interaction between L-Glu uptake and L-Gln release.

The first issue that we had to tackle before any biochemical experiment could even be designed, was the identification of the expression of L-Gln transporters that function in reverse mode within BGC. Since System N members could fulfill this requirement, and SNAT3 expression is prominent in the days just before birth and in the adulthood in the rat, we restricted our approach to SNAT3. However, we must mention that SNAT5 has been shown to be present in rat Bergmann glia cells (Cubelos *et al.* 2005). The results presented in Fig. 1, demonstrate, in the one hand, the specificity of our anti-peptide anti-GLAST/EAAT1 antibodies (Fig. 1a) as well as that SNAT3 is expressed in chick cerebellar BGC, both *in situ* as well as in our culture system. It is important to note the similar labeling of the Bergmann glia processes with anti-GLAST, anti-KBP, and anti-SNAT3 antibodies. Unfortunately, all these antibodies were generated in goat, preventing us to do double immunolabeling experiments. Nevertheless, if one compares the decoration with anti-calbindin antibodies, a Purkinje cells marker, it remains clear that SNAT3 co-localizes with KBP and GLAST.

The fact that the kinetic parameters detected for SNAT3 in our culture system are in the mM range as has been reported for other glia cells, made us confident that indeed, Bergmann glia express SNAT3 transporters. One could argue that several reports settle a K_m value of approximately 1 mM (Kilberg *et al.* 1980; Chaudhry *et al.* 2001; Broer *et al.* 2004) for SNAT3 and that the ones we report here are higher (2.9 mM). It should be noted, however, that the reported constants were obtained in heterologous glial cultures, whereas we use an enriched BGC culture (Ortega *et al.* 1991). Besides, our model system is avian origin in contrast to rodent cells used in the referred studies. Whether the apparent discrepancy is related to the cell population examined or the species used, it is not known at this moment. At this stage, we cannot rule out a plausible involvement of SNAT5 in our measurements of L-[^{3}H] Gln uptake or release. A pertinent observation could also be that if we expect that this carrier would function in a reverse manner, why we would be interested in the characterization of the uptake activity. The answer is simple: it is easier to measure uptake than release, and for kinetic purposes it is valid approach (Broer *et al.* 2004).

In any event, it became important to demonstrate a L-Glu-induced L-Gln release. Given the fact that in our experimental conditions, > 70% of the L-[^{3}H] Gln loaded in the cells remains as L-[^{3}H] Gln as judged by ion exchange chromatography, the experiments described in Fig. 4 show that D-Asp is capable to trigger L-Gln release in a more efficient manner than L-Glu. A plausible explanation to this finding is that L-Glu binds to receptors and transporters, whereas D-Asp would only binds to GLAST/EAAT1. These results strengthen our confidence in the hypothesis of a complex between these transporters. A detectable immunoreactive SNAT3 polypeptide is present in anti-GLAST immunoprecipitates and *vice versa* (Fig. 5a). Whether this is a direct protein–protein interaction between these two transporters, it is not known at this moment, work in progress in our lab is aimed at that direction. In support to our hypothesis, it is important to mention that recently the group of Billups, using electrophysiological recordings, has reported that astrocytes juxtaposed to the glutamatergic calyx of Held synapse in the rat medial nucleus of the trapezoid body release L-Gln as a consequence of L-Glu transport activation (Uwechue *et al.* 2012).

What could it be the purpose of a GLAST/SNAT3 association? One could postulate that in order for SNAT3 to work in reverse mode a significant rise in intracellular Na^+ within the vicinity of the transporter should be taking place. A functional coupling with GLAST would provide that local rise in Na^+ concentration, if this interpretation is correct then, first of all, D-Asp influx should prevent any L-[^{3}H] Gln uptake, and as demonstrated in Fig. 3, this is exactly the case. The fact that this prevention in L-[^{3}H] Gln uptake is dose dependent suggests that this is an specific effect. A valid argument in the interpretation of these results is that the

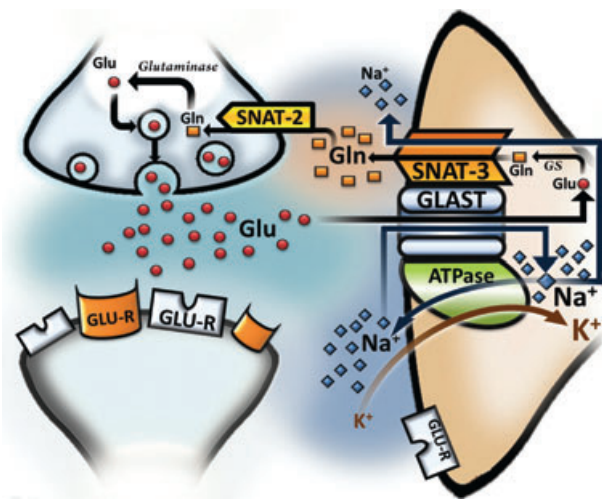

Fig. 6 Schematic representation of the Na^+-dependent glutamate/aspartate transporter (GLAST)/Na^+-dependent neutral amino acid transporter 3 (SNAT3) complex. L-Glu released from the parallel fibers is taken up into Bergmann glia cells through GLAST. The increase in $[Na^+]_i$ favors the operation, in reverse mode, of SNAT3 with the consequent release of L-Gln. Glu, L-glutamate; Gln, glutamine; GLU-R, Glutamate receptors; GLAST, sodium-dependent glutamate/aspartate transporter; SNAT, sodium-dependent neutral amino acid transporter.

reported K_m of BGC GLAST/EAAT1 is 62 μM and the IC_{50} values for the prevention in L-[^{3}H] Gln uptake is of 0.873 μM. A plausible explanation for this apparent discrepancy lies in the signal amplification inherent to cell signaling. For example, in BGC, a 1 mM L-Glu has to be applied to record a Na^+ inward current (Bennay *et al.* 2008), whereas the EC_{50} for L-Glu obtained through Oct-2/DNA binding activity is 164 μM (Mendez *et al.* 2004). Furthermore, it could be expected that D-Asp should increase GLAST/SNAT3 association whereas L-Gln not. Indeed, the results presented in Fig. 5c support this vision. A model of our interpretation of the results is shown in Fig. 6.

Taken together, our results provide a support to the critical involvement of glia cells in the modulation of L-Glu-mediated neurotransmission in what is nowadays known as the tripartite synapse.

Acknowledgements

This study was supported by grants from Conacyt-Mexico to A.O. (79502,188138) and PROMEP/SEP to A.R (UAQ-FOFI2012-FCQ201216). Z.M-L, A.M.G. and M.F-M are supported by Conacyt-Mexico fellowships. The technical assistance of Blanca Ibarra is acknowledged. The authors certify that there is no conflict of interest with any financial organization regarding the material discussed in the manuscript.

References

Albrecht J. (1989) L-glutamate stimulates the efflux of newly taken up glutamine from astroglia but not from synaptosomes of the rat. *Neuropharmacology* **28**, 885–887.

Anthony T. E., Klein C., Fishell G. and Heintz N. (2004) Radial glia serve as neuronal progenitors in all regions of the central nervous system. *Neuron* **41**, 881–890.

Araque A., Parpura V., Sanzgiri R. P. and Haydon P. G. (1999) Tripartite synapses: glia, the unacknowledged partner. *Trends Neurosci.* **22**, 208–215.

Bak L. K., Schousboe A. and Waagepetersen H. S. (2006) The glutamate/GABA-glutamine cycle: aspects of transport, neurotransmitter homeostasis and ammonia transfer. *J. Neurochem.* **98**, 641–653.

Balakrishnan S. and Bellamy T. C. (2009) Depression of parallel and climbing fiber transmission to Bergmann glia is input specific and correlates with increased precision of synaptic transmission. *Glia.* **57**, 393–401.

Bennay M., Langer J., Meier S. D., Kafitz K. W. and Rose C. R. (2008) Sodium signals in cerebellar Purkinje neurons and Bergmann glial cells evoked by glutamatergic synaptic transmission. *Glia.* **56**, 1138–1149.

Boulland J. L., Rafiki A., Levy L. M., Storm-Mathisen J. and Chaudhry F. A. (2003) Highly differential expression of SN1, a bidirectional glutamine transporter, in astroglia and endothelium in the developing rat brain. *Glia.* **41**, 260–275.

Broer A., Deitmer J. W. and Broer S. (2004) Astroglial glutamine transport by system N is upregulated by glutamate. *Glia.* **48**, 298–310.

Chaudhry F. A., Krizaj D., Larsson P., Reimer R. J., Wreden C., Storm-Mathisen J., Copenhagen D., Kavanaugh M. and Edwards R. H. (2001) Coupled and uncoupled proton movement by amino acid transport system. *N. EMBO J.* **20**, 7041–7051.

Cubelos B., Gonzalez-Gonzalez I. M., Gimenez C. and Zafra F. (2005) Amino acid transporter SNAT5 localizes to glial cells in the rat brain. *Glia.* **49**, 230–244.

Danbolt N. C. (2001) Glutamate uptake. *Prog. Neurobiol.* **65**, 1–105.

Deitmer J. W., Broer A. and Broer S. (2003) Glutamine efflux from astrocytes is mediated by multiple pathways. *J. Neurochem.* **87**, 127–135.

Dolinska M., Dybel A. and Albrecht J. (2000) Glutamine transport in C6 glioma cells. *Neurochem. Int.* **37**, 139–146.

Dolinska M., Dybel A., Zablocka B. and Albrecht J. (2003) Glutamine transport in C6 glioma cells shows ASCT2 system characteristics. *Neurochem. Int.* **43**, 501–507.

Espinoza-Rojo M., Lopez-Bayghen E. and Ortega A. (2000) GLAST: gene expression regulation by phorbol esters. *NeuroReport* **11**, 2827–2832.

Gonzalez-Mejia M. E., Morales M., Hernandez-Kelly L. C., Zepeda R. C., Bernabe A. and Ortega A. (2006) Glutamate-dependent translational regulation in cultured Bergmann glia cells: involvement of p70S6K. *Neuroscience* **141**, 1389–1398.

Grewal S., Defamie N., Zhang X., De Gois S., Shawki A., Mackenzie B., Chen C., Varoqui H. and Erickson J. D. (2009) SNAT2 amino acid transporter is regulated by amino acids of the SLC6 gamma-aminobutyric acid transporter subfamily in neocortical neurons and may play no role in delivering glutamine for glutamatergic transmission. *J. Biol. Chem.* **284**, 11224–11236.

Hagglund M. G., Sreedharan S., Nilsson V. C., Shaik J. H., Almkvist I. M., Backlin S., Wrange O. and Fredriksson R. (2011) Identification of SLC38A7 (SNAT7) protein as a glutamine transporter expressed in neurons. *J. Biol. Chem.* **286**, 20500–20511.

Halassa M. M., Fellin T. and Haydon P. G. (2007) The tripartite synapse: roles for gliotransmission in health and disease. *Trends Mol Med.* **13**, 54–63.

Hansson E. and Ronnback L. (1995) Astrocytes in glutamate neurotransmission. *FASEB J.* **9**, 343–350.

Haydon P. G., Blendy J., Moss S. J. and Rob Jackson F. (2009) Astrocytic control of synaptic transmission and plasticity: a target for drugs of abuse? *Neuropharmacology* **56**(Suppl 1), 83–90.

Henneberger C., Papouin T., Oliet S. H. and Rusakov D. A. (2010) Long-term potentiation depends on release of D-serine from astrocytes. *Nature* **463**, 232–236.

Jenstad M., Quazi A. Z., Zilberter M. *et al.* (2009) System A transporter SAT2 mediates replenishment of dendritic glutamate pools controlling retrograde signaling by glutamate. *Cereb. Cortex* **19**, 1092–1106.

Kilberg M. S., Handlogten M. E. and Christensen H. N. (1980) Characteristics of an amino acid transport system in rat liver for glutamine, asparagine, histidine, and closely related analogs. *J. Biol. Chem.* **255**, 4011–4019.

Lehmann C., Bette S. and Engele J. (2009) High extracellular glutamate modulates expression of glutamate transporters and glutamine synthetase in cultured astrocytes. *Brain Res.* **1297**, 1–8.

Lopez-Bayghen E., Rosas S., Castelan F. and Ortega A. (2007) Cerebellar Bergmann glia: an important model to study neuron-glia interactions. *Neuron Glia Biol.* **3**, 155–167.

Magistretti P. J. (2009) Role of glutamate in neuron-glia metabolic coupling. *Am. J. Clin. Nutr.* **90**, 875S–880S.

Malatesta P., Hack M. A., Hartfuss E., Kettenmann H., Klinkert W., Kirchhoff F. and Gotz M. (2003) Neuronal or glial progeny: regional differences in radial glia fate. *Neuron* **37**, 751–764.

Martinez-Lozada Z., Hernandez-Kelly L. C., Aguilera J., Lopez-Bayghen E. and Ortega A. (2011) Signaling through EAAT-1/GLAST in cultured Bergmann glia cells. *Neurochem. Int.* **59**, 871–879.

Mendez J. A., Lopez-Bayghen E., Rojas F., Hernandez M. E. and Ortega A. (2004) Glutamate regulates Oct-2 DNA-binding activity through alpha-amino-3-hydroxy-5-methylisoxazole-4-propionate receptors in cultured chick Bergmann glia cells. *J. Neurochem.* **88**, 835–843.

Mongin A. A., Hyzinski-Garcia M. C., Vincent M. Y. and Keller R. W., Jr (2011) A simple method for measuring intracellular activities of glutamine synthetase and glutaminase in glial cells. *Am. J. Physiol. Cell Physiol.* **301**, C814–822.

Ortega A., Eshhar N. and Teichberg V. I. (1991) Properties of kainate receptor/channels on cultured Bergmann glia. *Neuroscience* **41**, 335–349.

Ottersen O. P., Chaudhry F. A., Danbolt N. C., Laake J. H., Nagelhus E. A., Storm-Mathisen J. and Torp R. (1997) Molecular organization of cerebellar glutamate synapses. *Prog. Brain Res.* **114**, 97–107.

Regan M. R., Huang Y. H., Kim Y. S., Dykes-Hoberg M. I., Jin L., Watkins A. M., Bergles D. E. and Rothstein J. D. (2007) Variations in promoter activity reveal a differential expression and physiology of glutamate transporters by glia in the developing and mature CNS. *J. Neurosci.* **27**, 6607–6619.

Rosas S., Vargas M. A., Lopez-Bayghen E. and Ortega A. (2007) Glutamate-dependent transcriptional regulation of GLAST/EAAT1: a role for YY1. *J. Neurochem.* **101**, 1134–1144.

Ruiz M. and Ortega A. (1995) Characterization of an Na(+)-dependent glutamate/aspartate transporter from cultured Bergmann glia. *NeuroReport* **6**, 2041–2044.

Sager C., Tapken D., Kott S. and Hollmann M. (2009) Functional modulation of AMPA receptors by transmembrane AMPA receptor regulatory proteins. *Neuroscience* **158**, 45–54.

Seger R. and Krebs E. G. (1995) The MAPK signaling cascade. *FASEB J.* **9**, 726–735.

Shank R. P. and Campbell G. L. (1984) Glutamine, glutamate, and other possible regulators of alpha-ketoglutarate and malate uptake by synaptic terminals. *J. Neurochem.* **42**, 1162–1169.

Somogyi P., Eshhar N., Teichberg V. I. and Roberts J. D. (1990) Subcellular localization of a putative kainate receptor in Bergmann glial cells using a monoclonal antibody in the chick and fish cerebellar cortex. *Neuroscience* **35**, 9–30.

Uwechue N. M., Marx M. C., Chevy Q. and Billups B. (2012) Activation of glutamate transport evokes rapid glutamine release from perisynaptic astrocytes. *J. Physiol.* **590**, 2317–2331.

Volterra A. and Meldolesi J. (2005) Astrocytes, from brain glue to communication elements: the revolution continues. *Nat. Rev. Neurosci.* **6**, 626–640.

Wieronska J. M. and Pilc A. (2009) Metabotropic glutamate receptors in the tripartite synapse as a target for new psychotropic drugs. *Neurochem. Int.* **55**, 85–97.

Neurochemistry International 73 (2014) 139–145

Contents lists available at ScienceDirect

Neurochemistry International

journal homepage: www.elsevier.com/locate/nci

GLAST/EAAT1 regulation in cultured Bergmann glia cells: Role of the NO/cGMP signaling pathway

Alberto Balderas [a], Alain M. Guillem [a], Zila Martínez-Lozada [a], Luisa C. Hernández-Kelly [a,b], José Aguilera [b], Arturo Ortega [a,*]

[a] Departamento de Genética y Biología Molecular, Centro de Investigación y de Estudios Avanzados del Instituto Politécnico Nacional, Apartado Postal 14-740, México DF 07000, Mexico

[b] Institut de Neurosciénces i Departament de Bioquímica i Biología Molecular, Universitat Autònoma de Barcelona, Cerdanyola del Vallès, Barcelona, Spain

ARTICLE INFO

Article history:
Available online 6 November 2013

Keywords:
GLAST/EAAT1
Bergmann glia
Nitric oxide
cGMP

ABSTRACT

Glutamate, the major excitatory amino acid, activates a wide variety of signal transduction cascades. Ionotropic and metabotropic glutamate receptors are critically involved in long-term synaptic changes, although recent findings suggest that the electrogenic Na^+-dependent glutamate transporters, responsible for its removal from the synaptic cleft participate in the signaling transactions triggered by this amino acid. Glutamate transporters are profusely expressed in glia therefore most of its uptake occurs in this cellular compartment. In the cerebellar cortex, Bergmann glial cells enwrap glutamatergic synapses and participate in the recycling of its neurotransmitter through the glutamate/glutamine shuttle. It has long been acknowledged that glutamatergic transmission in the cerebellar molecular layer results in cGMP accumulation within Bergmann glia cells. In this context, we decided to investigate a plausible role of the nitric oxide/cGMP-signaling pathway in the regulation of Bergmann glia glutamate transporters. To this end, the well-established model of primary cultures of chick cerebellar Bergmann glial cells was used. Confluent monolayers were exposed to the nitric oxide donor, sodium nitroprusside, or to the non-hydrolysable cGMP analog dbcGMP and the [^{3}H] D-aspartate uptake activity measured. An increase in uptake activity, related to an augmentation in V_{Max}, was detected with both treatments. The signaling cascade includes NO/cGMP/PKG and Ca^{2+} influx through the Na^+/Ca^{2+} exchanger and might be related to the plasma membrane glutamate transporters turnover. Interestingly enough, an inhibitor of the cGMP dependent protein kinase was capable to abolish the sodium nitroprusside induced Ca^{2+} influx. These results provide an insight into the physiological role of cGMP in the cerebellum.

1. Introduction

Excitatory neurotransmission in the vertebrate Central Nervous System (CNS) is mediated mostly by glutamate (Glu). This excitatory amino acid exerts its actions through the activation of two main subtypes of receptors defined in terms of structure and signaling mechanisms: ionotropic (iGluRs) and metabotropic receptors (mGluRs). Three iGluRs have been defined: *N*-methyl-D-aspartate (NMDA), α-amino-3-hydroxy-5-methyl-4-isoaxazolepropionate (AMPA) and kainate (KA) receptors (Hollmann and Heinemann, 1994). Metabotropic receptors have been divided in terms of sequence similarity, signal transduction mechanisms and pharmacology in three groups. Group I receptors are coupled to the stimulation of phospholipase C with the consequent release of intracellular Ca^{2+}, while Groups II and III are coupled to the inhibition of adenylate cyclase. These three groups are activated preferentially by (RS)-3,5-dihydroxyphenylglycine (DHPG) for Group I, (*S*)-4-carboxy-3-hydroxyphenylglycine (*S*)-4C3HPG activates Group II while L-(+)-2-amino-4-phosphonobutyric acid (L-AP4) acts upon Group III (Coutinho and Knopfel, 2002).

A family of sodium-dependent Glu transporters are responsible for the removal of the excitatory transmitter from the synaptic cleft (Danbolt, 2001). These proteins are known as excitatory amino acid transporters (EAATs) and five different subtypes, numbered from 1 to 5 have been described. Although Glu uptake activity has been described in neurons and glia, more than 80% of the total brain removal of this excitatory amino acid from the synaptic cleft, is carried out by glial cells, which express EAAT1/GLAST (Glu/aspartate transporter) and/or EAAT2/Glt-1 (Glu transporter 1). In the cerebellum, the bulk of the Glu uptake takes place in Bergmann glia, which express GLAST/EAAT1, while in most of the other CNS structures, except for retina, Glt-1/EAAT2 is the major Glu carrier, in fact, it is known that this transporter represents roughly 2% of the total brain protein (Lehre and Danbolt, 1998).

* Corresponding author. Address: Departamento de Genética y Biología Molecular, Cinvestav-IPN, Apartado Postal 14-740, México DF 07000, Mexico. Tel.: +52 5 55747 3769; fax: +52 5 55747 3800x5317.
E-mail address: arortega@cinvestav.mx (A. Ortega).

0197-0186/$ - see front matter © 2013 Elsevier Ltd. All rights reserved.
http://dx.doi.org/10.1016/j.neuint.2013.10.011

Bergmann glia cells (BGC) are the most abundant glia cells in the cerebellum, comprising more than 90% of the cerebellar glia. These cells span the entire cerebellar molecular layer and encapsulate neuronal somata, dendrites and axons. BGC are involved in neurotransmitter uptake, K^+ homeostasis, lactate supply and pH regulation due to the expression of a battery of receptors and transporters (Lopez-Bayghen et al., 2007). In terms of glutamatergic transmission, BGC are in a very close proximity to the parallel fiber-Purkinje cell synapses, and are involved in the Glu/glutamine (Gln) shuttle that assures Glu supply to the presynaptic terminals. In this sense, BGC respond to glutamatergic stimulation, as we have been able to characterize over the years (Barrera et al., 2010).

The ability of Glu to induce large increases in the levels of guanosine 3′,5′-cyclic monophosphate (cGMP) in the cerebellum has been known since 1980 (Foster and Roberts, 1980). Exposure of rat cerebellar slices to NMDA, KA or sodium nitroprusside (SNP), an NO donor, results in a robust accumulation of cGMP in Bergmann glia fibers, that is inhibited by methylene blue, by the blockage of nitric oxide synthesis or by the depletation of extracellular Ca^{2+} (De Vente et al., 1990). Interestingly, both subunits of soluble guanylate cyclase (sGC) have been detected in BGC suggesting that these cells may be responsive to NO generated by a NMDA-dependent stimulation of neuronal nitric oxide synthase in granule cells (Ding et al., 2004). To gain insight into the role of cGMP in the physiology of BGC, we decided to evaluate its effects in one of the most characterized functions of BGC, the removal of Glu via GLAST/EAAT1. An augmentation of [^{3}H]-D-Asp uptake was found upon activation of the NO/cGMP pathway, suggesting a rapid up-regulation of the uptake process that might counter-balance the previously characterized reduction in GLAST/EAAT-1 activity by Glu (Gonzalez and Ortega, 2000).

2. Materials and methods

2.1. Materials

Tissue culture reagents were obtained from GE Healthcare (Carlsbad, CA, USA). A23187 (5-(methylamino)-2-({(2*R*,3*R*,6*S*,8*S*,9*R*,11*R*)-3,9,11-trimethyl-8-[(1*S*)-1-methyl-2-oxo-2-(1*H*-pyrrol-2-yl) ethyl]-1,7-dioxaspiro[5.5] undec-2-yl}methyl)-1,3-benzoxazole-4-carboxylic acid), D-aspartate (D-Asp) and Glu were all obtained from Tocris-Cookson (St. Louis, MO, USA). [^{3}H]-D-aspartate and [$^{45}Ca^{2+}$] were from Perkin Elmer (Boston, MA, USA). SNP, methylene blue, dbcGMP and Rp-8-Bromo-β-phenyl-1,N^2-ethenoguanosine 3′,5′-cyclic monophosphorothioate sodium salt hydrate (Rp-8-Br-PET-cGMPS), were obtained from Sigma–Aldrich, Mexico.

2.2. Cell culture and stimulation protocol

Primary cultures of cerebellar BGC were prepared from 14-day-old chick embryos as previously described (Ortega et al., 1991). Cells were plated in 24-well plastic culture dishes in DMEM containing 10% fetal bovine serum, 2 mM Gln, and gentamicin (50 μg/ml) and used on the 4th to 7th day after culture. Before any treatment, confluent monolayers were switched to non-serum DMEM media containing 0.5% bovine serum albumin (BSA) for 30 min and then treated as indicated. Inhibitors were added 30 min before agonists.

2.3. [^{3}H]-D-aspartate influx

Confluent BGC monolayers seeded in 24-well plates were washed three times to remove all non-adhering cells with 0.5 ml aliquots of solution A containing 25 mM HEPES-Tris, 130 mM NaCl, 5.4 mM KCl, 1.8 mM $CaCl_2$, 0.8 mM $MgCl_2$, 33.3 mM glucose and 1 mM NaH_2PO_4 at pH 7.4. When indicated, NaCl was replaced by choline chloride. The [^{3}H]-D-Asp influx was initiated at $t = 0$ by the addition of 0.5 ml solution A containing 0.4 μCi/ml of [^{3}H]-D-Asp. When inhibitors or modulators were tested, they were added 30 min prior to the beginning of the [^{3}H]-D-Asp influx assay. The reaction was stopped by aspirating the radioactive medium and washing each well within 15 s with 0.5 ml aliquots of an ice-cold solution A. For the determination of the kinetic parameters, the cold aspartate concentration was modified to a final 10, 25, 50, 100, 200 μM concentrations and the uptake time was 30 min a time which we have previously shown that uptake is linear (Ruiz and Ortega, 1995). The uptake was stopped as described above. The cells in the wells were then exposed for 2 h at 37 °C to 0.5 ml NaOH 0.1 M and an aliquot of that solution counted in a Beckmann 7800LS scintillation counter in the presence of a scintillation cocktail. Experiments were carried out as a minimum of quadruplicates.

2.4. [^{3}H]-D-aspartate binding

Confluent BGC monolayers seeded in 24-well culture plates were washed three times to remove all non-adhering cells with 0.5 ml aliquots of solution A. In the Na^+-free solution, NaCl was replaced by choline chloride. In the Ca^{2+}-free solution the $CaCl_2$ was supressed and 5 mM EDTA was added. The [^{3}H]-D-Asp binding was initiated at $t = 0$ by the addition of 0.5 ml solution A with or without modifications containing 0.4 μCi/ml of [^{3}H]-D-Asp at 4 °C. Glu was added 30 min and SNP 12 min prior to the beginning of the [^{3}H]-D-Asp binding assay. The assay was stopped by aspirating the radioactive medium and washing each well within 15 s with 0.5 ml aliquots of an ice-cold solution A. The cells in the wells were then exposed for 2 h at 37 °C to 0.5 ml NaOH and an aliquot of that solution counted in a Perkin Elmer TriCarb 2910 TR scintillation counter in the presence of a scintillation cocktail. Experiments were carried out as a minimum of quadruplicates.

2.5. [$^{45}Ca^{2+}$] influx

Confluent BGC monolayers seeded in 24-well plates were washed three times to remove all non-adhering cells with 0.5 ml aliquots of solution A containing 25 mM HEPES-Tris, 130 mM NaCl, 5.4 mM KCl, 1.8 mM $CaCl_2$, 0.8 mM $MgCl_2$, 33.3 mM glucose and 1 mM NaH_2PO_4 at pH 7.4. The SNP-induced influx of [$^{45}Ca^{2+}$] ions was initiated at $t = 0$ by the addition of 0.5 ml solution A containing 1.5 μCi/ml of [$^{45}Ca^{2+}$], and SNP at the specified concentration. When inhibitors or modulators were tested, they were added 30 min prior to the beginning of the [$^{45}Ca^{2+}$] influx assay. The reaction was stopped by aspirating the radioactive medium and washing each well within 15 s with 0.5 ml aliquots of an ice-cold solution A. The cells in the wells were then exposed for 2 h at 37 °C to 0.5 ml NaOH 0.1 M and an aliquot of that solution counted in a Perkin Elmer TriCarb 2910 TR scintillation counter in the presence of a scintillation cocktail. Experiments were carried out at least three times in quadruplicates.

2.6. Statistical analysis

Data are expressed as the mean (average) ± standard error (S.E.). A one-way analysis of variance (ANOVA) was performed to determine significant differences between conditions. When this analysis indicated significance (at the 0.05 level), post-hoc Student–Newman–Keuls test analysis was used to determine which conditions were significantly different from each other with the Prism software.

3. Results

3.1. The NO/cGMP signaling pathway increases [^{3}H]-D-aspartate uptake in Bergmann glial cells

More than thirty years have passed since the establishment of a Glu-dependent, Ca^{2+}-sensitive, increase in cGMP levels in cerebellar slices and the physiological consequence of the rise in the concentration of this nucleotide in glia cells remains obscure. In order to gain insight into the plausible role of NO as a modulator of glia cell function, we decided to concentrate in one established role of glia cells: Glu uptake (Danbolt, 2001). To this end, we exposed confluent BGC monolayers to the NO donor SNP. The results are depicted in Panel A of Fig. 1. A substantial increase in [^{3}H]-D-Asp was found in the presence of SNP. Two fundamental biochemical mechanisms are responsible of NO action: nitration and/or activation of sGC with the rise in cGMP intracellular concentrations. Treatment of the cultured cells with the non-hydrolysable cGMP analog, dbcGMP also results in an augmentation of the Glu uptake activity, similar but not identical the SNP effect (Panel B of Fig. 1). As expected, methylene blue, a guanylate cyclase inhibitor, prevents the SNP increase in [^{3}H]-D-Asp uptake without affecting the dbcGMP response (Panel C of Fig. 1).

3.2. GLAST/EAAT1 is regulated by the NO/cGMP pathway

D-Asp uptake through GLAST/EAAT1 is Na^+-dependent; therefore if the SNP effect is specific for this transporter, the replacement of NaCl in the external solution with an equimolar concentration of choline chloride would prevent the SNP effect. As expected, in a Na^+-free solution, SNP is no longer capable to increase [^{3}H]-D-Asp uptake (Fig. 2, panel A) it favor the idea of a specific effect over GLAST/EAAT1. As a control, cells were treated for 30 min with 1 mM Glu, which we have previously shown that reduces [^{3}H]-D-Asp uptake in a receptor-independent manner (Gonzalez and Ortega, 2000). At this stage, we decided to explore the kinetic parameters of the [^{3}H]-D-Asp uptake process, as a way to gain insight into the biochemical mechanism of the cGMP effect. The results are shown in panel B of Fig. 2. A change in GLAST/EAAT1 K_M is present upon cGMP and SNP that is reflected in an increase in the V_{Max} value, suggesting that an augmentation of available transporters in the plasma membrane. Note that this effect is not present when cells were pre-incubated with MB, the guanylate cyclase blocker blocking SNP effect. To corroborate this hypothesis, [^{3}H]-D-Asp binding experiments were performed in cells treated with SNP in the presence or absence of Na^+ and Ca^{2+}. As shown in Fig. 2C SNP increases the number of transporters in the plasma membrane, in a Ca^{2+}-dependent manner.

3.3. Sodium nitroprusside induces [$^{45}Ca^{2+}$] influx via PKG

The fact that dbcGMP was able to mimic the SNP effect, suggested the involvement of its downstream kinase, the cGMP-dependent protein kinase (PKG). To test this hypothesis, we pre-incubated confluent BGC monolayers with the PKG inhibitor, Rp-8-Br-PET-cGMPS, and then treated them with SNP, and as shown in Fig. 3A, the PKG inhibitor blocks SNP effect, demonstrating the involvement of PKG in the NO signaling in BGC.

It has been reported that the SNP triggered increase in cGMP intracellular levels is Ca^{2+} dependent in cerebellar slices (Linden et al., 1995). In the same vain, Kitao and co-workers demonstrated that SNP and cGMP stimulate Ca^{2+} influx through the activation in reverse mode of Na^+/Ca^{2+} exchanger (NCX) in astrocytes (Kitao et al., 2010). Therefore, we decided to analyze the involvement of Ca^{2+} and the NCX in the SNP effect observed in BGC. With this in mind, cells were treated with 100 μM SNP in normal or Ca^{2+}-free solution A and with the specific NCX inhibitor, KB-R7943 (15 μM). As clearly shown in Fig. 3B, the SNP effect is Ca^{2+}-dependent and sensitive to KB-R7943, suggesting that the NO response (augmentation of plasma membrane transporters) increases Na^+ influx, which activates the NCX leading to an increase in Ca^{2+} influx. To corroborate this idea, [$^{45}Ca^{2+}$] influx experiments were done. As clearly shown in Fig. 3C, exposure of the cultured cells to 100 μM SNP results in a significant increase in [$^{45}Ca^{2+}$] influx that is similar to that induced by the Ca^{2+} ionophore A231887. Pre-incubation of BGC cultures with the PKG inhibitor Rp-8-Br-PET-cGMPS prevents the SNP effect, demonstrating a NO-dependent PKG activation in BGC that in a undefined mechanism participates in the NCX function.

4. Discussion

The process of neurotransmitter removal or inactivation is critically involved in the proper function of the synapses, and the glutamatergic system is not an exemption (Tzingounis and Wadiche, 2007). It has been assumed that the physiological role of glial Glu transporters is restricted to the recycling of the neurotransmitter (Holz and Fisher, 2006), nevertheless, we, and others, have been able to demonstrate the involvement of these proteins as signaling entities (Martinez-Lozada et al., 2011; Abe and Saito, 2001; Martinez-Lozada et al., 2013). In any event, it is clear that the dysfunction of the neurotransmitter transporter systems results in a plethora of neurological and psychiatry disorders ranging from epilepsy to depression (Kanner, 2011; Wankerl et al., 2010).

Glu uptake and its rapid transformation into Gln to complete the Glu/Gln shuttle provides a biochemical framework for the involvement of glia cells in glutamatergic neurotransmission (Shank and Campbell, 1984). The expression and characterization of neurotransmitter receptors in glia cells favored the concept of a *tripartite* synapse (Araque et al., 1999). In this context, glia cells associated to glutamatergic synapses respond to synaptic activity via receptors: Ca^{2+} waves in radial glia cells (Muller et al., 1996) and via transporters: the Glu/Gln shuttle and its associated inward Na^+ current (Owe et al., 2006). Of particular interest, has been the regulation of the glia protein repertoire by Glu through transcriptional and translational control (Balazs, 2006; Gallo and Ghiani, 2000; Lopez-Bayghen and Ortega, 2010; Lopez-Bayghen et al., 2007).

In an effort to advance in our understanding of the role of glia cells in synaptic function we analyzed the plausible effect of NO in the regulation of [^{3}H]-D-Asp uptake activity. We were able to demonstrate that exposure to SNP or dbcGMP results in augmentation in the activity of the sole Glu transporter expressed in these cells: GLAST/EAAT-1 (Ruiz and Ortega, 1995; Danbolt, 2001). Note that the SNP effect is transient whereas the dbcGMP is more sustained (Fig. 1), most possible reflecting its resistance to hydrolysis by the cGMP phosphodiesterase. The extent of [^{3}H]-D-Asp uptake in BGC depends upon the abundance and affinity of GLAST/EAAT1 transporters in the plasma membrane; both SNP and dbcGMP increase V_{Max} values (Panel B of Fig. 2). It is important to mention that at first sight, it could be difficult to reconcile the magnitude of SNP and dbcGMP increase in [^{3}H] D-Asp uptake shown in Fig. 1 with the V_{Max} values reported in panel B of Fig. 3. A plausible explanation for this apparent discrepancy might be linked to the [^{3}H] D-Asp final concentration used in Fig. 1 [35 nM]. This concentration is below the affinity of GLAST/EAAT1 (Fig. 2). Since an augmentation of [^{3}H]-D-Asp uptake in one-point experiments as those in Fig. 1, can be the result of a different affinity of the transporters or to the fact that there could be more transporters in the plasma membrane, it was important to measure the Michaelis–Menten

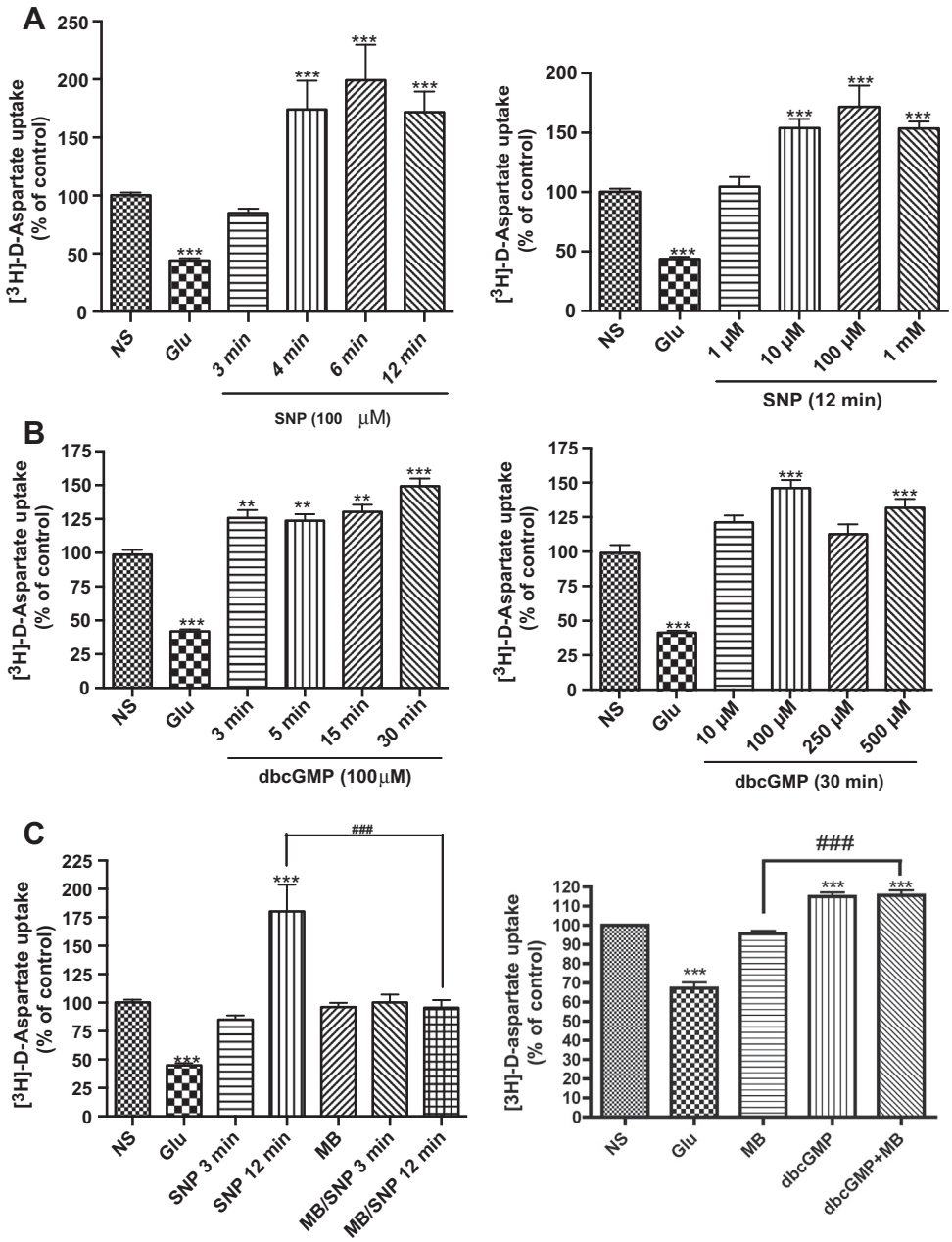

Fig. 1. NO and cGMP increase [^{3}H]-D-Asp uptake. (A) BGC were pre-incubated with the nitric oxide (NO) donor, SNP at a 100 μM concentration for indicated time periods (3, 4, 6 or 12 min); or pre-incubated 12 min with increasing SNP concentrations (1 μM, 10 μM, 100 μM and 1 mM), the [^{3}H]-D-Asp uptake time was 30 min. (B) BGC were pre-treated with the non-metabolizable analog of cGMP, dbcGMP at a 100 μM concentration for the indicated time periods (3, 5, 15 or 30 min); or pre-incubated 30 min with increasing dbcGMP concentrations (10 μM, 100 μM, 250 μM and 500 μM), the [^{3}H]-D-Asp uptake was measured as in panel A. (C) BGC were pre-treated with 100 μM SNP for 3 or 12 min or 100 μM dbcGMP, both in presence or absence of the sGC inhibitor, Methylene blue (MB); the [^{3}H]-D-Asp uptake assay done as in panel A. In all panels cells pre-incubated with 1 mM Glu for 30 min was used as a control of the experiment (Gonzalez and Ortega, 2000). Data are expressed as the mean ± SEM at least of 3 independent experiment, each tested in quadruplicate; a Student's *t*-test with a Dunnett's Multiple comparison test was performed to analyze the data ($^{***}p < 0.001$, $^{**}p < 0.01$). In Panel C a Newman–Keuls Multiple Comparison Test was performed to analyze MB/SNP effect ($^{###}p < 0.001$).

parameters. In fact, what we found is that either SNP or dbcGMP augments V_{Max}, albeit to a different extent probably due to the transient increase in cGMP levels in the cells exposed to SNP.

The amount Gln released by BGC is a function of the intracellular concentration of this neutral amino acid. It should be noted that the affinity of GLAST/EAAT1 is the 13–20 μM range, whereas the affinity of the Gln transporters involved the Gln release is in the 1–2 mM range (Ruiz and Ortega, 1995; Martinez-Lozada et al., 2013), therefore it is not surprising that a high (1 mM) Glu concentration inhibits [^{3}H]-D-Asp uptake (Figs. 1 and 2), (Gonzalez and Ortega, 2000).

It is tempting to speculate that *in vivo*, in periods of intense electrical activity in the cerebellar molecular layer, Glu-dependent increase in NO synthase results in a significant NO production that diffuses and activates soluble guanylate cyclase in BGC with the concomitant increase in cGMP levels. Activated PKG would facilitate the insertion of already synthetized GLAST/EAAT1 in the plasma membrane, increasing by these means the capacity of glial cells to bind Glu and therefore shape the post synaptic excitatory potential (Tzingounis and Wadiche, 2007; Takayasu et al., 2004). In support of our interpretation is the fact that the SNP effect of the increase in [^{3}H]-D-Asp uptake is present already after 4 min of

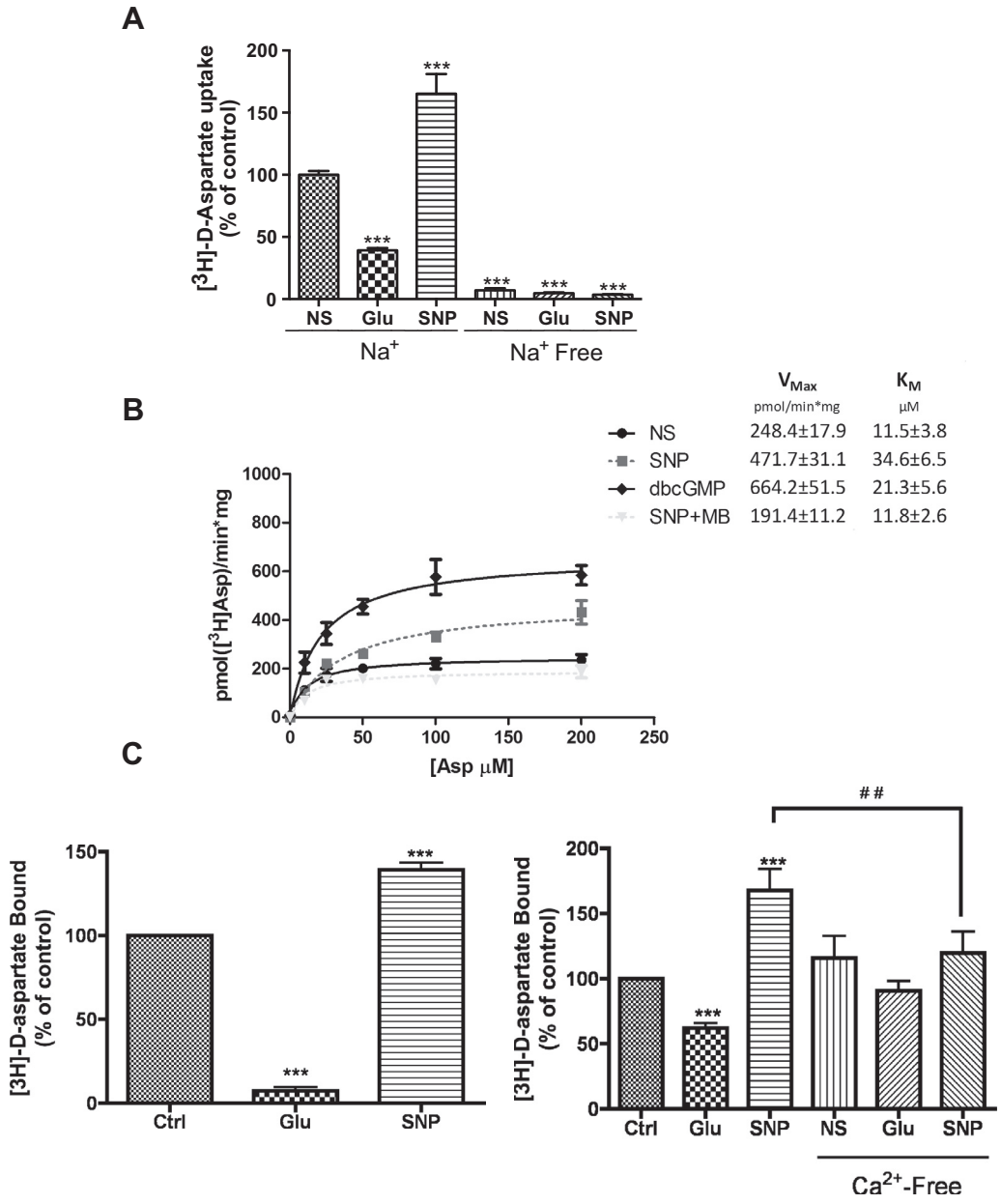

Fig. 2. SNP increases [^{3}H]-D-Asp uptake through the augmentation of available transporters in the plasma membrane. (A) BGC were pre-incubated with 1 mM Glu for 30 min and with 100 μM SNP for 12 min, both in presence or absence of Na^+; [^{3}H]-D-Asp uptake measured as in Fig. 1 in presence or absence of Na^+. Cells treated with 1 mM for Glu 30 min were used as a control of the experiment. Data are expressed as the mean ± SEM of at least 3 independent experiments, each tested in quadruplicate; a Student's *t*-test with a Dunnett's multiple comparison test was performed to analyze the data (***$p < 0.001$). (B) BGC were pre-incubated with 100 μM SNP for 12 min both in presence or absence of the sGC inhibitor, Methylene blue (MB); or with 100 μM dbcGMP for 30 min and the D-[^{3}H]-Asp uptake assay was performed with increasing non-labeled D-Asp concentrations (10 μM, 25 μM, 50 μM, 100 μM and 200 μM) for 30 min. Data are expressed as the mean ± SEM at least of 3 independent experiments, each tested in quadruplicate. Transport kinetics V_{Max} (pmol/min*mg) and K_M (μM) were determined by non-linear regression with the Prism 5 software (GraphPad). (C) BGC were stimulated with 1 mM Glu for 30 min or with 100 μM SNP both in presence or absence of Na^+ and Ca^{2+} (as indicated in the figure). Then a D-[^{3}H]-Asp binding assay was performed at 4 °C. Data are expressed as the mean ± SEM of at least 3 independent experiments, each tested in quadruplicate; a Student's *t*-test with a Dunnett's Multiple comparison test was performed to analyze the data (***$p < 0.001$, **$p < 0.01$). In Panel C a Newman–Keuls Multiple Comparison Test was performed to analyze SNP without Ca^{2+} effect (##$p < 0.01$).

treatment with the NO donor, whereas the Glu effect of reduction of [^{3}H]-D-Asp influx is present only after a Glu stimulation of 30 min. The actual target for PKG phosphorylation is not known at this moment. A direct PKG mediated GLAST/EAAT1 phosphorylation is unlikely given the fact that up to date it has not been possible to ascribe a role for the phosphorylation in the regulation of this protein (Conradt and Stoffel, 1997). Interestingly, all these effects are dependent on a NCX-mediated Ca^{2+} influx (Figs. 2 and 3). At this stage, one could speculate that the traffic of the transporter is mediated by the cytoskeleton, a structure tightly regulated though Ca^{2+}-mediated phosphorylation events. Work in progress in our lab is aimed to the characterization of the molecular mechanism of this regulation.

In summary, a complex set of biochemical transactions are triggered by Glu not only in the post-synaptic neuron but also in the glia cells that regulate the turnover and therefore the availability of releasable Glu in the presynaptic terminal. A model of our present findings is depicted in Fig. 4, the arrival of an action potential to

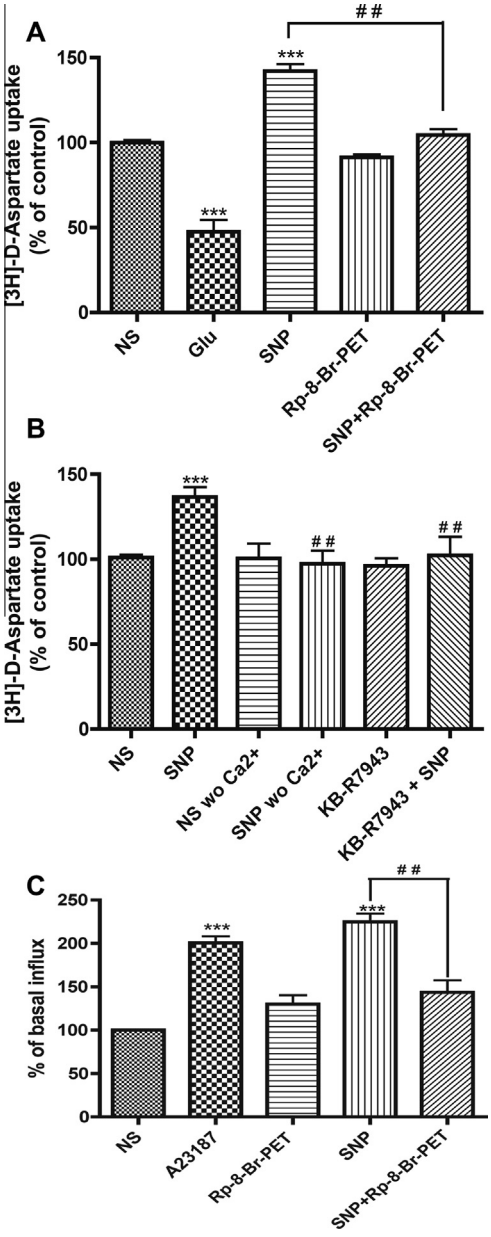

Fig. 3. SNP induced [$^{45}Ca^{2+}$] influx is PKG-dependent. (A) Cells were stimulated with 100 μM SNP for 12 min in presence or absence of PKG inhibitor, Rp-8-Br-PET-cGMPS 10 μM; the [^{3}H]-D-Asp uptake assay done as in Fig. 1. Cells pre-incubated with 1 mM Glu for 30 min were used as a control of the experiment. (B) BGC were treated with 100 μM SNP for 12 min in presence or absence of Ca^{2+}, or pre-incubated for 30 min with the NCX inhibitor, KB-R7943 (15 μM) and then treated with SNP; the [^{3}H]-D-Asp uptake assay done as in panel A. (C) Confluent BGC cultures were pre-exposed for 30 min to the PKG inhibitor, Rp-8-Br-PET-cGMPS 10 μM as indicated, and then incubated with 100 μM SNP and the [$^{45}Ca^{2+}$] uptake performed for 3 min. The Ca^{2+} ionophore A23187 (10 μM) was used as a positive control. Data are expressed as the mean ± SEM of at least 3 independent experiments, each tested in quadruplicate; a Student's *t*-test with a Dunnett's Multiple comparison test was performed to analyze the data ($^{***}p < 0.001$, $^{**}p < 0.01$) also a Newman–Keuls Multiple Comparison Test was performed to analyze SNP effect *vs* SNP + inhibitors ($^{\#\#}p < 0.01$).

the granule cells terminals results in Glu release. Glu activates ionotropic as well as metabotropic receptors in Purkinje cells, leading to the synthesis and release of NO, which would diffuse and activate sGC in Bergmann glia activating guanylate cyclase, augmented cGMP levels activate PKG activation, that together with the increased Na^{+} levels due to the Glu transport, activates of NCX with the resulting Ca^{2+} influx, which then would favor GLAST/EAAT1 containing vesicles movement to plasma membrane to increase GLAST/EAAT1 insertion in the plasma membrane and therefore an augmentation of Glu uptake.

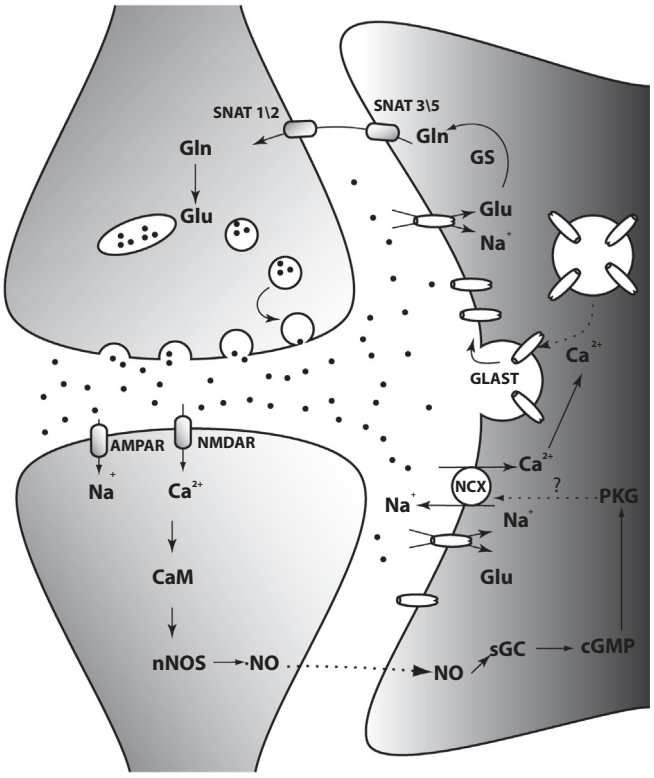

Fig. 4. Current working model. Once granule cells are depolarized, the released Glu activates ionotropic receptors in Purkinje cells, leading to the synthesis and release of NO, which would diffuse and activate sGC in Bergmann glia resulting in an increase in cGMP levels and PKG activation, resulting in the activation of NCX with the resulting Ca^{2+} influx, which then would favor GLAST/EAAT1 containing vesicles movement to plasma membrane to increase GLAST/EAAT1 insertion in the plasma membrane and therefore an augmentation of Glu uptake.

5. Conclusion

Nitric oxide regulates GLAST/EAAT1 through the activation of guanylate cyclase. A role for PKG and Ca^{2+} in this effect could be demonstrated.

Acknowledgements

This work was supported by grants from Conacyt-Mexico to A.O. (79502 and 123625). A.B., A.M.G., and Z.M. are supported by Conacyt-Mexico fellowship. The technical assistance of Luis Cid and Blanca Ibarra is acknowledged.

References

Abe, K., Saito, H., 2001. Possible linkage between glutamate transporter and mitogen-activated protein kinase cascade in cultured rat cortical astrocytes. J. Neurochem. 76, 217–223.
Araque, A., Parpura, V., Sanzgiri, R.P., Haydon, P.G., 1999. Tripartite synapses: glia, the unacknowledged partner. Trends Neurosci. 22, 208–215.
Balazs, R., 2006. Trophic effect of glutamate. Curr. Top. Med. Chem. 6, 961–968.
Barrera, I., Flores-Mendez, M., Hernandez-Kelly, L.C., Cid, L., Huerta, M., Zinker, S., Lopez-Bayghen, E., Aguilera, J., Ortega, A., 2010. Glutamate regulates eEF1A phosphorylation and ribosomal transit time in Bergmann glial cells. Neurochem. Int. 57, 795–803.
Conradt, M., Stoffel, W., 1997. Inhibition of the high-affinity brain glutamate transporter GLAST-1 via direct phosphorylation. J. Neurochem. 68, 1244–1251.
Coutinho, V., Knopfel, T., 2002. Metabotropic glutamate receptors: electrical and chemical signaling properties. Neuroscientist 8, 551–561.

Danbolt, N.C., 2001. Glutamate uptake. Prog. Neurobiol. 65, 1–105.
De Vente, J., Bol, J.G., Berkelmans, H.S., Schipper, J., Steinbusch, H.M., 1990. Immunocytochemistry of cGMP in the cerebellum of the immature, adult, and aged rat: the involvement of nitric oxide. A micropharmacological study. Eur. J. Neurosci. 2, 845–862.
Ding, J.D., Burette, A., Nedvetsky, P.I., Schmidt, H.H., Weinberg, R.J., 2004. Distribution of soluble guanylyl cyclase in the rat brain. J. Comp. Neurol. 472, 437–448.
Foster, G.A., Roberts, P.J., 1980. Pharmacology of excitatory amino acid receptors mediating the stimulation of rat cerebellar cyclic GMP levels in vitro. Life Sci. 27, 215–221.
Gallo, V., Ghiani, C.A., 2000. Glutamate receptors in glia: new cells, new inputs and new functions. Trends Pharmacol. Sci. 21, 252–258.
Gonzalez, M.I., Ortega, A., 2000. Regulation of high-affinity glutamate uptake activity in Bergmann glia cells by glutamate. Brain Res. 866, 73–81.
Hollmann, M., Heinemann, S., 1994. Cloned glutamate receptors. Annu. Rev. Neurosci. 17, 31–108.
Holz, R.W., Fisher, S.K., 2006. Synaptic transmission and cellular signaling: an overview. In: Siegel, G., Wayne, A.R., Brady, S., Price, D. (Eds.), Basic Neurochemistry: Molecular, Cellular and Medical Aspects. Elsevier Academic Press, Canada, pp. 167–181.
Kanner, A.M., 2011. Depression and epilepsy: a bidirectional relation? Epilepsia 52 (Suppl. 1), 21–27.
Kitao, T., Takuma, K., Kawasaki, T., Inoue, Y., Ikehara, A., Nashida, T., Ago, Y., Matsuda, T., 2010. The Na+/Ca^{2+} exchanger-mediated Ca^{2+} influx triggers nitric oxide-induced cytotoxicity in cultured astrocytes. Neurochem. Int. 57, 58–66.
Lehre, K.P., Danbolt, N.C., 1998. The number of glutamate transporter subtype molecules at glutamatergic synapses: chemical and stereological quantification in young adult rat brain. J. Neurosci. 18, 8751–8757.
Linden, D.J., Dawson, T.M., Dawson, V.L., 1995. An evaluation of the nitric oxide/cGMP/cGMP-dependent protein kinase cascade in the induction of cerebellar long-term depression in culture. J. Neurosci. 15, 5098–5105.
Lopez-Bayghen, E., Ortega, A., 2010. Glial cells and synaptic activity: translational control of metabolic coupling. Rev. Neurol. 50, 607–615.
Lopez-Bayghen, E., Rosas, S., Castelan, F., Ortega, A., 2007. Cerebellar Bergmann glia: an important model to study neuron–glia interactions. Neuron Glia Biol. 3, 155–167.
Martinez-Lozada, Z., Guillem, A.M., Flores-Mendez, M., et al., 2013. GLAST/EAAT1-induced glutamine release via SNAT3 in Bergmann glial cells: evidence of a functional and physical coupling. J. Neurochem. 125, 545–554.
Martinez-Lozada, Z., Hernandez-Kelly, L.C., Aguilera, J., Lopez-Bayghen, E., Ortega, A., 2011. Signaling through EAAT-1/GLAST in cultured Bergmann glia cells. Neurochem. Int. 59, 871–879.
Muller, T., Moller, T., Neuhaus, J., Kettenmann, H., 1996. Electrical coupling among Bergmann glial cells and its modulation by glutamate receptor activation. Glia 17, 274–284.
Ortega, A., Eshhar, N., Teichberg, V.I., 1991. Properties of kainate receptor/channels on cultured Bergmann glia. Neuroscience 41, 335–349.
Owe, S.G., Marcaggi, P., Attwell, D., 2006. The ionic stoichiometry of the GLAST glutamate transporter in salamander retinal glia. J. Physiol. 577, 591–599.
Ruiz, M., Ortega, A., 1995. Characterization of an Na(+)-dependent glutamate/aspartate transporter from cultured Bergmann glia. Neuroreport 6, 2041–2044.
Shank, R.P., Campbell, G.L., 1984. Glutamine, glutamate, and other possible regulators of alpha-ketoglutarate and malate uptake by synaptic terminals. J. Neurochem. 42, 1162–1169.
Takayasu, Y., Iino, M., Ozawa, S., 2004. Roles of glutamate transporters in shaping excitatory synaptic currents in cerebellar Purkinje cells. Eur. J. Neurosci. 19, 1285–1295.
Tzingounis, A.V., Wadiche, J.I., 2007. Glutamate transporters: confining runaway excitation by shaping synaptic transmission. Nat. Rev. Neurosci. 8, 935–947.
Wankerl, M., Wust, S., Otte, C., 2010. Current developments and controversies: does the serotonin transporter gene-linked polymorphic region (5-HTTLPR) modulate the association between stress and depression? Curr. Opin. Psychiatry 23, 582–587.

Neurochem Res
DOI 10.1007/s11064-015-1721-z

ORIGINAL PAPER

Methylphenidate Increases Glutamate Uptake in Bergmann Glial Cells

Alain M. Guillem[1] · Zila Martínez-Lozada[1] · Luisa C. Hernández-Kelly[1] · Esther López-Bayghen[1] · Bruno López-Bayghen[1] · Oscar A. Calleros[2] · Marco R. Campuzano[2] · Arturo Ortega[1]

Received: 10 June 2015 / Revised: 10 September 2015 / Accepted: 12 September 2015

Abstract Glutamate, the main excitatory transmitter in the vertebrate brain, exerts its actions through the activation of specific membrane receptors present in neurons and glial cells. Over-stimulation of glutamate receptors results in neuronal death, phenomena known as excitotoxicity. A family of glutamate uptake systems, mainly expressed in glial cells, removes the amino acid from the synaptic cleft preventing an excessive glutamatergic stimulation and thus neuronal damage. Autism spectrum disorders comprise a group of syndromes characterized by impaired social interactions and anxiety. One or the most common drugs prescribed to treat these disorders is Methylphenidate, known to increase dopamine extracellular levels, although it is not clear if its sedative effects are related to a plausible regulation of the glutamatergic tone via the regulation of the glial glutamate uptake systems. To gain insight into this possibility, we used the well-established model system of cultured chick cerebellum Bergmann glia cells. A time and dose-dependent increase in the activity and protein levels of glutamate transporters was detected upon Methylphenidate exposure. Interestingly, this increase is the result of an augmentation of both the synthesis as well as the insertion of these protein complexes in the plasma membrane. These results favour the notion that glial cells are Methylphenidate targets, and that by these means could regulate dopamine turnover.

✉ Arturo Ortega
arortega@cinvestav.mx

[1] Laboratorio de Neurotoxicología, Departamento de Toxicología, Centro de Investigación y de Estudios Avanzados del Instituto Politécnico Nacional, Apartado Postal 14-740, 07000 Mexico, DF, Mexico

[2] Clínica Neurocom, 03100 Mexico, DF, Mexico

Keywords Methylphenidate · Excitatory amino acid transporters · Bergmann glia · Translational control

Introduction

Glutamate (Glu) is the main excitatory amino acid neurotransmitter in the Central Nervous System (CNS). As many as 80–90 % of the synapses in the brain are glutamatergic [1], therefore this neurotransmitter is involved in a plethora of functions, from sensory motor information and coordination to emotions and cognition. Glu exerts its actions through the activation of specific membrane receptors that have been traditionally divided into two main categories: ionotropic (iGluRs) and metabotropic receptors (mGluRs).

A family of sodium-dependent Glu transporters, also known as excitatory amino acid transporters (EAATs) are responsible for Glu removal from the synaptic cleft [2]. Thus far, five EAAT subtypes have been described, being EAAT1 and EAAT2 preferentially expressed in glial cells and their activity represents more than 80 % of the total brain Glu uptake activity. Within the cerebellum, most of the Glu uptake takes place in Bergmann glial cells (BGC), which express exclusively EAAT1, a transporter also known as Na^{+}- glutamate/aspartate transporter (GLAST). In contrast, in other CNS structures, EAAT2 or Glutamate transporter 1 (GLT-1) is the major Glu carrier, in fact, it is known that this transporter represents roughly 2 % of total brain protein [3].

Glu has a critical role in brain physiology and higher brain functions [4, 5]. A tight control of its extracellular levels is critical to prevent its well-characterized neurotoxic effect. In fact, all known neurodegenerative diseases are related to an excess of extracellular Glu, as in amyotrophic lateral sclerosis (ALS) and Alzheimeŕs disease

Published online: 18 September 2015

[6, 7]. Moreover, it has also been suggested that dysregulation of Glu extracellular concentrations is involved in autism spectrum disorders (ASD) [8–10].

Autism comprises a complex neurodevelopment disorders characterized by social interaction impairment, communication and stereotyped behaviours [11, 12]. Multiple factors participate in its pathophysiology, it is known that genetic and environmental cues are involved, although the precise mechanisms underlying these disorders remain to be determined. In this scenario, the selection of an appropriate treatment is difficult.

Methylphenidate (MPH) is currently used for ASD treatment, although its efficacy is highly controversial [13]. Even though its effects over the dopaminergic system have been described, MPH also targets the glutamatergic system [10, 14]. Given the fact that Glu turnover is dependent on the *glutamate/glutamine shuttle,* a biochemical interplay between neurons and glial cells, in this contribution we focused on the effect of MPH on EAAT-1/GLAST-mediated [^{3}H]-D-Aspartate (D-Asp) uptake activity. To this end, we decided to use the model of cultured cerebellar Bergmann glial cells.

A time and dose-dependent increase in [^{3}H]-D-Asp uptake was observed, suggesting a rapid up-regulation of the Glu removal, likely to be relevant for the anti-anxiety effect of MPH. These results support the involvement of glial cells in the pathological features of complex brain disorders such as autism.

Methods

Materials

Tissue culture reagents were obtained from GE Healthcare (Carlsbad, CA, USA). D-Asp and Glu were obtained from Tocris-Cookson (St. Louis, MO, USA). [^{3}H]-D-Asp was from Perkin Elmer (Boston, MA, USA). Actinomycin D, cycloheximide, cytochalasin B, choline chloride, Rp-8-Bromo-β-phenyl-1,N2-ethenoguanosine 3′,5′-cyclic monophosphorothioate (8-Br-cGMP), bisindolylmaleimide II (Bis), 12-O-Tetradecanoylphorbol-13-acetate (TPA) and methylphenidate hydrochloride (MPH) were obtained from Sigma-Aldrich, Mexico. A 1:1000 dilution of GLAST-antibody (produced and characterized in our laboratory [15]) was used. Horseradish peroxidase-linked anti-rabbit antibodies (1:4000 dilution), and the enhanced chemiluminescence reagents were obtained from Amersham Biosciences (Buckinghamshire, UK).

Cell Culture and Stimulation Protocol

Primary cultures of cerebellar Bergmann glial cells were prepared from 14-day-old chick embryos as previously described [16]. Cells were plated in 24-well plastic culture dishes in DMEM containing 10 % foetal bovine serum, 2 mM glutamine, and gentamicin (50 μg/ml) and used on the 4th–7th day after culture. Before any treatment, confluent monolayers were switched to solution A containing 25 mM HEPES-Tris, 130 mM NaCl, 5.4 mM KCl, 1.8 mM $CaCl_2$, 0.8 mM $MgCl_2$, 33.3 mM glucose and 1 mM NaH_2PO_4 at pH 7.4, for experiments that included long-term exposure to MPH, confluent monolayers were switched to non-serum DMEM media containing 0.5 % bovine serum albumin (BSA). Inhibitors were added 30 min before agonists.

[^{3}H]-D-Asp Influx

Confluent Bergmann glial monolayers seeded in 24-well plates were washed three times to remove all non-adhering cells with 0.25 ml of solution A. When indicated, NaCl was replaced by choline chloride. The [^{3}H]-D-Asp influx was initiated at $t = 0$ by the addition of 0.25 ml solution A containing 0.4 μCi/ml of [^{3}H]-D-Asp. The reaction was stopped by aspirating the radioactive medium and washing each well within 15 s with 0.25 ml aliquots of an ice-cold solution A. For the determination of the kinetic parameters, the Asp concentration was modified to a final 10, 25, 50, 100 μM concentrations with unlabelled Asp and the uptake time was 30 min [17]. The uptake was stopped as described above. The cells in the wells were then exposed for 2 h at 37 °C to 0.25 ml NaOH 0.1 M and an aliquot of the radioactivity present determined in a Perkin Elmer scintillation counter in the presence of a scintillation cocktail. Experiments were carried at least three times with a minimum of quadruplicate determinations.

[^{3}H]-D-Asp Binding

Equilibrium-binding experiments were performed in confluent Bergmann glial cells monolayers that were washed three times to remove all non-adhering cells with 0.5 ml of solution A. Cells were incubated for 30 min with or without a fixed 100 μM MPH concentration. Na^+-free solutions were prepared replacing NaCl with choline chloride. In the Ca^{2+}-free solutions, $CaCl_2$ was omitted and 5 mM EDTA was added. The [^{3}H]-D-Asp binding was initiated at $t = 0$ by the addition of 0.5 ml solution A with or without modifications containing 0.4 μCi/ml of [^{3}H]-D-Asp at 4 °C. The assay was stopped after 15 min by aspirating the radioactive medium and washing each well within 15 s with 0.5 ml aliquots of an ice-cold solution A. The cells in the wells were solubilized for 2 h at 37 °C to 0.5 ml NaOH and an aliquot of that solution mixed with scintillation cocktail and the radioactivity present determined counted in a Perkin Elmer scintillation counter.

Experiments were carried out at least three times with a minimum of quadruplicate determinations. Non-specific binding was determined in the presence of 100 μM Asp. [^{3}H]-D-Asp binding to GLAST/EAAT1 was defined as the difference between the specific binding in normal solution A minus the binding in Na^+-free solution A.

SDS-PAGE and Western blots

Cells from confluent monolayers were harvested with phosphate buffer saline (PBS) (10 mM K_2HPO_4/KH_2PO_4, 150 mM NaCl, pH 7.4) containing phosphatase inhibitors (10 mM NaF, 1 mM Na_2MoO_4 and 1 mM Na_3VO_4). The cells were lysed with RIPA buffer (50 mM Tris-HCl, 1 mM EDTA, 150 mM NaCl, 1 mM phenylmethylsufonyl fluoride, 1 mg/ml aprotinin 1 mg/ml leupeptin, 1 % NP-40, 0.25 % sodium deoxycholate, 10 mM NaF, 1 mM Na_2MoO_4 and 1 mM Na_3VO_4, pH7.4). Cell lysates were denatured in Laemmli's sample buffer, resolved through 10 % SDS-PAGE and then electro blotted to nitrocellulose membranes. Blots were stained with Ponceau S stain to confirm that protein content was equal in all lanes. Membranes were soaked in PBS to remove the Ponceau S and incubated in TBS containing 5 % dried skimmed milk and 0.1 % Tween 20 for 60 min to block the excess of non-specific protein binding sites. Membranes were then incubated overnight at 4 °C with the primary antibodies indicated in each figure, followed by the adequate secondary antibodies. Immunoreactive polypeptides were detected by chemiluminescence with a MicroChemi (DNR Bio-Imaging System). Densitometric analyses were performed and data analysed with the Prism 5, GraphPad Software (San Diego, CA, USA).

RNA Extraction and qRT-PCR

Total RNA was isolated from confluent Bergmann glial cell cultures (treated, non-treated) and extracted using the Tri-Reagent (Sigma). Every treatment condition per experiment was analysed as technical duplicates. PCR was performed in a reaction volume of 10 μl. Real-time quantitative reverse transcription-PCR (qRT-PCR) was performed by a one-step method with 20 ng of total RNA and using KAPA SYBR FAST One Step qRT-PCR system (KAPA BIOSYSTEMS). Samples were subjected to quantitative PCR (qPCR) using Step one Plus Real time PCR system (Applied Biosystems). The qPCR profile consisted of an initial cDNA synthesis by M-MuLV Reverse Transcriptase at 42 °C for 5 min, an inactivation of the reverse transcriptase at 95 °C for 5 min, followed by 40 cycles of 95 °C for 3 s, 60 °C 30 s. A melt curve stage was added. To quantify GLAST mRNA levels, we used previously reported oligonucleotides designed by our workgroup as *chGLAST*: GLAST Forward 5′-GGCTGCGGGCATTCCTC-3′ and GLAST Reverse 5′-CGGAGACGATCCAAGAACCA-3′. As an endogenous control we amplified ribosomal protein S17 mRNA with the following primers: S17 Forward 5′-CCGCTGGATGCG CTTCATCAG-3′ and S17 Reverse 5′-TACACCCGTCTG GGCAAC-3′. The relative abundance of GLAST mRNA is expressed as sample versus a control normalized to S17 chick ribosomal mRNA levels and was calculated as $2 - \Delta\Delta C_t$. Data are presented as mean values ± SDs and analysed by one-way ANOVA ($p < 0.05$ was considered statistically significant).

Statistical Analysis

Data are expressed as the mean (average) ± standard error (SEM). A one-way analysis of variance (ANOVA) was performed to determine significant differences between conditions. When this analysis indicated significance (at the 0.05 level), a Dunnett's multiple comparison analysis was used to determine which conditions were significantly different from each other with the Prism 5, GraphPad Software (San Diego, CA, USA).

Results

Glutamate Uptake is Up-Regulated by MPH in Bergmann Glial Cells

The possibility that MPH could have an important effect on the glutamatergic transmission has long been suggested [14, 18, 19]. Despite of these contributions, its effect in glial cells have not been well characterized. Therefore, we decided to investigate whether an established glial cell function such as Glu uptake, could be modified by MPH.

As depicted in panel a of Fig. 1, when the cultured cells were treated with 100 μM MPH, a significant increase in [^{3}H]-D-Asp was detected as early as 2 h after MPH and the effect was still present after 12 h. In order to characterize the effect from a pharmacological perspective, we decided to expose the cultured cells to different MPH concentrations (1, 10, 100, 1000 μM) for 1 or 4 h. The results are shown in panels b and c of Fig. 1. Note that the MPH effect is not detected after 1 h, but after a 4 h pre-incubation a significant increase in uptake is detected at a 100 and 1000 μM MPH doses. As a control of our experiments we pre-treated the cells for 30 min with 1 mM D-Asp, treatment that we have shown, down-regulates GLAST-mediated [^{3}H]-D-Asp uptake [20].

MPH Increases Plasma Membrane GLAST Transporters

The results described in the previous section, demonstrate an increase in GLAST activity after MPH treatment; this

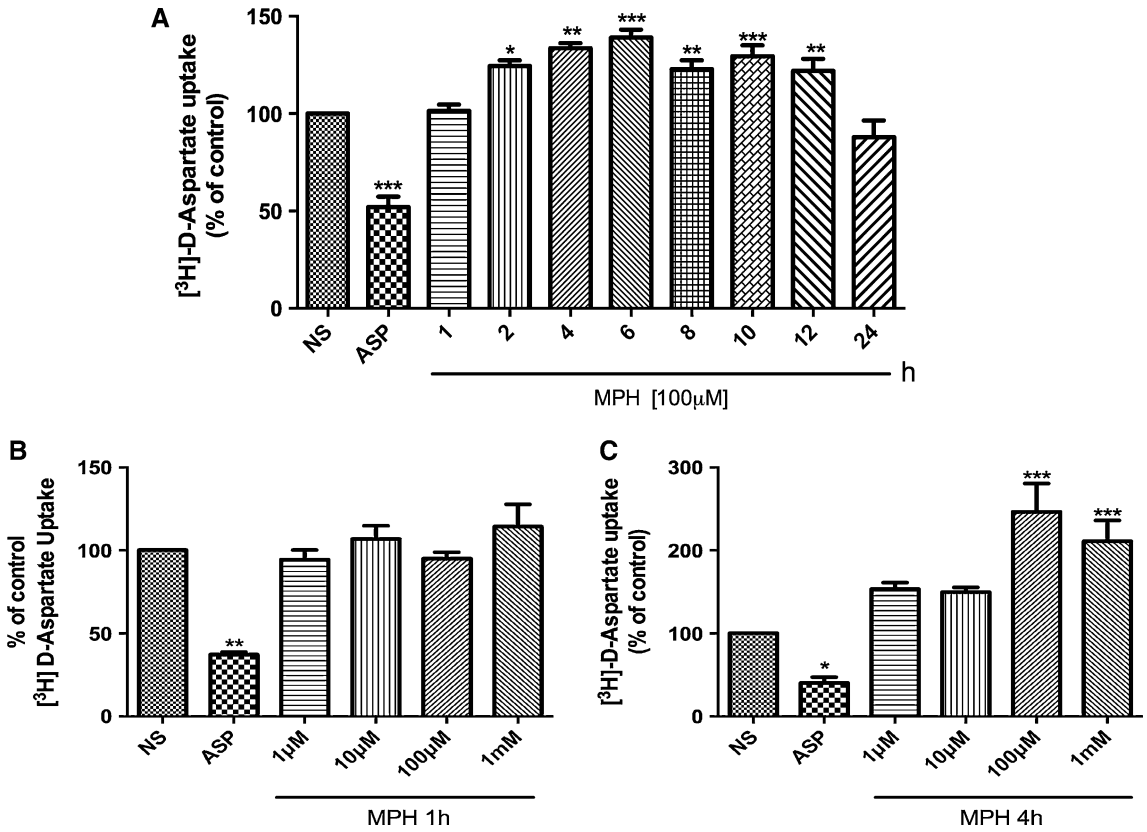

Fig. 1 Methylphenidate (MPH) increases GLAST activity. BGC were pre-incubated with MPH at a 100 μM concentration for indicated time periods (1, 2, 4, 6, 8, 10, 12 or 24 h) (**a**); or pre-incubated for 1 h (**b**) or 4 h (**c**) with increasing MPH concentrations (1, 10, 100 or 1000 μM), the [3H]-D-Asp uptake was performed for 30 min. As control of the experiment, cells were pre-incubated 30 min with 1 mM Glu [20]. *Non-stimulate* (NS), *Glutamate* 1 mM (Glu). Data are expressed as the mean ± SEM of at least three independent experiments, each tested in quadruplicate; a one-way analysis of variance (ANOVA) with a Dunnett's multiple comparison test was performed to analyse the data (***$p < 0.001$, **$p < 0.01$, *$p < 0.05$)

increase could be the result of an increased number plasma membrane transporters or a change in the affinity of the transporter towards its substrate. In order to clarify this issue, we decided to perform a Michaelis–Menten analysis of [^{3}H]-D-Asp uptake in control or MPH treated cells. The results are shown in Fig. 2 panel a. An increase in V_{MAX} (NS = 102.8 ± 13.7 pmol/min*mg, MPH = 206.4 ± 41.7 pmol/mg*min) was detected with a decrease in affinity (K_M = NS: 8.946 ± 5.2 M, MPH: 15.62 ± 10.8 M). These results suggest that MPH increases the number of Glu transporters in the plasma membrane. To confirm this interpretation, we measured the number of plasma membrane transporters via [^{3}H]-D-Asp equilibrium binding experiments. As shown in panel b of Fig. 2, MPH treatment increases plasma membrane [^{3}H]-D-Asp binding sites, an index of GLAST molecules present in that compartment. If indeed, MPH is linked to the regulation of plasma membrane GLAST molecules, manipulation of the cytoskeleton dynamics by means of treatment with cytochalasin B should be sufficient to block the MPH effect. This is the case, a pre-exposure to 50 μM cytochalasin-B for 30 min is sufficient to prevent the documented MPH increase in GLAST at the plasma membrane (Fig. 2c).

Signalling of MPH Increase in [^{3}H]-D-Asp Uptake

Previous findings from our group have demonstrated that signalling through the Ca^{2+}/diacylglicerol dependent protein kinase (PKC) or through the cGMP-dependent protein kinase (PKG) regulates GLAST. In the former case, PKC down regulates GLAST activity and even its gene expression [27, 28]. In contrast, cGMP through PKG, increases GLAST activity in a very similar manner as described in this contribution [21]. With this in mind, we pre-exposed the cultured cells to blockers of PKC, bisindlolylmaleimide I (BisI) and of PKG (Rp-8-Br-PET-cGMPS), and to a PKC activator (12-*O*-Tetradecanoylphorbol-13-acetate, TPA) prior to MPH treatment. A slight decrease in the MPH effect could be noticed in presence of the PKG blocker, although the reduction was not statistically significant. Blockage of PKC did not

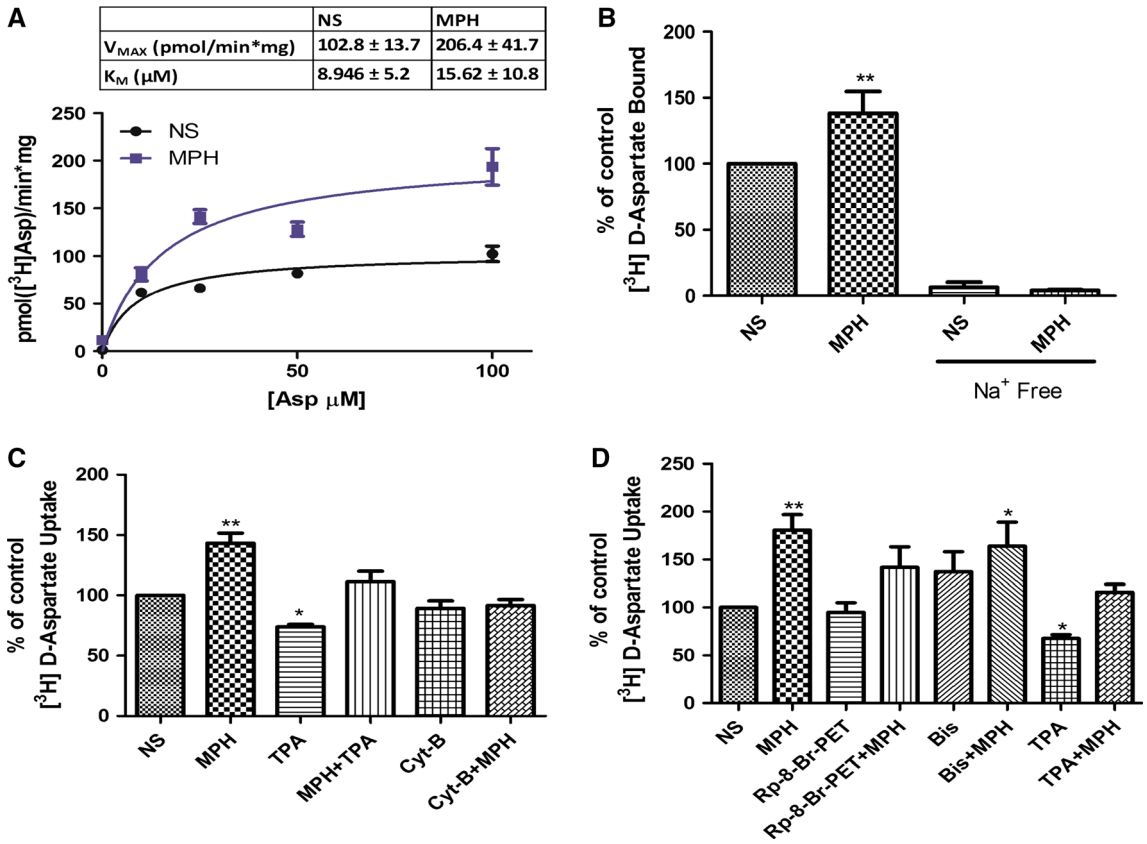

Fig. 2 MPH increases plasma membrane GLAST molecules. **a** BGC were pre-incubated with 100 μM MPH (*filled square*) or vehicle (NS) (*filled circle*) for 4 h and the [^{3}H]-D-Asp uptake assay was performed with increasing non-labelled D-Asp concentrations (0, 10, 25, 50 and 100 μM) for 30 min. Data are expressed as the mean ± SEM of at least three independent experiments, each assayed in quadruplicate. Transport kinetics V_{MAX} (pmol/min*mg) and K_M (μM) were determined by non-linear regression with Prism 5 software (GraphPad). **b** BGC monolayers were stimulated with MPH 100 μM for 4 h in normal or Na^+-free solution A. [^{3}H]-D-Asp binding assay was performed at 4 °C. Data are expressed as the mean ± SEM of at least three independent experiments, each tested in quadruplicate; a one-way analysis of variance (ANOVA) with a Dunnett's multiple comparison test was performed to analyse the data (**$p < 0.01$, *$p < 0.05$). **c** BGC were pre-incubated with 50 μM cytochalasin B (Cyt-B) for 30 min and exposed to 100 μM MPH or vehicle for 4 h; [^{3}H]-D-Asp uptake was performed for 30 min. Statistical analysis was performed as in (**b**). As experimental control, cells were pre-incubated 30 min with 12-O-Tetradecanoylphorbol-13-acetate (TPA). **d** BGC were treated for 4 h with 100 μM h MPH 4 h in the presence or absence of the indicated drugs; PKG inhibitor, Rp-8-Br-PET 10 μM, PKC inhibitor, Bisindolylmaleimide I (Bis) 2 μM, or PKC activator TPA 100 nM; the kinase inhibitors were added 30 min before MPH treatment; [^{3}H]-D-Asp uptake was performed for 30 min. Data are expressed as the mean ± SEM of at least three independent experiments, each performed in quadruplicate; a one-way analysis of variance (ANOVA) with a Dunnett's multiple comparison test was performed to analyse the data (**$p < 0.01$)

modify the MPH response, however TPA slightly decreases MPH effect. At this point, we cannot rule out the involvement of PKC or PKG in MPH signalling (Fig. 3d). A detailed analysis of these signalling cascades in the context of MPH treatment is needed to clarify this issue.

Given the fact that the MPH effect is slow, meaning it is present only after a 2 h treatment, we decided to explore the role of protein synthesis in the MPH effect. To this end, we pre-incubated the cultured cells with a 1 mM concentration of the protein synthesis inhibitor cycloheximide (CHX). As shown in panel a of Fig. 3, CHX treatment prevents the MPH-induced increase in [^{3}H]-D-Asp uptake, suggesting that MPH increases GLAST translation. Moreover, a transcription inhibitor such as actinomycin D, used at a 0.2 g/ml concentration does not modify the MPH effect, again suggesting an augmentation of GLAST mRNA translation (Fig. 3b). Accordingly, GLAST mRNA levels are not changed upon exposure of the cultured cells to 100 M MPH (Fig. 4a), whereas an increase in GLAST protein is present (Fig. 4b). These results are consistent with our interpretation that this psychostimulant regulates the efficacy of GLAST mRNA translation and its plasma membrane insertion.

Discussion

MPH is one of the most widely used CNS stimulants, commonly prescribed for attention-deficit/hyperactivity disorder, depression, obesity and autism spectrum disorders, among other mental illness [22, 23]. Although it has

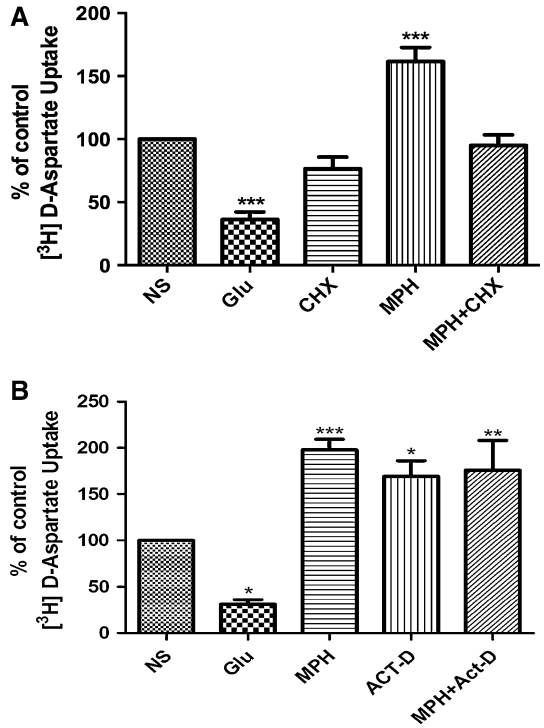

Fig. 3 MPH increases GLAST translation. **a** BGC were pre-incubated with MPH 100 μM for 4 h in the presence or absence of the protein synthesis inhibitor, cycloheximide (CHX) 1 mM, the [^{3}H]-D-Asp uptake was performed for 30 min. Data are expressed as the mean ± SEM of at least three independent experiments, each tested in quadruplicate; a Student *t test* with a Dunnett's multiple comparison test was performed to analyse the data. **b** BGC were pre-incubated with MPH 100 μM for 4 h in the presence or absence of the transcription inhibitor, actinomycin D (ACT-D) 10 μg/ml, the [^{3}H]-D-Asp uptake was performed for 30 min. In (**a**) and (**b**), the cells were pre-incubated with 1 mM Glutamate (Glu) for 30 min as a control of the experiment [20]. Data are expressed as the mean ± SEM of at least three independent experiments, each tested in quadruplicate; a one-way analysis of variance (ANOVA) with a Dunnett's multiple comparison test was performed to analyse the data (***$p < 0.001$, **$p < 0.01$, *$p < 0.05$)

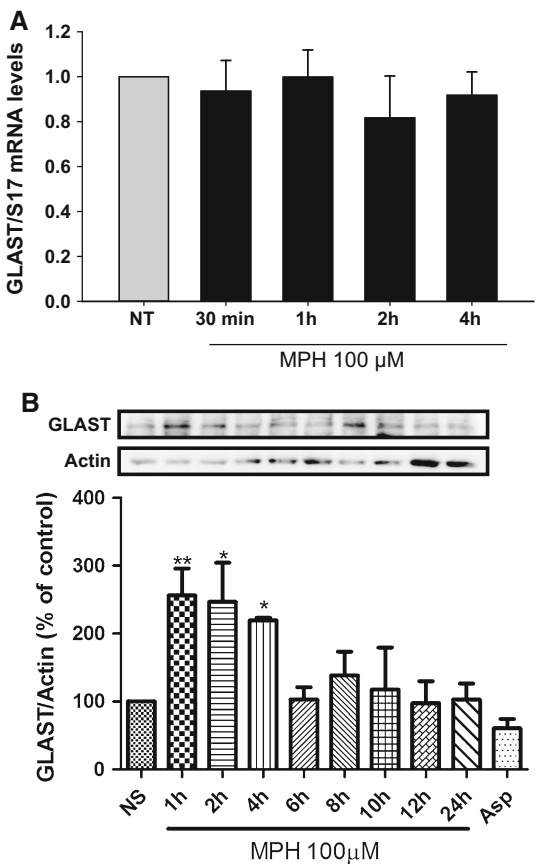

Fig. 4 MPH increases GLAST protein but not mRNA levels. **a** qRT-PCR assays were performed in primary cultures of BGC either non-treated or treated with MPH for the indicated time periods. Cells were harvested and total RNA was collected and analysed for *chglast* mRNA levels; data were normalized against ribosomal protein s17 mRNA levels. Data are expressed as the mean ± SEM of three independent experiments analysed in technical duplicates. A one-way ANOVA detected no significant difference amongst groups. **b** Confluent BGC monolayers were exposed to 100 μM MPH for the indicated time periods; GLAST was detected via Western blots (1:1000 GLAST-antibody was used); actin was used to normalize protein levels. 1 mM Aspartate (Asp) was used as a control. Results are presented as the mean ± SEM of at least three independent experiments, a representative Western blot is shown, a one-way analysis of variance (ANOVA) with a Dunnett's multiple comparison test was performed to analyse the data

been generally accepted that MPH blocks dopamine transporters and by these means increase dopamine intrasynaptic levels [24], it is clear that MPH actions are not restricted to dopamine transporters. In this context, we decided to explore a plausible interaction of MPH with the glutamatergic system, since it has been described that this drug enhances ionotropic Glu receptors response in dopaminergic neurons [25, 26]. Nevertheless, we reasoned that if MPH regulates dopaminergic tone by means of a direct modulation of Glu ionotropic receptors, then it might well be that MPH regulates the availability of this neurotransmitter in the synaptic cleft, availability that is controlled by glial-specific Glu transporters. To challenge our hypothesis, we decided to use the well-established model of glutamatergic neurons-associated glial, namely chick cerebellar Bergmann glial cells [28].

A relevant increase in GLAST activity was found upon exposure to 100 μM MPH, a concentration that has been widely used into evaluate MPH effects [14]. It should be noted that Bergmann glial cells express exclusively GLAST [17]. We were able to characterize a time and dose-dependent increase in [^{3}H]-D-Asp uptake. It is a rather slow phenomenon, since it is detected after a 2 h treatment and persists for up to 12 h. Kinetic analysis points out that the increase in Glu uptake activity is the result of an increase in the number of plasma membrane transporters, reflected in a significant two-fold increase in V_{MAX}. This interpretation was proved to be right, since

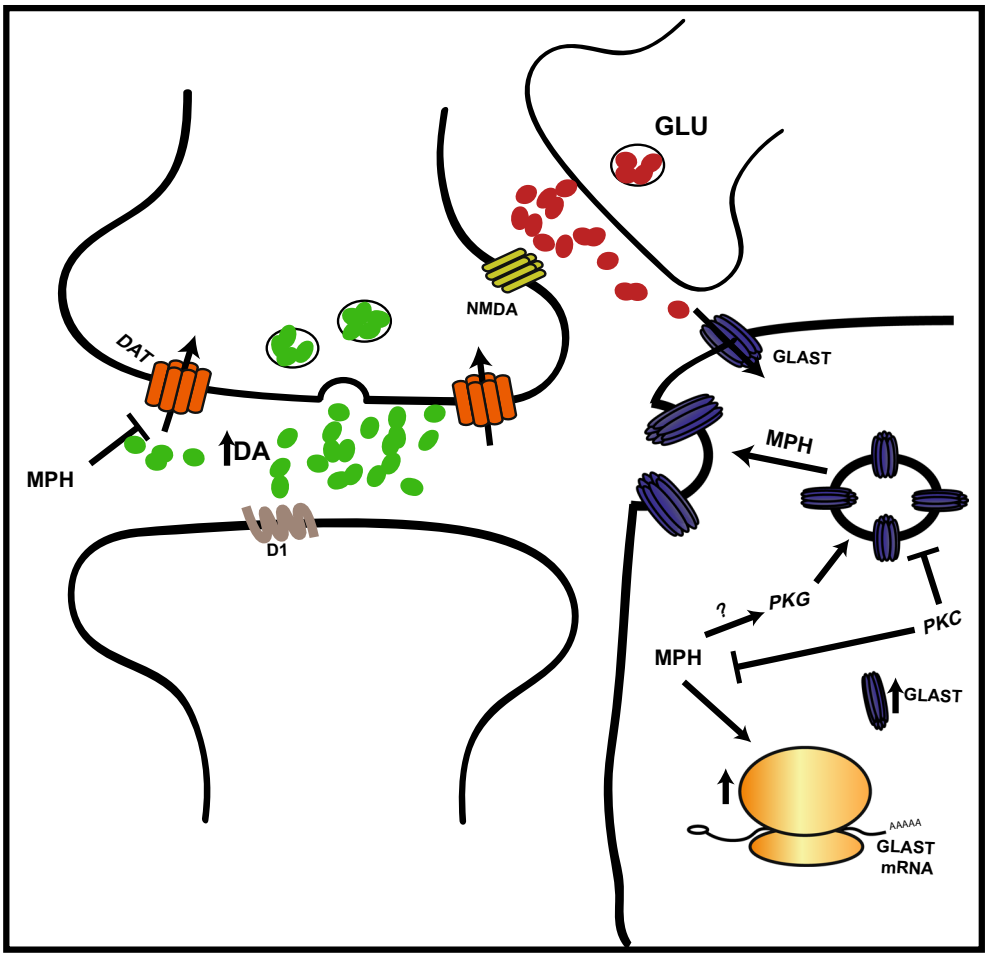

Fig. 5 Current model for MPH effect in GLAST/EAAT1 in cultured Bergmann glial cells. MPH affects GLAST-mediated Glu the uptake two levels: increasing GLAST mRNA translation and GLAST protein translocation to the plasma membrane, with a plausible role of PKG and PKC. This model illustrates that besides dopamine transporters, MPH also targets glutamate transporters in glial cells regulating both dopaminergic and glutamatergic transmission

[^{3}H]-D-Asp equilibrium binding experiments in whole cell monolayers, detected an augmentation in specific D-Asp binding sites in MPH treated cells, reflecting, once again, that the increase in uptake activity is related to an increase in functional transporters at the plasma membrane.

At this stage, an increased GLAST membrane trafficking was evident; therefore we decided to disrupt the cytoskeleton integrity by exposing the cells to cytochalasin B. As expected, MPH was no longer capable to increase GLAST activity. Our interpretation of the data, prompted us to explore the level(s) of regulation elicited by MPH, first we decided to evaluate if two signalling cascades, already known to regulate GLAST, could be the target of this psychostimulant. Although no conclusive evidence could be found, it is likely that the both PKG and PKC are involved in MPH action. Interestingly, while PKG might mediate some of MPH actions, PKC apparently blocks the MPH effect. In any event, it is clear that a detailed study of these signalling cascades in the context of MPH exposure, is mostly needed.

The fact that CHX but not actinomycin D reduces the MPH effect, points out that an increase in GLAST mRNA translation is present (Fig. 4). Note that actinomycin D treatment increases GLAST activity, this is probably due to a decrease in the expression of Ying–Yang 1, a transcription factor known to decrease *chglast* transcription in cultured chick Bergmann glia cells [27, 28]. Evidently, a MPH-dependent increase in plasma membrane GLAST molecules is present. Whether, this augmentation is related to an increase in the rate of plasma membrane transporter insertion or a decrease in its rate of removal is not known at this moment.

A schematic representation of our findings is presented in Fig. 5. Work currently in progress in our lab is aimed to the molecular characterization of the MPH effect in GLAST mRNA translation. In summary, we demonstrate

here that one of the most widely used psychostimulants targets ensheating glial cells associated to glutamatergic neurons.

Acknowledgments This work was supported by Grants from Conacyt-Mexico and Fundación Pandea to A.O. A.M.G. and Z.M-L were supported by a Conacyt-Mexico fellowships. The technical assistance of Luis Cid is acknowledged.

Compliance with Ethical Standards

Conflict of interest The authors certify that there is no conflict of interest with any financial organization regarding the material discussed in this manuscript.

References

1. Braitenberg V, Schüz A, Braitenberg VA (1998) Cortex : statistics and geometry of neuronal connectivity, 2nd edn. Springer, Berlin
2. Danbolt NC (2001) Glutamate uptake. Prog Neurobiol 65(1): 1–105
3. Danbolt NC, Chaudhry FA, Dehnes Y, Lehre KP, Levy LM, Ullensvang K, Storm-Mathisen J (1998) Properties and localization of glutamate transporters. Prog Brain Res 116:23–43
4. Solomonia RO, McCabe BJ (2015) Molecular mechanisms of memory in imprinting. Neurosci Biobehav Rev 50:56–69. doi:10.1016/j.neubiorev.2014.09.013
5. Pomierny-Chamiolo L, Rup K, Pomierny B, Niedzielska E, Kalivas PW, Filip M (2014) Metabotropic glutamatergic receptors and their ligands in drug addiction. Pharmacol Ther 142(3):281–305. doi:10.1016/j.pharmthera.2013.12.012
6. Sheldon AL, Robinson MB (2007) The role of glutamate transporters in neurodegenerative diseases and potential opportunities for intervention. Neurochem Int 51(6–7):333–355. doi:10.1016/j.neuint.2007.03.012
7. Paul P, de Belleroche J (2014) The role of D-serine and glycine as co-agonists of NMDA receptors in motor neuron degeneration and amyotrophic lateral sclerosis (ALS). Front Synaptic Neurosci 6:10. doi:10.3389/fnsyn.2014.00010
8. Fatemi SH (2008) The hyperglutamatergic hypothesis of autism. Prog Neuropsychopharmacol Biol Psychiatry 32(3):912–913. doi:10.1016/j.pnpbp.2007.11.004
9. Volk L, Chiu SL, Sharma K, Huganir RL (2015) Glutamate synapses in human cognitive disorders. Annu Rev Neurosci. doi:10.1146/annurev-neuro-071714-033821
10. Rojas DC (2014) The role of glutamate and its receptors in autism and the use of glutamate receptor antagonists in treatment. J Neural Transm 121(8):891–905. doi:10.1007/s00702-014-1216-0
11. Geschwind DH (2009) Advances in autism. Annu Rev Med 60:367–380. doi:10.1146/annurev.med.60.053107.121225
12. Muhle R, Trentacoste SV, Rapin I (2004) The genetics of autism. Pediatrics 113(5):e472–e486
13. Young NJ, Findling RL (2015) An update on pharmacotherapy for autism spectrum disorder in children and adolescents. Curr Opin Psychiatry 28(2):91–101. doi:10.1097/YCO.0000000000000132
14. Zhang CL, Feng ZJ, Liu Y, Ji XH, Peng JY, Zhang XH, Zhen XC, Li BM (2012) Methylphenidate enhances NMDA-receptor response in medial prefrontal cortex via sigma-1 receptor: a novel mechanism for methylphenidate action. PLoS ONE 7(12):e51910. doi:10.1371/journal.pone.0051910
15. Martinez-Lozada Z, Guillem AM, Flores-Mendez M, Hernandez-Kelly LC, Vela C, Meza E, Zepeda RC, Caba M, Rodriguez A, Ortega A (2013) GLAST/EAAT1-induced glutamine release via SNAT3 in Bergmann glial cells: evidence of a functional and physical coupling. J Neurochem 125(4):545–554. doi:10.1111/jnc.12211
16. Ortega A, Eshhar N, Teichberg VI (1991) Properties of kainate receptor/channels on cultured Bergmann glia. Neuroscience 41(2–3):335–349
17. Ruiz M, Ortega A (1995) Characterization of an Na(+)-dependent glutamate/aspartate transporter from cultured Bergmann glia. Neuroreport 6(15):2041–2044
18. Stoller BE, Garber HJ, Tishler TA, Oldendorf WH (1994) Methylphenidate increases rat cerebral cortex levels of *N*-acetyl-aspartic acid and *N*-acetyl-aspartyl-glutamic acid. Biol Psychiatry 36(9):633–636
19. Cavaliere C, Cirillo G, Bianco MR, Adriani W, De Simone A, Leo D, Perrone-Capano C, Papa M (2012) Methylphenidate administration determines enduring changes in neuroglial network in rats. Eur Neuropsychopharmacol 22(1):53–63. doi:10.1016/j.euroneuro.2011.04.003
20. Gonzalez MI, Ortega A (2000) Regulation of high-affinity glutamate uptake activity in Bergmann glia cells by glutamate. Brain Res 866(1–2):73–81
21. Balderas A, Guillem AM, Martinez-Lozada Z, Hernandez-Kelly LC, Aguilera J, Ortega A (2014) GLAST/EAAT1 regulation in cultured Bergmann glia cells: role of the NO/cGMP signaling pathway. Neurochem Int 73:139–145. doi:10.1016/j.neuint.2013.10.011
22. Perini E, Junqueira DR, Lana LG, Luz TC (2014) Prescription, dispensation and marketing patterns of methylphenidate. Rev Saude Publica 48(6):873–880. doi:10.1590/S0034-8910.2014004805234
23. Retz W, Retz-Junginger P (2014) Prediction of methylphenidate treatment outcome in adults with attention-deficit/hyperactivity disorder (ADHD). Eur Arch Psychiatry Clin Neurosci 264(Suppl 1):S35–S43. doi:10.1007/s00406-014-0542-4
24. Mergy MA, Gowrishankar R, Davis GL, Jessen TN, Wright J, Stanwood GD, Hahn MK, Blakely RD (2014) Genetic targeting of the amphetamine and methylphenidate-sensitive dopamine transporter: on the path to an animal model of attention-deficit hyperactivity disorder. Neurochem Int 73:56–70. doi:10.1016/j.neuint.2013.11.009
25. Prieto-Gomez B, Vazquez-Alvarez AM, Martinez-Pena JL, Reyes-Vazquez C, Yang PB, Dafny N (2005) Methylphenidate and amphetamine modulate differently the NMDA and AMPA glutamatergic transmission of dopaminergic neurons in the ventral tegmental area. Life Sci 77(6):635–649. doi:10.1016/j.lfs.2004.10.076
26. Di Miceli M, Gronier B (2015) Psychostimulants and atomoxetine alter the electrophysiological activity of prefrontal cortex neurons, interaction with catecholamine and glutamate NMDA receptors. Psychopharmacology 232(12):2191–2205. doi:10.1007/s00213-014-3849-y
27. Lopez-Bayghen E, Ortega A (2004) Glutamate-dependent transcriptional regulation of GLAST: role of PKC. J Neurochem 91(1):200–209. doi:10.1111/j.1471-4159.2004.02706.x
28. Rosas S, Vargas MA, Lopez-Bayghen E, Ortega A (2007) Glutamate-dependent transcriptional regulation of GLAST/EAAT1: a role for YY1. J Neurochem 101(4):1134–1144. doi:10.1111/j.1471-4159.2007.04517.x